Atmospheric Dispersal and Deposition of Tephra from a Potential Volcanic Eruption at Yucca Mountain, Nevada

Prepared for:
U.S. Department of Energy
Office of Civilian Radioactive Waste Management
Office of Repository Development
1551 Hillshire Drive
Las Vegas, Nevada 89134-6321

Prepared by:
Sandia National Laboratories
OCRWM Lead Laboratory for Repository Systems
1180 Town Center Drive
Las Vegas, Nevada 89144

Under Contract Number
DE-AC04-94AL85000

Atmospheric Dispersal and Deposition of Tephra from a Potential Volcanic Eruption at Yucca Mountain, Nevada

MDL-MGR-GS-000002 REV 03

October 2007

Model Signature Page/Change History

Complete only applicable items.

2. Type of Mathematical Model

☒ Process Model   ☐ Abstraction Model   ☐ System Model

Describe Intended Use of Model

The purpose of this model report is to provide documentation of a conceptual and mathematical model (Ashplume) for atmospheric dispersal and deposition of tephra from a potential volcanic eruption at Yucca Mountain, Nevada.

3. Title

Atmospheric Dispersal and Deposition of Tephra from a Potential Volcanic Eruption at Yucca Mountain, Nevada

4. DI (including Revision No. and Addendum No.):

MDL-MGR-GS-000002 REV 03

	Printed Name	Signature	Date
5. Originator	Gordon Keating		7.OCT.07
6. Independent Technical Reviewer	for Jean Younker	Ming Zhu	10/4/07
7. Checker	Jeff McCleary		10/4/7
8. QCS/Lead Lab QA Reviewer	Sounia Kassabian-Darnell		11/04/07
9. Responsible Manager/Lead	Greg Valentine for		10/4/07
10. Responsible Manager	Tom Pfeific for		10/4/07

11. Remarks

Change History	
12. Revision No. and Addendum No.	**13. Description of Change**
00	Initial issue
01	Revised in response to recommendations of the Regulatory Integration Team Evaluation, and management approval of those recommendations. An alternative model for ash redistribution was also developed and is documented in this AMR. In addition, a different version of the NOAA wind speed and direction data set was used to produce REV 01 from the one used in REV 00. This different version was used based on issues identified in CR 3205.

02	Revised to incorporate an alternative waste particle size distribution and alternative conceptual model for magma-waste interaction in the repository drifts, eruptive conduit, and eruption plume (Appendix J). This revision closes CRs 4126, 4509, 4734, 5088, 5919, 6098, and 6137. Changes to text are indicated by change bars, except for Appendix I, which was revised to be consistent with software documentation for the ash redistribution model under development; and Appendix J, which is entirely new. Additional text added in Section 7 to address Ashplume model validation acceptance criteria.
03	Revised to bring forward the revised waste particle size distribution (from Appendix J in Rev02), to revise certain Ashplume input parameter values, to introduce the magma partitioning factor, to document additional validation activities for the Ashplume model, and to remove the documentation of the tephra redistribution model (now included in MDL-MGR-GS-000006 REV00). These changes resulted in an extensive revision of the model report; therefore, change bars were not used. This revision closes CR 7837 by correcting values for the ASHPLUME code input parameter, dsigma, (ash particle size standard deviation). In addition, CR 6016 (associated with REV02 of this report) is resolved by enhanced discussion of the tephra redistribution model now contained in MDL-MGR-GS-000006 REV00.

CONTENTS

Page

CONTENTS (Continued)

CONTENTS (Continued)

Page

INTENTIONALLY LEFT BLANK

FIGURES

FIGURES (Continued)

FIGURES (Continued)

INTENTIONALLY LEFT BLANK

TABLES

TABLES (Continued)

ACRONYMS AND ABBREVIATIONS

BDCF	biosphere dose conversion factor
cm	centimeter
CDF	cumulative distribution function
DIRS	Document Input Reference System
DOE	U.S. Department of Energy
FEPs	features, events, and processes
g	gram
g_c	gravitation acceleration constant
kg	kilogram
km	kilometer
LHS	Latin Hypercube Sampling
m	meter
mm	millimeter
NRC	U.S. Nuclear Regulatory Commission
PDF	probability distribution function
RMEI	reasonably maximally exposed individual
s	second
TSPA	Total System Performance Assessment
TSPA-LA	Total System Performance Assessment for the License Application
TSPA-SR	Total System Performance Assessment for the Site Recommendation
TWP	technical work plan
YMRP	Yucca Mountain Review Plan

INTENTIONALLY LEFT BLANK

1. PURPOSE

The purpose of this model report is to provide documentation of the conceptual and mathematical model (Ashplume) for atmospheric dispersal and subsequent deposition of ash on the land surface from a potential volcanic eruption at Yucca Mountain, Nevada. Processes related to eruption and deposition of tephra are described in the context of the entire igneous disruptive events conceptual model in *Characterize Framework for Igneous Activity* (BSC 2004 [DIRS 169989], Section 6.1.1). The Ashplume conceptual model accounts for incorporation and entrainment of waste fuel particles associated with a hypothetical volcanic eruption through the Yucca Mountain repository and downwind transport of contaminated tephra. The Ashplume mathematical model describes the conceptual model in mathematical terms for estimating the concentration and thickness of radionuclide-contaminated tephra deposited on the ground surface from a hypothetical volcanic eruption at Yucca Mountain. Sensitivity analyses and model validation activities for the tephra dispersal model are also presented. Analyses documented in this model report update the previous documentation of the Ashplume mathematical model and its application to the Total System Performance Assessment (TSPA) for the License Application igneous scenarios.

In this report, 'Ashplume' is used when referring to the atmospheric dispersal model and 'ASHPLUME' is used when referencing the code representing that model (with 'ASHPLUME_DLL_LA V.2.1' as an example of a specific version of the ASHPLUME code). The term "tephra" is used as a general term for pyroclastic material regardless of size in favor of the term "ash," which means erupted material <2 mm in diameter (Fisher and Schmincke 1984 [DIRS 162806], pp. 89 to 90). The terms "fuel" and "waste" are used interchangeably.

This report describes the technical basis for the Ashplume model. The output of this report is a set of specific values (or ranges of values) for input parameters to the ASHPLUME code as implemented in TSPA. One analysis report provides direct inputs to this model report, namely *Characterize Eruptive Processes at Yucca Mountain, Nevada* (SNL 2007 [DIRS 174260]) and its product output (DTN: LA0612DK831811.001 [DIRS 179987]).

Revision 03 of this report has been prepared to document a revised waste-particle size distribution, several revised ASHPLUME input parameter values, new polar grid input parameters for ASHPLUME_DLL_LA V2.1 (for coupling to FAR V.1.2 (2007 [DIRS 182225]), the code developed as the basis for the tephra redistribution model), and the magma partitioning factor (a new parameter developed in this report for estimating the concentration of radioactive waste in the tephra) (SNL 2007 [DIRS 182219], Sections 2.2.3.2 and 2.6.5.1). Documentation of the revised ash redistribution model has been removed from this model report and is now presented in *Redistribution of Tephra and Waste by Geomorphic Processes Following a Potential Volcanic Eruption at Yucca Mountain, Nevada* (SNL 2007 [DIRS 179347]).

1.1 SCOPE OF WORK

The scope of this report is limited to description of a model of atmospheric dispersal of contaminated tephra during and after a violent Strombolian eruption of the type that could occur in the Yucca Mountain region (SNL 2007 [DIRS 174260], Section 6.3.1). If such an eruption were to intersect the repository, the possibility exists for wastes to become entrained in the

eruptive mixture and be transported via the same mechanisms as the ash plume. Although other eruption types that include nonviolent as well as violent phases exist, the violent Strombolian eruption has the greatest potential to erupt tephra and waste particles high into the atmosphere, thus increasing the potential distance of dispersal (SNL 2007 [DIRS 174260], Section 6.3.4.4). This type of eruption has been determined to be representative of the potential future eruptions occurring in the vicinity of Yucca Mountain (SNL 2007 [DIRS 174260], Section 6.3.4.4).

Figure 1-1 is a schematic representation of a possible future volcanic eruption at Yucca Mountain, showing transport of radioactive waste in an ash plume and deposition on the ground in the RMEI area. In Figure 1-1, the scope of the Ashplume conceptual model includes only the eruptive ash plume, convective/dispersive transport of contaminated ash particles downwind, and deposition on the ground surface. The Ashplume mathematical model may be used to evaluate ash and waste concentration (areal density) at any one point or multiple points on the surface relative to the volcanic vent.   The north-south orientation and 18-km distance shown in Figure 1-1 are for illustration purposes only.
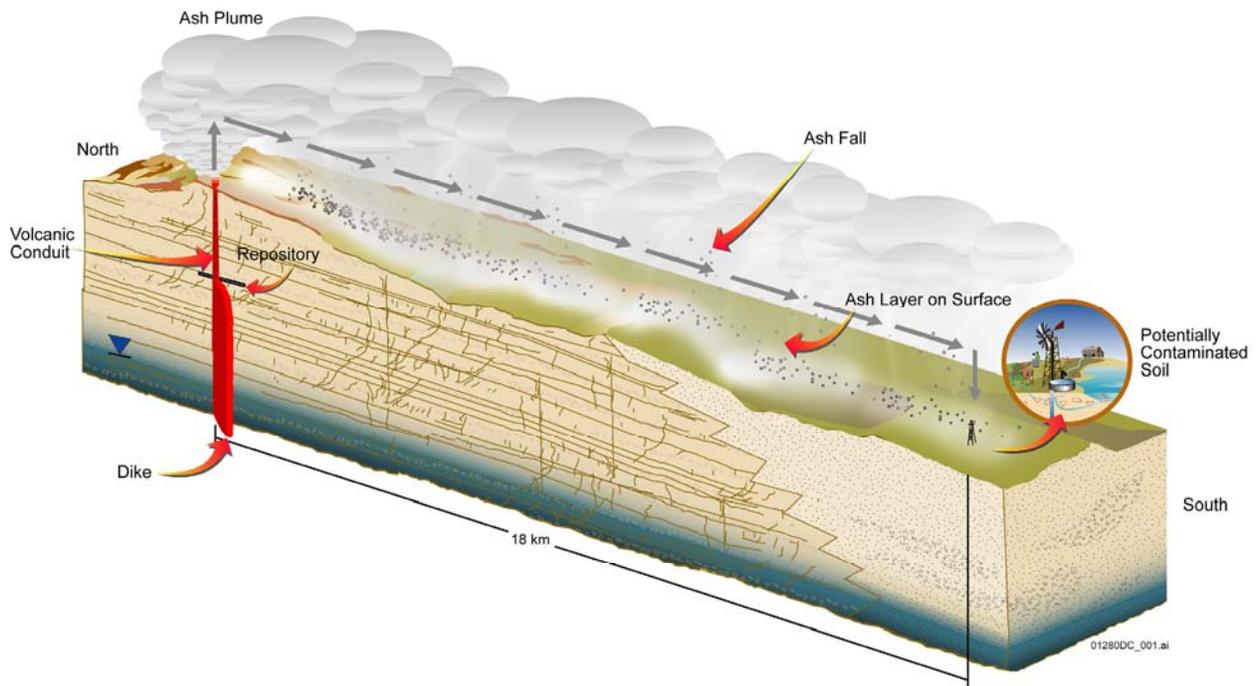
Source: SNL 2007 [DIRS 178871], Figure 6.5-12.

NOTE: For illustration purposes only.

Figure 1-1. Schematic Representation of a Volcanic Eruption at Yucca Mountain, Showing Transport of Radioactive Waste in an Ash Plume

1.2 BACKGROUND

The following sections discuss the ash dispersal model used for past Yucca Mountain TSPA analyses and present the objectives of this report as defined by *Technical Work Plan: Igneous Activity Assessment for Disruptive Events* (SNL 2007 [DIRS 182219]) for this activity.

1.2.1 Previous Use and Documentation

ASHPLUME Version 1.0–A Code for Contaminated Ash Dispersal and Deposition, Technical Description and User's Guide (Jarzemba et al. 1997 [DIRS 100987]) implements the mathematical model of atmospheric dispersal and deposition of tephra of Suzuki (1983 [DIRS 100489]) for estimation of the areal density of tephra deposits on the surface of the Earth following a volcanic eruption. The code includes estimation of the areal density of spent fuel particles incorporated into tephra particles due to a volcanic event that intersects the repository.

The original ASHPLUME V1.0 code (Jarzemba et al. 1997 [DIRS 100987]) was modified and verified for Yucca Mountain Project use to incorporate eruptive parameters developed from natural analogue volcanoes that would be representative of any future volcanic event in the Yucca Mountain region (CRWMS M&O 1999 [DIRS 132547]). The code was revised again—ASHPLUME_DLL_LA V.2.0 [DIRS 166571]—for calculations within the TSPA. ASHPLUME_DLL_LA V.2.0 was similar to previous versions of the code but employed a relationship for mass discharge rate and column height based on eruption power, rather than the less accurate empirical relationship between volume and column height used in ASHPLUME 1.4LV-dll [DIRS 154748]. This version of the code was more consistent with the state of practice among volcanologists.

A form of ASHPLUME V.2.0 [DIRS 152844], compiled for use on the Windows NT 4.0 platform, was used for some of the model validation and sensitivity studies presented in Section 7; this form of the code differs insignificantly from ASHPLUME_DLL_LA V.2.0 [DIRS 166571], which had been compiled to run on the Windows 2000 platform for TSPA. The change in the code from ASHPLUME 1.4LV-dll [DIRS 154748] to ASHPLUME_DLL_LA V.2.0 [DIRS 166571] and ASHPLUME V.2.0 [DIRS 152844] produced slightly higher calculated column heights than did ASHPLUME 1.4LV. Therefore, a new set of wind data collected at Desert Rock (near Mercury, Nevada) (NOAA 2004 [DIRS 171035]) was used to calculate wind speed and direction up to a height of 13 km. This data set replaces the Nevada Test Site data (Quiring 1968 [DIRS 119317]).

This report (Rev. 03) documents use of the latest version of the code, ASHPLUME_DLL_LA V2.1 [DIRS 178870]. The code was modified to provide the capability for computing on a radial (polar) grid for better performance when providing output for use by the tephra redistribution model, FAR (SNL 2007 [DIRS 179347]). Since the code modification as part of ASHPLUME_DLL_LA V2.1 affected only the routines that define the grid and did not affect the numerical solver routines, the validation activities using Version 2.0 remain valid and current for Version 2.1. Additional model validation activities using ASHPLUME V2.1 are presented in Section 7.5.

1.2.2   Technical Work Plan

This model report is governed by *Technical Work Plan: Igneous Activity Assessment for Disruptive Events* (SNL 2007 [DIRS 182219]). The technical work plan (TWP) specifies the activities to be carried out in consolidating and updating the documentation of the Ashplume conceptual and mathematical models.

1.3   MODEL LIMITATIONS

1.3.1   Ashplume Model Limitations

A mathematical model is generally considered to be a mathematical description of a conceptual model that approximates the behavior of a system, process, or phenomenon with determinable limits of uncertainty. The Ashplume mathematical model is an approximation of the physical systems involved in the atmospheric dispersal and deposition of contaminated tephra (ash and waste particles) associated with a possible future volcanic eruption through the repository at Yucca Mountain. Limitations inherent in all mathematical representations of complex geologic processes include: (1) incomplete knowledge of details of highly complex and heterogeneous natural processes involving localized regions of the Earth's crust; (2) use of a mathematical representation that approximates, but does not specifically represent, every detail of the process; and (3) lack of comprehensive data describing every aspect of the complex, heterogeneous geologic natural processes being represented. As a result of these limitations, the model provides predictive capability but does not provide an exact representation of the process.

The Ashplume model for Yucca Mountain is based on a model of Suzuki (1983 [DIRS 100489]) that Jarzemba et al. (1997 [DIRS 100987]) refined to represent violent Strombolian-type eruptions. Strombolian eruption involves ejection of magma into the atmosphere as a ballistic fountain of up to cm-sized scoria fragments from which μm- and mm-size ash is elutriated in a rising convective plume above the fountain. Whereas the fountain deposits a cone of potentially contaminated scoria around the vent orifice, the convective plume provides a source for distal transport of potentially contaminated ash downwind over a wide area. Fallout of ash from the plume forms a ground layer that generally thins with distance from the vent and is subject to redistribution by wind and water erosion. The Strombolian-type eruption is considered to be the most typical of the type of eruption possible in the Yucca Mountain region (SNL 2007 [DIRS 174260], Section 6.3.1). A Strombolian eruption includes violent phases as well as phases that are less violent, in which more effusive eruption processes dominate (SNL 2007 [DIRS 174260], Section 6.3.1). With increasing eruption violence, a larger fraction of the magma is fragmented to ash sizes, and a greater proportion of the magma contributes to the convective plume. The Ashplume model is limited to representation of the convective plume only and, thus, best models violent Strombolian eruptions. While the Ashplume model is mass conservative, accounting for overall mass balance is not explicitly provided in the model results.

The Ashplume model solves diffusive transport (by atmospheric turbulence and wind) of particles distributed in a column (plume) of a height determined by the heat flux (power) of the column source. The duration of this transport for individual particles is the fallout time for particles governed by their terminal fall velocity (a function of their individual size, density, and shape factor) and their upward velocity in the plume. One limitation of the model is that

Ashplume assumes a linear decrease in the plume's rise velocity from its initial rise velocity at the vent to zero at the top of the plume, and a detailed, buoyancy-driven velocity profile is not calculated. The linear rise velocity approximation does not differ substantially from a modeled buoyancy-driven velocity profile (Sparks et al. 1997 [DIRS 144352], p. 25).

Another limitation of the Ashplume model is its inability to accurately represent the transport of ash particles of mean diameter less than approximately 15 µm (Jarzemba et al. 1997 [DIRS 100987], Section 2.1). This cutoff in mean particle diameter is generally accepted to be the lower limit for the importance of gravitational settling. For particle sizes less than about 15 µm, atmospheric turbulence would tend to keep the particles aloft longer than would be estimated by the model. Because the typical mean diameter of ash particles after an eruption is generally much larger than 15 µm (see Section 6.5.2.4), the model described here is applicable to calculating the distribution of the majority of potential ash and radionuclide mass released during a possible future eruption at Yucca Mountain (CRWMS M&O 2001 [DIRS 174768], p. 9). For the small number (approximately 10%) of model realizations in which the mean particle size is <30 µm, the effect of the model limitation is to overestimate the deposition of these fine particles in the proximal Yucca Mountain region (rather than tens or hundreds of kilometers downwind), leading to conservative estimates of ash and waste areal densities at the location of the reasonably maximally exposed individual (RMEI). A related limitation is that Ashplume does not consider ash particle aggregation within the plume or removal of particles from the plume by rainfall. These processes would tend to increase the deposition of particles from the plume, and could either increase or decrease the ash-waste deposition in the RMEI location. The model is limited to solid waste only and does not consider gaseous waste species.

The Ashplume mathematical model uses the simplification that wind speed is assumed to be constant throughout the atmospheric column. This assumption is discussed further in Section 5. This limitation is accommodated within the TSPA models by treating wind speed as an uncertain parameter. In addition, wind-speed data are taken from the upper altitudes reached by the ash plume where the majority of ash is dispersed from the eruptive column of a violent Strombolian eruption. The full range of wind speeds from near zero to the maximum winds observed at the higher altitudes is represented in the wind-speed distribution used in the TSPA analyses. This stochastic treatment of wind speed captures the uncertainty that exists in future wind speeds at all altitudes of the vertical eruptive column. Wind direction and wind speed are treated in a similar manner within the TSPA implementation of the dispersion model. The Ashplume mathematical model limits wind direction to a single value for a given realization of the model. However, in the TSPA, wind direction is also treated stochastically so that the distribution of wind direction and velocity, as a function of height, reflects the wind directions actually observed near the Yucca Mountain site. The effects of the assumptions of constant column height and wind conditions during an eruption were evaluated in a sensitivity analysis of the coupled ASHPLUME-FAR models (Section 7.6). Variable column height and/or wind conditions during an eruption produced a variation of less than a factor of four on calculated tephra concentrations in sediment after redistribution; this variation is considered not significant in comparison to the orders-of-magnitude uncertainty in other Ashplume model inputs (e.g., eruptive duration and volume).

The final limitation of the Ashplume model is its sensitivity to eruptive power and initial rise velocity, which are, in turn, functions of total erupted volume and duration. These parameters (power and initial rise velocity) are uncertain. The range in values of eruptive power is defined by observations at analog volcanoes (Jarzemba 1997 [DIRS 100460], p. 136). The use of ASHPLUME_DLL_LA V.2.1 [DIRS 178870] assumes a condition in which magma is fragmented and enters the convective plume (violent Strombolian) such that the initial plume rise velocity can be derived using a relationship between power, duration, and conduit diameter (Section 6.5.1, Equation 6-7). This relationship is further defined through equations of bouyant magma rise velocity (for the minimum initial rise velocity) and multiphase modeling of the convective rise portion of an eruptive column (for the maximum initial rise velocity; Section 6.5.2.10).

In spite of these limitations, the Ashplume model is considered to be appropriate, although conservative, for the analysis of the atmospheric transport and deposition of contaminated tephra in the eruption model case because the model includes those parameters that apply specifically to conditions of incorporation of waste into volcanic tephra, maximum entrainment of contaminated tephra in an eruption column, dispersal of that tephra downwind, and deposition of the tephra at specified locations on the Earth's surface. The appropriateness of the model and the development of specific parameters are explained in detail in Section 6.

2. QUALITY ASSURANCE

This report documents a conceptual and mathematical model of atmospheric dispersal and subsequent deposition of contaminated tephra from a potential volcanic eruption at Yucca Mountain. The report contributes to the analysis and modeling of a process that might disrupt natural and engineered barriers, which are classified in *Q-List* (BSC 2005 [DIRS 175539], Section 5) as "safety category" because of their importance to meeting the performance objectives in 10 CFR 63.113 [DIRS 180319].

Development of this report revision and the supporting activities have been determined to be subject to the Yucca Mountain Project quality assurance program (DOE 2007 [DIRS 182051]; SNL 2007 [DIRS 182219], Section 8.1). The electronic management of data was accomplished in accordance with the controls specified in the TWP (SNL 2007 [DIRS 182219], Section 8.5) and the Lead Laboratory procedure IM-PRO-002, *Control of the Electronic Management of Information*. The revision of this report was performed with no variances to work described in the TWP (SNL 2007 [DIRS 182219]) and was developed in accordance with SCI-PRO-006, *Models*.

INTENTIONALLY LEFT BLANK

3. USE OF SOFTWARE

3.1 SOFTWARE TRACKED BY CONFIGURATION MANAGEMENT

The sequence of versions showing the evolution of the ASHPLUME software, as well as other qualified software, is provided in Table 3-1. ASHPLUME V.2.0 [DIRS 152844] and ASHPLUME V2.1 [DIRS 178870] are the versions used in this model report for the validation activities in Section 7. Both versions were obtained from Software Configuration Management and are appropriate for each application. These qualified codes were adequate for their intended uses as required by IM-PRO-003, *Software Management*.

Table 3-1. Computer Software

Software Title/ Version (V)	Software Tracking Number (STN)	Description / Range of Use	Computer Platform and Operating System
ArcGIS v. 9.1 Desktop [DIRS 176015]	11205-9.1-00	Qualified geographical data visualization and basic spatial analysis; used for visualization of ASHPLUME and ASHFALL model output in the code comparison model validation activity (Section 7.5)	PC, Windows XP
ASHPLUME_DLL_LA V2.1 [DIRS 180147]	11117-2.1-01	This version is used by TSPA	PC, Windows Server 2003
ASHPLUME_DLL_LA V2.1 [DIRS 178870]	11117-2.1-00	Parameterization developed in this model report directly feeds this version of the software for TSPA usage. This version is used for model validation studies described in Section 7.	PC, Windows 2000, XP
ASHPLUME V.2.0 [DIRS 152844]	10022-2.0-00	This version is used in validation studies as described in Section 7.	PC, Windows NT 4.0
ASHPLUME_DLL_LA V.2.0 [DIRS 166571]	11117-2.0-00	This version is used for model validation studies described in Section 7.	PC, Windows 2000
ASHPLUME 1.4LV [DIRS 154748]	10022-1.4LV-dll-00	This version is used corroboratively with V 2.0 for comparison of calculated and measured ash deposition thickness for 1995 Cerro Negro eruption (see Section 7.3).	PC, Windows 2000
FAR V.1.2 [DIRS 182225]	11190-1.2-00	This software was used in the Ashplume model validation activity reported in Section 7.6	PC, Windows 2000 & 2003
GoldSim V.9.60.000 [DIRS 180224]	10344-9.60-00	This software was used to run the ASHPLUME_DLL_LA V2.1 and FAR V.1.2 codes in the Ashplume model validation activity reported in Section 7.6	PC, Windows 2000, 2003, & XP

3.2 EXEMPT SOFTWARE

Commercial, off-the-shelf software used in support of this model report is listed in Table 3-2. This software is exempt from the requirements of IM-PRO-003. Formulas, inputs, and outputs used in these software and other information required for a technically qualified person to reproduce the work are documented in each section or appendix where the analysis is presented.

Table 3-2.   Exempt Software

Software Name and Version (V)	Description	Computer Platform and Operating System
Microsoft Excel, v97 SR-2 and v2000	The commercial software was used for plotting graphs and statistical calculations. Only built-in standard functions in this software were used. No software routines or macros were used with this software to prepare this report.	PC, Windows 2000/NT/XP
Microsoft Access, 2000	The commercial software, Microsoft Access 2000, was used for unit conversions and data segregation. Only built-in standard query functions in this software were used. No software routines or macros were used with this software to prepare this report.	PC, Windows 2000, XP
OriginPro 7.5	The commercial software, OriginPro 7.5, was used for data visualization and generation of basic statistics using built-in functions. No software routines or macros were used with this software to prepare this report.	PC, Windows 2000/XP
Microsoft PowerPoint 97 SR-2	The commercial software was used for visualizing model validation results in context of published data. Only built-in standard functions in this software were used. No software routines or macros were used with this software to prepare this report.	PC, Windows NT
Golden Software's Surfer Version 6.01.	The commercial software was used for visualizing model validation results in context of published data. Only built-in standard functions in this software were used. No software routines or macros were used with this software to prepare this report.	PC, Windows NT
Matlab release 11	The commercial software was used for generation of synthetic ash plume data sets based on simple equations. Only built-in standard functions in this software were used. No software routines or macros were used with this software to prepare this report.	PC, Windows XP
Tecplot 360	The commercial software was used for visualization and grid processing, using only built-in standard functions. No software routines or macros were used with this software to prepare this report.	PC, Windows XP

4. INPUTS

4.1 DIRECT INPUT

This section discusses data, parameters, and inputs to the modeling activities that are documented in this report. External data used as direct input have been qualified as documented in Appendix A.

4.1.1 Data

Sources for data supporting the development of input parameters to the Ashplume model, and documented in this report, are listed in Table 4-1. These data are used to develop primary model inputs as described in Section 6.5.2. Ash physical characteristics required as inputs to the Ashplume model are developed in *Characterize Eruptive Processes at Yucca Mountain, Nevada* (SNL 2007 [DIRS 174260]). The report provides information about natural volcanic systems and the parameters that can be used to model their behavior and is appropriate for use as input to the ash dispersion model documented in this report.

The wind speed cumulative distribution functions (CDFs) and wind direction probability distribution functions (PDFs) appropriate for use in modeling a potential future volcanic eruption in the Yucca Mountain region are developed in this model report from data provided in *Upper Air Data: Desert Rock, Nevada Years 1978-2003* (NOAA 2004 [DIRS 171035]). The development of the CDFs and PDFs from the raw climatological data is described in Sections 6.5.2.7 and 6.5.2.8 and Appendix D. The waste-particle-size distribution used as input to this model report is supported by documentation included in Appendix F. Air physical characteristics are taken from *CRC Handbook of Chemistry and Physics, A Ready-Reference Book of Chemical and Physical Data* (Lide 1994 [DIRS 147834]), as discussed in Sections 6.2.3.13 and 6.2.3.14.

The qualification status of the input sources is provided in the Technical Data Management System and listed in the Document Input Reference System (DIRS) database. Data from external sources are used as direct input to the development of this model report. The data from these sources have been qualified for intended use within the document using the process found in SCI-PRO-006, and the methods and attributes required for qualification of data per SCI-PRO-001, *Qualification of Unqualified Data*. These qualifications are documented in Appendix A.

Separate data were used for development of the model and input parameter values (Section 6.5) versus those used to validate the model (Section 7).

Table 4-1.   Input Data

Data Description	Data Tracking Number (DTN) or Source
Column diffusion constant (beta)	Jarzemba et al. 1997 [DIRS 100987], Suzuki 1983 [DIRS 100489]
Air physical characteristics (air viscosity)	Lide 1994 [DIRS 147834]
Air physical characteristics (air density)	Lide 1994 [DIRS 147834]
Eddy diffusivity constant	Suzuki 1983 [DIRS 100489]
Specific heat capacity of magma	Drury 1987 [DIRS 156447], Bacon 1977 [DIRS 165512]
Basaltic magma liquidus temperature	LA0612DK831811.001 [DIRS 179987]
Eruptive volume based upon the estimated eruption volumes of Quaternary volcanoes in the Yucca Mountain region	LA0612DK831811.001 [DIRS 179987]
Duration of a single explosive phase constituting a violent Strombolian eruptive event	LA0612DK831811.001 [DIRS 179987]
Eruptive power	Jarzemba 1997 [DIRS 100460]
Basaltic magma density	LA0612DK831811.001 [DIRS 179987]
Basaltic magma density and viscosity as a function of initial water content	LA0612DK831811.001 [DIRS 179987]
Conduit diameter	LA0612DK831811.001 [DIRS 179987]
Clast characteristics (ash particle shape factor)	LA0612DK831811.001 [DIRS 179987]
Ash-particle density variation with particle size	LA0612DK831811.001 [DIRS 179987]
Log ash-particle size at minimum, maximum ash density	LA0612DK831811.001 [DIRS 179987]
Mean ash-particle diameter	LA0612DK831811.001 [DIRS 179987]
Ash particle diameter standard deviation	LA0612DK831811.001 [DIRS 179987]
Ash particle shape factor	LA0612DK831811.001 [DIRS 179987]
Ash settled density	LA0612DK831811.001 [DIRS 179987]
Elevation of Yucca Mountain crest	MO9912GSC99492.000 [DIRS 165922]
Maximum initial rise velocity	Woods 1988 [DIRS 172081]
Wind data	NOAA 2004 [DIRS 171035]

4.1.2   Parameters and Parameter Uncertainty

The treatment of uncertainty for the values or ranges of values for input parameters is described in Section 6.5.2 as part of the rationale for each parameter value. Values for ASHPLUME input parameters are specified as: 1) point values for well-established geophysical data (e.g., properties of air) or constants that control numerical functions in ASHPLUME_DLL_LA V.2.1 [DIRS 178870] code; 2) as stochastic ranges of a specified form for parameters whose

uncertainty has been bounded by analogue studies (e.g., eruptive power); or 3) as tables of values for parameters based on environmental observations (e.g., cumulative distribution functions of wind speed and direction by altitude).

The TSPA model, of which Ashplume is a component, uses Monte Carlo simulation as a method for mapping uncertainty in model parameters and future system states, expressed as probability distributions, into predictions of model output (SNL 2007 [DIRS 178871]). Large uncertainties exist in Ashplume model input parameters due to the uncertainty of future atmospheric conditions at the time of the hypothetical eruption and uncertainty in the characterization of the physical attributes of a future eruption. Ashplume model parameters that contain uncertainty and may significantly affect the results of TSPA calculations are developed in this model report as probability distributions for compatibility with the Monte Carlo methods used in the TSPA model.

4.2   CRITERIA

The regulatory requirements for performance assessment that must be satisfied by the TSPA are stated in 10 CFR 63.114 [DIRS 180319]. This report primarily addresses the integrated subissue of airborne transport of radionuclides, and *Yucca Mountain Review Plan, Final Report* (YMRP) (NUREG-1804; NRC 2003 [DIRS 163274]) associates the integrated subissue of airborne transport of radionuclides with the requirements listed in 10 CFR 63.114(a) to (c) and (e) to (g) [DIRS 180319]. The YMRP (NRC 2003 [DIRS 163274], Section 2.2.1.3.11.3) describes the acceptance criteria that the NRC will use to evaluate the adequacy of information addressing the airborne transport of radionuclides in the license application. Information addressing the YMRP acceptance criteria is presented in Appendix B.

Model validation acceptance criteria associated with SCI-PRO-006 are discussed in Section 7.

4.3   CODES, STANDARDS, AND REGULATIONS

No other codes, standards or regulations other than those referenced in Section 4.2 apply to this model report.

INTENTIONALLY LEFT BLANK

5. ASSUMPTIONS

This section describes the assumptions applicable to the use of the Ashplume model. Each assumption listed is followed by a rationale for use and its disposition in this report. Assumptions are grouped within this section according to whether they apply to the conceptual or mathematical model or to the model parameters. A summary of the described assumptions is provided in Table 5-1. Assumptions made in source documents are not discussed in this report.

Table 5-1. Summary of Key Assumptions

Item #	Assumption	Summary Comment on Impact
MODEL ASSUMPTIONS		
5.1.1	Volcanic eruption is violent Strombolian for entire duration	Represents the most energetic aspect of expected eruption styles and creates sustained eruptive column consistent with transport modeled by ASHPLUME.
5.1.2	Waste incorporation into magma via energetic conduit environment	Provides basis for conceptual model of waste package failure and incorporation of fragmented waste into ascending magma.
5.1.3	Waste particles form well-mixed suspension in magma	By analogy with suspension of refractory wall-rock xenoliths within the magma, this assumption informs the choice of a neutral value for the input parameter, waste incorporation ratio.
5.1.4	Waste-Particle Incorporation into Tephra	Tephra and waste are combined according to the natural size distributions of tephra and waste particles. Sensitivity analysis indicates that impact of this assumption is small.
PARAMETER ASSUMPTIONS		
5.2.1	Future wind speed and direction	Global climate model studies with available paleoclimate information support the assumption of little change to long-term average wind patterns. Postglacial qualitative trends include a lessening of frequency for northerly winds from the repository towards the RMEI.
5.2.2	Wind speed and direction remain constant during an eruptive event	Gives maximum distribution along centerline of wind direction and toward the RMEI for corresponding wind conditions. Sensitivity analysis indicates that this assumption has small impact on model results.
5.2.3	Ashplume utilization of wind speed and direction	Use of wind speed and direction corresponding with the top of plume results in high dispersal of ash and waste.
5.2.4	Waste particle size	Appropriate analogue data from igneous extrusion through engineered systems are lacking. This assumption uses a particle size distribution informed by laboratory tests studies of hot particles dispersed from the Chernobyl Nuclear Power Plant, fractured post-service spent fuel form, and observations of accretion of sub-micron-sized particles.
5.2.5	Initial rise velocity	Initial rise velocity of particles in plume is the minimum velocity necessary to supply eruptive thermal power to a convective plume; particles decelerate from the vent through the gas-thrust region to the base of the convective-thrust region. This assumption maximizes the dispersal of ash and waste in a high convective plume that is transported downwind.

5.1   MODEL ASSUMPTIONS

5.1.1   Volcanic Eruption is Violent Strombolian for Entire Duration

Assumption–The Ashplume model assumes that volcanic eruptions in the Yucca Mountain region are violent Strombolian for the entire duration of the explosive phase. Erupted magma is presumed to be fragmented and dispersed in the convective plume for the entire duration of the eruption. This assumption is conservative in that it maximizes the potential for ash and waste dispersal during Strombolian activity. (Violent Strombolian does not reach the dispersive potential of more violent types of events that are not associated with the Yucca Mountain region, such as Vulcanian/Surtseyan [hydrovolcanic] eruptions or eruptive phases.) The validity of this assumption received support from the Igneous Consequences Peer Review Panel (Detournay et al. 2003 [DIRS 169660], Section 4.2).

Rationale–This assumption is considered to be conservative because normal Strombolian activity is dominated by short-duration bursts that throw relatively coarse fragments of melt out of the vent on ballistic trajectories, where most of the fragments are deposited immediately around the vent with only a very small fraction of finer particles rising higher and being dispersed by wind to form minor fallout sheets (SNL 2007 [DIRS 174260], Section 6.3.5.1). In contrast, the Ashplume model represents the most violent type of Strombolian activity, in which the near-vent ballistic component is minimal and tephra dispersal in a wind-blown convective plume dominates, according to the conceptual model (Jarzemba et al. 1997 [DIRS 100987], p. 2-1). Clearly, this assumption maximizes the dispersal of contaminants for Strombolian activity. While all of the analogue volcanoes studied in the Yucca Mountain region exhibit evidence of explosive eruption by the violent Strombolian style for at least part of their eruptive history (SNL 2007 [DIRS 174260], Section 6.3.4.4), uncertainties associated with the nature of violent Strombolian eruptive phases include their duration, eruption power (the heat flux carried by the tephra), and the volume of the erupted tephra (SNL 2007 [DIRS 174260], Section 6.3.4.4). These uncertainties are included in the model through the development of distribution functions for these parameters. The volume of the Lathrop Wells volcano is used to provide realistic bounds for these input parameters since it is the preferred analogue to a potential future volcanic eruption at Yucca Mountain (Section 6.5.2).

It is conservative to assume that an eruptive event can be modeled as being in the violent Strombolian phase during the entire period of eruption because typical eruptions include only a minor component, if any, of violent Strombolian activity. Most of a typical eruption is less energetic.

Where Used–This assumption is used in Section 6.3 to support the conceptual model for the volcanic eruption release.

5.1.2   Waste Incorporation Into Magma via Energetic Conduit Environment

Assumption–Physical damage to the waste package in the energetic conduit environment is assumed to provide a means for waste package failure and entrainment of fragmented waste within the rising magma.

Rationale–Analyses of waste package and waste form in the intrusion scenario indicate that the integrity of the waste package would be compromised via corrosion, heating, and differential pressures associated with magmatic intrusion (SNL 2007 [DIRS 177430], Section 6.4.8.3). If the conduit intersects one or more repository drifts, the waste packages located partially or entirely within the conduit may be degraded and moved by fragmenting magma ascending toward the vent (SNL 2007 [DIRS 177430], Section 6.4.8.3.2). Physical damage to the waste package is considered likely in the turbulent and unsteady flow environment that creates and evolves the volcanic conduit, including magma pressure transients, shear stresses, wall-rock failure, and differential flow regimes (e.g., annular, channeled flow) (SNL 2007 [DIRS 174260], Appendix F). This condition is inherent in the input parameter for the amount of waste erupted and is given a technical basis in *Number of Waste Packages Hit by Igneous Intrusion* (SNL 2007 [DIRS 177432]) for use in the TSPA.

Where Used–This assumption is used in Section 6.5.1 in the development of the Ashplume mathematical model and in Section 6.5.2.6 in the development of the value for the Ashplume input parameter, waste incorporation ratio.

5.1.3 Waste Particles Form Well-Mixed Suspension in Magma

Assumption– Waste particles are well mixed in the magma within the conduit and are treated as refractory particles (xenoliths) in the melt during fragmentation.

Rationale– The energetic conduit environment exposes the spent fuel to flowing magma (Section 5.1.2; SNL 2007 [DIRS 177432] Section 5.2). Complex conduit processes, including differential magma flow regimes (e.g., annular, channeled flow), pressure transients and vesiculation, shear stresses, and wall-rock failure, produce a well-mixed suspension of fragmented waste particles within the magma. The analogy for this process is natural suspension of refractory wall-rock xenoliths within magma prior to eruption. The time scales for waste entrainment, transport in the conduit, and eruption are on the order of hours, which does not provide sufficient time for melting or dissolution into the magma (Codell 2004 [DIRS 181522], pp. 206 to 207). This assumption informs the choice of a neutral value of the model parameter, "waste incorporation ratio" (Section 6.5.2.6), such that tephra and waste particles are combined according to the compatibility of their respective particle size distributions.

Where Used–This assumption is used in Section 6.5 in the development of the Ashplume mathematical model.

5.1.4 Waste-Particle Incorporation into Tephra

Assumption–The mathematical formulation of the Ashplume model makes the simplifying assumption that tephra and waste are combined according to the natural size distributions of tephra and waste particles, consistent with the conceptual fragmentation of a well-mixed suspension of waste particles within the silicate melt (magma).

Rationale–This assumption is consistent with the conceptualization that all waste material in canisters intersected by an eruptive conduit is incorporated into the magma (and, subsequently, into the eruption column) (Sections 5.1.2 and 5.1.3). This mathematical formulation is required to correct the density of tephra particles for the density of the incorporated waste particle prior to

transport. Immediately prior to eruption, magma consisting of a well-mixed suspension of waste particles (Section 5.1.3) fragments, and the resulting pyroclasts (tephra) are composed of particles that contain various proportions of silicate melt droplets, crystals, lithic (rock) fragments, and waste fragments. The mathematical model allows the natural size distributions of tephra (produced in the fragmentation process) and waste particles (retained from the original release of waste from the waste packages) to prevail in the tephra-waste mixture (Section 6.5.2.6), and the density of the resulting composite pyroclast is adjusted if waste is present. Thus the waste particles can be treated as refractory "xenoliths" in the melt, which, upon magma fragmentation, reappear in the tephra as mixed particles of waste and silicate melt (glass).

Where Used–This assumption is used in Section 6.5.1 in the development of the Ashplume mathematical model and in Section 6.5.2.6 in the development of the value for the Ashplume input parameter, waste incorporation ratio.

5.2   PARAMETER ASSUMPTIONS

5.2.1   Future Wind Speed and Direction

Assumption–Data characterizing variability in wind speed and wind direction under present climatic conditions in the Yucca Mountain region are provided in *Upper Air Data: Desert Rock, Nevada Years 1978-2003* (NOAA 2004 [DIRS 171035]; and Appendix D, this document). These data are assumed to be acceptable approximations of variability in wind speed and direction for future wind conditions.   Conceptually, this assumption corresponds to an assumption that climatic change will not significantly affect wind speed and direction.   The magnitude of short-term variability in wind speed and direction, which is included in the data that characterize present wind conditions, is presumed to be significantly greater than long-term variability introduced by potential future climatic changes.

Rationale–Justification for future wind conditions in future climates is based on the observation that the magnitude of short-term variability in meteorological phenomena is great compared to changes in long-term averages.   Emphasis for relatively brief volcanic events is appropriately placed on the short-term variability rather than on long-term averages in wind patterns.

Additional support for the reasonableness of this assumption comes from examination of published modeling studies of past climatic conditions that may be reasonable analogues for future climatic conditions at Yucca Mountain.   Kutzbach et al. (1993 [DIRS 119269], p. 60) have modeled global climates at 3,000-year intervals during the last 18,000 years, using general circulation models with available paleoclimatic information used to define boundary conditions. Resolution of the model is extremely coarse (grid blocks are 4.4 degrees latitude by 7.5 degrees longitude (Kutzbach et al. 1993 [DIRS 119269], p. 60)), and results are not intended to be interpreted at local scales.   However, model results (presented at a regional scale) provide qualitative information about modeled wind speeds and directions for the southwestern United States.   Model results are provided for 18,000 years ago, at the end of the last major glaciation of northern North America, at 12,000, 9,000, and 6,000 years ago and also for present conditions. Climatic conditions at these times span the range of conditions that might reasonably occur during a future transition from the present climate to a glacial climate.

Modeled surface winds for the southwestern United States in winter and summer show a slightly stronger westerly component (away from the location of the RMEI south of the repository) 18,000 years ago than at present and are essentially unchanged from the present at 12,000, 9,000, and 6,000 years ago (Kutzbach et al. 1993 [DIRS 119269], Figures 4.6 and 4.8). Modeled winter (January) winds at the 500-millibar (mb) pressure isobars (about 5.5-km altitude) blow strongly from the west at all times and were somewhat stronger at 18,000 years ago than at present (Kutzbach et al. 1993 [DIRS 119269], Figure 4.14). Modeled summer (July) winds at 500 mb are weaker and less consistent than winter winds, blowing from the southwest and west at 18,000 and 12,000 years ago and at the present, and from the northwest 9,000 and 6,000 years ago (Kutzbach et al. 1993 [DIRS 119269], Figure 4.15).

The information relevant to the assumption discussed here is that significant changes in wind speeds and directions in the southwestern United States, as modeled by Kutzbach et al. (1993 [DIRS 119269]), are not dramatic during the modeled transition from glacial to interglacial climates. The largest changes, occurring during full glacial conditions 18,000 years ago, appear qualitatively to correspond to a decrease in the relative frequency of winds blowing toward the RMEI location south of Yucca Mountain. Therefore, these changes are reasonably and conservatively neglected, and variability in present wind conditions is assumed to characterize variability adequately in future conditions.

Where Used–This assumption is used to justify the distributions of future wind speed and direction that are recommended for use in the TSPA analyses. The recommended wind direction and wind speed distribution functions are discussed in Section 6.5. Functionally, the assumption means that individual values of wind speed and direction can be sampled for time zero from distributions based on present data, and the same values can then be used for all time steps for each realization.

5.2.2 Wind Speed and Direction Remain Constant During an Eruptive Event

Assumption–Wind speed and direction are assumed to be constant during an eruptive event.

Rationale–This assumption prevents short-term variations in wind speed and direction from spreading the ash plume over a broader area and results in both a maximum quantity and maximum concentration of waste at the centerline of the plume. This is a reasonable simplification, given the relatively short duration of violent eruptive events. In addition, studies of the effects of variable wind conditions during an eruption on the concentration of tephra at the RMEI after redistribution (Section 7.6) indicate that the system is relatively insensitive to such variations.

Where Used–Section 6.5.

5.2.3 Ashplume Utilization of Wind Speed and Direction

Assumption–The Ashplume model assumes that the wind speed and direction that dictate tephra dispersal are those that occur at the top of the plume.

Rationale–Wind speed and wind direction vary with altitude above the ground, and, thus, tephra dispersed from the plume at different altitudes follows trajectories governed by altitude-dependent wind vectors. The column diffusion constant (β) determines which locations in the column contribute the most tephra dispersal. This constant was presumed to be a log-uniform distribution from 0.01 to 0.5 (Jarzemba et al. 1997 [DIRS 100987], p. 4-1) without justification (for the distribution type) other than it spans more than one order of magnitude. Because violent Strombolian eruptions typically form an anvil-shaped plume, most particles must rise to near the plume top before dispersal down wind. This suggests that large values of β are common such that the distribution is likely uniform, as is implemented in this report. With a uniform distribution of beta between 0.01 and 0.5, the majority (about 80%) of violent Strombolian eruptions are modeled with β greater or equal to 0.1, a level at and above which Suzuki (1983 [DIRS 100489], Figure 6) showed dominant dispersal from the upper half of the column. Hence, the wind speed and direction near the top of the plume are appropriate and maximize dispersal for modeled eruptions. In addition, a comparison of ASHPLUME to another tephra dispersal model that incorporates a wind field that is stratified with elevation (ASHFALL) indicates that the use of a single wind speed and direction condition (at the top of the eruption column) gives a good approximation of natural systems during an eruption (Section 7.5). This assumption is considered to be reasonable and consistent with the intended use of the Ashplume model.

Where Used–Section 6.5.

5.2.4 Waste-Particle Size

Assumption–For the purpose of estimating waste-particle diameters in the eruptive environment, all waste entrained in rising magma is assumed to be unaltered commercial spent fuel physically disaggregated to a size range that approximately relates to fuel form grain size.

Rationale–This assumption is considered reasonable for analyses of the postclosure performance period as specified in 10 CFR 63.311 [DIRS 180319].

A discussion of the rationale for defining the waste particle size criteria is included in Appendix B. Through an extensive literature review, aspects of waste (spent nuclear fuel) in the magmatic environment are discussed to support the characterization of a waste particle size range for Ashplume modeling purposes. These aspects include spent fuel form characterization, oxidation (aqueous and dry-air), mechanical shock, disaggregation experiments, and the Chernobyl nuclear power plant (ChNPP) accident analog. Based on this analysis, a waste particle size distribution is developed that places strong weight on the data from observed particulates dispersed from the ChNPP accident. The upper bound (0.2 mm) represents a typical fragment size from a fractured postservice spent fuel pellet, and the lower bound (1 μm) recognizes the observed tendency for accretion of sub-micron particles.

Where Used–Section 6.5.2.16 to develop the waste-particle size distribution.

5.2.5   Initial Rise Velocity

Assumption–The initial rise velocity of tephra particles in the plume is assumed to be the minimum velocity required to provide the plume the modeled thermal power. The Ashplume model stipulates that the convective rise velocity of tephra particles linearly decreases from the initial rise velocity at the base of the convective plume to zero at the top of the plume. The upward velocity profile of buoyant plumes generally decreases with height to zero at their tops, where neutral buoyancy is a complex relationship of plume and atmospheric density profiles and the rate of air entrainment and heating. Therefore, this assumption represents the model-equivalent of the plume's vertical velocity profile. In order for model-equivalence to give a reasonable numerical approximation, the initial rise velocity is constrained to values that are compatible with the plume height and, thus, eruptive power.

Rationale–Ashplume models a column (plume) instantaneously loaded with hot particles moving at some upward velocity. The height of the column determined by ASHPLUME is fixed by the power (heat flux) provided by erupting magma. The heat flux is directly proportional to the mass flux of magma from the vent, which, for continuity, is determined by the vent area, magma bulk density, and vent velocity. For any given vent area and mass flow rate, the density and velocity of the mixture are inversely related: minimum vent velocity occurs when the magma bulk density is at its maximum (gas-free) value and maximum vent velocity occurs when magma bulk density is at its minimum value. The eruption velocity may briefly exceed the sonic velocity of the mixture within or slightly above the eruptive vent, resulting in subatmospheric pressure in the jet; however, the pressure quickly adjusts to atmospheric conditions, which determine the mixture density and, indirectly, its velocity. For the purposes of this study then, the minimum realistic magma bulk density (and maximum vent velocity) arises when magma volatile components are expanded to atmospheric pressure. The minimum vent velocity is constrained by the minimum practical magma rise rate (maximum magma bulk density) (Appendix G). Realistic vent velocities fall between these two extremes.

Before the magma and gas mixture enters the convective-thrust part of the plume, it rapidly decelerates by its interaction with the atmosphere and gravitational forces in a region known as the gas-thrust region (Section 6.3). Because the height of the gas-thrust region is generally less than 10% of the total eruptive column height, a convective plume model such as Ashplume that neglects this gas-thrust region is justified (Wilson et al. 1978 [DIRS 162859], p. 1,830). The Ashplume model must account for gas expansion and air entrainment as well as the deceleration of tephra in the gas-thrust region while maintaining continuity in order for the column height to eruptive power relationship to hold. Implicit in the convective plume model is that: (1) height is solely determined by the convection produced by the supplied thermal power and that (2) the contribution to the plume height by the momentum of gas-thrust region is negligible. This approximation stipulates that the velocity of tephra entering the plume must only be that required to deliver the required power.

The variation in velocity of the plume from the vent, through the gas-thrust region, to the convective rise region is determined by complex interactions of the multiphase gas-pyroclast mixture and ambient air, at pressures varying from below atmospheric pressure to several times above it (Valentine 1998 [DIRS 181477], pp. 107 to 110). Calculations of the relationship between vent velocity and plume velocity at the base of the convective rise region require

numerical models like that of Woods (1988 [DIRS 172081]). Determination of the bounds on the range of reasonable values for initial rise velocity are developed from theoretical considerations of minimum and maximum velocities for the gas-pyroclast mixture entering the bouyant plume (Section 6.5.2.10). This assumption is considered reasonable and consistent with the intended use of the Ashplume model.

Where Used–Section 6.5.

6. MODEL DISCUSSION

The potential consequences associated with the eruption model case require consideration of both the eruption and deposition of contaminated tephra and redistribution of that material after deposition. This section presents the objectives, technical bases, and applications of the model that represents the eruption and deposition of volcanic tephra. Section 6.1 presents the modeling objectives. Section 6.2 presents the applicable features, events, and processes addressed by the model. Section 6.3 provides the conceptual basis for the eruptive transport and deposition of waste-contaminated tephra from a hypothetical volcanic eruption through a repository at Yucca Mountain. Section 6.4 discusses alternative conceptual models, and Section 6.5 presents the technical basis for application of the tephra dispersal and deposition model. Section 6.6 summarizes the model results and abstractions.

The Ashplume mathematical model is implemented for TSPA calculations by computer code ASHPLUME_DLL_LA V.2.1 [DIRS 178870]. The ASHPLUME_DLL_LA computer code is a component of the TSPA model of the nuclear waste repository at Yucca Mountain. The TSPA model is used to evaluate the performance of the geologic repository in protecting humans and the environment from the risk associated with exposure to spent nuclear fuel and high-level radioactive waste. Within the TSPA, the model of atmospheric dispersal and deposition of tephra implemented in the ASHPLUME code is used to estimate the ground-level concentration or areal density (g/cm^2) of tephra and waste after a violent Strombolian eruption that intersects the repository. The code is called twice within each TSPA realization, and the results are passed to FAR, the model of tephra redistribution and soil diffusion (SNL 2007 [DIRS 179347]). The first call to ASHPLUME calculates tephra deposition at the location of the RMEI (a single point located 18 km south of the repository). The second call calculates tephra fall at numerous points within the Fortymile Wash watershed as a basis for calculating the redistribution of waste-contaminated tephra by sediment transport processes in FAR. The waste concentration is then converted to activity concentrations of individual radionuclides and combined with biosphere dose conversion factors (BDCFs) in TSPA to calculate a radiation dose to the RMEI.

6.1 MODELING OBJECTIVES

A model has been developed to simulate the dispersal and deposition processes for volcanic tephra contaminated with radioactive waste from a hypothetical eruption through the repository at Yucca Mountain. The overall objectives of this model are to

- Represent the processes related to atmospheric transport and deposition of contaminated tephra at and near the RMEI location and within the Fortymile Wash watershed

- Provide model output in a format that is compatible with the input requirements of the FAR model of tephra redistribution, within the TSPA modeling framework.

The Ashplume conceptual model provides the basis, supported by analogue descriptions, for the applicability of using the ASHPLUME code to model volcanic ash and waste dispersal during a hypothetical future volcanic eruption through the repository. Development of the model uses the eruptive processes conceptual model (SNL 2007 [DIRS 174260], Section 6) and is based on

comparison of the expected scenario characteristics with the physical processes modeled by Ashplume.

The Ashplume model implements the conceptual and mathematical model of Suzuki (1983 [DIRS 100489]) for estimation of the areal density of tephra deposits on the surface of the earth following a violent Strombolian-type volcanic eruption. The computer code, developed by Jarzemba et al. (1997 [DIRS 100987]) from the Suzuki mathematical model, includes estimation of the areal density on the Earth's surface of spent fuel particles incorporated into tephra particles due to an eruption that intersects the repository at Yucca Mountain. Areal densities can be converted to deposit thickness by dividing the areal density by the value of settled (deposit) density (typically 1.0 g/cm^3 (SNL 2007 [DIRS 174260], Table 7-1)).

ASHPLUME_DLL_LA V.2.1 [DIRS 178870] includes a dynamically linked library module for use as a component of the TSPA GoldSim model to assess dose to the RMEI from exposure to contaminated ash from possible volcanic activity at the Yucca Mountain site. The results of the Ashplume model calculations (tephra and waste areal densities) are used by the TSPA model in conjunction with the results of the tephra redistribution model, FAR, and BDCFs to calculate annual doses to a hypothetical individual, the RMEI. The annual doses to the RMEI, calculated in the TSPA model, are used to demonstrate that the postclosure performance objectives for the repository have been met. ASHPLUME V.2.1 [DIRS 178870] also includes an executable module for stand-alone use, which is applied to making calculations shown in Section 7 of this report. The stand-alone version calls the dynamically linked library module for making the calculations and serves only to format user input parameters for the dynamically linked library. Thus, the following discussions in this report apply equally to both stand-alone and dynamically linked library implementations of ASHPLUME V.2.1.

6.2 FEATURES, EVENTS, AND PROCESSES INCLUDED IN THE MODELS

As stipulated in *Technical Work Plan: Igneous Activity Assessment for Disruptive Events* (SNL 2007 [DIRS 182219], Section 1), this model report addresses the FEPs pertaining to igneous activity that are included (i.e., Included FEPs) for TSPA LA listed in Table 6-1. Table 6-1 provides a list of FEPs that are relevant to this model analysis in accordance with their assignment in the LA FEP list (DTN: MO0706SPAFEPLA.001 [DIRS 181613]). Specific reference to the various sections within this document where issues related to each FEP are addressed is provided in Table 6-1.

For the igneous eruptive scenario, the TSPA assumes that a hypothetical dike propagates upward and intersects the repository, providing a source for magma to enter the repository drifts. Magma with entrained waste moves to the Earth's surface through a conduit, is transported into the atmosphere as contaminated tephra, dispersed downwind, deposited on the ground, and redistributed by sedimentary processes. The FEPs listed in Table 6-1 (pertaining to the atmospheric transport and deposition of tephra) are part of the conceptual basis for such a scenario. However, this report does not provide a direct basis for the inclusion in TSPA of the FEPs listed in Table 6-1; rather, this report develops a basis for implementing the FEPs in TSPA by helping to constrain the potential consequences of the listed FEPs. As such, a partial treatment of the included FEPs is provided herein, and the results of this model report and listed FEPs are considered to be implicitly included in the TSPA.

Table 6-1.   Included FEPs for This Model Report

FEP Number	FEP Name	Relevant Sections
1.2.04.06.0A	Eruptive conduit to surface intersects repository	6.3, 6.5.2
1.2.04.07.0A	Ashfall	6.5, 7.3, 7.5, 7.6

Source: DTN: MO0706SPAFEPLA.001 [DIRS 181613].

6.3   BASIS OF ASHPLUME CONCEPTUAL MODEL

The basis for the conceptual model of a Strombolian eruption (including violent Strombolian) in the Yucca Mountain region is discussed in *Characterize Eruptive Processes at Yucca Mountain, Nevada* (SNL 2007 [DIRS 174260], Section 6, Table 7-1), including details of volcanic eruption characteristics and supporting parameters, values, and distributions. The following discussion develops the conceptual model using information from this source.

In the conceptual model for the atmospheric dispersal and deposition of contaminated tephra, the volcanic eruption is preceded by ascent of a basaltic dike through the Earth's crust, intersection of the proposed repository at Yucca Mountain, and subsequent propagation of the dike to the ground surface. An eruptive conduit, or conduits, can form when a portion of the erupting dike begins to widen and provides a preferential pathway to focus magma flow to the surface. Analyses of waste package and waste form in the intrusion scenario indicate that the integrity of the waste package would be compromised via corrosion, heating, and differential pressures associated with magmatic intrusion (SNL 2007 [DIRS 177430], Section 6.4.8.3). If the conduit intersects one or more repository drifts, the waste packages located partially or entirely within the conduit may be degraded and moved by fragmenting magma ascending toward the vent (SNL 2007 [DIRS 177430], Section 6.4.8.3.2). Physical damage to the waste package in this energetic conduit environment is assumed to provide a means for waste package failure and entrainment of fragmented waste within the rising magma (Section 5.1.2). This condition is inherent in the input parameter for the amount of waste erupted and is given a technical basis in *Number of Waste Packages Hit by Igneous Intrusion* (SNL 2007 [DIRS 177432]) for use in the TSPA.

The waste form has been degraded during reactor service and by exposure to the magmatic environment, and it consequently consists of particles in the size range of 1 μm to 2 mm (reduced by fracturing from the original 9×11 mm pellet size, Appendix F). Some portion of these waste particles is suspended and well-mixed with the magma, carried to the surface through the conduit, and erupted at the vent. The eruption typically involves several phases, including Strombolian and violent Strombolian activity (cone building and tephra sheet deposition) and effusion of lava flows. The Ashplume model abstraction assumes that the various eruption phases are condensed into a single violent Strombolian phase (Section 5.1.1), with concurrent effusion of lava, sustained eruption column, and construction of a scoria cone. The waste incorporated into the magma is therefore deposited in various eruptive products—scoria cone, lava flows, and tephra blanket—over the course of the eruption.

Existing data are limited regarding the expected state of the waste particles resulting from a basaltic eruptive event and associated thermal, chemical, and physical processes, but an expected grain size distribution has been developed using a combination of the results of diverse analyses

of degraded spent reactor fuel (Section 6.5.2.16 and Appendix F). The model assumes that fine-grained waste particles are mixed directly into the magma prior to magma fragmentation, and accounting is made for the proportion of waste-containing magma that is eventually deposited in geologically resistant eruptive products (scoria cone, lava flows) that do not contribute to dose (Section 6.5.2.22). The waste particles within the magma are treated as refractory particles (analogous to xenoliths) that form a component of tephra particles upon magma fragmentation (Section 5.1.3). For transport calculations, the combined ash/waste particles are modeled as density-corrected ash particles.

The Ashplume model begins with the thermal and mass characteristics of the erupted material entering the convective-thrust part of the eruption column. A violent Strombolian eruption is characterized by the eruption of a high-speed column of a gas-pyroclast-waste-particle mixture. The column consists of two regions. The lower region directly above the vent is called the gas-thrust region, and it behaves as a ballistic fountain of tephra moving under the influence of its eruption momentum. The upper region of the column is called the convective-thrust region, in which tephra rises by buoyant convective currents (Self and Walker 1994 [DIRS 162831]). Hence, a violent Strombolian eruption is one that is dominated by heating of entrained air, and the atmospheric transport of the fragmented magma and gas mixture approximates a thermally buoyant plume.

As the eruptive mixture rises in the plume of a violent Strombolian eruption, it entrains and heats air. This, in turn, reduces the bulk density of the mixture, and the plume becomes buoyant and continues to rise (SNL 2007 [DIRS 174260], Section 6.4), forming the initial conditions for the ASHPLUME code calculations. The plume rises to an altitude of neutral buoyancy compared to the surrounding atmosphere, at which point it then spreads laterally (x and y directions for the model) as an anvil-shaped cloud and is transported down wind (x direction). Tephra particles fall out (z direction) from the vertical eruption column and from the anvil cloud according to their settling velocities. Such eruptions produce a fallout sheet of varying thickness extending from the volcanic vent. The thickness of the deposit depends on factors such as particle density, eruptive parameters, wind speed and direction, and distance from the vent (Suzuki 1983 [DIRS 100489], p. 95).

The Ashplume mathematical model is based on a two-dimensional diffusion model in which only horizontal (x-y) turbulent diffusion is considered. The movement of air in the atmosphere is relatively random due to the many eddy currents that exist (Suzuki 1983 [DIRS 100489], p. 96). The movement of particles within the air mass is treated as random for the same reason. Particles diffuse in the atmosphere in both vertical (z) and horizontal directions (x-y), but because the scale of horizontal turbulence is much greater than the scale of the vertical turbulence (Suzuki 1983 [DIRS 100489], p. 98), horizontal diffusion is the dominant factor in determining the width of a plume as it moves downwind. Therefore, the Ashplume model is based on a two-dimensional diffusion equation in which only horizontal turbulent diffusivity is considered; given that the x-direction is aligned downwind, the main component of horizontal turbulent diffusivity is in the y-direction.

Ashplume is designed to model violent Strombolian eruption behavior as a thermally buoyant plume, calculating the atmospheric dispersal of tephra and its deposition on the ground. Furthermore, Ashplume quantifies the entrainment of waste in the erupted plume by an

"incorporation ratio," which provides a mathematical combination of ash and waste particle size distributions (Section 6.5.2.6). The scope of this conceptual model begins with the intersection of waste by the magma and ends with the ash-waste mixture settling to the ground surface. Outputs of the Ashplume model include estimates of ash-waste areal densities (g/cm^2) at prescribed points surrounding the volcanic vent.

6.4 CONSIDERATION OF ALTERNATIVE CONCEPTUAL MODELS FOR AIRBORNE TRANSPORT OF TEPHRA

Several alternative conceptual models were considered to evaluate the violent Strombolian eruption and transport of the tephra-waste mixture. The qualitative evaluations conducted are summarized in the following discussions.

6.4.1 Gaussian-Plume Model

Methods used previously to estimate radionuclide dispersal by volcanism (Wescott et al. 1995 [DIRS 100476]) theorize that the ash cloud travels as a Gaussian plume, released at a stack height one half the volcanic column height. Application of the Gaussian-plume model presumes that a plume of contaminants travels in the same direction as the prevailing wind (*x*-direction) but may be somewhat depressed toward the Earth's surface due to gravitational settling. Contaminant concentration in the plume follows a Gaussian distribution in the dimensions perpendicular to the direction of travel (*y*- and *z*-directions).

The Gaussian-plume model does not accurately account for the effects of gravitational settling of volcanic particles with large diameters (i.e., centimeters). This shortcoming could lead to estimates of a higher upper limit on the particle-size range for particles dispersed a significant distance downwind than would be the case in reality. The increased particle size would result in the distribution of a larger amount of waste farther downwind than would normally be expected after a basaltic eruption. Based on these factors, the Gaussian-plume alternative conceptual model is excluded from further evaluation because the model does not adequately portray a volcanic eruption column and is not conservative in the distribution of contaminated ash.

6.4.2 PUFF

PUFF (Searcy et al. 1998 [DIRS 101015]) was evaluated conceptually based on descriptions in the scientific literature. The PUFF model was developed primarily to predict airborne distribution of ash plumes to aid aircraft navigation near volcanic eruptions. The PUFF conceptual model does not include incorporation of contaminated particles with the ash plume or calculate ground-level concentrations of ash resulting from settling. The PUFF model was excluded from further evaluation because of these limitations.

6.4.3 Gas-Thrust Code

Another alternative conceptual model considered was the gas-thrust code that was proposed in the NRC "Igneous Activity Issue Resolution Status Report" (Reamer 1999 [DIRS 119693], Section 4.2.2.3). Use of the code would require either the development of an atmospheric transport and deposition model to couple to the gas-thrust code or a code would have to be developed to retrofit the gas-thrust code to an existing atmospheric transport model. The

ash-dispersion controlling constant (beta) within the ASHPLUME code has an analogous effect to the gas-thrust code. The parameter beta has the effect of generating a vertical distribution of particles above the volcano. The gas-thrust code is a variation on this concept and falls within the uncertainties associated with the input parameter values used in forming the beta distribution. The gas-thrust alternative conceptual model was excluded from further evaluation because the ASHPLUME code, without modification, uses input parameters that incorporate the vertical distribution of particles above a volcano.

6.4.4 Alternative Igneous Source Term Model

The Alternative Igneous Source Term model was developed by Codell (2003 [DIRS 165503]) as an extension of Ashplume to investigate the processes of waste fragmentation and incorporation into the tephra. Despite an in-depth review of thermal, chemical, and physical processes of waste degradation in the presence of magma, no reliable means have been identified to predict the grain size of incorporated waste, and Codell (2003 [DIRS 165503]) concludes that one should assume that all waste from damaged waste packages is incorporated homogeneously into the magma-pyroclast medium as a fine-grained material. Codell's (2003 [DIRS 165503]) main improvement over Ashplume is the addition of a more-detailed model for the mixing of ash and fuel particles. While Ashplume uses a fixed incorporation ratio to specify the mixing of fuel and ash by particle size, Codell's (2003 [DIRS 165503]) alternative model allows for a range of fuel concentrations on a given ash particle, following the rule that the fraction of mass of fuel incorporated into ash is proportional to the mass of the ash. To accomplish this, the alternative conceptual model bins the ash-particle-size distribution, develops symbolic "indicator particles" to represent the mass of ash in each bin, and then distributes the available mass of fuel to those indicator particles according to a probability function. Therefore, Codell's (2003 [DIRS 165503]) particles range much more widely in density than those used in the current Ashplume model, which produces the possible existence of dense particles that would fall out of the column sooner than is estimated by the current model. However, Codell (2003 [DIRS 165503]) found that the difference in results between Ashplume and the alternative conceptual model was, on average, within a factor of two for fuel concentration and that Ashplume typically estimates higher concentrations, and is, therefore, more conservative. Codell (2003 [DIRS 165503]) concludes that given other, larger, uncertainties in modeling volcanism, Ashplume is credible.

In summary, this alternative model explores aspects of waste incorporation into the magma and ash beyond the scope of previous work. However, despite the detailed analysis of concepts of waste-magma mixing and a complex approach to the mixing of waste and ash particles, the resulting estimates of waste concentration on the ground are not significantly different from the current model and may, therefore, be excluded from consideration.

6.4.5 ASHFALL

ASHFALL is based on a three-dimensional model of tephra dispersal by Armienti et al. (1988 [DIRS 179762]). Like ASHPLUME, ASHFALL is based on the method of Suzuki (1983 [DIRS 100489]), but ASHFALL extends the work of Armienti et al. (1988 [DIRS 179762]), using time- and altitude-dependent wind conditions while retaining the two-dimensional dispersion downwind (Hurst and Turner 1999 [DIRS 176897], p. 615). Another difference

between the two codes is the way that each defines the distribution of tephra particle sizes: ASHFALL uses a set of prescribed settling velocities for ash particles rather than the mean and standard deviation of particle size used in ASHPLUME. The transport methods differ in that ASHFALL incorporates variations in wind conditions in time and space, while ASHPLUME assumes a single, constant value for wind speed and direction based on conditions at the top of the plume. Both codes use the method of Suzuki (1983 [DIRS 100489]) to prescribe the initial conditions of tephra mass distribution with height in the eruption column.

The results of a code comparison between ASHPLUME and ASHFALL (Section 7.5, Appendix J) indicate that ASHPLUME can produce tephra thickness results (using reasonable input parameter values) that are within a factor of two of ASHFALL results, despite the use of complex wind fields (variable with altitude and in time) in the ASHFALL model. In addition, the ASHFALL code does not include the explicit transport of radionuclides in its formulation. Based on the lack of significant improvement in transport results and the lack of radionuclide incorporation in tephra particles, the ASHFALL model is excluded from consideration.

6.4.6 TEPHRA

The TEPHRA code (Bonadonna et al. 2005 [DIRS 179753]) is based on the models of Suzuki (1983 [DIRS 100489]) and Armienti et al. (1988 [DIRS 179762]), similar to ASHFALL, but includes the increased sophistications of grain-size-dependent diffusion and particle settling velocities that account for Reynolds number variations. Like the ASHPLUME and ASHFALL codes, the initial mass distribution in the column is defined in an extension of the concepts of Suzuki (1983 [DIRS 100489]), and transport and deposition downwind are accomplished by advection, turbulent eddy diffusion, and gravitational settling. The wind field is divided into layers, each with distinct conditions of speed and direction, and particle fall time is based on a combination of linear and power-law diffusion from the column.

The main improvements of the TEPHRA code over earlier atmospheric dispersal codes include increased sophistication in the calculation of particle settling and resulting deposition patterns, the capability to handle stochastic input parameter ranges, and parallelization of the code for rapid computing. Bonadonna et al. (1998 [DIRS 181521]) used some of these techniques to investigate the relationship of complex tephra thickness patterns to possible eruptive column dynamics. The rapid calculation times for large problems represents an excellent advancement for real-time volcanic hazards assessments at active volcanoes.

Although this code manifests several improvements in sophistication over the ASHPLUME code, it can be excluded from consideration for use in TSPA for several reasons. First, the current implementation of the TEPHRA code does not include consideration of the incorporation of radionuclides into volcanic tephra for transport. Second, the additional capacity for using complex wind conditions to transport tephra is immaterial for estimates of impacts of tephra deposition thousands of years in the future, when the uncertainties associated with wind conditions do not support the use of complex or time-variant wind fields during an eruption. Third, the increased sophistication of the physics controlling particle settling, which may produce more complex tephra deposits similar to the effects of unsteady column heights or variable wind fields, does not necessarily increase the accuracy of estimated tephra concentrations in sediment after redistribution, given the controlling influence of topography and

the larger uncertainties in model input parameters (as demonstrated in the coupled ASHPLUME-FAR study documented in Section 7.6).

6.4.7 Summary of Alternative Conceptual Models

Table 6-2 summarizes the alternative conceptual models considered for the volcanic direct release scenario. Based on the screening of the alternative conceptual models considered, the Ashplume model was determined to be the most appropriate model for use in TSPA calculations of atmospheric dispersal and deposition of tephra due to a volcanic eruption through the repository. The Ashplume model was specifically chosen because it incorporates both the ash dispersal and waste incorporation mechanisms required for the TSPA analysis of ash-waste deposition, redistribution, and dose to man. In addition, the mathematical model embodied in the ASHPLUME code has been confirmed as robust and valid in the light of continuing evolution of other codes (e.g., ASHFALL and TEPHRA). The alternative conceptual models considered in Table 6-2 do not provide the full functionality required for the TSPA analysis nor do they provide additional value in the context of the long time frame for the risk assessment.

There are two general categories of tephra dispersal models: 1) research models with a high degree of complexity in the physics meant mostly for a posteriori analysis of past eruptions for which there is abundant observational data (wind conditions, column height, ash deposition and grain size distribution); these models are computationally intensive and are most useful for understanding the dynamics of plume development and sedimentation of tephra. 2) Hazards assessment models capable of fast, first-order predictions of tephra deposition to be run in the case of real-time hazards predictions (i.e., tephra fall predictions during an eruption); these models typically have simplified physics and can be run on a small desktop computer. While models in the first category (e.g., TEPHRA) incorporate complex physics (e.g., variable Reynolds number sedimentation) and are often coupled with atmospheric models for time- and height-varying wind conditions, the degree of complexity required for input parameterization makes these models difficult to use for predictive hazards assessments. In particular, the required detail in the input wind conditions (time-varying wind speed and direction at multiple altitudes) is not realistic for use in the Yucca Mountain TSPA for events hundreds to thousands of years in the future, when the uncertainties in wind conditions at Yucca Mountain are large. The ASHPLUME model uses generalized statistics for wind conditions at a single altitude (top of eruption column) for each model realization, with the assumption that such generalized wind conditions will be valid for the performance assessment period. This degree of generalization of present wind conditions and assumption of validity for the performance period is reasonable; however, it is not reasonable to explicitly define complex, time-varying wind conditions for a tephra dispersal model realization that estimates tephra dispersal thousands of years in the future.

An analysis of the effects of unsteady eruption (i.e., variable eruption column height) and variable wind conditions during an eruption has been undertaken with the ASHPLUME code in order to assess the importance of the coupled tephra dispersal/deposition and redistribution models (Section 7.6). Composite tephra distributions resulting from varying column height or wind conditions ranged from diffuse (spreading) to bilobate (diverging) patterns, with up to 180 degrees of separation between lobes and considering plume orientations ranging over the entire Fortymile Wash watershed. The results of this analysis demonstrate that, for unsteady column heights or variable wind speed and direction during a single eruption event, the

maximum expected variation in tephra concentration in sediment at the outlet of Fortymile Wash after erosion, transport, and mixing of tephra is on the order of a factor of 3 or 4; this is small in comparison to the uncertainty of other ASHPLUME input parameters (eruption characteristics) which vary over 1 to 2 orders of magnitude. Therefore, the added sophistication of models such as ASHFALL or TEPHRA in the consideration of the physics of tephra transport and deposition is neglible when coupled to the landscape-scale redistribution model, FAR.

Table 6-2.   Alternative Conceptual Models Considered for Airborne Transport of Tephra

Alternative Conceptual Model	Key Assumptions	Screening Assessment and Basis
Gaussian Plume	Point source, Gaussian distribution of plume	Excluded—larger particles are not accurately accounted for in gravitational settling.
PUFF	Convection and dispersion of ash from a volcanic eruption	Excluded—model still in development, waste-fuel interaction not included, surface concentrations not available.
Gas-Thrust	Buoyancy of a vertical erupting column	Excluded—atmospheric transport not available, surface concentrations of waste and ash not available.
Alternative Igneous Source Term	Ashplume plus probability model for size of waste particles mixing with a given ash particle	Excluded—results of alternative conceptual model not significantly different from those of Ashplume.
ASHFALL	Ashplume plus time/space dependent wind field and explicit definition of range of particle settling velocities	Excluded—lack of transport of radionuclides; direct comparison with ASHPLUME indicates less than factor of two difference in model results.
Tephra	Ashplume plus time/space dependent wind field, complex particle diffusion and settling velocity formulation, parallelized code, stochastic input parameter	Excluded—lack of transport of radionuclides; lack of basis for realizing the benefits of complex tephra deposition patterns or variable wind conditions for future eruptions.

6.5   TEPHRA DISPERSAL CONCEPTUAL MODEL DESCRIPTION

The model of atmospheric dispersal and deposition of tephra used in the TSPA and implemented with the Ashplume mathematical model is based on a theoretical model for the dispersion of tephra developed by Suzuki (1983 [DIRS 100489]). Jarzemba et al. (1997 [DIRS 100987], pp. 2-5 to 2-7) extended the mathematical model to include the incorporation of waste-fuel particles with tephra particles. This section presents the mathematical formulation of the Suzuki/Jarzemba dispersion model and discusses model inputs developed for use in the TSPA.

6.5.1   Mathematical Description of the Base-Case Conceptual Model

The movement of air mass in the atmosphere is relatively random within the scale of eddy motions in wind currents (Suzuki 1983 [DIRS 100489], p. 96). Therefore, the dispersion of the ash-waste particles in the atmosphere is treated as random. Particles disperse in the atmosphere in both vertical and horizontal directions. However, the scale of horizontal turbulence is much greater than the scale of vertical turbulence (Suzuki 1983 [DIRS 100489], p. 98). Therefore, in Suzuki's (1983 [DIRS 100489]) development of the mathematical model, particle diffusion is considered to be two-dimensional in the horizontal x-y plane. Particle movement in the third (vertical) direction is accounted for by settling velocity in the Suzuki model.

The underlying two-dimensional partial differential equation relating the change in concentration, $\partial \xi$, at a point x-y (with x downwind) to wind velocity, u, and an eddy diffusivity constant, K, follows (Suzuki 1983 [DIRS 100489], Equation 1):

$$\frac{\partial \xi}{\partial t} = -u \frac{\partial \xi}{\partial x} + \frac{\partial}{\partial x}\left(K \frac{\partial \xi}{\partial x} \right) + \frac{\partial}{\partial y}\left(K \frac{\partial \xi}{\partial y} \right) \qquad \text{(Eq. 6-1)}$$

By selecting an appropriate value for the diffusivity constant, K, Equation 6-1 is appropriate for estimating the two-dimensional diffusion of particulate matter in the atmosphere downwind from a source of contamination. Because the x direction is assumed to be aligned with the wind, the y component of the convective term in Equation 6-1 is zero.

Suzuki (1983 [DIRS 100489]) developed the mathematical model shown in Equation 6-1 for application to atmospheric dispersal of tephra by applying source conditions and settling velocities suitable for explosive volcanic eruptions (violent Strombolian; Jarzemba 1997 [DIRS 100460], p. 133) that characterize basaltic volcanoes in the Yucca Mountain region (SNL 2007 [DIRS 174260], Section 6.4). Jarzemba et al. (1997 [DIRS 100987]) further developed the model to calculate the concentration of spent-fuel waste particles that become incorporated with ash particles in the case of a hypothetical volcanic eruption through the Yucca Mountain repository. A summary of the mathematical development by Suzuki (1983 [DIRS 100489]) and Jarzemba et al. (1997 [DIRS 100987]) of the ash-waste dispersal model follows.

To derive a solution to Equation 6-1 suitable for application to calculation of tephra dispersion in the atmosphere after a volcanic eruption, Suzuki (1983 [DIRS 100489], pp. 95-96) used the following boundary and initial conditions.

- Erupted material (the source boundary) consists of a finite mass of volcanic tephra particles

- The source of tephra particles is described by the distribution of the diameter of the released particles, and the distribution has a single mode

- Tephra particles have a probability to diffuse out of the eruption column during upward travel in the column as well as during transport of the plume downwind

- All particles fall at the terminal velocity and finally accumulate on the ground.

The solution to the mathematical model described in Equation 6-1 is provided by Suzuki (1983 [DIRS 100489], p. 104), modified by Jarzemba et al. (1997 [DIRS 100987], p. 2-2), and can be summarized by the following equation that describes the areal density of accumulated ash on the Earth's surface after an eruption:

$$X(x,y) = \int_{\rho=\rho_{min}}^{\rho_{max}} \int_{z=0}^{H} \frac{5Q p(z) f(\rho)}{8\pi C (t+t_s)^{5/2}} \exp\left[\frac{-5\left\{(x-ut)^2 + y^2\right\}}{8C(t+t_s)^{5/2}} \right] dz\, d\rho \qquad \text{(Eq. 6-2)}$$

where

$X(x, y)$ = mass of ash per unit area accumulated at location (x, y) in g/cm^2

ρ = common logarithm of particle diameter d, where d is in cm

ρ_{min} = minimum value of ρ

ρ_{max} = maximum value of ρ

z = vertical distance of particle from ground surface in km

H = height of eruption column above vent in km

x = x coordinate on the surface of the Earth oriented in the same direction as the prevailing wind in cm

y = y coordinate on the surface of the Earth, oriented perpendicular to the direction of the prevailing wind in cm

Q = total quantity of erupted material in g

$p(z)$ = distribution function for particle diffusion out of the column within $\pm dz$ of height z

$f(\rho)$ = distribution function for log-diameter of particles within $\pm d\rho$ of ρ normalized per unit mass

C = constant relating eddy diffusivity and particle fall time in cm^2/s$^{5/2}$

t = particle fall time in s

t_s = particle diffusion time in eruption column in s

u = wind speed in cm/s.

The probability density distribution function for particle diffusion out of the eruption column $p(z)$ is given by (Suzuki 1983 [DIRS 100489], Equation 7):

$$p(z) = \frac{\beta W_0 Y e^{-Y}}{V_0 H \left\{ 1 - (1 + Y_0) e^{-Y_0} \right\}}$$

(Eq. 6-3)

where

Y = $\dfrac{\beta W(z)}{V_0}$

Y_0 = $\dfrac{\beta W_0}{V_0}$

β = a constant controlling diffusion of particles in the eruption column (dimensionless)

W_0 = initial particle rise velocity in cm/s, that represents initial rise velocity of the convective part of the plume.

V_0 = particle terminal velocity at mean sea level in cm/s

$W(z)$ = particle velocity as a function of height = $W_0\left(1 - \dfrac{z}{H}\right)$ in cm/s.

According to Jarzemba et al. (1997 [DIRS 100987], p. 2-4), the definitions of Y and Y_0 differ from those found by Suzuki (1983 [DIRS 100489], p. 103), that is, $Y = \dfrac{\beta(W(z) - V_0)}{V_0}$ and $Y_0 = \dfrac{\beta(W_0 - V_0)}{V_0}$, for two reasons:

- The definitions by Suzuki (1983 [DIRS 100489], p. 103) lead to negative values of $p(z)$ at heights approaching the top of the column

- $p(z)$ (Equation 6-3) integrated over all column heights does not equal one using the definitions of Y and Y_0 found in Suzuki (1983 [DIRS 100489], p. 103).

The particle terminal velocity at mean sea level is given by (Suzuki 1983 [DIRS 100489], Equation 4'; modified by Jarzemba et al. 1997 [DIRS 100987], Equation 2-3):

$$V_0 = \frac{\psi_p g_c d^2}{9\eta_a F^{-0.32} + \sqrt{81\eta_a^2 F^{-0.64} + \dfrac{3}{2}\psi_p \psi_a g_c d^3 \sqrt{1.07 - F}}} \qquad \text{(Eq. 6-4)}$$

where

Ψ_a, Ψ_p = density of air and of particles, respectively in g/cm^3

g_c = gravitational acceleration constant = 980 cm/s^2

η_a = dynamic viscosity of air in g/(cm·s)

F = shape factor for particles—for an elliptically shaped particle with principal axes a, b, and c, $F = (b+c)/2a$, where a is the longest axis

d = mean particle diameter in cm.

The value for the gravitational acceleration constant, 980 cm/s^2, was programmed into the ASHPLUME code (CRWMS M&O 2001 [DIRS 174768], p. 38). Jarzemba et al. (1997 [DIRS 100987], p. 2-4) define particle density, Ψ_p in g/cm^3, to be a function of the particle log-diameter, ρ_a in cm, as follows:

$$\Psi_p = \Psi_p^{\,high} \qquad \text{for } \rho_a < \rho_a^{\,low}$$

$$\Psi_p = \Psi_p^{\,low} + (\Psi_p^{\,high} - \Psi_p^{\,low})(\rho_a^{\,high} - \rho_a)/(\rho_a^{\,high} - \rho_a^{\,low}) \quad \text{for } \rho_a^{\,low} < \rho_a < \rho_a^{\,high} \qquad \text{(Eq. 6-5)}$$

$$\Psi_p = \Psi_p^{\,low} \qquad \text{for } \rho_a > \rho_a^{\,high}$$

where $\Psi_p^{\,high}$, $\Psi_p^{\,low}$, $\rho_a^{\,high}$, and $\rho_a^{\,low}$ are defined by user inputs.

The particle fall time (in s) is given by (Suzuki 1983 [DIRS 100489], p. 102):

$$t = 0.752 \times 10^6 \left[\frac{1 - e^{-0.0625z}}{V_0} \right]^{0.926}$$

(Eq. 6-6)

Suzuki (1983 [DIRS 100489], p. 103) assumed that the eruption column radius is equal to 0.5z (z is height in km) and is equal to 3σ_r, where σ_r is the standard deviation of the column radius. The particle diffusion time in the eruption column, t_s, is given by (Suzuki (1983 [DIRS 100489], p. 103):

$$t_s = \left(\frac{5z^2}{288C} \right)^{2/5}$$

(Eq. 6-6a)

where C is the constant relating eddy diffusivity and particle fall time.

Suzuki (1983 [DIRS 100489], pp. 98 to 104) and Jarzemba et al. (1997 [DIRS 100987], Section 2.2) provide a detailed derivation of Equations 6-2 through 6-6.

The height of the eruption column or plume, H, used in Equation 6-2, follows buoyant plume theory applied to volcanic eruptions by Wilson et al. (1978 [DIRS 162859]) and discussed by Jarzemba et al. (1997 [DIRS 100987], p. 4-4). In ASHPLUME, height in km is given as:

$$H = 0.0082 P^{0.25}$$

(Eq. 6-7a)

where the eruption column power, P, in watts, is determined by the eruption mass flux and heat content:

$$P = \dot{Q} \left(C_p \Delta TE \right)$$

(Eq. 6-7b)

The parameters in parentheses in Equation 6-7b represent the heat content and its efficiency in adding buoyancy; they are fixed by magma and tephra characteristics. The mass flux, $\dot{Q}$, can be evaluated by assuming a constant eruptive mass flux over the duration of the eruption, which is related to the erupted-ash settled volume by Equation 6-7c. In that equation, the transformation, for purposes of power calculation, neglects the smaller mass and heat contribution from gas.

$$\dot{Q} = \frac{Q}{T_d} = \frac{V \psi_s}{T_d} = \psi_m W_0 \pi \left(\frac{d_c}{2} \right)^2$$

(Eq. 6-7c)

where

C_p = heat capacity of magma (J/kgK)

ΔT = temperature difference between magma and ambient (°C)

E = efficiency factor of heat usage (1.0 for Equation 6-7b)

Q = total mass of erupted material (kg)

V = ash erupted volume (m³)

T_d = eruption duration (s)

ψ_s = ash settled density (kg/m³)

ψ_m = bulk density of erupting magma and gas mixture (kg/m³)

W_0 = initial particle rise velocity (m/s)

d_c = effective conduit (vent) diameter (m).

The units listed above are for Equations 6-7a through Equation 6-7c only. The ASHPLUME input parameters of initial rise velocity, power, and duration are linked in Equations 6-7b and 6-7c and determine the plume height in Equation 6-7a; velocity also contributes to the probability density distribution function (Equation 6-3). Accordingly, the basis for selecting these parameters is further discussed in Section 6.2.3. The value for the efficiency factor (E) is assumed to be equal to 1 (one significant digit) in this analysis, given the uncertainties in values for C_p and ΔT. As already noted, the calculation neglects the mass and thermal content of gas in the plume. In the ASHPLUME code, the total mass of erupted material, Q, is calculated from input values for power, P, and eruption duration, T_d.

In the Suzuki mathematical model (Suzuki 1983 [DIRS 100489], p. 102), the volcanic ash size is distributed log-normally:

$$f(\rho^a) = \frac{1}{\sqrt{2\pi}\sigma_d} \exp\left[-\frac{(\rho^a - \rho_{mean}^a)^2}{2\sigma_d^2}\right] \qquad \text{(Eq. 6-8)}$$

where

$f(\rho^a)$ = probability distribution for log diameter of ash

ρ^a = log-diameter of ash particle size, with particle size in cm

ρ_{mean}^a = mean of log-diameter of ash particle size, with particle size in cm

σ_d = standard deviation of log particle size.

The TSPA analyses for Yucca Mountain require an estimate of spent fuel per unit area on the ground surface as a function of location relative to the volcanic vent (i.e., relative to the repository) after a hypothetical eruption through the repository. It is assumed that the transport mechanism for waste fuel particles is by combination with tephra particles by relative size according to an incorporation ratio (Section 5.1.4).

The rationale for limiting the amount of fuel mass available for incorporation into a volcanic-ash particle of a given size is that for smaller volcanic-ash particles, an amount of fuel mass will be

too large to be incorporated into these small particles. For example, it is unlikely that a 1-cm-diameter fuel particle could be incorporated into a 0.5-cm-diameter volcanic ash particle. Assuming a cutoff on the ratio of incorporable fuel diameter to volcanic ash diameter of 1:10 is equivalent to assuming an incorporation ratio (ρ_c) of 1. Mathematically, the incorporation ratio is defined as (Jarzemba et al. 1997 [DIRS 100987], Equation 2-7):

$$\rho_c = \log_{10}\left[\frac{d_{min}^a}{d^f}\right] \tag{Eq. 6-9}$$

where

d_{min}^a = minimum ash particle size needed for incorporation, in cm

d^f = fuel particle size in cm.

Setting the incorporation ratio ρ_c equal to 0.3 is roughly equivalent to allowing all fuel mass of size less than or equal to one-half of the volcanic-ash particle size to be available for incorporation. See Section 6.5.2.6 for more discussion of the appropriate value for the waste incorporation ratio.

Fuel mass is defined by Jarzemba et al. (1997 [DIRS 100987], pp. 2-5 to 2-6) as following a log-triangular distribution function of the log-diameter of fuel particles (specifically, a log-triangular distribution for fuel mass within $\pm d\rho^f$ of ρ^f normalized per unit mass). The log-triangular distribution is defined in Equation 6-10.

$$
\begin{aligned}
m(\rho^f) \quad &= k_1(\rho^f - \rho_{min}^f) && \text{for } \rho_{min}^f < \rho^f \le \rho_{mode}^f \\
&= k_1(\rho_{mode}^f - \rho_{min}^f) - k_2(\rho^f - \rho_{mode}^f) && \text{for } \rho_{mode}^f < \rho^f \le \rho_{max}^f \\
&= 0 && \text{otherwise}
\end{aligned}
\tag{Eq. 6-10}
$$

where

$m(\rho^f)$ = log-triangular distribution of fuel particle size

ρ^f = log-diameter of fuel particle size, with particle size in cm

$k_1 = \dfrac{2}{(\rho_{max}^f - \rho_{min}^f)(\rho_{mode}^f - \rho_{min}^f)}$

$k_2 = \dfrac{2}{(\rho_{max}^f - \rho_{min}^f)(\rho_{max}^f - \rho_{mode}^f)}$

ρ_{min}^f = minimum log-diameter of fuel particle size, with particle size in cm

ρ_{max}^f = maximum log-diameter of fuel particle size, with particle size in cm

ρ_{mode}^f = mode log-diameter of fuel particle size, with particle size in cm.

Jarzemba et al. (1997 [DIRS 100987], pp. 2-6 to 2-7) determined the fuel fraction (ratio of fuel mass to ash mass) as a function of ρ^a by considering that all fuel particles of size smaller than $(\rho^a - \rho_c)$ have the ability to be incorporated simultaneously into volcanic-ash particles of size ρ^a or larger. The fuel fraction as a function of ρ^a is determined by summing all the incremental contributions of fuel mass to the volcanic ash mass from fuel sizes smaller than $(\rho^a - \rho_c)$. An expression for the fuel fraction is given as:

$$FF\left(\rho^a\right) = \frac{U}{Q} \cdot \int_{\rho=-\infty}^{\rho=\rho^a} \frac{m\left(\rho - \rho_c\right)}{1 - F\left(\rho\right)} d\rho \qquad \text{(Eq. 6-11)}$$

where

Q =   the total mass of ash ejected in the event in g
U =   total mass of fuel ejected in the event in g
m =   probability density function of fuel particle size
$F(\rho^a)$ =   cumulative distribution of $f(\rho^a)$.

Equation 6-11 assumes the resulting contaminated particles have the same size distribution as the original volcanic ash particles. This assumption seems reasonable because the total mass of volcanic ash erupted will be much greater than the total mass of fuel available for incorporation. Introduction of a relatively small amount of fuel mass into the ash mass is unlikely to alter the size distribution of the ash. The mathematical and computational models do, however, adjust the density of ash particles to account for the incorporation of fuel. The particle density used in the calculation of the terminal velocity of a particle is adjusted as a combined particle in the dispersion calculation. The combined-particle density is adjusted by a statement in the ASHPLUME code: ashden = ashden × [1 + fuel fraction]. In this statement, "ashden" represents the ash particle density and "fuel fraction" represents the mass fraction of fuel in the combined particle. The integrand of Equation 6-2 is multiplied by $FF(\rho^a)$ and then recalculated to find the spent fuel density at the (x, y) location.

6.5.2 Ashplume Model Inputs

The values for input parameters to Ashplume are developed from observed, or primary, data from analogue volcanoes. This development is based on the approach outlined in *Characterize Eruptive Processes at Yucca Mountain, Nevada* (SNL 2007 [DIRS 174260], Section 6.3.4), but it has been altered to meet the needs of this model. While field measurements provide ranges for the values of individual eruption parameters, field measurements do not provide integrated or mathematically self-consistent sets of eruption parameters such as those that are required as input for Ashplume. Therefore, the input parameters required in the model abstraction are developed from observed (field) measurements by applying mathematical relationships (Section 6.5.1). The resulting set of self-consistent eruption input parameters may differ slightly from the field measurements but honors the ranges of important parameters (e.g., erupted volume) observed at analogue volcanoes.

Self-consistent relationships among eruptive duration, eruptive volume, and vent radius are used in Equations 6-7b and 6-7c to derive values for eruptive duration and mass flux. Eruptive height, calculated from power using Equation 6-7a, is used to define the atmospheric height bin from which wind speed and direction are sampled. The model is kept self-consistent by the use of appropriate ranges, developed from data for the Yucca Mountain region (e.g., eruptive volume, eruptive duration, and vent radius) developed in *Characterize Eruptive Processes at Yucca Mountain, Nevada* (SNL 2007 [DIRS 174260], Section 6.3.4). These values, combined with reasonable material properties data (ash settled density, magma density, magma specific heat, and temperature difference), provide a firm link between the model performance and primary data. The ash settled density, which is the bulk density of the ash that settles on the ground after an eruption, is provided in DTN: LA0612DK831811.001 [DIRS 179987] as a range from 300 to 1,500 kg/m^3 with a mean of 1,000 kg/m^3; a standard deviation of 100 kg/m^3 is chosen based on expectations that the value will be near 1,000 kg/m^3 (SNL 2007 [DIRS 174260], Section 6.3.5.3). A value of 2,600 kg/m^3 (two significant figures) is used for magma density to represent the likely magmatic water contents (DTN: LA0612DK831811.001 [DIRS 179987], Table 6-5). Note that while eruptive volume is not a direct input parameter for ASHPLUME_DLL_LA V.2.1 [DIRS 178870], it is used in the modeling process as one of the primary means to constrain the realism of the combinations of input parameters that define each modeled eruption (Sections 6.5.2.2 and 8.2). Once the primary input parameter values have been developed (e.g., eruptive power and duration), they are used within the ASHPLUME code at run time to calculate values for column height (from power) and total mass of ash (from power and duration), among others, for use in transport calculations. Because these values are calculated using equivalent mathematical relationships, the results of the model are consistent with the primary data used to develop the input parameter values.

Because of the model simplification in which the observed data (e.g., eruptive volume and power) are treated as independent variables, the result is a broader range in derived parameters (e.g., eruptive duration) than would be seen in natural analogues. For example, eruption volume and power have some general correlation in the natural world, and the range in possible eruptive duration is therefore more restricted than is calculated by assuming the two variables are independent. The conservatism introduced by this simplification is mitigated by restricting the set of input parameters for each model realization such that the overall erupted volume is realistic (Section 8.2). The end result is that each model realization is reasonable and the simplification does not adversely affect the model results.

For the ASHPLUME_DLL_LA V.2.1 computer code [DIRS 178870] to calculate the concentration of tephra and waste fuel on the ground surface according to Equation 6-2, parameter values must be provided for all of the unknown coefficients in the governing Equations 6-2 to 6-11 (Section 6.5.1). ASHPLUME_DLL_LA V.2.1 [DIRS 178870] allows parameters that are distributions to be sampled outside of the ASHPLUME code (within the TSPA GoldSim model). GoldSim then passes the sampled point values for each parameter into the ASHPLUME_DLL_LA V.2.1 code. Each realization simulates only one volcanic event at a time, and the single volcanic event in each realization represents the entire output of the volcano as one violent Strombolian eruption. All input parameters used in the ASHPLUME code are listed in Table 6-3. The following sections discuss each of these parameters in more detail and provide the technical basis for the parameter values and distributions.

Table 6-3. Inputs for the Ashplume Model

Coefficient [ASHPLUME Parameter] (Equation Number)	Parameter Description	Type of Parameter	Data Source	Location of Discussion in Text
x and y [xmin, xmax, ymin, ymax,nx and ny] (Equation 6-2)	Grid coordinates, corresponding to RMEI location and Fortymile Wash watershed	Constant	See text	Section 6.5.2.17
Ψ_p^{high} [ashdenmax] (Equation 6-5)	Ash particle density at minimum particle size	Constant	DTN: LA0612DK831811.001 [DIRS 179987]	Section 6.5.2.11
Ψ_p^{low} [ashdenmin] (Equation 6-5)	Ash particle density at maximum particle size	Constant	DTN: LA0612DK831811.001 [DIRS 179987]	Section 6.5.2.11
ρ_a^{high} [ashrhohi] (Equation 6- 5)	Log ash particle size at minimum ash density	Constant	DTN: LA0612DK831811.001 [DIRS 179987]	Section 6.5.2.11
ρ_a^{low} [ashrholow] (Equation 6-5)	Log ash particle size at maximum ash density	Constant	DTN: LA0612DK831811.001 [DIRS 179987]	Section 6.5.2.11
F [fshape] (Equation 6-4)	Ash particle shape factor	Constant	DTN: LA0612DK831811.001 [DIRS 179987]	Section 6.5.2.12
Ψ_a [airden](Equation 6- 4)	Air density	Constant	Lide 1994 [DIRS 147834]	Section 6.5.2.13
η_a [airvis] (Equation 6-4)	Air viscosity	Constant	Lide 1994 [DIRS 147834]	Section 6.5.2.14
C [C] (Equation 6-2)	Eddy diffusivity constant	Constant	Suzuki 1983 [DIRS 100489]	Section 6.5.2.15
d_{max} [dmax]	Maximum particle diameter for transport	Constant	SNL 2007 [DIRS 174260]	Section 6.5.2.18
ρ_{min}^f, ρ_{mode}^f, ρ_{max}^f [fdmin, fdmean, fdmax] (Equation 6-10)	Minimum, mode, maximum waste particle size	Constant	Appendix F	Section 6.5.2.16
H_{min} [hmin]	Minimum height of eruption column	Constant	Minimum practical value	Section 6.5.2.19
$Ash\ Cutoff$ [acutoff]	Threshold limit on ash accumulation	Constant	Minimum practical value	Section 6.5.2.20
β [beta] (Equation 6-3)	Column diffusion constant	Stochastic	Jarzemba et al. 1997 [DIRS 100987], Suzuki 1983 [DIRS 100489]	Section 6.5.2.3
d [dmean] (Equation 6-4)	Mean ash particle diameter	Stochastic	DTN: LA0612DK831811.001 [DIRS 179987]	Section 6.5.2.4
σ_d [dsigma] (Equation 6-8)	Ash particle diameter standard deviation	Stochastic	DTN: LA0612DK831811.001 [DIRS 179987]	Section 6.5.2.5

Table 6-3.   Inputs for the Ashplume Model (Continued)

Coefficient [ASHPLUME Parameter] (Equation Number)	Parameter Description	Type of Parameter	Data Source	Location of Discussion in Text
ρ_c [rhocut] (Equation 6-9)	Waste incorporation ratio	Constant	See Section 6.5.2.6	Section 6.5.2.6
U [uran] (Equation 6-11)	Mass of waste to incorporate	Stochastic	N/A	Section 6.5.2.9
Wind Direction [udir]	Wind direction	Stochastic	NOAA 2004 [DIRS 171035]	Section 6.5.2.8
u [u] (Equation 6-2)	Wind speed	Stochastic	NOAA 2004 [DIRS 171035]	Section 6.5.2.7
W_o [werupt0] (Equation 6-3)	Initial rise velocity	Stochastic	Wilson and Head 1981 [DIRS 101034], Woods 1988 [DIRS 172081]	Section 6.5.2.10
P [power] (Equations 7a and 6-7b)	Eruptive power	Stochastic	Jarzemba 1997 [DIRS 100460]	Section 6.5.2.1
T_d [tdur]	Eruption duration	Stochastic	DTN: LA0612DK831811.001 [DIRS 179987]	Section 6.5.2.2
rmin [rmin]	Minimum radius (polar grid)	Constant	Appendix I	Section 6.5.2.17
rfactor [rfactor]	Radial increment factor	Constant	Appendix I	Section 6.5.2.17
nr [nr]	Number of radial divisions	Constant	Appendix I	Section 6.5.2.17
nthet [nthet]	Number of angular increments	Constant	Appendix I	Section 6.5.2.17
Numapts [numapts]	Number of points in tephra/waste histogram output	Constant	See text	Section 6.5.2.21
—	Magma partioning factor	Stochastic	See text	Section 6.5.2.22

6.5.2.1 Eruptive Power, P

Type: log-uniform distribution
Value: 1×10^9 to 1×10^{12}
Units: watts.

The range of eruptive power is derived from observations at analogue volcanoes summarized in Table 6-4 (and also summarized in SNL 2007 [DIRS 174260], Table 6-9). The values for six historic eruptions at four small-volume basalt volcanoes are distributed across four orders of magnitude and provide a minimum basis to expect that the power for an eruption defined by this distribution may take any value in the range; therefore a log-uniform distribution type is specified.

Table 6-4.   Explosive Eruptive Events and Power at Analogue Volcanoes

Event	Log (P) P in W
Cerro Negro, 1992	12.0
Tolbachik, 1975	11.7
Parícutin, 1944 I	11.1
Parícutin, 1944 II	11.5
Parícutin, 1946	9.0
Heimaey, 1973	9.9

Source: Jarzemba 1997 [DIRS 100460], p. 136.

NOTE: Values for eruptions at Hekla reported by Jarzemba 1997 [DIRS 100460], p. 136, are
not included because they represent magma flux and eruptive style characteristic of
ocean island (spreading center) tectonic settings and are not representative of potential
eruptions in the Yucca Mountain Region as characterized in SNL 2007 [DIRS 174260],
Section 6.3.

6.5.2.2   Eruption Duration, Td

Type: log-uniform distribution
Value: calculated in TSPA (see Section 8.2)
Units: seconds.

The range of eruption duration and the rationale for using this range of values are discussed in *Characterize Eruptive Processes at Yucca Mountain, Nevada* (SNL 2007 [DIRS 174260], Section 6.3.4.4). The range of values provided in that document spans 18 hours to 75 days $(6.48 \times 10^4$ to 6.48×10^6 seconds) for the duration of a single explosive phase constituting a violent Strombolian eruption (DTN: LA0612DK831811.001 [DIRS 179987]), as observed at analogue volcanoes; this range is specified as a log-uniform distribution.

The actual limits on the range of eruption duration used in each TSPA model realization are established at run-time, as determined by Equations 8-1a and 8-1b (Section 8.2) such that the total volume of the eruption remains within the bounds provided in DTN: LA0612DK831811.001 [DIRS 179987]. The primary considerations used to verify the realism of each TSPA model realization (Section 8.2) are eruptive power and eruptive volume, two parameters that well characterize the magnitude of violent Strombolian eruptions (SNL 2007 [DIRS 174260], Section 6.3.4.4). While the range of duration developed in a TSPA model realization for a given sampled value of power (Equations 2-1a and 2-1b) may range from about 1 hour to 4.4 years, the limits of total eruptive volume $(0.004 \text{ km}^3$ to 0.14 km^3; DTN: LA0612DK831811.001 [DIRS 179987]) are honored. The upper end of the possible range of eruptive duration remains within the range of the duration for the formation of an entire volcano (4.4 years versus 90th percentile duration 3 years), while the lower end is less than the minimum duration for a single violent Strombolian eruptive phase (1 hour versus 18 hours) (DTN: LA0612DK831811.001 [DIRS 179987]). The uncertainty of the range in values calculated for each TSPA realization reflects uncertainties in the ranges for power and eruptive volume, which are derived from limited observational data. The distribution in eruptive duration is specified as log-uniform, given that all values within the range have an equal probability.

6.5.2.3 Column Diffusion Constant, β

Type: uniform distribution
Value: 0.01 to 0.5
Units: N/A.

The column diffusion constant (β) is set at a uniform distribution with a minimum value of 0.01 and a maximum value of 0.5.

The column diffusion constant was discussed by Suzuki (1983 [DIRS 100489], pp. 104 to 107). This parameter affects the distribution of particles vertically in the ash column and helps determine where particles exit the column. The erupted ash cloud is assumed (by Suzuki) to spread axially a distance of half the height. Ashplume takes a beta value and determines the vertical profile of particle sizes in the erupted column that will then be transported down wind. Suzuki discussed beta values of 0.01, 0.1, and 0.5. The larger beta becomes, the more the particle distribution becomes skewed towards the top of the column. A value of 0.5 generates a column particle distribution that contains very few particles in the lower 70% of the column, whereas a beta value of 0.01 gives an upwardly decreasing distribution that contains the most particles lower in the column. The beta parameter, in effect, is related to the buoyancy of particles in the eruptive column and determines how high most particles will travel before exiting the column. Based on comparisons of modeled and observed tephra distributions, Suzuki (1983 [DIRS 100489], p. 104) suggests that beta values of 0.5 or greater are not representative of typical eruptions. Jarzemba et al. (1997 [DIRS 100987], pp. 4-1 and 4-6) uses a log-uniform distribution for beta that has a minimum value of 0.01 and a maximum value of 0.5. This range of values spans more than an order of magnitude and encompasses the range that is valid for the Ashplume model. However, in order to simulate the anvil cloud associated with a violent Strombolian eruption properly, samples from the range in beta should be focused toward the upper end of the range; therefore, a uniform (rather than log-uniform) distribution is recommended. Uncertainty in this value originates from the relationship between the mathematical coefficient and physical processes; the limits of the range have been established by theory and judgment of the developer (Suzuki 1983 [DIRS 100489]), and the type of distribution that emphasizes the upper end of the range also reflects scientific judgment.

6.5.2.4 Mean Ash Particle Diameter, d

Type: log-triangular distribution
Value: 0.001-0.01-0.1
Units: cm.

The ash particle diameter is defined within the Ashplume model by two parameters: the mean ash particle diameter and the ash particle diameter standard deviation. The mean ash particle diameter for the volcanic eruption is defined in DTN: LA0612DK831811.001 [DIRS 179987], as a log-triangular distribution with a minimum value of 0.001 cm, a mode value of 0.01 cm, and a maximum value 0.1 cm. The rationale for using this range of mean ash particle diameter is discussed in *Characterize Eruptive Processes at Yucca Mountain, Nevada* (SNL 2007 [DIRS 174260] Sections 6.3.5.1 and Table 7-1). The mode (0.01 cm) honors the frequency of values near this value in samples from Lathrop Wells volcano, while the tails honor the

variability in mean grain size observed at historical violent Strombolian eruptions (SNL 2007, [DIRS 174260], Tables 6-10 and 6-11). For comparison, Jarzemba (1997 [DIRS 100460], p. 137) gives a log-triangular distribution with a minimum of 0.01 cm, a median of 0.1 cm, and a maximum of 10 cm. Although this upper range would account for the larger lapilli sizes and smaller blocks and bombs, these particles would fall on or near the cone and would not contribute much or any mass to the downwind tephra deposit, as is demonstrated by measurements of historic violent Strombolian eruptions (SNL 2007 [DIRS 174260], Table 6-11).

6.5.2.5 Ash Particle Diameter Standard Deviation, σ_d

Type: uniform distribution
Value: 0.301 to 0.903
Units: log (cm).

The ash particle diameter standard deviation is discussed in *Characterize Eruptive Processes at Yucca Mountain, Nevada* (SNL 2007 [DIRS 174260], Section 6.3.5.1) and is derived from analogue data. A uniform distribution from 1 phi to 3 phi units is recommended based on the range of observed tephra deposits from violent Strombolian eruptions at analogue volcanoes (DTN: LA0612DK831811.001 [DIRS 179987]). The upper and lower bounds of the range were chosen based on scientific judgment to bracket the sparse observations, and the uniform distribution reflects sparseness of the data and the equal likelihood of any value within the range.

Phi units are defined (Fisher and Schmincke 1984 [DIRS 162806], p.118) as

$$\phi = -\log_2(d \times 10) \qquad \text{(Eq. 6-12)}$$

where

ϕ = particle diameter in phi units, and

d = particle diameter in cm.

The ASHPLUME code needs to have the particle size standard deviation (σ_ϕ) specified in Log base 10 space. To do this, σ_ϕ in Log base 2 space must be converted to σ_d in Log base 10 space.

Tephra particle populations resulting from sediment transport often reflect a normal size distribution due to sorting (Fisher and Schmincke 1984 [DIRS 162806], p. 118). For a normal distribution, 68.26% of the frequency lies within one standard deviation of the mean (Davis 1986 [DIRS 123714], p. 66). Therefore, σ_ϕ and σ_d can be approximated by

$$\sigma_\phi = \frac{\phi_{16} - \phi_{84}}{2} \qquad \text{(Eq. 6-13)}$$

where

ϕ_{84} = the 84th percentile grain size in phi units, and

ϕ_{16} = the 16th percentile grain size in phi units.

and

$$\sigma_d = \frac{\rho_{84} - \rho_{16}}{2} \qquad \text{(Eq. 6-14)}$$

where

ρ_{84} = log base 10 of the 84th percentile grain size in cm, and

ρ_{16} = log base 10 of the 16th percentile grain size in cm.

The sign reversal between Equations 6-13 and 6-14 is due to the fact that ϕ increases with decreasing particle size and ρ decreases with decreasing particle size.

Combining Equations 6-12 and 6-13 gives:

$$2\sigma_\phi = \log_2(d_{84} \times 10) - \log_2(d_{16} \times 10) \qquad \text{(Eq. 6-15)}$$

Utilizing the identities $log_a xy = log_a x + log_a y$ and $log_a x = log_b x \, / \, log_b a$ (Selby 1975 [DIRS 106143], p. 181), Equation 6-15 can be written as

$$2\sigma_\phi = \log_2 d_{84} + \log_2 10 - \log_2 d_{16} - \log_2 10$$
$$2\sigma_\phi = \frac{\log_{10} d_{84} - \log_{10} d_{16}}{\log_{10} 2} \qquad \text{(Eq. 6-16)}$$

or

$$\sigma_\phi \log_{10} 2 = \frac{\log_{10} d_{84} - \log_{10} d_{16}}{2} \qquad \text{(Eq. 6-17)}$$

Because the right side of Equation 6-17 is equivalent to σ_d in Equation 6-14, the relationship between σ_d and σ_ϕ is

$$\sigma_d = \sigma_\phi \log_{10} 2$$
$$or \qquad \text{(Eq. 6-18)}$$
$$\sigma_d = 0.301\sigma_\phi$$

Therefore, for use by ASHPLUME in the TSPA model, σ_d should be sampled from a uniform distribution between $\sigma_d = 0.301$ and $\sigma_d = 0.903$ log(cm). The uniform distribution of the values

for standard deviation is unrelated to the presumed normal distribution of the underlying particle size distribution.

6.5.2.6 Waste Incorporation Ratio, ρ_c

Type: point value
Value: 0.0
Units: N/A.

The incorporation ratio describes the ratio of ash/waste particle sizes that can be combined for transport. In the original formulation, Jarzemba (1997 [DIRS 100460], pp. 134 to 135) conceived of magma-waste mixing by the model:

$$R(x, y) = X(x, y) \frac{A}{Q},$$ (Eq. 6-19)

where

$R(x,y)$ = quantity of radioactivity per unit area accumulated at location (x,y) (Ci/cm^2)
$X(x,y)$ = mass of ash per unit area accumulated at location (x,y) (g/cm^2)
A = total amount of radioactivity released (Ci)
Q = total mass of ash erupted (g).

This relationship simply multiplies the mass of ash deposited in a particular location by the ratio of total masses of waste and ash erupted. While this model does not account for the gravitational influence of the waste's relatively higher density on the transported particles, it is suitable for a homogeneous mix of waste in magma prior to fragmentation and eruption.

The waste incorporation model included in the ASHPLUME V1.4, V2.0, and V2.1 codes is more sophisticated, involving a conceptual model of the combination of two particle streams. The particles of waste are "instantaneously" homogenized in ash particles, and the controlling parameter is related to the relative sizes of the waste and ash particle populations:

$$\rho_c = \log_{10}\left[\frac{d_{min}^a}{d^f}\right]$$ (Eq. 6-20)

where

ρ_c = waste incorporation ratio
d_{min}^a = minimum ash particle size needed for incorporation in cm
d^f = fuel particle size in cm.

For a value of $\rho_c = 0.3$ (Jarzemba et al. 1997 [DIRS 100987], p. 2-6), waste particles can only be incorporated into ash particles twice their size.

The mass of waste deposited on the ground at a particular location is calculated in this model by the use of a fuel fraction term ($FF(\rho^a)$) (Jarzemba et al. 1997 [DIRS 100987], pp. 2-6 to 2-7):

$$FF\left(\rho^a\right) = \frac{U}{Q} \cdot \int_{\rho=-\infty}^{\rho=\rho^a} \frac{m\left(\rho-\rho_c\right)}{1-F\left(\rho\right)} d\rho \qquad\qquad \text{(Eq. 6-21)}$$

where

Q =total mass of ash ejected in the event in g

U =total mass of fuel ejected in the event in g

$m(\rho)$ =probability density function of mass of fuel as a function of fuel particle size

ρ^a = $\log_{10}$ of the ash particle diameter in cm

$F(\rho^a)$ = cumulative distribution of $f(\rho^a)$, the distribution of ash mass as a function of ash particle size.

This model assumes that all fuel particles of a size smaller than (ρ^a-ρ_c) will be simultaneously incorporated into volcanic ash particles of size ρ^a or larger. The combination of particles is carried out in the integrand by dividing the mass of waste in particles of size (ρ-ρ_c) by the mass of ash in particles less than (ρ^a-ρ_c). The fuel fraction is calculated by summing up all the incremental contributions of fuel mass to the volcanic ash mass from fuel sizes smaller than (ρ^a-ρ_c) (Jarzemba et al. 1997 [DIRS 100987], p. 2-6). The density of the combined ash-waste particles is adjusted to account for the presence of the high-density waste. To determine the mass of fuel deposited at a particular location, the main model equation that calculates ash distribution (Equation 6-2) is multiplied by this fuel fraction term and re-integrated by particle size and eruption column height (Section 5.2.2).

This mathematical model is appropriate for the conceptual model of two separate particle streams combining in the rising ash plume, but its application is less meaningful in the conceptual model of magma interactions with waste in a repository drift. Considering the effusive end-member of magma-waste interaction in a conduit-intersected repository drift, the liquid magma flows through the portion of the drift within the footprint of the conduit, degrades the waste packages, releases the waste, and incorporates it as a suspension of waste particles in the silicate melt (SNL 2007 [DIRS 177432], Section 5.2). These particles are assumed to be relatively inert; that is, no melting or dissolution of the particles occurs that would dissolve waste material into solution in the melt. Flow dynamics within the magma in the conduit prior to eruption are assumed to produce a well-mixed (homogeneous) suspension of waste particles throughout the magma (Section 5.1.2). At the vent, the waste-containing magma erupts to produce various deposits, and the portion destined for the tephra blanket is fragmented and becomes entrained in the buoyant plume. In this scenario, the waste is already incorporated into the melt prior to magma fragmentation, and the mathematical formulation in Equation 6-20, using the waste incorporation ratio, ρ_c, does not pertain conceptually. However, this mathematical model can still be used by prescribing a neutral value for ρ_c, which would simply allow the natural size distributions of tephra (produced in the fragmentation process) and waste particles (retained from the original release of waste from the waste packages) to prevail in the tephra-waste mixture. Thus the waste particles can be treated as refractory "xenoliths" in the

melt, which, upon magma fragmentation, will reappear in the tephra as mixed particles of waste and silicate melt (glass).

The appropriate "neutral" value for ρ_c is one that simply allows the combination of the original particle size distributions of waste and ash. In this case, a value of $\rho_c=0$ is used in Equations 6-11 and 6-21 (that is, the ratio of ash and waste particle sizes is 1:1, Equation 6-20).

In a second scenario for magma-waste interaction in the drift, gas-dominated (fragmented) magma erupts explosively into the drift. In this case, the path through the conduit to eventual eruption at the vent will arguably involve homogenization of the once-fragmented melt with other rising liquid-dominated magma, resulting in a well-mixed magma-waste suspension. The conceptual model of partitioning of the rising magma into various eruptive products also pertains in this case; simultaneous eruption of a violent Strombolian plume and effusion of lava flows has been documented in historic eruptions (e.g., Paricutin, February 24, 1943; Luhr and Simpkin 1993 [DIRS 144310], p. 69). The waste incorporation ratio should also be used in a neutral mode ($\rho_c=0$) here as well, since the partitioning of magma into eruptive products will have already reduced the eruptive mass of waste (Sections 6.5.2.22 and 8.2), and the turbulent rise of the (fragmented) magma-waste suspension in the conduit will allow the refractory waste particles to form composite tephra particles with the silicate melt according to a simple mixture of grain sizes, as described for the first scenario, above.

6.5.2.7   Wind Speed, u

Type: empirical distribution
Value: Individual tables in DTN
Units: cm/s.

Upper Air Data for Desert Rock, Nevada Years 1978-2003 (NOAA 2004 [DIRS 171035]) provides wind speed data for the Desert Rock area for a 26-yr period from 1978 to 2003 (see Appendix D). Desert Rock is located near Mercury, Nevada, about 40 km east of Yucca Mountain; it is the closest atmospheric observation station to Yucca Mountain at which atmospheric conditions are measured to altitudes required by this modeling study. After converting height data to height above Yucca Mountain, data were grouped into 1-km increments from 0 km up to 13 km. (Although the current range of values for eruptive power result in a maximum column height of 8.2 km, the values for eruptive power under consideration at the time the wind data were analyzed required wind data up to 13-km altitude.) The wind speed data for each height interval were then used to calculate CDFs with bins set to 100 cm/s intervals. Appendix D contains a detailed description of the steps required to develop the wind speed CDFs. The data are listed in Output DTN: MO0408SPADRWSD.002, in individual Excel worksheets. For reference by TSPA, each wind speed elevation bin is located in the DTN files following a consistent format for workbook/worksheet naming convention. For instance, the 0 to 1 km elevation (above Yucca Mountain crest) data are contained in the "0 to 1 CDF for TSPA" worksheet within the *0 to 1 CDF.xls* workbook. Uncertainty in these empirical data is captured in the distribution functions.

Although Quiring (1968 [DIRS 119317]) provides wind speed data for the Yucca Mountain region for a seven-year period from 1957 to 1964, those data do not extend to sufficiently high

altitudes to address fully the range of potential column heights that the Ashplume model considers; thus, the data from Desert Rock are more appropriate.

6.5.2.8 Wind Direction, Determines *x* and *y*

Type: empirical distribution
Value: Individual tables in DTN
Units: Ashplume degrees (relative to due east, Figure D-1).

Upper Air Data for Desert Rock, Nevada Years 1978-2003 (NOAA 2004 [DIRS 171035]) provides wind direction data for the Desert Rock area for a 26-yr period from 1978 to 2003. Desert Rock is located near Mercury, Nevada, about 40 km east of Yucca Mountain; it is the closest atmospheric observation station to Yucca Mountain at which atmospheric conditions are measured to altitudes required by this modeling study. After converting Desert Rock height data to height above Yucca Mountain, data were grouped into 1-km increments from 0 km up to 13 km. (Although the current range of values for eruptive power result in a maximum column height of 8.2 km, the values for eruptive power under consideration at the time the wind data were analyzed required wind data up to 13-km altitude.) The wind direction data for each height interval were then used to calculate PDFs and associated wind-rose diagrams, with bins set to 30-degree intervals. Appendix D contains a detailed description of the steps required to develop the wind direction PDFs. The data are listed in Output DTN: MO0408SPADRWSD.002, in individual Excel worksheets. For reference by TSPA, each wind direction elevation bin is located in the DTN files following a consistent format for workbook/worksheet naming convention. For instance, the data for 0 to 1 km elevation (above Yucca Mountain crest) are contained in the "0 to 1 PDF for TSPA" worksheet within the *0 to 1 PDF.xls* workbook. Uncertainty in these empirical data is captured in the distribution functions.

Although Quiring (1968 [DIRS 119317]) provides wind direction data for the Yucca Mountain region for a seven-year period from 1957 to 1964, those data do not extend to sufficiently high altitudes to address fully the range of potential column heights that the Ashplume model considers; thus, the data from Desert Rock are more appropriate.

6.5.2.9 Mass of Waste Available for Incorporation, U

Value: distribution will be passed to Ashplume; determined by the TSPA model
Units: grams

The mass of waste available for incorporation with ash particles is an input for the ASHPLUME_DLL_LA V.2.1 [DIRS 178870] code, but this parameter is not developed within this report. The waste mass depends upon factors such as waste inventory and the number of waste packages impacted by a volcanic eruption, described in *Number of Waste Packages Hit by Igneous Intrusion* (SNL 2007 [DIRS 177432]). These factors are defined elsewhere in the TSPA model, multiplied by the magma partitioning factor (Sections 6.5.2.22, 8.2), and the resulting waste mass available is passed to ASHPLUME_DLL_LA V.2.1 [DIRS 178870] at run time. Uncertainty in this parameter is captured by the development of supporting parameters, including the LHS methods employed in *Number of Waste Packages Hit by Igneous Intrusion* (SNL 2007 [DIRS 177432]) and development of the range of values for the magma partitioning factor.

6.5.2.10 Initial Rise Velocity, W_o

Type: uniform distribution
Value: 1.0 to 1.0×10^4
Units: cm/s.

Termed "the eruption velocity at the vent" for previous versions of ASHPLUME software, the initial rise velocity is assumed to be the minimum velocity required to provide the modeled power to the plume (Section 5.2.5). This velocity is related to, but typically much lower than, vent velocity. Vent velocities are related to magma volatile content (SNL 2007 [DIRS 174260], Section 6.3.4.3) and acceleration due to volatile exsolution, and these values do not reflect the deceleration of the tephra particles that occurs near the top of the gas thrust portion of the eruptive column before their entry into the convectively rising plume, which must be assumed for application of the Ashplume model (Section 5.2.5). The function of the initial rise velocity parameter is to deliver the thermal mass (power) to the eruption column, and the velocity of the material entering the plume must only be that required to deliver the necessary power (i.e., without additional momentum due to volatile exsolution). Neglecting the gas-thrust part of the eruption column and given that the heat flux is directly proportional to the mass flux of magma at the vent, the simplest approach to developing the initial rise velocity is to calculate the mass flux of magma below the vent. This mass flux is calculated by Equations 6-7a through 6-7c, a function of eruption power and conduit diameter, using maximum magma bulk density (i.e., unexpanded magma prior to gas exsolution and fragmentation). The range in power is specified in Section 6.5.2.1, and the conduit diameter is specified in DTN: LA0612DK831811.001 [DIRS 179987] as a range with a minimum of 1 m, a mean of 15 m, and a 95th percentile value of 21 m (at 300 m depth). The heat capacity (Cp) used for magma is 1,000 J/(kg·K) derived as a rounded value from Bacon (1977 [DIRS 165512], Figures 1 and 2) and Drury (1987 [DIRS 156447], Table 2). The difference in temperature between magma and ambient is approximated at 1,000 K (lowest liquidus magma temperature is 1,046°C (DTN: LA0612DK831811.001 [DIRS 179987]), ambient is about 25°C at repository depth; temperature difference is rounded to 1,000°C or 1,000 K).

The minimum initial rise velocity can be derived via Equation 6-7c from the minimum mass flux (1×10^3 kg/s) and "maximum" radius (chosen for this analysis as 12 m, slightly above the 95th percentile value of 10.5 m). The maximum is derived from maximum mass flux (1×10^6 kg/s) and minimum radius (0.5 m). Given the ranges in these values and a magma density of 2.6 g/cm³ (Section 6.5.2), the range in W_0 is 9×10^{-2} cm/s to 5×10^4 cm/s. However, Wilson and Head (1981 [DIRS 101034], p. 2,977) report that the minimum practical value for rise speed of basalt in a 0.22-m-radius conduit is 0.12 m/s (12 cm/s). The minimum practical value for initial rise velocity can be better defined using a relationship for magma ascent velocity below the fragmentation depth (Wilson and Head 1981 [DIRS 101034], Equation 12) discussed in *Characterize Eruptive Processes at Yucca Mountain, Nevada* (SNL 2007 [DIRS 174260], Section 6.3.4.1), presented in Appendix G.

Given basalt density and viscosity appropriate for 0 to 4 wt. % H_2O (DTN: LA0612DK831811.001 [DIRS 179987], Table 6-5) and buoyant rise driven solely by a small density contrast ($\rho_c = \rho_m + 10\%$), the magma ascent rate ranges from 1 cm/s to 3,500 cm/s (Appendix G) for a conduit 1- to 24-m in diameter (range expected for Yucca Mountain region;

DTN: LA0612DK831811.001 [DIRS 179987], Table 7-1). The minimum value for W_0 is therefore specified as 1.0 cm/s to provide a realistic lower bound while providing appropriate velocity values that successfully deliver the thermal mass to the eruption column.

The maximum value reflects the upper end of possible velocities of the plume as it transitions from the gas-thrust to convective rise portions of the plume. The velocity of the eruptive mixture decreases markedly from the vent to the base of the convective rise zone. Results of the multiphase eruption column model of Woods (1988 [DIRS 172081], pp. 178 to 179) provide the basis for realistic maximum values. Figure 2a of Woods (1988 [DIRS 172081]) illustrates the variation in vertical plume velocity with height for a simulated eruption (initial column temperature of 1,000 K) for various vent radii. The curves representing 20 m and 50 m vent radii exhibit a rapid decrease in velocity through the gas-thrust region, resulting in a residual upward velocity of about 100 m/s at the base of the convective rise region (≤ 1,000 m above vent). Above that velocity transition within the convective rise region, the velocities of the 20 and 50 m curves decrease monotonically, consistent with (and approximated by) the Ashplume model assumption of linear decrease in velocity with height (Equation 6-3 and following). (Larger vent radii promote increasing mixing with ambient atmosphere, enhanced heat transfer, and superbuoyant convective plumes (Woods 1988 [DIRS 172081], pp. 178 to 179), which are inconsistent with the assumptions of the Ashplume model.) For the 95th percentile conduit diameter of 21 m (DTN: LA0612DK831811.001 [DIRS 179987]) and moderate conduit widening at the vent (SNL 2007 [DIRS 174260], Appendix F), these 20- and 50-m vent radius curves on Figure 2a of Woods (1988 [DIRS 172081]) provide a reasonable upper bound on velocity—100 m/s—at the base of the convective thrust part of the eruption column.

Due to the lack of data to emphasize one part of the velocity range over another, a uniform distribution between 1 cm/s and 10,000 cm/s is specified.

6.5.2.11 Ash Particle Density, Ψp

Type: point values
Values: Table 8-2
Units: g/cm^3.

The ash particle density used in Equation 6-4 is defined in Equation 6-5. The ash particle density is defined to be a function of particle diameter in *Characterize Eruptive Processes at Yucca Mountain, Nevada* (SNL 2007 [DIRS 174260], Section 6.3.5.2). The ASHPLUME_DLL_LA V.2.1 [DIRS 178870] code requires inputs for the densities of large and small ash particles. *Characterize Eruptive Processes at Yucca Mountain, Nevada* defines the densities of ash particles as a function of the magma density (2.6 g/cm^3; Section 6.5.2). The density of a 0.001-cm ash particle (and smaller) is defined as 80% of the magma density (2.08 g/cm^3), whereas a 1.0-cm (and larger) ash particle has a density of 40% of the magma density (1.04 g/cm^3) as a result of the typically greater volume of voids (vesicles) in larger pyroclasts (DTN: LA0612DK831811.001 [DIRS 179987]). The density of intermediate sized particles varies linearly between these end-members. ASHPLUME requires two sets of values to be entered related to the ash particle density, ash particle density at minimum (ψ_p^{high}) and maximum (ψ_p^{low}) particle size (described above) and log ash particle size at minimum (ρ_a^{high}) and maximum

(ρ_a^{low}) ash density. The particle diameters for input to parameters ρ_a^{high} and ρ_a^{low} must be entered as log values, that is, as log (cm).

The values for minimum and maximum particle size and associated densities (and the linear trend between them) are based on studies of basaltic pyroclasts (SNL 2007 [DIRS 174260], Section 6.3.5.2) and considerations of magma fragmentation, pyroclast formation, and void (vesicle) concentration.

6.5.2.12 Ash Particle Shape Factor, *F*

Type: point value
Value: 0.5
Units: N/A.

The ash-particle shape factor is a parameter that is used to describe the shape of the ash particles being transported in the model. The shape factor is used in determining the settling velocity according to Equation 6-4. The shape factor (F) is defined as F = (b + c)/2a, where a, b, and c are the length of the longest, middle, and shortest axes of the particles (Suzuki 1983 [DIRS 100489], pp. 99 to 100). DTN: LA0612DK831811.001 [DIRS 179987] provides a particle shape factor of 0.5. This parameter applies to the ash and does not apply to the waste. The waste is incorporated into ash particles in order to be transported downwind, and the Ashplume model treats all particles (ash and ash-waste combined) as having the same shape factor. Jarzemba (1997 [DIRS 100460], p. 139) used a value of *F* = 0.5 as a shape factor likely to be representative of common clast shapes, following analyses by Suzuki (1983 DIRS 100489], pp. 100 to 101); consistent with DTN: LA0612DK831811.001 [DIRS 179987], *F* = 0.5 is provided for use by TSPA as a point value.

6.5.2.13 Air Density, Ψa

Type: point value
Value: 0. 001734
Units: g/cm^3.

The air density is used in calculating the particle-settling velocity in Equation 6-4. Because the density is nearly constant within the altitude range of interest, air density was selected as a point value (constant). The density was calculated for an ambient temperature of 25°C (298 K) and a pressure of 1 bar, using a linear interpolation between density values provided at 200 K and 300 K in Lide (1994 [DIRS 147834], p. 6-1), resulting in a value of 0.001734 g/cm^3.

6.5.2.14 Air Dynamic Viscosity, η_a

Type: point value
Value: 0. 000185
Units: g/(cm·s).

The air viscosity is used in calculating the particle-settling velocity in Equation 6-4. Because the viscosity is nearly constant within the altitude range of interest, air viscosity was selected as a

point value (constant). The viscosity was calculated for an ambient temperature of 25°C (298 K), using a linear interpolation between viscosity values provided at 200 K and 300 K in Lide (1994 [DIRS 147834], p. 6-239), resulting in a value of 0.000185 g/(cm·s).

6.5.2.15 Eddy Diffusivity Constant, *C*

Type: point value
Value: 400
Units: $cm^2/s^{5/2}$

The constant (C) controlling eddy diffusivity relative to particle fall time was modeled by Suzuki (1983 [DIRS 100489], pp. 98 to 99). The eddy diffusivity (K) of the particles is expressed by Suzuki as a function of the particle fall time, $K = Ct^{3/2}$, where t is the particle fall time. This relationship is based on turbulent particle diffusion and the simplification that the particle diffusion time equals the particle fall time (i.e., time to settle to the ground in seconds). The above relationship is obtained from Suzuki (1983 [DIRS 100489], pp. 98 to 99) because eddy turbulent diffusion occurs over large-scale eddies and can, thus, be related to the particle fall times. The apparent eddy diffusivity (A_L) of particles in the atmosphere is related to the scale of diffusion (L) according to Suzuki (1983 [DIRS 100489], p. 98) by $A_L = 0.08073C^{2/5}L^{6/5}$ with A_L given in cm^2/s and L in cm. Suzuki (1983 [DIRS 100489], Figure 2) shows a linear relationship between $log(A_L)$ and $log(L)$ in the atmosphere; the correlation between L and A_L is defined as $A_L = 0.887L^{6/5}$. Combining these equations yields a constant value for C of 400 $cm^2/s^{5/2}$.

6.5.2.16 Waste Particle Size (Minimum, Mode, Maximum)

Type: point values
Values: 0.0001 minimum, 0.0013 mode, 0.2 maximum
Units: cm.

Waste fuel mass is treated as a log-triangular distribution with particle size in the Ashplume model (Equation 6-10). The minimum, mode, and maximum values defining the distribution are fixed values in the TSPA analyses and are provided to the ASHPLUME_DLL_LA V.2.1 [DIRS 178870] code in units of cm. The values are converted to log (cm) within the code. The rationale for the minimum (0.0001), mean (0.003), and maximum (0.2) particle diameter in centimeters is presented in Appendix F. Because ASHPLUME_DLL_LA V.2.1 requires a mode value for the log-triangular distribution, the mean value, 0.0030 cm, (Appendix F) was converted to a mode value of 0.0013 cm according to $\mu = (a + b + c)/3$ where μ is the log of the mean value, a is the log of the minimum value, b, is the log of the mode value, and c is the log of the maximum value (Evans et al. 1993 [DIRS 112115], p. 187).

6.5.2.17 Grid Location and Spacing, X_{min}, X_{max}, Y_{min}, Y_{max}, N_x, N_y (Cartesian) and rmin, rfactor, nr, ntheta (Polar)

The combined Ashplume/FAR models simulate atmospheric dispersion, deposition, and redistribution of waste-contaminated tephra within the Fortymile Wash watershed. As described in Section 8.2, the Ashplume model is run twice per TSPA realization. The first time TSPA calls the ASHPLUME_DLL_LA V.2.1 [DIRS 178870] code, it is provided with Cartesian coordinates

for the location of the RMEI. Any grid (receptor) location can be specified for calculation of ash and fuel concentrations in the ASHPLUME_DLL_LA V.2.1 [DIRS 178870] code. The only limitation is that the volcanic vent location (0, 0) cannot be specified. The grid locations are defined by specifying a minimum and maximum X and Y location and the number of desired grid locations between the minimum and maximum. These parameters are shown in Table 8-1 for the TSPA model feeds. As an example, to calculate the ash and fuel concentrations at a single point corresponding to the RMEI located approximately 18 km due south of the repository (see below), the minimum and maximum X locations would be specified as 0.0 each, and the minimum and maximum Y locations would be specified as −18 km each. The number of X and Y locations would be specified as 1 and 1, respectively. In the ASHPLUME coordinate system, the point (0, 0) corresponds to the volcanic vent, 0 degrees is due east, 90 degrees is due north, 180 degrees is due west, and −90 degrees is due south. The appropriate coordinate transformations are made within the ASHPLUME_DLL_LA V.2.1 [DIRS 178870] code to be consistent with Equation 6-2.

The second call to the ASHPLUME_DLL_LA V.2.1 [DIRS 178870] code calculates the concentrations of tephra and waste aerially within the Fortymile Wash watershed, requiring adequate grid coverage of the entire basin. As described in Appendix I, the most efficient approach to developing adequate grid coverage is through the use of polar coordinates. The values for the ASHPLUME input parameters controlling the polar grid (*rmin, rfactor, nr, ntheta*, Table 8-2) were developed in the course of sensitivity analyses based on grid resolution (Appendix I). Since these parameter values are specifications of the calculational grid, no uncertainty is associated with them.

The location of the RMEI is specified with respect to the groundwater transport of radionuclides as approximately 18 km due south of the repository, along Fortymile Wash. The basis for this location is derived from the definition of the controlled area in 10 CFR 63.302 [DIRS 180319] and the requirement in 10 CFR 63.312(a) that the RMEI lives in the accessible environment (i.e., outside the controlled area) above the highest concentration of radionuclides in the plume of groundwater contamination. The Yucca Mountain controlled area is defined to extend no further south than 36º 40′ 13.6661″ N latitude in the predominant direction of groundwater flow. This location is discussed further in *Characteristics of the Receptor for the Biosphere Model* (BSC 2005 [DIRS 172827], Section 6.1) as referring to an area north of Highway 95 near the southern boundary of the Nevada Test Site. The path of the contaminated plume has been modeled as occurring under Fortymile Wash (SNL 2007 [DIRS 181650], Figure 6-1[a]). The location of the RMEI, as described above, has been used for calculations of ash and waste concentration (both from primary tephra fall and secondary tephra redistribution) representative of the RMEI location to ensure that estimates of dose are calculated at a consistent location for the nominal, intrusive, and eruptive modeling cases.

The TSPA parameter, Grid_Flag, is used externally (separate from the vector of 36 ASHPLUME inputs listed in Table 8-1) to establish whether a Cartesian or a polar grid will be used. While zero values input for the Cartesian values signals a polar grid within ASHPLUME (and vice versa), non-zero values throughout will result in both grid types being used for a given ASHPLUME realization. The Grid_Flag parameter is used to signal both the Ashplume and FAR codes unambiguously that either a Cartesian or a polar grid will be used.

6.5.2.18 Maximum Particle Diameter for Transport, d_{max}

The maximum particle diameter that can be transported down wind is specified as 10 cm in this model report. This parameter is a simple check within the code to limit the maximum size of particles that are considered for transport in the model. *Characterize Eruptive Processes at Yucca Mountain, Nevada* (SNL 2007 [DIRS 174260], Section 6.3.5.1) describes the range in tephra particle sizes observed at Tolbachik and Cerro Negro volcanoes, which are analogues for a volcano that could possibly form in the Yucca Mountain region. Mean tephra particle sizes from these volcanoes range from 0.19 to 0.37 mm. Thus, these data support the hypothesis that grain sizes greater than about 1 cm are not transported a significant distance down wind but, rather, fall ballistically near the cone. Therefore, the use of a 10-cm tephra-size cutoff for transport provides reasonable efficiency of the numerical code without biasing the model results.

6.5.2.19 Minimum Height of Eruption Column, H_{min}

This parameter allows the definition of a lower threshold height below which particle transport is not calculated within the code. It represents the lower limit of the inner integral of Equation 6-2. A value of 1 m is chosen because this is essentially zero, considering the heights of eruption that are simulated from Equation 6-7b. A value identically equal to zero is not numerically possible in the ASHPLUME_DLL_LA V.2.1 [DIRS 178870].

6.5.2.20 Threshold Limit on Ash Accumulation, *Ash Cutoff*

The value of 10^{-10} (g/cm^2) selected in this model report defines the lower limit for the calculation of ash accumulation; below this value, the ash-concentration value is set to zero in the ASHPLUME_DLL_LA V.2.1 [DIRS 178870] code. This limit is reasonable because any values lower than this will have a negligible effect on model results. This limit is intended to speed code calculations for large grids by eliminating calculations that result in concentrations below this value.

6.5.2.21 Number of Points for Particle Size Histogram, *Numapts*

The ASHPLUME_DLL_LA V.2.1 [DIRS 178870] code includes the capability to calculate histograms of tephra or waste concentration (g/cm^2) per particle size interval, reported for each of the grid output points. The value entered in sequence number 36 (Table 8-1) defines the number of particle size bins, and the contribution of tephra and waste concentration (g/cm^2) is reported for each bin. This code capability is mainly used during model development, testing, and validation, and it is not used by TSPA; therefore a value of 0 is specified for the TSPA parameter, **Num_pts**, in Table 8-2.

6.5.2.22 Magma Partitioning Factor

Type: uniform distribution
Value: 0.1 to 0.5
Units: none.

The Ashplume model of the eruption column, ash dispersal, and ash deposition assumes that violent Strombolian activity dominates, and the model considers only the portion of the eruption

products that are transported aerially away from the vent (Section 5.1.1). This assumption conceptually excludes the volume of magma and waste incorporated into the scoria cone and lava flows. The input parameter values for the Ashplume model are based on estimates of eruptive style and volumes in the Yucca Mountain region, especially Lathrop Wells volcano, the youngest and best-preserved of the scoria cones in the region (SNL 2007 [DIRS 174260], Section 6.3.3.1). Analysis of the Lathrop Wells volcano indicates that a significant proportion of the eruptive products resulted from Strombolian and violent Strombolian activity, contributing mass to the cone, lava flows, and tephra sheet (SNL 2007 [DIRS 174260], Section 6.3.3.1). However, the Ashplume model assumes that waste mixed with the magma at depth enters the eruptive column and is deposited in the tephra sheet only. Therefore the mass of waste available for magmatic transport due to waste package failure must be reduced by a factor that reflects the proportion of waste-containing magma that is erupted to form the scoria cone and lava flows; this reduced mass of waste (mixed with magma) is then provided to ASHPLUME for transport and deposition in the tephra sheet.

Estimates of the relative proportions of magma deposited in various eruptive products are available from studies at Lathrop Wells and at other sites described in the literature (DTN: LA0702PADE03GK.001), focusing on Holocene eruption analogues (and Lathrop Wells) because erosive loss is minimal and tephra sheets are typically well preserved. The range in values for the proportion of dense magma volume deposited in the tephra sheet at eight basaltic volcanoes worldwide is 0.04 to 0.50; at Lathrop Wells, the tephra proportion is 0.38. The suggested range for the value of the "magma partitioning factor" (i.e., the proportion of magma partitioned into the eruptive column and deposited in the tephra sheet), based on these eight volcanoes, is 0.1 to 0.5, with a uniform distribution due to the sparseness of the data. The remainder of the waste is deposited with the magma in relatively stable geologic features (scoria cone and lava flows) and is not available for aerial transport to the RMEI location.

If the magma entering the repository drifts is not liquid-dominated, but instead has fragmented into a gas-dominated fluid containing silicate melt pyroclasts, partitioning of waste-containing magma into various eruptive products is still reasonable, given that multiple states of magma may exist in the conduit below the vent as a result of complex magma pathways, transient blockages, variations in magma flux and pressure, and annular flow. Field observations support this conceptual model, including simultaneous pyroclastic and effusive eruptions (e.g., Luhr and Simkin 1993 [DIRS 144310], p. 69; SNL 2007 [DIRS 174260], Section 6.3.1).

6.5.3 Summary of the Computational Model

Ashplume model results are primarily produced within the TSPA model (GoldSim). The model results presented in this report are limited to the validation activity in Section 7. The Ashplume mathematical model is implemented as a computer code using the standard FORTRAN 77 language. The integrations defined in the mathematical model are solved using standard numerical integration techniques. For use in the TSPA, the ASHPLUME_DLL_LA V.2.1 [DIRS 178870] code is implemented directly within the GoldSim software as a dynamically linked library. All model inputs are entered in GoldSim templates and passed directly to the ASHPLUME DLL. Table 8-2 provides a summary of all inputs required by GoldSim and relates Ashplume input parameters to the corresponding GoldSim variable names. These variables are passed to the ASHPLUME_DLL_LA V.2.1 [DIRS 178870] module at run time, and

ASHPLUME calculates ash and fuel deposition in g/cm^2, passing the values back to the GoldSim model.

6.6 ASHPLUME MODEL RESULTS AND ABSTRACTIONS

No Ashplume model results and abstractions are presented in this report. The output of this report consists of technical basis and instructions for use of the Ashplume model in TSPA. The procedure for the implementation of the Ashplume model in TSPA is described in Section 8.

INTENTIONALLY LEFT BLANK

7. VALIDATION

Validation, or confidence building, is a means to ensure that the system behavior simulated by models is sufficiently consistent with observed behavior to give confidence in model outcomes.

Model validation guidelines, presented in SCI-PRO-002, are based on two levels of model importance and are commensurate with each level. These levels of model importance were based on the TSPA system sensitivity analyses and conclusions presented in *Risk Information to Support Prioritization of Performance Assessment Models* (BSC 2003 [DIRS 168796]), referred to herein as the prioritization report. The prioritization report stated, with regard to the atmospheric transport of erupted radionuclides, the only parameters that bear significantly on the estimate of the mean annual dose to the RMEI are wind speed and direction (BSC 2003 [DIRS 168796], Sections 3.3.13 and 5.1.10). In keeping with the level of confidence required for TSPA component models (SCI-PRO-002, Attachment 3), confidence in the Ashplume model is developed through a Level II model validation.

Ashplume model validation was performed in phases under several revisions of the TWP. Appendix C of REV 04 of *Technical Work Plan: Igneous Activity Assessment for Disruptive Events* (BSC 2003 [DIRS 166289]) described the planned validation of the Ashplume model, which was originally presented in REV 00 of this report. Additional validation discussion has been added to Section 7 of this revision of the model report, per REV 08 of the TWP (BSC 2005 [DIRS 174773], Section 2.6.3.1) and per REV 10 of the TWP (SNL 2007 [DIRS 182219], Section 2.6.5.1).

7.1 VALIDATION PROCEDURES

SCI-PRO-002, Attachment 3 requires at least two postdevelopment model validation methods for Level II importance models; the validation methods are described in SCI-PRO-006 (Section 6.3.2). Specifically, three postdevelopment model validation methods were completed for the Ashplume model. Table 7-1 summarizes the validation activities carried out to satisfy the validation criteria, defined in SCI-PRO-006 (Section 6.3.2), for the Ashplume model and specifies the location in this model report in which each activity is discussed.

Table 7-1.   Confidence-Building and Post-Model Development Validation Activities

Validation Approaches	Location of Discussion in this Model Report
Confidence-Building Activities Related to Model Development (SCI-PRO-002, Attachment 3)	
Evaluate and select input parameters and/or data that are adequate for the model's intended use	Input parameters were selected to represent conditions expected for a volcanic eruption specific to the Yucca Mountain region and to include the range of values representing uncertainty in future eruption parameters and atmospheric conditions. Model input discussion is in Section 6.5.
Formulate defensible assumptions and simplifications that are adequate for the model's intended use	Model assumptions and simplifications are discussed in Section 5.

Table 7-1. Confidence-Building and Post-Model Development Validation Activities (Continued)

Validation Approaches	Location of Discussion in this Model Report
Ensure consistency with physical principles, such as conservation of mass, energy, and momentum, to an appropriate degree commensurate with the model's intended use	A special calculation has been completed to demonstrate that the model is mass conservative (CRWMS M&O 2000 [DIRS 161492]).
Represent important future state (aleatoric), parameter (epistemic), and alternative model uncertainties to an appropriate degree commensurate with the model's intended use	Parameter uncertainties, including wind speed and direction, are discussed in Sections 4, 6.5, 7.2, and 7.6. Alternative models are discussed in Section 6.4. The representation of important model parameters with distributions of values to be used in the TSPA Monte Carlo approach ensures that the range of possible outcomes is fully represented. Discussion of selection of the parameter distributions is in Section 6.5. Parametric uncertainties are discussed in Sections 7.3.1.4 and 7.3.2.2.
Ensure simulation conditions have been designed to span the range of intended use and avoid inconsistent outputs or that those inconsistencies can be adequately explained and demonstrated to have little impact on results	A sensitivity analysis was performed in which model simulations were carried out to span the entire range of all parameters represented by distributions; outputs were checked for consistency (Section 7.2).
Ensure that model predictions (performance parameters) adequately represent the range of possible outcomes, consistent with important uncertainties and modeling assumptions, conceptualizations, and implementation	In addition to the other validation activities described above, a coupled Ashplume-FAR model sensitivity analysis was performed to assess the effect of the range of important Ashplume input parameters (power, wind speed and direction) on the composite output of the coupled models of tephra dispersal, deposition, and redistribution (Section 7.6)
Postdevelopment Model Validation Activities (SCI-PRO-006, Section 6.3.2)	
Corroboration of model results with data acquired from the laboratory, field experiments, analogue studies or other relevant observations (or published in refereed journals), not previously used to develop or calibrate the model	Calculations were performed to compare Ashplume model results to data collected for three volcanoes (Cerro Negro, Lathrop Wells, and Cinder Cone) that are considered representative of volcanic ash deposits that could result from an eruption at Yucca Mountain (Section 7.3).
Technical review, planned in the applicable TWP, by reviewers independent of the development, checking, and interdisciplinary review of the model documentation	An independent review was performed by Dr. Frank Spera of the University of California to assess the applicability of the Ashplume model. The independent review is documented in Section 7.4 (see Appendix E for text of the technical review).
Corroboration of model results with other model results obtained from the implementation of other independent mathematical models developed for similar or comparable intended use/purpose	A comparison between the ASHPLUME and ASHFALL codes was performed to develop confidence in the mathematical approach incorporated in the ASHPLUME code. The results of this code comparison are summarized in Section 7.5 and Appendix J.

7.2 SENSITIVITY ANALYSIS

A sensitivity analysis was performed to test the Ashplume model over the entire range of model input parameter values to be used in the TSPA analysis. This sensitivity analysis both ensured that the model operated as expected over the parameter ranges selected and ensured that there were no limits to model validity due to any numerical constraints. In addition, the sensitivity analysis identified the model parameters to which the calculated waste concentration is most sensitive and are thus important in the TSPA dose calculations. The uncertainty in these

parameters is represented in the TSPA analysis by a distribution of values covering the ranges developed in the input selection process. This sensitivity analysis was performed using ASHPLUME_DLL_LA V.2.1 [DIRS 178870] and ranges of base-case parameter values documented in Table 8-2.

The sensitivity analyses were performed by varying the value of the following input parameters: eruptive power, mean ash particle diameter, ash particle diameter standard deviation, column diffusion constant (beta), initial rise velocity, wind speed, wind direction, eruption duration, waste incorporation ratio, and waste particle size statistics (minimum, mode, maximum). The values for each of these parameters used in the analysis are provided in Table C-1, based on ranges of values defined in Table 8-2. During a TSPA simulation, these parameters might take on any value within the defined distributions. The model was run over the full range of values for each parameter shown in the tables. Further details of the methods used in this analysis are described in Appendix C.

The results of each ASHPLUME run for a given parameter were plotted and evaluated for sensitivity to change in value. The plots shown in Appendix C (Figures C-1 to C-10) exhibit expected trends that are in accordance with the underlying mathematical model (Suzuki 1983 [DIRS 100489], Jarzemba et al. 1997 [DIRS 100987]). No discontinuities in results were detected, which indicates numerical convergence in all simulations. The analysis indicates that the Ashplume model results are most sensitive to variations in wind speed and wind direction and mean ash particle diameter, which produce orders-of-magnitude changes in tephra and waste thickness at the RMEI location. Moderate sensitivity (factor of 2 to 10 change) was displayed for variations in values for the parameters defining eruptive power, duration, and tephra particle size standard deviation. The model showed only minor sensitivity (less than factor of two change) to variations in beta, initial rise velocity, eruption duration, waste incorporation ratio, and waste particle size.

The sensitivity of the coupled tephra dispersal/deposition and redistribution models (ASHPLUME and FAR, respectively) to variations in key eruptive parameters is discussed in Section 7.6.

7.3   NATURAL ANALOGUE STUDIES

Natural analogue studies addressed the adequacy and accuracy of the Ashplume model by comparing model results to observed tephra fall thickness distributions at Cerro Negro volcano, Nicaragua; Lathrop Wells volcano, Nevada; and Cinder Cone, California.

7.3.1   Validation Criteria

Based on a review of relevant published tephra dispersal modeling studies (Appendix H), the Ashplume studies used in natural analogue comparisons of computed versus measured tephra thickness below will be deemed sufficiently accurate for the model's intended use if any of the following occur:

  I.   The error in match between computed and measured tephra thickness at specific locations is within a factor of 2

II. The correlation coefficient (R) is greater than or equal to 0.9 and the slope of the regression line is within 30% of unity (B statistic = 0.7 to 1.3)

III. There is a reasonable match between the computed and observed pattern of the tephra deposit, in terms of two-dimensional profile or three-dimensional tephra sheet pattern. A reasonable match will be one in which there is consistency in tephra thicknesses and dispersal patterns, based on visual inspection.

Criterion I compares computed versus measured tephra thicknesses at each observation point independently. Criterion II is more stringent than criterion I (which could result in regression slopes ≤2), and it includes the general goodness-of-fit of the modeled thickness to *all* measured points (via the correlation coefficient). Criterion III provides a means to evaluate the overall goodness-of-fit of the modeled pattern of the tephra blanket compared to interpretations of field data (e.g., an isopach map). If the validation exercise is successful in meeting these accuracy acceptance criteria while using reasonable input parameter values, the scientific basis for the model is deemed to be adequate. Reasonable input parameter values are those which are either derived from field observations native to the case study at hand or input parameter values generalized from worldwide studies (e.g., Section 6.5.2).

A Note on Matching Observed Tephra Thickness–Tephra-dispersal models, such as ASHPLUME and others based on Suzuki's (1983 [DIRS 100489]) mathematical model, simplify the eruption column as a vertical line source, rather than explicitly modeling eruption column physics. As a result, the computed tephra concentrations are valid only for distances sufficiently far from the source that the tephra dispersal processes can be described by advection-dispersion and particle settling processes (Pfeiffer et al. 2005 [DIRS 174826], pp. 273 and 274). In practice, this means that, in model validation comparisons of computed versus observed tephra thicknesses, greater weight should be given to matching distal data. For example, modeling studies that fitted proximal data in order to reconstruct tephra distributions resulted in extreme underestimation of total erupted mass (Pfeiffer et al. 2005 [DIRS 174826], pp. 291 and 292). In the modeling studies of analogue cases in the following sections, fits to the distal data have been emphasized in the evaluation of the performance of the model relative to accuracy criteria.

7.3.2 Cerro Negro

The Cerro Negro volcano is one of a number of active basaltic volcanoes within an active volcanic chain in Nicaragua. Cerro Negro is located on the Caribbean tectonic plate, and the volcanic activity expressed within this long volcanic chain, which continues from southern Mexico to Costa Rica, is directly related to subduction of the Pacific tectonic plate under the Caribbean tectonic plate. This convergent tectonic setting differs from extensional Basin and Range setting for the basaltic cinder cones in the Yucca Mountain region (e.g., Lathrop Wells). The convergent setting is generally expected to produce larger volume (longer-lived) volcanoes than a continental extensional setting. Volcanism at Cerro Negro has a 150-year history with at least 22 documented eruptions. Its last eruption (1995) produced a tephra volume (0.004 km^3) (Hill et al. 1998 [DIRS 151040]) similar to, but less than, that of the Lathrop Wells volcano (> 0.07 km^3) (SNL 2007 [DIRS 174260], Section 6.3.4.4). The 1995 Cerro Negro eruption may be analogous to the type of eruption that could occur in the Yucca Mountain region. However, Cerro Negro's relatively long history, shape, and magma production rate suggest that it may

represent a young composite volcano rather than a simple, long-lived cinder cone (McKnight and Williams 1997 [DIRS 162827]).

The measured eruption parameters published by Hill et al. (1998 [DIRS 151040]) for their study using a model similar to Ashplume were used to develop input parameters for the ASHPLUME code (versions 1.4LV and 2.0), and are documented in Appendix L. Because these field measurements were assumed to accurately represent the actual 1995 eruption of Cerro Negro, these parameters were not varied in ASHPLUME to attempt to match the field data. Because of the uncertainties associated with the atmospheric and eruption conditions of the Cerro Negro event, comparison of ash fall thicknesses between the observed distribution and the Ashplume result is qualitative. However, this comparison provides confidence that the Ashplume model can give a reasonable representation of ash deposition for a possible future eruption at Yucca Mountain.

As shown in Figure 7-1 the Ashplume calculations compare well with the observed data for distances from the volcanic vent greater than 10 km. For distances less than 10 km, the Ashplume results give ash thickness values greater than the observed data. The lobe on the northern side of the measured ash thickness data is interpreted to be a result of a variation in wind direction and/or speed that occurred during the eruption. This variation probably accounts for some of the discrepancy because Ashplume assumes a constant wind speed and direction for a given simulation. In addition, comparison of results using ASHPLUME 1.4LV [DIRS 154748] and ASHPLUME V.2.0 [DIRS 152844] show the overall consistency between the two versions (Figure 7-1) in terms of ash thickness and dispersal patterns. This study meets the qualitative accuracy criterion III.
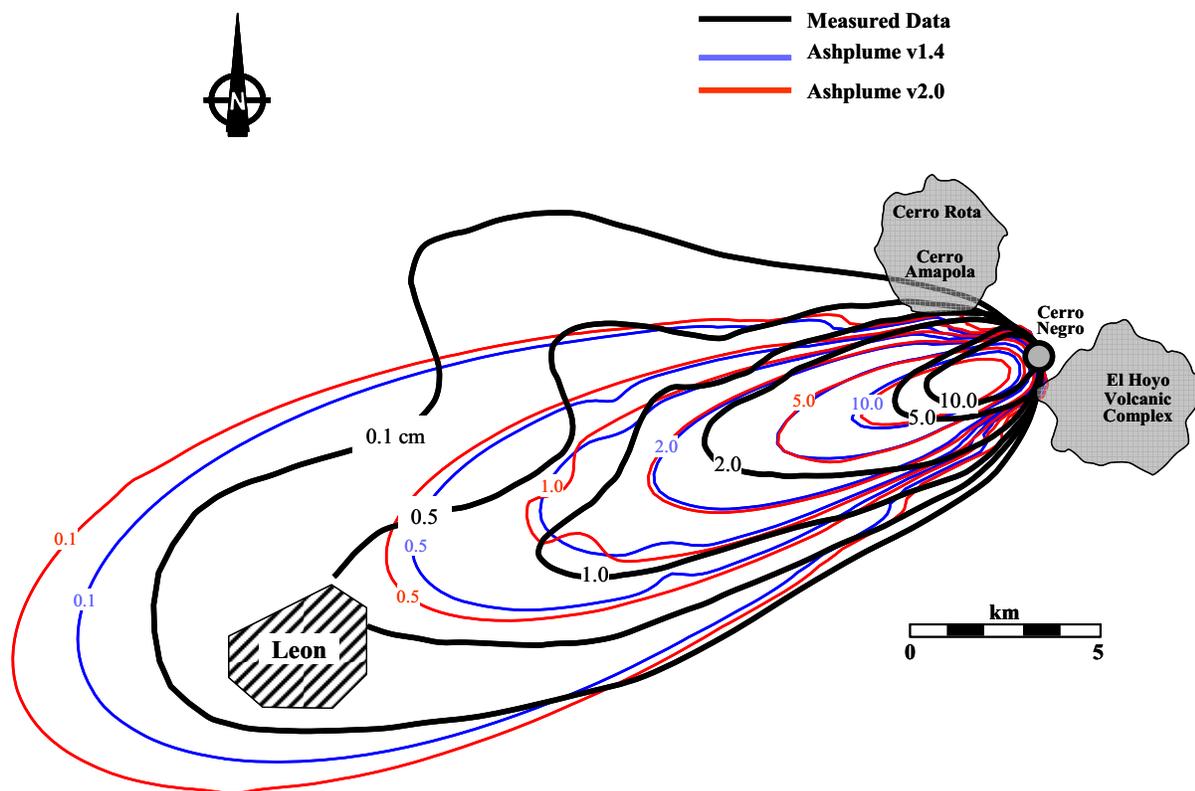
Source: Appendix L.

Figure 7-1   Comparison of Calculated and Measured Ash Deposition Thickness (cm) for 1995 Cerro Negro Eruption: Isopachs of Model Results from ASHPLUME 1.4LV and V.2.0 Compared to Observed (Measured) Ash Thickness

7.3.3   Lathrop Wells

At 77,000 years old (Heizler et al. 1999 [DIRS 107255], p. 803), the Lathrop Wells volcano, Nevada, is the youngest basaltic volcano in the Yucca Mountain region. It is the southern-most surface expression of the Plio-Pleistocene Crater Flat Volcanic Zone (CFVZ) (Crowe and Perry 1990 [DIRS 100973], p. 328) and is located approximately 18 km south of Yucca Mountain. Characteristics of the volcanism comprising the CFVZ are documented in Perry et al. (1998 [DIRS 144335], Chapters 2 and 4). Eruptive history of the Lathrop Wells volcano and volume estimates of the cone, lava flows, and eruptive tephra are provided in *Characterize Eruptive Processes at Yucca Mountain, Nevada* (SNL 2007 [DIRS 174260], Appendix C). The volume of tephra was estimated from field sample points, which located ash fall deposits that are now shallowly buried beneath younger colluvium and eolian deposits. Due to deeper burial or non-deposition of the tephra, data points to the south of the cone are largely absent, and this results in an apparent tephra fall pattern directed northward from the vent area. Additionally, there are no data for ash deposits less than 1-cm thick, which limits the identification of the northward extent of the ash fall. The tephra distribution presented in *Characterize Eruptive Processes at Yucca Mountain, Nevada* (SNL 2007 [DIRS 174260], Appendix C) is, therefore, a minimum distribution.

For the Lathrop Wells volcano simulation, all parameters were set to base-case values (Table 8-2); those parameters with distributed ranges in Table 8-2 were set to midrange values, except ash particle size standard deviation, for which a representative value was used from *ASHPLUME, V2.0, User's Manual* (CRWMS M&O 2001 [DIRS 174768], Table 2). Sample input and output files are presented at the end of this section. Several calculations were performed using wind speed sampled from the range that is used in TSPA and results were compared to the Lathrop Wells volcano data (Figure 7-2). The figure also shows the results of a simulation using wind speeds of 800 cm/s (Model 4), which most closely matches the Lathrop Wells volcano tephra data. The simulations showed that observed Lathrop Wells data fall within the range of results produced by ASHPLUME V.2.0 [DIRS 152844], except at very proximal locations, using wind speeds within the range provided to TSPA (Section 8.2).
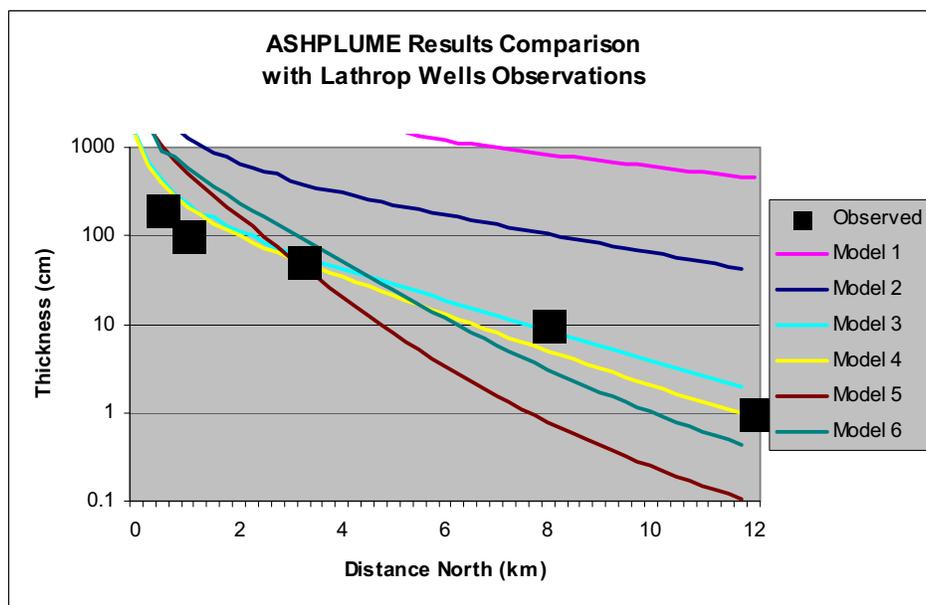
NOTE: Observed data are from an isopach map in SNL 2007 [DIRS 174260], Figure C-2c, measured north from the vent. The 300-cm thickness observed value is not shown for clarity (falls close to 200-cm point). Models are realizations for a wind blowing to the north. Parameters held constant for these comparisons are β = 0.3, d = 0.0572 cm, σ_d = 0.2518 log(cm), ρ_c = 0.3, and U = 0. The following list shows the varied parameters in each model with V calculated from P and T_d by Equations 6-7a through 6-7c for a conduit diameter of 10 m (Models 1 and 2) and 4.5 m (Models 3 to 6):

Model 1: P = 5.0 x 10^{12} W, V = 0.08 km^3, Td = 0.2 d, W_0 = 24.5 m/s, u = 1,000 cm/s
Model 2: P = 5.0 x 10^{11} W, V = 0.04 km^3, Td = 1.0 d, W_0 = 12.1 m/s, u = 1,000 cm/s
Model 3: P = 5.0 x 10^{10} W, V = 0.004 km^3, Td = 1.0 d, W_0 = 1.2 m/s, u = 1,000 cm/s
Model 4: P = 5.0 x 10^{10} W, V = 0.004 km^3, Td = 1.0 d, W_0 = 1.2 m/s, u = 800 cm/s
Model 5: P = 6.2 x 10^8 W, V = 0.004 km^3, Td = 75.0 d, W_0 = 0.01 m/s, u = 1,000 cm/s
Model 6: P = 6.2 x 10^8 W, V = 0.004 km^3, Td = 75.0 d, W_0 = 0.01 m/s, u = 1,400 cm/s.

Figure 7-2.   Comparison of Ashplume Results to Lathrop Wells Ash-Thickness Observations

For the purposes of model validation, tephra thicknesses computed by the ASHPLUME model were compared to distances from vent to isopachs along the centerline of the plume developed from field measurements, reported in *Characterize Eruptive Processes at Yucca Mountain, Nevada* (SNL 2007 [DIRS 174260], Figure C-2c) (Figure 7-3). Model fits to the medial and distal data are generally good (within a factor of 4 to 5 proximally and within 10% medially and

distally. The overall pattern of the centerline profile of the deposit was reproduced by the better model fits (Figure 7-2). The correlation figure (Figure 7-3) illustrates this good fit for small tephra thicknesses and larger overestimates for higher thicknesses (proximal deposits). Models 3 and 4 provide the best fits overall.
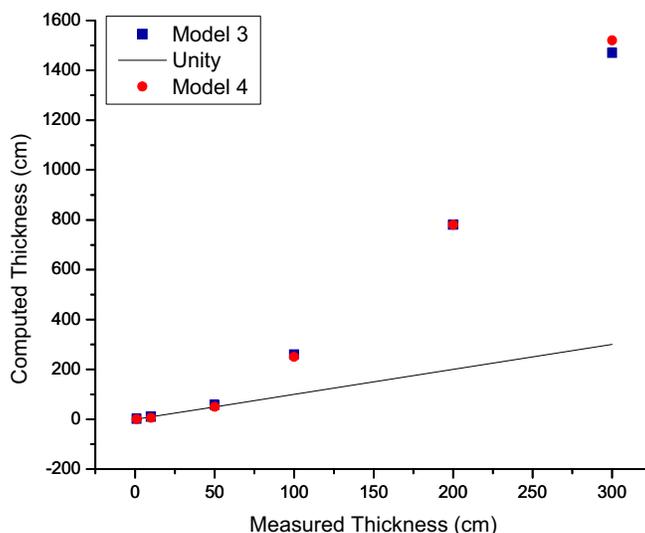
Source: Developed Validation DTN: LA0508GK831811.002.

NOTE: Measured data are from an isopach map in SNL 2007 [DIRS 174260], Figure C-2c. Black line represents perfect correlation. The best model runs (3 and 4) matched the distal deposits well but overestimate proximal deposits (computed thicknesses above 300 cm).

Figure 7-3.   Results of Lathrop Wells Validation Runs, Plotted as Measured versus Computed Tephra Thickness

The statistics of the correlations provide a means to assess the adequacy of the validation exercise. Linear regressions were performed on the data in Figure 7-3 using built-in functions of OriginPro V7.5. Linear regressions that include model values for all six points (Table 7-2) show the effects of the overestimates for larger ash thicknesses (proximal areas). Models 3 and 4 produce linear regression slopes of about 5. These regression slopes approach unity (1.2 and 1.03) when only the medial and distal data (3 to 12 km) are considered, indicating that the model did a good job of matching the observed deposits in distal areas. These statistics compare well to the acceptance criteria developed from published tephra modeling studies, including model estimates within a factor of 2 of observed values and regression slopes within 30% of unity. Computed proximal deposits ($\leq$1 km) fit less well to the measured values, but the ASHPLUME model does not calculate the dispersal of tephra associated with the construction of the cinder cone, which is generally emplaced by ballistic trajectories. Because of this aspect of the model, model fits of medial and distal deposit thicknesses are deemed to be more important in the validation exercise.

Table 7-2. Lathrop Wells Model Validation Statistics: Correlation of Modeled versus Observed Tephra Thickness

ASHPLUME Run Number	Linear Regression Slope (all data)	Correlation Coefficient, R (all data)	Linear Regression Slope (3 to 12 km)	Correlation Coefficient, R (3 to 12 km)
3	4.9	0.98	1.2	0.999
4	5.0	0.98	1.03	0.997

 Source: Developed validation DTN: LA0508GK831811.002.

Based on the model validation acceptance criteria described in Section 7.3.1, the goodness-of-fit of computed versus measured tephra thickness demonstrated by this validation exercise indicate that the model is sufficiently accurate and adequate for its intended use.

Input file for Lathrop Wells Model 4:

```
ASHPLUME v2.0 Lathrop Wells 4
1                                  ! iscrn, 0 = no screen output, 1 = yes
0    0                             ! xmin, xmax in km
0    12.0                          ! ymin, ymax in km
1                                  ! numptsx
49                                 ! numptsy
2.08    1.04                       ! ashdenmin, ashdenmax in g/cm3
-3.0    0.0                        ! ashrholow, ashrhohi
0.5                                ! fshape
0.001117  0.0001758               ! airden in g/cm3, airvis in g/cm-s
400.0                              ! c in cm2/s to the 5/2
10.0                               ! dmax in cm
0.0001  0.002  0.05               ! fdmin, fdmean, fdmax all in cm
0.001                              ! hmin in km
1.0e-10                            ! acutoff in g/cm2
0.3                         ***    ! the constant beta (unitless)
0.0572                      ***    ! the mean ash particle diameter (cm)
.2518                       ***    ! sigma for the ash lognormal dist.
0.3                                ! the incorporation ratio (unitless)
0.0                         ***    ! the mass of fuel to incorporate (g)
90.0                        ***    ! the wind direction- relation to due east (deg)
800.                        ***    ! the wind speed (cm/s)
121.                        ***    ! the initial eruption velocity (cm/s)
5.00e+10                    ***    ! the power (watts)
8.64e+04                    ***    ! the event duration (s)  (24 hours)

*** Parameters sampled in TSPA model
```

Output file for Lathrop Wells Model 4:

```
ASHPLUME version 2.00-dll


**********************************************************************
     Input Parameters (From vin vector):
        Minimum x location (km)...............    0.0000
        Maximum x location (km)...............    0.0000
        Minimum y location (km)...............    0.0000
        Maximum y location (km)...............   12.0000
        Number of grid points in x...........        1
        Number of grid points in y...........       49
        Minimum ash density (g/cm^3)..........    2.0800
        Maximum ash density (g/cm^3)..........    1.0400
```

```
        Minimum particle size [log(cm)].......    -3.0000
        Maximum particle size [log(cm)].......     0.0000
        Particle shape parameter..............     0.5000
        Air density (g/cc)....................  1.1170E-03
        Air viscosity (g/cm-s)................  1.7580E-04
        Eddy diff. constant (cm^2/s^[5/2])....   400.0000
        Size cutoff (cm)......................    10.0000
        Minimum waste particle diameter (cm)..     0.0001
        Mode waste particle diameter (cm).....     0.0020
        Maximum waste particle diameter (cm)..     0.0500
        Minimum height of column (km).........     0.0010
        Lower limit for ash deposits (g/cm^2). 1.0000E-10
        Dispersion constant, beta.............     0.3000
        Mean particle diameter (cm)...........     0.0572
        Log particle standard deviation.......     0.2518
        Incorporation ratio...................     0.3000
        Total fuel mass available (g)......... 0.0000E+00
        Wind direction (deg).................     90.0000
        Wind speed (cm/s)....................    800.0000
        Vent exit velocity (cm/s)............    121.0000
        Event power (w)...................... 5.0000E+10
        Event duration (s)................... 8.6400E+04


****************************************************************
     Derived Parameters:
        Ash particle minimum log-diameter.....    -2.5016
        Ash particle mean log-diameter........    -1.2426
        Ash particle maximum log-diameter.....     0.0164
        Fuel particle minimum log-diameter....    -4.0000
        Fuel particle mode log-diameter.......    -2.6990
        Fuel particle maximum log-diameter....    -1.3010
        Column height (km)....................     3.8775
        Ash mass (g)......................... 5.8870E+12


****************************************************************
     Results (To vout vector):
     Note: If more than one location is specified here, only the last
           one will be returned in vout.

      x(km)       y(km)       xash(g/cm^2)      xfuel(g/cm^2)

      0.000       0.250        1.3703E+03        0.0000E+00
      0.000       0.500        6.2883E+02        0.0000E+00
      0.000       0.750        3.9328E+02        0.0000E+00
      0.000       1.000        2.8015E+02        0.0000E+00
      0.000       1.250        2.1013E+02        0.0000E+00
      0.000       1.500        1.7456E+02        0.0000E+00
      0.000       1.750        1.3576E+02        0.0000E+00
      0.000       2.000        1.2017E+02        0.0000E+00
      0.000       2.250        9.9560E+01        0.0000E+00
      0.000       2.500        8.4997E+01        0.0000E+00
      0.000       2.750        7.3656E+01        0.0000E+00
      0.000       3.000        6.4218E+01        0.0000E+00
      0.000       3.250        5.6208E+01        0.0000E+00
      0.000       3.500        4.9368E+01        0.0000E+00
      0.000       3.750        4.3481E+01        0.0000E+00
      0.000       4.000        3.8363E+01        0.0000E+00
      0.000       4.250        3.3893E+01        0.0000E+00
      0.000       4.500        2.9985E+01        0.0000E+00
      0.000       4.750        2.6555E+01        0.0000E+00
      0.000       5.000        2.3522E+01        0.0000E+00
      0.000       5.250        2.0832E+01        0.0000E+00
      0.000       5.500        1.8454E+01        0.0000E+00
```

```
0.000        5.750        1.6359E+01        0.0000E+00
0.000        6.000        1.4511E+01        0.0000E+00
0.000        6.250        1.2873E+01        0.0000E+00
0.000        6.500        1.1419E+01        0.0000E+00
0.000        6.750        1.0130E+01        0.0000E+00
0.000        7.000        8.9886E+00        0.0000E+00
0.000        7.250        7.9807E+00        0.0000E+00
0.000        7.500        7.1049E+00        0.0000E+00
0.000        7.750        6.3132E+00        0.0000E+00
0.000        8.000        5.6140E+00        0.0000E+00
0.000        8.250        4.9926E+00        0.0000E+00
0.000        8.500        4.4476E+00        0.0000E+00
0.000        8.750        3.9652E+00        0.0000E+00
0.000        9.000        3.5383E+00        0.0000E+00
0.000        9.250        3.1604E+00        0.0000E+00
0.000        9.500        2.8259E+00        0.0000E+00
0.000        9.750        2.5297E+00        0.0000E+00
0.000       10.000        2.2673E+00        0.0000E+00
0.000       10.250        2.0345E+00        0.0000E+00
0.000       10.500        1.8280E+00        0.0000E+00
0.000       10.750        1.6445E+00        0.0000E+00
0.000       11.000        1.4814E+00        0.0000E+00
0.000       11.250        1.3350E+00        0.0000E+00
0.000       11.500        1.2052E+00        0.0000E+00
0.000       11.750        1.0893E+00        0.0000E+00
0.000       12.000        9.8592E-01        0.0000E+00
```

7.3.4   Cinder Cone

Basaltic ash thickness data from Cinder Cone, a 277-m-high Holocene cone in Lassen Volcanic National Park, California, is provided by Heiken (1978 [DIRS 162817]). Cone and tephra-sheet volume (0.038 km^3 and 0.032 km^3, respectively), composition, monogenetic behavior, and eruptive sequence make Cinder Cone a good analogue for a future eruption in the Yucca Mountain region. Several ASHPLUME V.2.0 [DIRS 152844] simulations were carried out to compare ASHPLUME results (estimates) to observed ash-thickness data. For the Cinder Cone simulation (Figure 7-4), all parameters were set to base-case values (Table 8-2); those parameters with distributed ranges in Table 8-2 were set to midrange values, except for mean ash particle size and ash particle size standard deviation (see note to Figure 7-4). These parameters were set to match specific ash particle size data at Cinder Cone (Heiken 1978 [DIRS 162817]). Sample input and output files are included at the end of this section. Several calculations were performed using wind speeds sampled from the full range used for the TSPA and results were compared to the Cinder Cone data. Figure 7-4 shows the results of the simulation in terms of profiles along the centerline of the tephra deposit. The 2,000-cm/s (model 2) wind speed provides a good fit to the >1 km data. The simulations show that observed Cinder Cone data fall well within the range of results produced by Ashplume using values from the TSPA range of wind speeds.
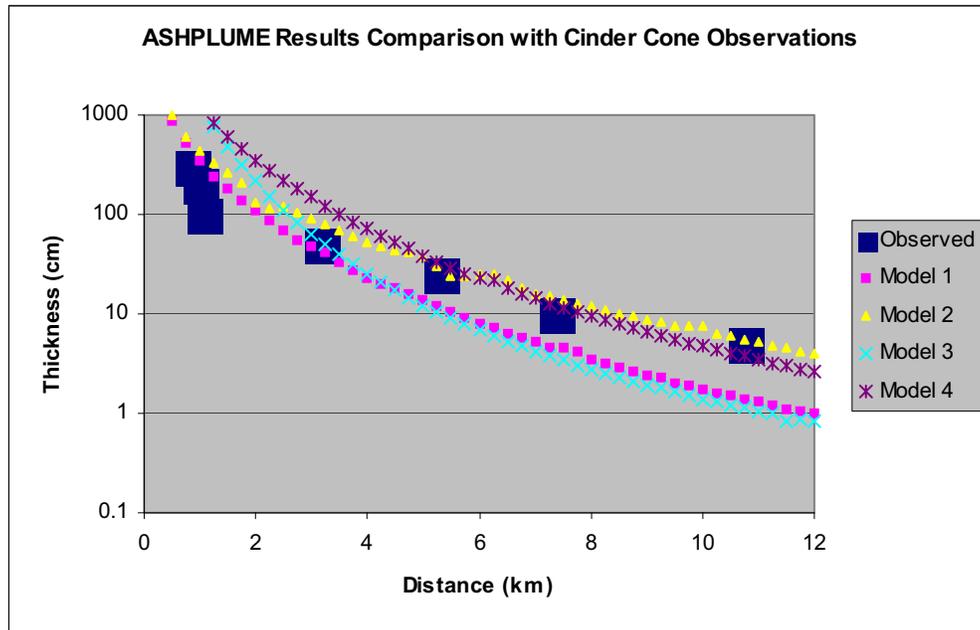
NOTE: Observed data are from Heiken (1978 [DIRS 162817], Figure 3). Models are realizations for a wind blowing to the east. Parameters held constant for these comparisons are β = 0.3, d = 0.193 cm, σ_d = −0.78 log(cm), ρ_c = 0.3, and U = 0. The following list shows the varied parameters in each model with V calculated from P and T_d by Equations 6-7a to 6-7c for a conduit diameter of 5.0 m (Models 1 and 2) and 8 m (Models 3 and 4):

Model 1: P = 5.0 x 10^{10} W, V = 0.004 km^3, Td = 1.0 d, W_0 = 24.5 m/s, u = 1,000 cm/s
Model 2: P = 5.0 x 10^{10} W, V = 0.004 km^3, Td = 1.0 d, W_0 = 1.2 m/s, u = 2,000 cm/s
Model 3: P = 7.5 x 10^{10} W, V = 0.065 km^3, Td = 10.0 d, W_0 = 0.5 m/s, u = 200 cm/s
Model 4: P = 6.8 x 10^{10} W, V = 0.018 km^3, Td = 3.0 d, W_0 = 0.5 m/s, u = 800 cm/s.

Figure 7-4.   Comparison of Ashplume Results to Cinder Cone Ash Thickness Observations

For the purposes of model validation, tephra thickness estimates from the ASHPLUME model were compared to observed data at specific points (distances from vent to isopachs along the centerline of the plume described by Heiken (1978 [DIRS 162817], Figure 3) (Figure 7-5). Model fits to the medial and distal data are generally good (within a factor of 2 proximally and within 10% medially and distally. The overall pattern of the centerline profile of the deposit was reproduced by the better model fits (Figure 7-4). The correlation figure (Figure 7-5) illustrates this good fit for small tephra thicknesses and larger overestimates for higher thicknesses (proximal deposits). Models 1 and 2 provide the best fits overall.
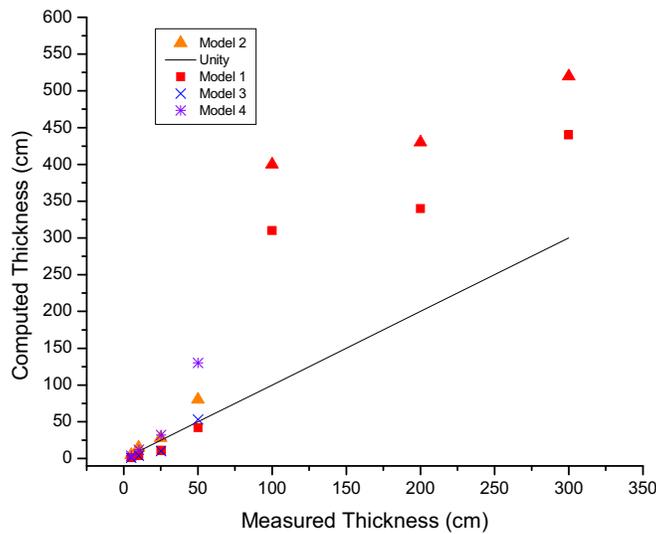
Source: Developed validation DTN: LA0508GK831811.002.

NOTE: Measured thickness points are taken from distances from vent to isopachs in Heiken (1978 [DIRS 162817], Figure 3). Proximal (large computed thickness) points for Models 3 and 4 are not shown, as the computed thicknesses were above 1,000 cm. Black line represents perfect correlation. The best model runs (1 and 2) matched the distal deposits well but overestimate proximal deposits (computed thicknesses above 300 cm).

Figure 7-5. Results of Cinder Cone Validation Runs, Plotted as Measured versus Computed Tephra Thickness

The statistics of the correlations provide a means to assess the adequacy of the validation exercise. Linear regressions were performed on the data in Figure 7-5 using built-in functions of OriginPro V7.5. Linear regressions including model values for all seven points (Table 7-3) show the effects of the estimates for larger ash thicknesses (proximal areas). Models 1 and 2 produce linear regression slopes of 1.6 to 1.9. These regression slopes approach unity (0.9, Model 1) when only the medial and distal data (3 to 10 km) are considered, indicating that the model did a good job of matching the observed deposits in distal areas. These statistics compare well to the acceptance criteria developed from published tephra modeling studies, including model estimates within a factor of 2 of observed values and regression slopes within 30% of unity. Computed proximal deposits ($\leq$1 km) fit less well to the measured values, but the ASHPLUME model does not calculate the dispersal of tephra associated with the construction of the cinder cone, which is generally emplaced by ballistic trajectories. Because of this aspect of the model, model fits of medial and distal deposit thicknesses are deemed to be more important in the validation exercise.

Table 7-3. Cinder Cone Model Validation Statistics: Correlation of Modeled versus Observed Tephra Thickness

ASHPLUME Run Number	Linear Regression Slope (all data)	Correlation Coefficient, R (all data)	Linear Regression Slope (3 to 10 km)	Correlation Coefficient, R (3 to 10 km)
1	1.6	0.94	0.91	0.98
2	1.9	0.92	1.6	0.99
3	6.9	0.95	1.2	0.96
4	5.4	0.94	2.8	0.97

Source: Developed validation DTN: LA0508GK831811.002.

Based on the model validation acceptance criteria described in Section 7.3.1, the goodness-of-fit of computed versus measured tephra thickness demonstrated by this validation exercise indicate that the model is sufficiently accurate and adequate for its intended use.

The Lathrop Wells and Cinder Cone simulations of tephra thicknesses provide additional confidence that the Ashplume model and model parameters selected for use in the TSPA can produce ash thickness results that cover the range of values expected for volcanoes in the Yucca Mountain region.

Input File for Cinder Cone Model 2:

```
ASHPLUME v2.0 Cinder Cone, Lassen NP, run 2
1                              ! iscrn, 0 = no screen output, 1 = yes
0.5    14.0                    ! xmin, xmax in km
0.0     0.0                    ! ymin, ymax in km
28                             ! numptsx
1                              ! numptsy
2.08    1.04                   ! ashdenmin, ashdenmax in g/cm3
-3.0    0.0                    ! ashrholow, ashrhohi
0.5                            ! fshape
0.001117  0.0001758            ! airden in g/cm3, airvis in g/cm-s
400.0                          ! c in cm2/s to the 5/2
10.0                           ! dmax in cm
0.0001  0.002  0.05            ! fdmin, fdmean, fdmax all in cm
0.001                          ! hmin in km
1.0e-10                        ! acutoff in g/cm2
0.3                    ***  ! the constant beta (unitless)
0.193                  ***  ! the mean ash particle diameter (cm)
-0.78                  ***  ! sigma for the ash lognormal dist.
0.3                         ! the incorporation ratio (unitless)
0.0                    ***  ! the mass of fuel to incorporate (g)
0.0                    ***  ! the wind direction- relation to due east (deg)
2600.                  ***  ! the wind speed (cm/s)
57.6                   ***  ! the initial eruption velocity (cm/s)
8.82e+10               ***  ! the power (watts)
2.59e+06               ***  ! the event duration (s)  (3 days)

*** Parameters sampled in TSPA model
```

Output File for Cinder Cone Model 2:

```
ASHPLUME version 2.00-dll
```

```
************************************************************************
    Input Parameters (From vin vector):
        Minimum x location (km)................      0.5000
        Maximum x location (km)................     14.0000
        Minimum y location (km)................      0.0000
        Maximum y location (km)................      0.0000
        Number of grid points in x.............         28
        Number of grid points in y.............          1
        Minimum ash density (g/cm^3)...........      2.0800
        Maximum ash density (g/cm^3)...........      1.0400
        Minimum particle size [log(cm)].......      -3.0000
        Maximum particle size [log(cm)].......       0.0000
        Particle shape parameter...............      0.5000
        Air density (g/cc).....................  1.1170E-03
        Air viscosity (g/cm-s).................  1.7580E-04
        Eddy diff. constant (cm^2/s^[5/2])....    400.0000
        Size cutoff (cm).......................     10.0000
        Minimum waste particle diameter (cm)..      0.0001
        Mode waste particle diameter (cm).....      0.0020
        Maximum waste particle diameter (cm)..      0.0500
        Minimum height of column (km).........      0.0010
        Lower limit for ash deposits (g/cm^2).  1.0000E-10
        Dispersion constant, beta.............      0.3000
        Mean particle diameter (cm)...........      0.1930
        Log particle standard deviation.......     -0.7800
        Incorporation ratio...................      0.3000
        Total fuel mass available (g)........  0.0000E+00
        Wind direction (deg)..................      0.0000
        Wind speed (cm/s).....................   2600.0000
        Vent exit velocity (cm/s).............     57.6000
        Event power (w).......................  8.8200E+10
        Event duration (s)....................  2.5900E+06


************************************************************************
    Derived Parameters:
        Ash particle minimum log-diameter.....      3.1856
        Ash particle mean log-diameter........     -0.7144
        Ash particle maximum log-diameter.....     -4.6144
        Fuel particle minimum log-diameter....     -4.0000
        Fuel particle mode log-diameter.......     -2.6990
        Fuel particle maximum log-diameter....     -1.3010
        Column height (km)....................      4.4687
        Ash mass (g)..........................  3.1130E+14


************************************************************************
    Results (To vout vector):
    Note: If more than one location is specified here, only the last
          one will be returned in vout.

        x(km)       y(km)       xash(g/cm^2)    xfuel(g/cm^2)
        0.500       0.000       4.6638E+04      0.0000E+00
        1.000       0.000       2.1376E+04      0.0000E+00
        1.500       0.000       1.3087E+04      0.0000E+00
        2.000       0.000       9.0748E+03      0.0000E+00
        2.500       0.000       6.7211E+03      0.0000E+00
        3.000       0.000       5.1783E+03      0.0000E+00
        3.500       0.000       4.1145E+03      0.0000E+00
        4.000       0.000       3.3241E+03      0.0000E+00
        4.500       0.000       2.8717E+03      0.0000E+00
        5.000       0.000       2.2572E+03      0.0000E+00
        5.500       0.000       1.8986E+03      0.0000E+00
        6.000       0.000       1.6249E+03      0.0000E+00
        6.500       0.000       1.3867E+03      0.0000E+00
```

```
    7.000      0.000       1.2748E+03        0.0000E+00
    7.500      0.000       1.1229E+03        0.0000E+00
    8.000      0.000       7.3215E+02        0.0000E+00
    8.500      0.000       7.2602E+02        0.0000E+00
    9.000      0.000       7.9481E+02        0.0000E+00
    9.500      0.000       7.0444E+02        0.0000E+00
   10.000      0.000       5.3725E+02        0.0000E+00
   10.500      0.000       4.5336E+02        0.0000E+00
   11.000      0.000       4.3927E+02        0.0000E+00
   11.500      0.000       3.6888E+02        0.0000E+00
   12.000      0.000       3.5214E+02        0.0000E+00
   12.500      0.000       3.1642E+02        0.0000E+00
   13.000      0.000       3.0284E+02        0.0000E+00
   13.500      0.000       2.5930E+02        0.0000E+00
   14.000      0.000       2.3622E+02        0.0000E+00
```

7.4   ASHPLUME INDEPENDENT TECHNICAL REVIEW

An independent technical review was conducted for the Ashplume model as part of the validation activities (Pfeifle 2007 [DIRS 182321]). This section presents a summary of the review that is presented in its entirety in Appendix E.

Consistent with the guidance in AP-SIII.10Q[1], *Models*, for validation of mathematical models, an independent technical review was conducted to assess the application of Ashplume for representing potential future volcanic events at Yucca Mountain. The review was conducted by Dr. Frank Spera, Professor of Geology at the University of California, Santa Barbara, from March 24, to April 10, 2003. Revision 00, Draft B of this model report was made available to Dr. Spera for his review (see Appendix E) along with other requested material. Dr. Spera was also a member of the Peer Review Panel that addressed the approach used by the Yucca Mountain Project to evaluate igneous consequences from a potential igneous event intersecting a repository at Yucca Mountain, Nevada (Detournay et al. 2003 [DIRS 169660]). Dr. Spera was requested to consider whether the mathematical model is appropriate for representing the conceptual model (i.e., is Ashplume appropriate for its intended use), which is to represent the atmospheric dispersal of waste-contaminated tephra from a potential volcanic eruption at Yucca Mountain.

Dr. Spera observed that the fundamental factors governing the fallout distribution of volcanic tephra include the height of the steady-state volcanic column, a function of eruptive mass flow rate, total eruptive volume, and the wind speeds and direction affecting the tephra being ejected into the atmosphere at different levels above the volcanic vent. He concluded that, if available, additional analogues should be considered. Since his review, work to characterize the Lathrop Wells tephra sheets has been completed and documented in the revision to *Characterize Eruptive Processes at Yucca Mountain, Nevada* (SNL 2007 [DIRS 174260], Appendix C). This study provides additional basis for validation of Ashplume in this model report.

Dr. Spera also recommended that the Ashplume model be compared to other similar mathematical models. He specifically recommended ASHFALL for this purpose. This comparison has been performed and is documented in Section 7.5.

---

[1] This historical procedure was in effect at the time the review was performed.

Finally, Dr. Spera recommended that greater mass discharge rates and corresponding higher plume heights be considered when Ashplume is implemented. In response to this recommendation, new wind information (NOAA 2004 [DIRS 171035]) has been implemented in this model report to better represent eruption mechanics, including consideration of greater eruptive power and mass discharge rate, and consideration of the behavior of an ash plume at greater altitudes.

Based on information available and a full understanding of its limitations, Dr. Spera concluded that the outputs of Ashplume provide reasonable representations of products that could result from a volcanic eruption at Yucca Mountain. In response to Dr. Spera's discussion of strengths and weaknesses of the Ashplume model, an additional validation study (Section 7.3) and a code comparison (versus the ASHFALL code, Section 7.5) have been performed and parametric uncertainties have been characterized and propagated to the TSPA.

7.5   ASHPLUME – ASHFALL CODE COMPARISON

Two of the postdevelopment model validation methods that can be used to validate the Ashplume model are: 1) corroboration of model results with results obtained from the implementation of an alternative mathematical model; and 2) corroboration of model results with information published in refereed journals or literature (SCI-PRO-006, Section 6.3.2). The results from the Ashplume model have been compared to those from another ash dispersal code, ASHFALL (Hurst and Turner 1999 [DIRS 176897]), using equivalent input parameters, as recommended in the April 2003 independent technical review of the Ashplume model by Dr. Frank Spera (Section 7.4.2). A description of the code comparison is presented in Appendix J and is summarized here. The code comparison was carried out per the technical workplan (SNL 2007 [DIRS 182219], Section 2.6.5.1) by configuring the inputs to the ASHPLUME_DLL_LA V.2.1 [DIRS 178870] code to simulate conditions of the 1995 and 1996 eruptions of Ruapehu volcano in New Zealand. Equivalent ASHPLUME inputs were developed to those of an ASHFALL modeling study of these eruptions published by Hurst and Turner (1999 [DIRS 176897]) and provided directly by Dr. Tony Hurst (Appendix J, Addendum). ASHPLUME input and output files for this modeling activity are contained in validation DTN: LA0706GK150308.001. The ASHPLUME results were visually and quantitatively compared with the results reported by Hurst and Turner (1999 [DIRS 176897]) per specific validation criteria defined above (Section 5.3.2.1) and in the TWP (SNL 2007 [DIRS 182219], Section 2.6.5.1 and consistent with SNL 2007 [DIRS 182219]).

The ASHPLUME code was used in two sets of model runs to attempt to match published output from the ASHFALL code for constant wind conditions and a variable wind field (Hurst and Turner 1999 [DIRS 176897], Figs. 1b and 1d) (Appendix J). In both cases the results of the ASHPLUME code were similar to ASHFALL in terms of the shape and distribution of the tephra deposit. ASHPLUME input parameter values were adjusted within reasonable ranges to fine-tune the match between the two models. In both cases the best fits were obtained using base-case parameter values (those derived from direct equivalencies between the two mathematical models) with adjustment to wind speeds appropriate for the center of mass of the eruptive column and to values of the Suzuki constant to match the usage of Hurst and Turner (1999 [DIRS 176897]).

A consistent difference occurred in the shape of the axial profiles of the results of the two models: the ASHPLUME model typically resulted in greater proximal (<80 km) tephra thickness and less distal (>140 km) deposition. The distribution of tephra from the ASHFALL model was generally wider than that of ASHPLUME, most likely due to the slight variation in wind speed and direction at the 13 altitude bins used by the former model versus the single wind condition at the top of the eruption column used by the latter. The 25° spread in ASHFALL wind directions with elevation resulted in a slight fanning of the eruption plume.

Composite-plume tephra distributions were created from two separate ASHPLUME model runs that were identical except for varying wind direction. The distribution of tephra from this combination was compared to the results of an ASHFALL run that used a wind field that shifted in direction during the eruption. Similar to the single-plume runs, the ASHFALL tephra deposit was more diffuse than that of ASHPLUME due to the variation of wind conditions with height. ASHPLUME wind speeds for the model runs that compared most favorably to ASHFALL were slightly slower than what would be expected from the meteorological data appropriate for the altitude of greatest ash concentration in the eruptive column. This may result from the need to match ASHFALL, which transports tephra using a combination of lower wind speeds near the ground and higher speed winds that exist near the top of the eruption column.

The consistent difference in downwind tephra thickness profile shape between ASHPLUME and ASHFALL may result from a fundamental difference between the codes, perhaps as a result of differences in the way fall velocities are defined for the tephra particles. ASHPLUME calculates particle settling and deposition by the use of a mean and standard deviation for particle size, together with values for particle density, shape factor, and properties of air. In contrast, ASHFALL uses direct input of a probability distribution of particle settling velocities, which may produce a more complex tephra distribution pattern. A 60% increase in mean particle size in ASHPLUME resulted in a 10% to 50% decrease in transport (tephra thickness), but it did not change the shape of the ASHPLUME tephra profile.

The single- and composite-plume simulation exercises both provided results that were close to the results of ASHFALL, indicating that, while the exact shape of the plume was not reproduced, the overall distribution of tephra could be reproduced within a factor of two. This level of precision is consistent with acceptance criteria for other ASHPLUME model validation exercises, as defined in Section 7.3.1. As a result of this code comparison activity, it has been demonstrated that the ASHPLUME code can use reasonable input parameter values to produce results comparable to the ASHFALL code, which uses more complex treatments of tephra particle settling velocities and variable wind conditions with height and with time.

7.6 INVESTIGATION OF SENSITIVITY OF COUPLED ASHPLUME-FAR MODELS

The ASHPLUME_DLL_LA V.2.1 code [DIRS 178870] simulates the dispersal of volcanic tephra and incorporated waste by assuming that volcanic activity during an eruption is consistently energetic (violent Strombolian), with constant eruptive power for the duration of the eruption. According to the algorithm used in the code, this translates into a constant eruption column height (Section 6.5.1). Additionally, ASHPLUME calculates advective transport utilizing a single value each for wind speed and direction, which remain constant during the

eruption. These values are assigned based on conditions at the maximum column height. These code limitations have recently been set aside in other tephra dispersal models that utilize time and altitude-dependent wind conditions or unsteady column height (Section 6.5.4; Folch and Falpeto 2005 [DIRS 181523]). However, given that the ASHPLUME code is coupled to the tephra redistribution model (FAR; SNL 2007 [DIRS 179347]), the effects of these code limitations on the tephra/waste concentration at the RMEI location after atmospheric dispersal and fluvial redistribution are not obvious. This section summarizes an analysis of the effects of 1) unsteady column height and 2) variable wind conditions on the concentration of waste-containing tephra in sediment at the outlet of Fortymile Wash after the combined processes of atmospheric dispersal and fluvial redistribution. The full description of the analysis is included in Appendix K. Model input and output files for the ASHPLUME_DLL_LA V.2.1 [DIRS 178870] and FAR V.1.2 (2007 [DIRS 182225]) codes are archived in model validation DTN: LA0708GK150308.001.

The effect of variable column height during an eruption was assessed by dividing the base-case eruption volume among three small eruptions, each with constant wind direction but variable power, column height, wind speed, and duration. The sets of model runs were combined to form composite tephra sheets for comparison to other model cases. The effect of variation in wind direction during an eruption was assessed in two separate cases: 1) *spread*, caused by minor variations in wind direction throughout an eruption, and 2) *divergence*, caused by two distinct wind directions during the eruptive period. Sets of three small component eruptions simulated varying wind direction (spread) over 30°, 60°, and 90° compared to the base-case, east-directed run.

Unsteady eruption column height simulated in a series of ASHPLUME model runs produced only slight change in the distribution of tephra deposited in the Fortymile Wash watershed compared to the instantaneous, constant-column-height base case, despite varying the component eruption volume by an order of magnitude, the column height by a factor of 2, and the wind speed by 30%. The aspect ratio for the composite tephra sheet changed by ±20% versus the simple diffusive plume base case. When the composite tephra mass from these variable column height eruptions was routed through the FAR sediment-transport model, the concentration of tephra in sediment at the outlet of Fortymile Wash varied by less than 15% compared to the base case.

The effect of wind variation during an eruption (spread or divergence of the eruptive plume) produced a maximum variation in sediment tephra concentration a factor of 2.24 greater than that of the base case. The variation in amount of tephra mobilized off steep slopes and through active channels varied non-monotonically with azimuth in these studies, suggesting that factors other than unsteady eruption or variable wind conditions were controlling tephra remobilization efficiency.

The controlling effects of watershed geometry and terrain were identified in an analysis in which the wind direction for simple single-eruption, constant-wind Ashplume runs was rotated in 30° increments within an 180° azimuthal band downwind of the vent area. The output of these runs provided input into FAR to evaluate the resulting variation in tephra concentration in stream sediments. Notably, the span of tephra concentrations in sediment at the Fortymile watershed outlet calculated for the simple azimuthal rotation case (0.2 to 2.6 times the base case)

encompasses all variation resulting from the more complex eruptive cases involving variation in column height and wind conditions during an eruption.

This variation in tephra concentration in sediment at the watershed outlet is considered in light of uncertainties in the model system. The tephra concentration in Fortymile Wash sediment varied by less than a factor of three overall in these studies. In contrast, the uncertainty is much higher in other risk parameters used to develop the inputs to the Ashplume model; for instance, the range of likely values for eruptive conduit size (which directly determines the quantity of radioactive waste entrained into the eruption), eruptive volume, and eruption duration range over one to two orders of magnitude (SNL 2007 [DIRS 174260], Table 7-1). Therefore, from a tephra dispersal and deposition modeling perspective, variations in tephra concentration at the Fortymile Wash outlet due to unsteady eruption or variable winds during an eruption are not significant in the context of the uncertainty in other eruption parameters.

Despite its simplification relative to recent tephra dispersal models, the Ashplume model is considered to be adequate for its intended purpose within TSPA. The analysis of risk due to tephra remobilization is highly dependent on the nature of the specific geometry and terrain in the study area, and these effects outweigh sensitivities to eruption parameters in the coupled-model risk assessment. The use of more sophisticated tephra dispersal models that incorporate more complex physics would arguably not provide a more meaningful result once the details of the tephra thickness distributions on the landscape had been diffused by the tephra redistribution model.

7.7   UNCERTAINTY

The Ashplume model has been validated by comparisons to tephra deposits at three analogue volcanoes and by extensive sensitivity analyses on individual parameters (Sections 7.2, 7.3, 7.6 and Appendix C). The results of the validation studies indicate that the model can successfully reproduce the pattern and thickness of tephra deposits when the model input parameters are derived from available site-specific eruption information supplemented by generalized "base-case" parameter values (Table 8-2) derived from the volcanological literature and field studies. Sensitivity studies indicate that the model results are relatively insensitive to variation in most parameters, the exceptions being wind speed and direction, mean ash particle diameter, eruption power, eruption duration and tephra particle size standard deviation (Section 7.2, Appendix C). These six parameters were reasonably well constrained for each of the analogue studies: in the case of Cerro Negro, field observations constrained four; in the case of Cinder Cone and Lathrop Wells, the tephra deposits were reproduced within the accuracy criteria by specifying reasonable "base-case" parameter values and specific grain size statistics for these parameters. The coupled model (ASHPLUME-FAR) sensitivity study provides a characterization of the propagation of uncertainty of these key Ashplume input parameters through the tephra redistribution model (Section 7.6, Appendix K).

8. CONCLUSIONS

The objectives of this model report are the following:

- Update documentation of the Ashplume conceptual and mathematical models, including parameterization and validation for the ASHPLUME_DLL_LA V.2.1 code [DIRS 178870] as implemented in the TSPA

- Provide representative wind speed and direction data for the Yucca Mountain region at altitudes up to 13 km

- Address the criteria of Section 4.2 as shown in Appendix B

- Summarize the implementation of the Ashplume model in TSPA.

8.1 SUMMARY OF MODELING ACTIVITY

The Ashplume conceptual model accounts for incorporation and entrainment of waste particles in an eruption plume and atmospheric transport of the contaminated tephra. The Ashplume mathematical model describes the conceptual model in mathematical terms to allow for estimates of radioactive waste-ash deposition on the ground surface in case the hypothetical eruptive event occurs. A key activity in the development of these models is the identification of realistic and representative values for the input parameters. The Ashplume mathematical model is implemented by the ASHPLUME_DLL_LA V.2.1 [DIRS 178870] computer code, which is a required component of the TSPA model of the nuclear waste repository at Yucca Mountain. Within the TSPA, the model for atmospheric dispersal and deposition of tephra, implemented in the ASHPLUME code, is used to estimate the ground-level concentration (areal density) of ash and waste after a violent Strombolian eruption that intersects the repository. The waste concentration is modified by processes in the ash redistribution model (SNL 2007 [DIRS 179347]) and then converted to activity concentrations of individual radionuclides and combined with BDCFs in the TSPA model to calculate an annual dose to the RMEI. Other uses of ASHPLUME have not been evaluated in this report.

8.2 PRODUCT OUTPUT INTENDED FOR USE IN THE TSPA MODEL

The output from this model report consists of two components, which are summarized in Table 8-1. First, a set of input parameter values (points and ranges of values) for ASHPLUME_DLL_LA V.2.1 [DIRS 178870] are summarized in Table 8-2 for use in the TSPA modeling. Second, a set of summary data characterizing wind speed and direction in the Yucca Mountain region for heights above the surface of Yucca Mountain up to 13 km are presented in Tables 8-3 and 8-4, respectively. (Methods for development of the wind speed and wind direction data are described in Appendix D, and the full data are given in Output DTN: MO0408SPADRWSD.002.) These outputs are described in detail in the following paragraphs.

Table 8-1.   Output Data

Data Description	Data Tracking Number	Location of Use of Output DTNs in this Report
Parameter values to be used as input for the ASHPLUME_DLL_LA V.2.1 model for TSPA	LA0702PADE03GK.002	Table 8-2
Desert Rock wind speed and wind direction data analyses for years 1978 – 2003	MO0408SPADRWSD.002	Tables 8-3 and 8-4; Figure 8-1; Tables D-8, D-9, and D-10; Figure D-2
Summary of calculations of values for the proportion of basaltic eruptive products that are deposited as fallout tephra based on analysis of Holocene eruptions worldwide and Lathrop Wells volcano, Nevada. This information forms the basis for the range of values of the new parameter, magma partitioning factor.	LA0702PADE03GK.001	Section 6.5.2.22

Four developed DTNs support analyses and parameter values documented in this report.

- DTN: MO0506SPACHERN.000 was developed in the revised waste particle size analysis described in Appendix F, Section F3.6, presenting the results of the evaluations of Chernobyl data

- Validation DTN: LA0508GK831811.002 documents the Ashplume model validation statistics for the Cinder Cone and Lathrop Wells Volcano case studies (Section 7.3.1)

- Validation DTN: LA0706GK150308.001 contains input and output files for ASHPLUME_DLL_LA V.2.1 that were used in the ASHPLUME-ASHFALL code comparison (Section 7.5)

- Validation DTN: LA0708GK150308.001 contains input and output files for the ASHPLUME_DLL_LA V2.1 and FAR V.1.2 codes that were used in the ASHPLUME-FAR coupled model sensitivity analysis (Section 7.6).

The coupled models Ashplume and Fortymile Ash Redistribution (FAR) calculate the areal concentration of waste in sediment after atmospheric transport, deposition, and redistribution through the Fortymile Wash watershed.   Inputs to the FAR model are documented in *Redistribution of Tephra and Waste by Geomorphic Processes Following a Potential Volcanic Eruption at Yucca Mountain, Nevada* (SNL 2007 [DIRS 179347]). The model coupling requires that the ASHPLUME_DLL_LA V2.1 [DIRS 178870] code be run twice per TSPA realization: 1) a single point waste concentration at the location of the reasonably maximally exposed individual (RMEI) (18 km south of the repository) is passed via the ASHPLUME output vector to FAR; and 2) the Fortymile Wash drainage basin is sampled on a polar grid and output to a text file, *ashplume.out*. In this second run, the final grid sample is output by ASHPLUME DLL, but this information is ignored in favor of the entire grid written to the external file. The FAR DLL then reads the grid of values from the text file. In these two ASHPLUME_DLL_LA V.2.1 [DIRS 178870] code runs, the values for the input parameters are identical except for values that specify the model grid. The basis for the location of the RMEI (18 km south of the repository) is

discussed in Section 6.5.2.17. The use of the parameter, Grid_Flag, in relation to input values for the ASHPLUME and FAR codes, is also discussed in Section 6.5.2.17.

Table 8-2 lists the parameterization and other code inputs required to run the ASHPLUME_DLL_LA V.2.1 code [DIRS 178870] within the TSPA model, which is implemented within the GoldSim modeling system. GoldSim requires a vector of Ashplume inputs for each realization of the model. Some of the Ashplume parameters required in GoldSim are represented as point values and do not change from one realization to the next. Some input parameters are represented by distributions that are sampled by GoldSim. The sampled values are then passed to Ashplume for each realization. Following are instructions for sampling the distributed parameter values and building an input file for each realization (using TSPA parameter names; see Table 8-2 for mathematical model equivalencies):

1. Sample distributions for the parameters Beta_Dist_a, Dash_mean_a, Dash_sigma_a, Erupt_Velocity_a, and Erupt_Power_a

2. Sample distribution for ash settled density (Ash_Density_a)

3. Calculate limits for the total eruption duration (T_{d_min}, T_{d_max}, in seconds) using Equations 8-1a and 8-1b such that the range of allowable total eruption volume (0.004 to 0.14 km^3) is respected (using Erupt_Power_a, (P, in watts), Ash_Density_a (ψ_s, in kg/m^3, see Section 6.5.2), and the units conversion factors of 10^9 m^3/km^3 and 1 W/J/s):

$$T_{d\_min} = \frac{V_{min}\psi_s}{\dot{Q}} = \frac{V_{min}\psi_s}{P/(C_p\Delta T)} = \frac{\left(0.004\,km^3\right)\cdot\psi_s\left(\frac{kg}{m^3}\right)\cdot\left(10^{15}\frac{J\cdot m^3}{kg\cdot km^3}\right)}{P(W)} \quad \text{(Eq. 8-1a)}$$

$$T_{d\_max} = \frac{V_{max}\psi_s}{\dot{Q}} = \frac{V_{max}\psi_s}{P/(C_p\Delta T)} = \frac{\left(0.14\,km^3\right)\cdot\psi_s\left(\frac{kg}{m^3}\right)\cdot\left(10^{15}\frac{J\cdot m^3}{kg\cdot km^3}\right)}{P(W)} \quad \text{(Eq. 8-1b)}$$

4. Sample Erupt_Time_a (T_d, in seconds) from the range (log-uniform) bounded by T_{d_min}, T_{d_max}

5. Calculate eruption column height by the equation: $H = 0.0082(P^{0.25})$, with H in km and P in watts

6. Use eruption column height, H, as index to sample the appropriate altitude bin in the cumulative distribution functions for wind direction (e.g., Wind_Dir_2_3_km_a) and wind speed (e.g., Wind_Speed_2_3_km_a); if the column height is exactly equal to an altitude bin boundary (e.g., 8.00 km), sample the next higher bin (e.g., 8 to 9 km)

7. Sample distribution for Magma_Partitioning_a (magma partitioning factor) and multiply the sampled value by the mass of waste available for transport. The product in grams is the value used for the ASHPLUME input parameter #26, *uran* (mass of waste to incorporate, Table 8-2). The mass of waste available for transport is derived in upstream calculations in the TSPA GoldSim model based on the number of waste packages hit and package inventory data and is not provided in this report.

Two outputs are contained in the output vector from Ashplume after a single realization within the GoldSim model: (1) x_{ash}, the tephra deposition in g/cm^2, and (2) x_{fuel}, the fuel deposition in g/cm^2. In addition, if a grid of calculation points is used, the tephra and waste concentrations at each grid point are written to an external file, *ashplume.out*.

All output feeds from this model report to the TSPA model are identified in Tables 8-1 and 8-2. Table 8-2 indicates the relative position within the input vector required by Ashplume (i.e., the sequence number), the variable name used within GoldSim, a brief description of the parameter, the units of the parameter, the value(s) for the parameter, and the distribution type. Two parameters–wind speed and wind direction–are identified in Table 8-2 as having distribution type "table." For this distribution type, the TSPA model requires a tabular listing of the CDF or PDF of the parameter. In this report, wind speed and wind direction data tables were formulated to be used as input to the TSPA model (Output DTN: MO0408SPADRWSD.002). These data have also been modified further to fit the specific form and function of the model. The methods used for producing these tables are described in Appendix D.

Table 8-3 (also included as Table D-9) gives a summary of wind speed in relation to height above Yucca Mountain. The tabular listings for wind direction PDF for incremental distances above Yucca Mountain and corresponding wind rose diagrams are given in Output DTN: MO0408SPADRWSD.002. Tables 8-3 and 8-4 and Figure 8-1 below are representative samples of the more complete listings found in Output DTN: MO0408SPADRWSD.002.

Table 8-2. Input Parameter Values for the ASHPLUME_DLL_LA V.2.1 Model for TSPA

Seq. No.*	ASHPLUME Parameter (variable name) [Equation No.]	TSPA Parameter Name	Description	Units	Value	Distribution Type
1	Iscrn (iscrn) [n/a]	iscrn	Run type (0 = no screen output)	None	0	point value
2	X_{min} (xmin) [n/a]	X_RMEI [1] X_Min_Grid [2]	Minimum X grid location	km	0[1] 0[2]	point value
3	X_{max} (xmax) [n/a]	X_RMEI [1] X_Max_Grid [2]	Maximum X grid location	km	0[1] 0[2]	point value
4	Y_{min} (ymin) [n/a]	Y_RMEI [1] Y_Min_Grid [2]	Minimum Y grid location	km	−18[1] 0[2]	point value
5	Y_{max} (ymax) [n/a]	Y_RMEI [1] Y_Max_Grid [2]	Maximum Y grid location	km	−18[1] 0[2]	point value
6	N_x (numptsx) [n/a]	Nxx_Grid	Number of X grid locations (0 for no Cartesian grid)	None	1[1] 0[2]	point value
7	N_y (numptsy) [n/a]	Ny_Grid	Number of Y grid locations	None	1[1] 0[2]	point value

Table 8-2. Input Parameter Values for the ASHPLUME_DLL_LA V.2.1 Model for TSPA (Continued)

Seq. No.*	ASHPLUME Parameter (variable name) [Equation No.]	TSPA Parameter Name	Description	Units	Value	Distribution Type
8	Ψ_p^{low} (ashdenmin) [Equation 6-5]	AshDen_MaxD	Ash particle density at maximum particle size	g/cm^3	1.04	point value
9	Ψ_p^{high} (ashdenmax) [Equation 6-5]	AshDen_MinD	Ash particle density at minimum particle size	g/cm^3	2.08	point value
10	ρ_a^{low} (ashrholow) [Equation 6-5]	LogD_maxDen	Log ash particle size at maximum ash density	log (cm)	−3	point value
11	ρ_a^{high} (ashrhohi) [Equation 6-5]	LogD_minDen	Log ash particle size at minimum ash density	log (cm)	0	point value
12	F (fshape) [Equation 6-4]	Fshape	Ash particle shape factor	None	0.5	point value
13	Ψ_a (airden) [Equation 6-4]	AirDen	Air density	g/cm^3	0.001734	point value
14	η_a (airvis) [Equation 6-4]	AirVis	Air viscosity	g cm^{-1} s^{-1}	0.000185	point value
15	C (C) [Equation 6-2]	C	Eddy diffusivity constant	cm^2/s$^{5/2}$	400.0	point value
16	d_{max} (dmax) [n/a]	Dmax_trans	Maximum particle diameter for transport	cm	10	point value
17	ρ_{min}^f (fdmin) [Equation 6-10]	D_min	Minimum waste particle size	cm	0.0001	point value
18	ρ_{mode}^f (fdmean) [Equation 6-10]	D_mode	Mode waste particle size	cm	0.0013	point value
19	ρ_{max}^f (fdmax) [Equation 6-10]	D_max	Maximum waste particle size	cm	0.2	point value
20	H_{min} (hmin) [n/a]	H_min	Minimum height of eruption column	km	0.001	point value
21	Ash Cutoff (acutoff) [n/a]	A_cutoff	Threshold limit on ash accumulation	g/cm^2	1×10^{-10}	point value
22	β (beta) [Equation 6-3]	Beta_dist_a	Column diffusion constant (Beta)	none	0.01 to 0.5	uniform
23	d (dmean) [Equation 6-4]	Dash_mean_a	Mean ash particle diameter	cm	0.001 to 0.01 to 0.1	log triangular
24	σ_d (dsigma) [Equation 6-8]	Dash_sigma_a	Ash particle diameter standard deviation	log (cm)	0.301 to 0.903	uniform
25	ρ_c (rhocut) [Equation 6-9]	Rhocut	Waste incorporation ratio	None	0.0	point value
26	U (uran) [Equation 6-11]		Mass of waste to incorporate	g	Calculated within the TSPA model	N/A
27	Wind Direction (udir) [n/a]	Varies by column height bin (e.g., Wind_Dir_1_2_k	Wind Direction	degrees	DTN: MO0408SPADRWSD.002	table

Table 8-2.   Input Parameter Values for the ASHPLUME_DLL_LA V.2.1 Model for TSPA (Continued)

Seq. No.*	ASHPLUME Parameter (variable name) [Equation No.]	TSPA Parameter Name	Description	Units	Value	Distribution Type
		m_a)				
28	U (u) [Equation 6-2]	Varies by column height bin (e.g., Wind_Speed_1_2_km_a)	Wind Speed	cm/s	DTN: MO0408SPADRWSD.002	table
29	W_0 (werupt0) [Equation 6-3]	Erupt_Velocity_a	Initial rise velocity	cm/s	1.0×10^0 to 1.0×10^4	uniform
30	P (power) [Equation 6-7b]	Erupt_Power_a	Eruptive power	W	1.0×10^9 to 1.0×10^{12}	log-uniform
31	T_d (tdur) [Equation 6-7c]	Erupt_Time_a	Eruption duration	s	See Equations 8-1a and 8-1b	log-uniform
32	$rmin$ (rmin) [n/a]	Min_Rad [2]	Minimum radius (polar grid)	km	0.2	point value
33	$rfactor$ (rfactor) [n/a]	R_Factor [2]	Radial increment factor	None	1.2	point value
34	nr (nr) [n/a]	Nrr_Grid [2]	Number of radial divisions (0 for no polar grid)	None	31	point value
35	$nthet$ (nthet) [n/a]	Ntheta_Grid [2]	Number of angular increments	None	36	point value
36	$numapts$ (numapts) [n/a]	Num_pts	Number of points in ash/waste histogram output (0 for no hist)	None	0	point value
N/A	N/A	Magma_Partitioning_a	Fractional multiplier on waste mass to account for waste-containing magma erupted in scoria cone and lava flows	None	0.1 to 0.5	uniform
N/A	N/A	Vol_Time_Converter	Conversion factor for calculating min and max eruption duration bounds (Equations 8-1a, 8-1b)	$\dfrac{J \cdot m^3}{kg \cdot km^3}$	10^{15}	Point value
N/A	N/A	Grid_Flag	Model flag for grid type 0 = Cartesian Grid 1 = Polar Grid	None	0[1] 1[2]	Point value

Source: Output DTN: LA0702PADE03GK.002.

NOTES: *Seq. No. = GoldSim sequence number.

[1]   The ASHPLUME DLL is called twice. The [1] TSPA parameters are used in the first call to calculate ash deposition at the RMEI location only.
[2]   The second call to the ASHPLUME DLL uses the [2] TSPA parameters to calculate ash deposition on either a radial or Cartesian grid.

Table 8-3. Wind Speed in Relation to Height Above Yucca Mountain

Height above YM (km)	Minimum Wind Speed (cm/s)	Maximum Wind Speed (cm/s)	Average Wind Speed (cm/s)
0 to 1	0	4,670	668
1 to 2	0	4,480	817
2 to 3	0	5,000	1,007
3 to 4	0	6,400	1,215
4 to 5	0	10,500	1,486
5 to 6	0	14,100	1,695
6 to 7	0	10,300	1,949
7 to 8	0	11,000	2,160
8 to 9	0	8,700	2,294
9 to 10	0	8,640	2,416
10 to 11	0	8,900	2,437
11 to 12	0	9,900	2,311
12 to 13	0	7,300	2,064

Source: NOAA 2004 [DIRS 171035]; Output DTN: MO0408SPADRWSD.002.

NOTE: This table is also given as Table D-9 in Appendix D. The data listed in this table are representative of the wind-speed data listed in the attachment.

Table 8-4. Wind Direction PDF at 3 to 4 km Above Yucca Mountain

Compass Degrees	Ashplume Degrees	Count	PDF
165 to 195	90 (North)	5,788	0.0818
195 to 225	60	9,821	0.1388
225 to 255	30	12,019	0.1699
255 to 285	0 (East)	11,030	0.1559
285 to 315	−30	10,186	0.1440
315 to 345	−60	7,486	0.1058
345 to 15	−90 (South)	4,402	0.0622
15 to 45	−120	2,497	0.0353
45 to 75	−150	1,639	0.0232
75 to 105	180 (West)	1,407	0.0199
105 to 135	150	1,743	0.0246
135 to 165	120	2,730	0.0386
Total		70,748	1.0000

Source: NOAA 2004 [DIRS 171035]; Output DTN: MO0408SPADRWSD.002.

NOTE: The data listed in this table are representative of the wind-direction data listed
             Output DTN: MO0408SPADRWSD.002.
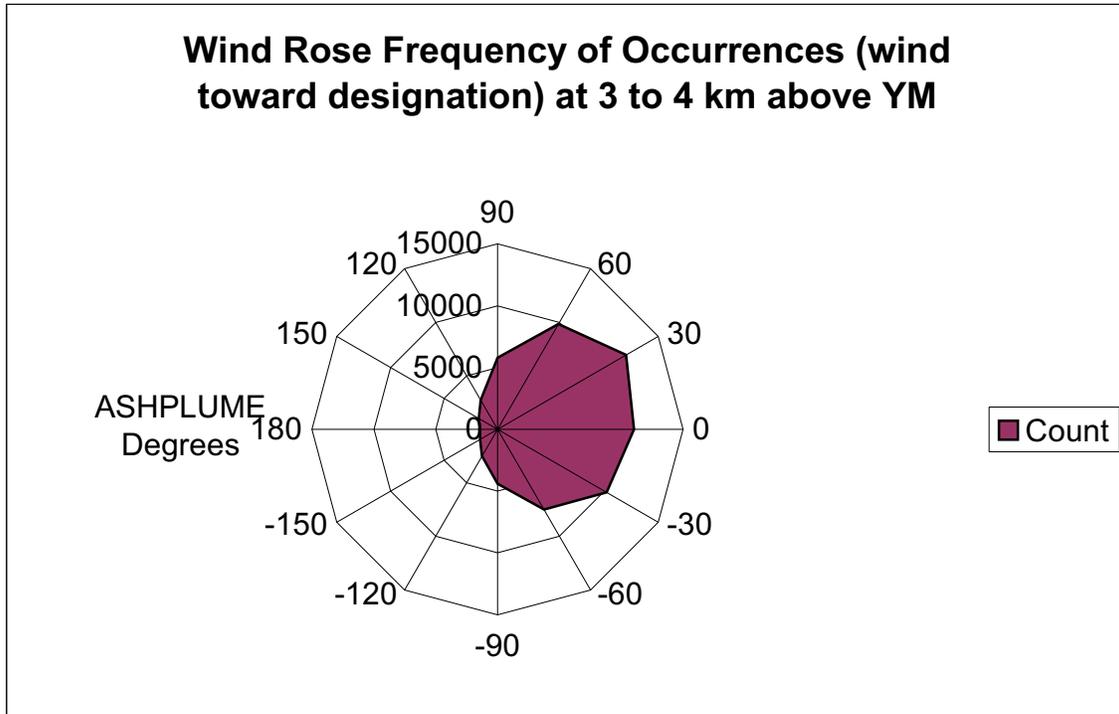
Source: NOAA 2004 [DIRS 171035]. Output DTN: MO0408SPADRWSD.002.

NOTE: The wind rose frequency of occurrences shown in this figure is a representation of the wind-direction data listed in Table 8-4.

Figure 8-1. Wind-Rose Frequency of Occurrences at 3 to 4 km Above Yucca Mountain

A new parameter has been added to the TSPA model for atmospheric dispersal and deposition of waste-containing tephra, entitled the "magma partitioning factor". This parameter is coded into GoldSim upstream of the call to ASHPLUME_DLL_LA V.2.1 [DIRS 178870]. The magma partitioning factor is provided as a range (0.1 to 0.5, uniform, Table 8-2). In a given TSPA realization, the value of total waste mass available for transport derived from sampling the number of waste packages hit (SNL 2007 [DIRS 177432]) is multiplied by the magma partitioning factor to result in a value for the input parameter, "mass of waste to incorporate," in the Ashplume model component (Seq. #26 in Table 8-2). The basis for the distribution of values for this parameter is discussed in Section 6.5.2.22.

8.3 OUTPUT UNCERTAINTY

The TSPA model uses Monte Carlo simulation as a method for mapping uncertainty in model parameters and future system states, expressed as probability distributions, into predictions of model output (SNL 2007 [DIRS 178871]). Quantification of the treatment of uncertainty for each uncertain parameter is discussed as part of the description of each parameter in Section 6.5.2. Epistemic uncertainties exist in Ashplume model input parameters due to the uncertainty in underlying data or imperfect knowledge of other required inputs (model for volcanic eruption). The uncertain parameter values for ASHPLUME input parameters (e.g., eruptive power, duration) have been derived from sparse observations of basaltic volcanoes worldwide, and the distributions are defined to reflect the generally low level of statistical knowledge. For example,

the distribution of values for eruptive power spans three orders of magnitude and is defined as log-uniform to reflect an equal likelihood of small or large events: data are not sufficiently abundant to define a more specific distribution, such as log-normal. Methods for the development of tabulated wind speed and direction parameters are described in Appendix D; values for these input parameters are listed in Output DTN: MO0408SPADRWSD.002 as cumulative distribution functions (wind speed) or probability distribution functions (wind direction) for each 1-km altitude bin above Yucca Mountain (for 1 to 13 km), as reported at Desert Rock for the years 1978 through 2003 (NOAA 2004 [DIRS 171035]). Table 8-2 shows all ASHPLUME input parameters and indicates those that are represented by probability distributions and those that use fixed values. These parameter uncertainties, represented by the parameter distributions developed and documented in this model report, are propagated throughout the TSPA model and reflected in the annual dose to the RMEI calculated by the TSPA model.

The Ashplume model has been validated by comparisons to tephra deposits at three analogue volcanoes and by extensive sensitivity analyses on individual parameters (summarized in Section 7). The results of the validation studies indicate that the model can successfully reproduce the pattern and thickness of tephra deposits when the model input parameters are derived from available site-specific eruption information supplemented by generalized "base-case" parameter values derived from the volcanological literature and field studies. Sensitivity studies indicate that the model results are relatively insensitive to variation in most parameters, the exceptions being wind speed and direction, and mean ash particle diameter, and, to a lesser extent, eruption power, and eruption duration. These parameters were reasonably well constrained for each of the analogue studies: in the case of Cerro Negro, field observations constrained all of these sensitive parameters; in the cases of Cinder Cone and Lathrop Wells, the tephra deposits were reproduced within the accuracy criteria by specifying reasonable "base-case" parameter values for these parameters.

Additional validation studies include independent technical review (Section 7.4), a code comparison (ASHPLUME to ASHFALL) (Section 7.5) and evaluation of the sensitivity of the coupled ASHPLUME-FAR models to variation in input parameter values (Section 7.6). These additional validation activities provide additional confidence that the uncertainties in the approach and parameter values for the Ashplume model have been adequately defined and propagated through the TSPA model.

INTENTIONALLY LEFT BLANK

9.   INPUTS AND REFERENCES

9.1   DOCUMENTS CITED

The following is a list of the references cited in this document. Column 1 represents the unique six-digit numerical identifier (the Document Input Reference System [DIRS] number), which is placed in the text following the reference callout (e.g., BSC 2003 [DIRS 168796]). The purpose of these numbers is to assist the reader in locating a specific reference in the DIRS database.

179761   Aloisi, M.; D'Agostino, M.; Dean, K.G.; Mostaccio, A.; and Neri, G. 2002. "Satellite Analysis and PUFF Simulation of the Eruptive Cloud Generated by the Mount Etna Paroxysm of 22 July 1998." *Journal of Geophysical Research, 107,* (B12), ECV 9-1-ECV 9-12. Washington, D.C.: American Geophysical Union. TIC: 257632.

179762   Armienti, P.; Macedonio, G.; and Pareschi, M.T. 1988. "A Numerical Model for Simulation of Tephra Transport and Deposition: Applications to May 18, 1980, Mount St. Helens Eruption." *Journal of Geophysical Research, 93,* (B6), 6463-6476. Washington, D.C.: American Geophysical Union. TIC: 257633.

165512   Bacon, C.R. 1977. "High Temperature Heat Content and Heat Capacity of Silicate Glasses: Experimental Determination and a Model for Calculation." *American Journal of Science, 277,* 109-135. New Haven, Connecticut: Yale University, Kline Geology Laboratory. TIC: 255125.

179747   Barberi, F.; Ghigliotti, M.; Macedonio, G.; Orellana, H.; Pareschi, M.T.; and Rosi, M. 1992. "Volcanic Hazard Assessment of Guagua Pichincha (Ecuador) Based on Past Behaviour and Numerical Models." *Journal of Volcanology and Geothermal Research, 49,* 53-68. Amsterdam, The Netherlands: Elsevier. TIC: 257637.

179753   Bonadonna, C.; Connor, C.B.; Houghton, B.F.; Connor, L.; Byrne, M.; Laing, A.; and Hincks, T.K. 2005. "Probabilistic Modeling of Tephra Dispersal: Hazard Assessment of a Multiphase Rhyolitic Eruption at Tarawera, New Zealand." *Journal of Geophysical Research, 110,* (B03203), 1-21. Washington, D.C.: American Geophysical Union. TIC: 257638.

181521   Bonadonna, C.; Ernst, G.G.J.; and Sparks, R.S.J. 1998. "Thickness Variations and Volume Estimates of Tephra Fall Deposits: The Importance of Particle Reynolds Number." *Journal of Volcanology and Geothermal Research, 81,* 173-187. New York, New York: Elsevier. TIC: 259539.

168796   BSC (Bechtel SAIC Company) 2003. *Risk Information to Support Prioritization of Performance Assessment Models.* TDR-WIS-PA-000009 REV 01 ICN 01 Errata 001. Las Vegas, Nevada: Bechtel SAIC Company. ACC: MOL.20021017.0045; DOC.20031014.0003.

166289   BSC 2003. *Technical Work Plan: Igneous Activity Assessment for Disruptive Events.* TWP-WIS-MD-000007 REV 04. Las Vegas, Nevada: Bechtel SAIC Company. ACC: DOC.20031125.0006.

170026   BSC 2004. *Atmospheric Dispersal and Deposition of Tephra from a Potential Volcanic Eruption at Yucca Mountain, Nevada.* MDL-MGR-GS-000002 REV 01. Las Vegas, Nevada: Bechtel SAIC Company. ACC: DOC.20041025.0003; DOC.20050606.0004.

169989   BSC 2004. *Characterize Framework for Igneous Activity at Yucca Mountain, Nevada.* ANL-MGR-GS-000001 REV 02. Las Vegas, Nevada: Bechtel SAIC Company. ACC: DOC.20041015.0002; DOC.20050718.0007.

174067   BSC 2005. *Atmospheric Dispersal and Deposition of Tephra from a Potential Volcanic Eruption at Yucca Mountain, Nevada.* MDL-MGR-GS-000002 REV 02. Las Vegas, Nevada: Bechtel SAIC Company. ACC: DOC.20050825.0001; DOC.20050908.0001; DOC.20060306.0008.

172827   BSC 2005. *Characteristics of the Receptor for the Biosphere Model.* ANL-MGR-MD-000005 REV 04. Las Vegas, Nevada: Bechtel SAIC Company. ACC: DOC.20050405.0005.

175539   BSC 2005. *Q-List.* 000-30R-MGR0-00500-000-003. Las Vegas, Nevada: Bechtel SAIC Company. ACC: ENG.20050929.0008.

174773   BSC 2005. *Technical Work Plan for: Igneous Activity Assessment for Disruptive Events.* TWP-WIS-MD-000007 REV 08. Las Vegas, Nevada: Bechtel SAIC Company. ACC: DOC.20050815.0001.

165503   Codell, R. 2003. "Alternative Igneous Source Term Model for the Yucca Mountain Repository." Proceedings of the 10th International High-Level Radioactive Waste Management Conference (IHLRWM), March 30-April 2, 2003, Las Vegas, Nevada. Pages 405-412. La Grange Park, Illinois: American Nuclear Society. TIC: 254559.

181522   Codell, R.B. 2004. "Alternative Igneous Source Term Model for Tephra Dispersal at the Yucca Mountain Repository." *Nuclear Technology, 148,* 205-212. La Grange Park, Illinois: Nuclear Technology. TIC: 259537.

179760   Connor, L.J. and Connor, C.B. 2006. "Inversion is the Key to Dispersion: Understanding Eruption Dynamics by Inverting Tephra Fallout." In *Statistics in Volcanology,* No. 1, Pages 231-242 of *Special Publications of the IAVCEI.* Mader, H.M., Coles, S.G., Connor, C.B., and Connor, L.J., eds. Tulsa, Oklahoma: Geological Society. TIC: 259238.

100973   Crowe, B.M. and Perry, F.V. 1990. "Volcanic Probability Calculations for the Yucca Mountain Site: Estimation of Volcanic Rates." *Proceedings of the Topical Meeting on Nuclear Waste Isolation in the Unsaturated Zone, FOCUS '89, September 17-21, 1989, Las Vegas, Nevada.* Pages 326-334. La Grange Park, Illinois: American Nuclear Society. TIC: 212738.

100116   CRWMS M&O 1996. *Probabilistic Volcanic Hazard Analysis for Yucca Mountain, Nevada.* BA0000000-01717-2200-00082 REV 0. Las Vegas, Nevada: CRWMS M&O. ACC: MOL.19971201.0221.

132547   CRWMS M&O 1999. *ASHPLUME Version 1.4LV Design Document.* 10022-DD-1.4LV-00, Rev. 00. Las Vegas, Nevada: CRWMS M&O. ACC: MOL.20000424.0415.

161492   CRWMS M&O 2000. *ASHPLUME Version 1.4LV Validation Test Report.* 10022 VTR-1.4LV-00 REV 00. Las Vegas, Nevada: CRWMS M&O. ACC: MOL.20000424.0419.

174768   CRWMS M&O 2001. *ASHPLUME, V2.0, User's Manual.* Software Document Number: 10022-UM-2.0-00. Las Vegas, Nevada: CRWMS M&O. ACC: MOL.20011119.0008.

123714   Davis, J.C. 1986. *Statistics and Data Analysis in Geology.* 2nd Edition. New York, New York: John Wiley and Sons. TIC: 214516.

164019   Dehaudt, P. 2001. "Physical and Chemical State of the Nuclear Spent Fuel After Irradiation." Section 5.2 of *Synthesis on the Long Term Behavior of the Spent Nuclear Fuel.* Poinssot, C., ed. CEA-R-5958(E). Volume I. Paris, France: Commissariat à l'Énergie Atomique. TIC: 253976.

169660   Detournay, E.; Mastin, L.G.; Pearson, J.R.A.; Rubin, A.M.; and Spera, F.J. 2003. *Final Report of the Igneous Consequences Peer Review Panel, with Appendices.* Las Vegas, Nevada: Bechtel SAIC Company. ACC: MOL.20031014.0097; MOL.20030730.0163.

166027   DOE (U.S. Department of Energy) 2003. *Review of Oxidation Rates of DOE Spent Nuclear Fuel Part 2. Nonmetallic Fuel.* DOE/SNF/REP-068, Rev. 0. Idaho Falls, Idaho: U.S. Department of Energy, Idaho Operations Office. ACC: DOC.20030905.0009.

182051   DOE 2007. *Quality Assurance Requirements and Description.* DOE/RW-0333P, Rev. 19. Washington, D. C.: U.S. Department of Energy, Office of Civilian Radioactive Waste Management. ACC: DOC.20070717.0006.

156447   Drury, M.J. 1987. "Thermal Diffusivity of Some Crystalline Rocks." *Geothermics, 16,* (2), 105-115. New York, New York: Pergamon Press. TIC: 251764.

101607   Einziger, R.E.; Thomas, L.E.; Buchanan, H.C.; and Stout, R.B. 1992. "Oxidation of Spent Fuel in Air at 175 to 195°C." *Journal of Nuclear Materials, 190,* 53-60. Amsterdam, The Netherlands: North-Holland Publishing Company. TIC: 238511.

171915   EPRI (Electric Power Research Institute) 2004.   *Potential Igneous Processes Relevant to the Yucca Mountain Repository: Extrusive-Release Scenario.* EPRI TR-1008169. Palo Alto, California: Electric Power Research Institute. TIC: 256654.

112115   Evans, M.; Hastings, N.; and Peacock, B. 1993. *Statistical Distributions.*   2nd Edition. New York, New York: John Wiley & Sons. TIC: 246114.

127332   Finch, R.J.; Buck, E.C.; Finn, P.A.; and Bates, J.K. 1999. "Oxidative Corrosion of Spent UO_2 Fuel in Vapor and Dripping Groundwater at 90°C." *Scientific Basis for Nuclear Waste Management XXII, Symposium held November 30-December 4, 1998, Boston, Massachusetts, U.S.A.* Wronkiewicz, D.J. and Lee, J.H., eds. *556,* 431-438. Warrendale, Pennsylvania: Materials Research Society. TIC: 246426.

179323   Finch, R. and Fortner, J. 2002. Petri Dish Tests. Spent Fuel. Scientific Notebook 1547. LL001104412241.019. ACC: MOL.19980731.0070; MOL.20040611.0040.

162806   Fisher, R.V. and Schmincke, H.-U. 1984.   *Pyroclastic Rocks.* New York, New York: Springer-Verlag. TIC: 223562.

181523   Folch, A. and Felpeto, A. 2005. "A Coupled Model for Dispersal of Tephra During Sustained Explosive Eruptions." *Journal of Volcanology and Geothermal Research, 145,* 337-349. New York, New York: Elsevier. TIC: 259538.

110277   Glaze, L.S. and Self, S. 1991. "Ashfall Dispersal for the 16 September 1986, Eruption of Lascar, Chile, Calculated by a Turbulent Diffusion Model." *Geophysical Research Letters, 18,* (7), 1237-1240. Washington, D.C.: American Geophysical Union. TIC: 245739.

100758   Gray, W.J. and Wilson, C.N. 1995.   *Spent Fuel Dissolution Studies FY 1991-1994.* PNL-10450. Richland, Washington: Pacific Northwest Laboratory. ACC: MOL.19960802.0035.

127061   Guenther, R.J.; Blahnik, D.E.; Campbell, T.K.; Jenquin, U.P.; Mendel, J.E.; Thomas, L.E.; and Thornhill, C.K. 1991. *Characterization of Spent Fuel Approved Testing Material - ATM-105.* PNL-5109-105. Richland, Washington: Pacific Northwest Laboratory. TIC: 203785.

109207   Guenther, R.J.; Blahnik, D.E.; Jenquin, U.P.; Mendel, J.E.; Thomas, L.E.; and Thornhill, C.K. 1991. *Characterization of Spent Fuel Approved Testing Material-- ATM-104.* PNL-5109-104. Richland, Washington: Pacific Northwest Laboratory. TIC: 203846.

173851   Harrison, R.M. 1993. "Atmospheric Pathways." Chapter 3 of *Radioecology after Chernobyl, Biogeochemical Pathways of Artificial Radionuclides.* Warner, F. and Harrison, R.M., eds. SCOPE 50. New York, New York: John Wiley & Sons. TIC: 257252.

179763   Heffter, J.L. 1996. "Volcanic Ash Model Verification Using a Klyuchevskoi Eruption." *Geophysical Research Letters, 23,* (12), 1489-1492. Washington, D.C.: American Geophysical Union. ACC: LLR.20070321.0103.

179744   Heffter, J.L. and Stunder, B.J.B. 1993. "Volcanic Ash Forecast Transport and Dispersion (VAFTAD) Model." *Weather and Forecasting, 8,* 533-541. Boston, Massachusetts: American Meteorological Society. TIC: 257635.

162817   Heiken, G. 1978. "Characteristics of Tephra from Cinder Cone, Lassen Volcanic National Park, California." *Bulletin of Volcanology, 41-2,* 119–130. New York, New York: Springer-Verlag. TIC: 235508.

107255   Heizler, M.T.; Perry, F.V.; Crowe, B.M.; Peters, L.; and Appelt, R. 1999. "The Age of Lathrop Wells Volcanic Center: An ^{40}Ar/^{39}Ar Dating Investigation." *Journal of Geophysical Research, 104,* (B1), 767-804. Washington, D.C.: American Geophysical Union. TIC: 243399.

151040   Hill, B.E.; Connor, C.B.; Jarzemba, M.S.; La Femina, P.C.; Navarro, M.; and Strauch, W. 1998. "1995 Eruptions of Cerro Negro Volcano, Nicaragua, and Risk Assessment for Future Eruptions." *Geological Society of America Bulletin, 110,* (10), 1231-1241. Boulder, Colorado: Geological Society of America. TIC: 245102.

110280   Hopkins, A.T. and Bridgman, C.J. 1985. "A Volcanic Ash Transport Model and Analysis of Mount St. Helens Ashfall." *JGR: Journal of Geophysical Research, 90,* (D6), 10,620-10,630. Washington, D.C.: American Geophysical Union. TIC: 245738.

176897   Hurst, A.W. and Turner, R. 1999. "Performance of the Program ASHFALL for Forecasting Ashfall During the 1995 and 1996 Eruptions of Ruapehu Volcano." *New Zealand Journal of Geology and Geophysics, 42,* (4), 615-622. Thorndon, Wellington, New Zealand: RSNZ Publishing. TIC: 257647.

100460   Jarzemba, M.S. 1997. "Stochastic Radionuclide Distributions After a Basaltic Eruption for Performance Assessments of Yucca Mountain." *Nuclear Technology, 118,* 132-141. Hinsdale, Illinois: American Nuclear Society. TIC: 237944.

100987   Jarzemba, M.S.; LaPlante, P.A.; and Poor, K.J. 1997. *ASHPLUME Version 1.0—A Code for Contaminated Ash Dispersal and Deposition, Technical Description and User's Guide.* CNWRA 97-004, Rev. 1. San Antonio, Texas: Center for Nuclear Waste Regulatory Analyses. ACC: MOL.20010727.0162.

119269   Kutzbach, J.E.; Guetter, P.J.; Behling, P.J.; and Selin, R. 1993. "Simulated Climatic Changes: Results of the COHMAP Climate-Model Experiments." Chapter 4 of *Global Climates Since the Last Glacial Maximum.* Wright, H., Jr.; Kutzbach, J.; Webb, T., III; Ruddiman, W.; Street-Perrott, F., Bartlein, P., eds. Minneapolis, Minnesota: University of Minnesota Press. TIC: 234248.

147834   Lide, D.R., ed. 1994. *CRC Handbook of Chemistry and Physics, A Ready-Reference Book of Chemical and Physical Data.* 75th Edition. Boca Raton, Florida: CRC Press. TIC: 102972.

144310   Luhr, J.F. and Simkin, T., eds. 1993. *Paricutin, The Volcano Born in a Mexican Cornfield.* Phoenix, Arizona: Geoscience Press. TIC: 247017.

179745   Macedonio, G.; Pareschi, M.T.; and Santacroce, R. 1988. "A Numerical Simulation of the Plinian Fall Phase of 79 A.D. Eruption of Vesuvius." *Journal of Geophysical Research, 93,* (B12), 14,817-14,827. Washington, D.C.: American Geophysical Union. TIC: 257641.

101726   McEachern, R.J. and Taylor, P. 1997. *A Review of the Oxidation of Uranium Dioxide at Temperatures Below 400°C.* AECL-11335. Pinawa, Manitoba, Canada: Atomic Energy of Canada Limited. TIC: 232575.

162827   McKnight, S.B. and Williams, S.W. 1997. "Old Cinder Cone or Young Composite Volcano?: The Nature of Cerro Negro, Nicaragua." *Geology, 25,* (4), 339–342. Boulder, Colorado: Geological Society of America. TIC: 254104.

170378   Mück, K.; Pröhl, G.; Likhtarev, I.; Kovgan, L.; Golikov, V.; and Zeger, J. 2002. "Reconstruction of the Inhalation Dose in the 30-km Zone After the Chernobyl Accident." *Health Physics, 82,* (2), 157-172. Philadelphia, Pennsylvania: Lippincott Williams & Wilkins. TIC: 256234.

174224   NEA (Nuclear Energy Agency) 2002. *Chernobyl, Assessment of Radiological and Health Impacts.* Paris, France: Organization for Economic Co-Operation and Development, Nuclear Energy Agency. TIC: 257424.

171035   NOAA (National Oceanic and Atmospheric Administration) 2004. *Upper Air Data for Desert Rock, Nevada Years 1978-2003. NCDC (National Climatic Data Center) Digital Upper Air Files TD 6201 and 6301 (Includes Compact Disk and Special Instruction Sheet with Listing of Files).* Asheville, North Carolina: National Oceanic and Atmospheric Administration. ACC: MOL.20040817.0103.

100297   NRC (U.S. Nuclear Regulatory Commission) 1998. *Issue Resolution Status Report Key Technical Issue: Igneous Activity.* Rev. 0. Washington, D.C.: U.S. Nuclear Regulatory Commission. ACC: MOL.19980514.0576.

159538   NRC 2002. *Integrated Issue Resolution Status Report.* NUREG-1762. Washington, D.C.: U.S. Nuclear Regulatory Commission, Office of Nuclear Material Safety and Safeguards. TIC: 253064.

163274   NRC 2003. *Yucca Mountain Review Plan, Final Report.* NUREG-1804, Rev. 2. Washington, D.C.: U.S. Nuclear Regulatory Commission, Office of Nuclear Material Safety and Safeguards. TIC: 254568.

144335   Perry, F.V.; Crowe, B.M.; Valentine, G.A.; and Bowker, L.M., eds. 1998. *Volcanism Studies: Final Report for the Yucca Mountain Project.* LA-13478. Los Alamos, New Mexico: Los Alamos National Laboratory. TIC: 247225.

174826   Pfeiffer, T.; Costa, A.; and Macedonio, G. 2005. "A Model for the Numerical Simulation of Tephra Fall Deposits." *Journal of Volcanology and Geothermal Research, 140,* 273-294. New York, New York: Elsevier. TIC: 257591.

182321   Pfeifle, T. 2007. "Independent Technical Review of ASHPLUME Model, Described in MDL-MGR-GS-000002, Rev 00B, by F.J. Spera, April 10, 2003. Accession Number: LLR.20070726.0119." Memorandum from T. Pfeifle to File, August 2, 2007, with attachment. ACC: LLR.20070807.0300; LLR.20070726.0119.

119317   Quiring, R.F. 1968. *Climatological Data Nevada Test Site and Nuclear Rocket Development Station.* ESSA Research Laboratories Technical Memorandum - ARL 7. Las Vegas, Nevada: U.S. Department of Commerce, Environmental Science Services Administration Research Laboratories. ACC: NNA.19870406.0047.

119693   Reamer, C.W. 1999. "Issue Resolution Status Report (Key Technical Issue: Igneous Activity, Revision 2)." Letter from C.W. Reamer (NRC) to Dr. S. Brocoum (DOE/YMSCO), July 16, 1999, with enclosure. ACC: MOL.19990810.0639.

145235   Sagar, B., ed. 1997. *NRC High-Level Radioactive Waste Program Annual Progress Report: Fiscal Year 1996.* NUREG/CR-6513, No. 1. Washington, D.C.: U.S. Nuclear Regulatory Commission. ACC: MOL.19970715.0066.

156313   Sandoval, R.P.; Weber, J.P.; Levine, H.S.; Romig, A.D.; Johnson, J.D.; Luna, R.E.; Newton, G.J.; Wong, B.A.; Marshall, R.W., Jr.; Alvarez, J.L.; and Gelbard, F. 1983. *An Assessment of the Safety of Spent Fuel Transportation in Urban Environs.* SAND82-2365. Albuquerque, New Mexico: Sandia National Laboratories. ACC: NNA.19870406.0489.

165740   Schlueter, J.R. 2003. "Igneous Activity Agreement 2.09, Additional Information Needed." Letter from J.R. Schlueter (NRC) to J.D. Ziegler (DOE/ORD), March 25, 2003, 0331036684, with enclosure. ACC: MOL.20031009.0249.

101015   Searcy, C.; Dean, K.; and Stringer, W. 1998. "PUFF: A High-Resolution Volcanic Ash Tracking Model." *Journal of Volcanology and Geothermal Research, 80,* 1-16. Amsterdam, The Netherlands: Elsevier. TIC: 238696.

106143   Selby, S.M., ed. 1975. *CRC Standard Mathematical Tables.* 23rd Edition. Cleveland, Ohio: CRC Press. TIC: 247118.

162831   Self, S. and Walker, G.P.L. 1994. "Ash Clouds: Characteristics of Eruption Columns." Volcanic Ash and Aviation Safety: Proceedings of the First International Symposium on Volcanic Ash and Aviation Safety held in Seattle, Washington in July 1991. Casadevall, T.J., ed. U.S. Geological Survey Bulletin 2047. Pages 65–74. Washington, D.C.: U.S. Government Printing Office. TIC: 254494.

174260   SNL (Sandia National Laboratories) 2007. *Characterize Eruptive Processes at Yucca Mountain, Nevada.* ANL-MGR-GS-000002 REV 03. Las Vegas, Nevada: Sandia National Laboratories. ACC: DOC.20070301.0001.

177430   SNL 2007. *Dike/Drift Interactions.* MDL-MGR-GS-000005 REV 02. Las Vegas, Nevada: Sandia National Laboratories.

177432   SNL 2007. *Number of Waste Packages Hit by Igneous Events.* ANL-MGR-GS-000003 REV 03. Las Vegas, Nevada: Sandia National Laboratories.

179347   SNL 2007. *Redistribution of Tephra and Waste by Geomorphic Processes Following a Potential Volcanic Eruption at Yucca Mountain, Nevada.* MDL-MGR-GS-000006 REV 00. Las Vegas, Nevada: Sandia National Laboratories.

181650   SNL 2007. *Saturated Zone Flow and Transport Model Abstraction*. MDL-NBS-HS-000021 REV03 AD01. Las Vegas, Nevada: Sandia National Laboratories.

182219   SNL 2007. *Technical Work Plan for: Igneous Activity Assessment for Disruptive Events.* TWP-WIS-MD-000007 REV 10. Las Vegas, Nevada: Sandia National Laboratories.

178871   SNL 2007. *Total System Performance Assessment Model /Analysis for the License Application.* MDL-WIS-PA-000005 REV 00. Las Vegas, Nevada: Sandia National Laboratories.

144352   Sparks, R.S.J; Bursik, M.I.; Carey, S.N.; Gilbert, J.S.; Glaze, L.S.; Sigurdsson, H.; and Woods, A.W. 1997. *Volcanic Plumes*. 574. New York, New York: John Wiley and Sons. TIC: 247134.

100489   Suzuki, T. 1983. "A Theoretical Model for Dispersion of Tephra." *Arc Volcanism: Physics and Tectonics, Proceedings of a 1981 IAVCEI Symposium, August-September, 1981, Tokyo and Hakone.* Shimozuru, D. and Yokoyama, I., eds. Pages 95-113. Tokyo, Japan: Terra Scientific Publishing Company. TIC: 238307.

153441   Swan, A.R.H. and Sandilands, M. 1998. *Introduction to Geological Data Analysis.* Malden, Massachusetts: Blackwell Science. TIC: 249127.

179741   Tanaka, H.L. and Yamamoto, K. 2002. "Numerical Simulation of Volcanic Plume Dispersal from Usu Volcano in Japan on 31 March 2000 Using PUFF Model." *Earth Planets and Space, 54,* 743-752. Tokyo, Japan: Terra Scientific Publishing. TIC: 257640.

179765   Turner, R. and Hurst, T. 2001. "Factors Influencing Volcanic Ash Dispersal from the 1995 and 1996 Eruptions of Mount Ruapehu, New Zealand." *Journal of Applied Meteorology, 40,* 56-69. Boston, Massachusetts: American Meteorological Society. TIC: 257636.

174141   Ushakov, S.V.; Burakov, B.E.; Shabalev, S.I.; and Anderson, E.B. 1997. "Interaction of UO_2 and Zircaloy During the Chernobyl Accident." *Scientific Basis for Nuclear Waste Management XX, Materials Research Society Symposium held December 2-6, 1996, Boston, Massachusetts.* Gray, W.J. and Triay, I.R., eds. *465,* 1313-1318. Pittsburgh, Pennsylvania: Materials Research Society. TIC: 238884.

181477   Valentine, G.A. 1998. "Eruption Column Physics." In *Developments in Volcanology 4,* Chapter 4 of *From Magma to Tephra, Modelling Physical Processes of Explosive Volcanic Eruptions.* Freundt, A. and Rosi, eds. New York, New York: Elsevier. TIC: 248078.

181319   Walker, G.P.L.; Wilson, L.; and Bowell, E.L.G. 1971. "Explosive Volcanic Eruptions-I The Rate of Fall of Pyroclasts." *Geophysical Journal of the Royal Astronomical Society, 22,* 377-383. Oxford, England: Blackwell Scientific Publications. TIC: 259489.

100476   Wescott, R.G.; Lee, M.P.; Eisenberg, N.A.; McCartin, T.J.; and Baca, R.G., eds. 1995. NRC Iterative Performance Assessment Phase 2, Development of Capabilities for Review of a Performance Assessment for a High-Level Waste Repository. NUREG-1464. Washington, D.C.: U.S. Nuclear Regulatory Commission. ACC: MOL.19960710.0075.

101034   Wilson, L. and Head, J.W., III 1981. "Ascent and Eruption of Basaltic Magma on the Earth and Moon." *Journal of Geophysical Research, 86,* (B4), 2971-3001. Washington, D.C.: American Geophysical Union. TIC: 225185.

162859   Wilson, L.; Sparks, R.S.J.; Huang, T.C.; and Watkins, N.D. 1978. "The Control of Volcanic Column Heights by Eruption Energetics and Dynamics." *Journal of Geophysical Research, 83,* (B4), 1829–1836. Washington, D.C.: American Geophysical Union. TIC: 254493.

172081   Woods, A.W. 1988. "The Fluid Dynamics and Thermodynamics of Eruption Columns." *Bulletin of Volcanology, 50,* 169-193. Berlin, Germany: Springer-Verlag. TIC: 256689.

152504   Wunderman, R. and Venzke, E., eds. 1995. "Global Volcanism Program." Bulletin of the Global Volcanism Network, Volume 20, Number 11/12 (December 1995). Washington, D.C.: Smithsonian Institution. Accessed November 10, 2000. TIC: 249090. http://nmnhwww.si.edu/gvp/archive/1995/2012_gvn.htm.

9.2   CODES, STANDARDS, REGULATIONS, AND PROCEDURES

180319   10 CFR 63. 2007. Energy: Disposal of High-Level Radioactive Wastes in a Geologic Repository at Yucca Mountain, Nevada. Internet Accessible.

IM-PRO-002, *Control of the Electronic Management of Information*.

IM-PRO-003, *Software Management*.

SCI-PRO-001, *Qualification of Unqualified Data*.

SCI-PRO-002, *Planning for Science Activities*.

SCI-PRO-006, *Models*.

9.3   SOFTWARE

176015   ArcGIS Desktop V. 9.1. 2005. WINDOWS XP. STN: 11205-9.1-00.

180147   ASHPLUME_DLL_LA V. 2.1. 2007. WINDOWS 2003. STN: 11117-2.1-01.

178870   ASHPLUME_DLL_LA. V. 2.1. 2006. WINDOWS 2000/XP. STN: 11117-2.1-00.

182225   FAR V. 1.2. 2007. WINDOWS 2000 & WINDOWS 2003. STN: 11190-1.2-00.

154748   ASHPLUME V. 1.4LV-dll. 2000. PC, Windows 95/NT. 10022-1.4LV-dll-00.

152844   ASHPLUME V. 2.0. 2001. PC. STN: 10022-2.0-00.

166571   ASHPLUME_DLL_LA V. 2.0. 2003. PC, Windows 2000. STN: 11117-2.0-00.

180224   GoldSim V. 9.60. 2007. PC, WINDOWS 2000, WINDOWS XP, WINDOWS 2003. STN: 10344-9.60-00.

9.4   SOURCE DATA, LISTED BY DATA TRACKING NUMBER

179987   LA0612DK831811.001. Magma and Eruption Properties for Potential Volcano at Yucca Mountain. Submittal date: 03/23/2007.

155224   LL001104412241.019. An Estimate of the Fuel-Particle Sizes for Physically Degraded Spent Fuel Following a Disruptive Volcanic Event Through the Repository. Submittal date: 11/29/2000.

165922   MO9912GSC99492.000. Surveyed USW SD-6 As-Built Location. Submittal date: 12/21/1999.

179527   MO0605SPAFORTY.000. Fortymile Wash Drainage Basin Dem. Submittal date: 05/23/2006.

181613   MO0706SPAFEPLA.001. FY 2007 LA FEP List and Screening. Submittal date: 06/20/2007.

9.5   DEVELOPED DATA AND PRODUCT OUTPUTS, LISTED BY DATA TRACKING NUMBER

LA0702PADE03GK.001. Proportion of Magma Deposited in Analog Tephra Sheets. Submittal date: 2/1/2007.

LA0702PADE03GK.002. Input Parameter Values for the ASHPLUME V 2.1_DLL_LA Model for TSPA. Submittal date: 2/2/2007.

MO0408SPADRWSD.002. Desert Rock Wind Speed and Wind Direction Analyses for Years 1978 - 2003. Submittal date: 8/19/2004.

MO0506SPACHERN.000. Analysis of Chernobyl Hot Particle Data to Assess Source-Term Maximum Particle Size. Submittal date: 06/16/2005.

LA0508GK831811.002. Ashplume Model Validation Statistics for Lathrop Wells Volcano and Cinder Cone Case Studies. Submittal date: 8/12/2005.

LA0706GK150308.001. Model Input/Output Files for Ashplume-Ashfall Code Comparison. Submittal date: 06/28/2007.

LA0708GK150308.001. Model Input/Output files for Ashplume-FAR Coupled Model Validation. Submittal date: 8/27/2007.

INTENTIONALLY LEFT BLANK

APPENDIX A
QUALIFICATION OF EXTERNAL SOURCES

APPENDIX A
QUALIFICATION OF INPUT DATA

External sources have provided unqualified data that have been used as direct input to this document. The inputs from these sources are qualified for intended use within this document using the criteria found in SCI-PRO-006, *Models*. These criteria represent a subset of the methods and attributes required for qualification of data per SCI-PRO-001, *Qualification of Unqualified Data*, Attachment 3.

Data for Qualification

There are six external sources of data used as direct input to this report:

- Jarzemba et al. 1997 [DIRS 100987], column diffusion constant, β, as discussed in Section 6.5.2.3

- Suzuki 1983 [DIRS 100489], eddy diffusivity constant, as discussed in Section 6.5.2.15, and column diffusion constant, β, as discussed in Section 6.5.2.3

- Bacon 1977 [DIRS 165512] and Drury (1987 [DIRS 156447], heat capacity of magma, as discussed in Section 6.5.2.10

- Jarzemba 1997 [DIRS 100460], ash particle shape factor, F, as discussed in Section 6.5.2.12, and eruptive power, as discussed in Section 6.5.2.1

- Woods 1988 [DIRS 172081], plots used to estimate the maximum value for the initial rise velocity of the convective-thrust region of an eruptive plume, as discussed in Section 6.5.2.10.

A1. METHOD OF QUALIFICATION SELECTED

The method for qualification of all five external sources of data is the "technical assessment method". The rationale for using this method is that all three of the qualification approaches for technical assessment (SCI-PRO-001, Attachment 3) of external source data are appropriate for consideration. Other qualification methods are not considered because they require information not available through the original source (i.e., scientific journal or publication). Qualification process attributes used in the technical assessment of each external source are selected from the list provided in Attachment 4 of SCI-PRO-001. Attributes used specifically as data qualification attributes in this report are:

1. Criterion 1 – Qualifications of personnel or organizations generating the data are comparable to qualification requirements of personnel generating similar data under an approved program that supports the YMP license application process or postclosure science

2. Criterion 3 – The extent to which the data demonstrate the properties of interest (e.g., physical, chemical, geologic, mechanical)

3. Criterion 7 – Prior peer or other professional reviews of the data and their results

4. Criterion 10 – Extent and quality of corroborating data or confirmatory testing results.

A2.   JARZEMBA, M.S., LAPLANTE, P.A., AND POOR, K.J. 1997

Reference—Jarzemba, M.S., LaPlante, P.A., and Poor, K.J. 1997. *ASHPLUME Version 1.0—A Code for Contaminated Ash Dispersal and Deposition, Technical Description and User's Guide.* CNWRA 97-004, Rev. 1. San Antonio, Texas: Center for Nuclear Waste Regulatory Analyses. ACC: MOL.20010727.0162 [DIRS 100987].

Description of Use—Jarzemba et al. (1997 [DIRS 100987]) is one of the sources for one parameter required by the ASHPLUME computer code. The parameter and its reference location in the report by Jarzemba et al. (1997 [DIRS 100987]) is as follows:

- Column Diffusion Constant, β (p. 4-1, Table 5-1).

The specific range of values for the column diffusion constant is discussed as in Section 6.5.2.3. The column diffusion constant (β) is set at a uniform distribution with a minimum value of 0.01 and a maximum value of 0.5. The column diffusion constant was discussed earlier by Suzuki (1983 [DIRS 100489], pp. 104 to 107). This parameter affects the distribution of particles vertically in the ash column and helps determine where particles exit the column. Jarzemba et al. (1997 [DIRS 100987], p. 4-1) uses a log-uniform distribution for beta that has a minimum value of 0.01 and a maximum value of 0.5. This range of values spans more than an order of magnitude and encompasses the range that is valid for the Ashplume model. However, to simulate the anvil cloud associated with a violent Strombolian eruption properly, samples from the range in beta should be focused toward the upper end of the range; therefore, a uniform (rather than log-uniform) distribution is recommended.

Extent to which the Data Demonstrate the Properties of Interest—The parameter value is provided in the documentation for the ASHPLUME code, *ASHPLUME Version 1.0—A Code for Contaminated Ash Dispersal and Deposition, Technical Description and User's Guide* (Jarzemba et al. 1997 [DIRS 100987]). The discussion of values for the column diffusion constant in the report by Jarzemba et al. (1997 [DIRS 100987]) build on theoretical considerations by Suzuki (1983 [DIRS 100489]), and therefore the values recommended by Jarzemba et al. (1997 [DIRS 100987]) provide the most thorough documentation of the technical basis for these parameter values.

Qualifications of Personnel or Organizations Generating the Data and Prior Use of the Data—The computer code, ASHPLUME, was developed at Southwest Research Institute, under contract to the NRC. The code is used to model volcanic ash and waste dispersal during a hypothetical future volcanic eruption through the repository. ASHPLUME Version 1.0, a code for contaminated ash dispersal and deposition, was prepared for the NRC under contract to the Center for Nuclear Waste Regulatory Analyses, San Antonio, Texas. The Center for Nuclear Waste Regulatory Analyses at Southwest Research Institute is a federally funded research and development center created to support the NRC. The source document (Jarzemba et al. 1997

[DIRS 100987]) is the technical description and user's guide for ASHPLUME, Version 1.0. The principal author of the code was Dr. Mark S. Jarzemba.

Qualifications of M.S. Jarzemba:

Education:

B.S. 1988, Engineering Physics, Ohio State University
M.S. 1991, Nuclear Engineering, Ohio State University
Ph.D. 1993, Nuclear Engineering, Ohio State University.

Dr. Jarzemba has over 15 years of research and professional experience. His background includes nuclear instrumentation and shielding, radon gas-phase transport modeling, environmental/dose pathway analyses and criticality analyses. At the time of publication, Dr. Jarzemba was a research scientist with Southwest Research Institute. Dr. Jarzemba is the author and co-author of numerous books and publications.

Based on the foregoing discussion, the data cited from the report by Jarzemba et al. (1997 [DIRS 100987]), can be accepted as qualified for use in this report.

A3.   SUZUKI, T. 1983

Reference—Suzuki, T. 1983. "A Theoretical Model for Dispersion of Tephra." *Arc Volcanism: Physics and Tectonics, Proceedings of a 1981 IAVCEI Symposium, August-September, 1981, Tokyo and Hakone.* Shimozuru, D. and Yokoyama, I., eds. Pages 95-113. Tokyo, Japan: Terra Scientific Publishing Company. TIC: 238307. [DIRS 100489]

Description of Use—Suzuki (1983 [DIRS 100489], p. 99, Figure 2) is the source for eddy diffusivity constant (400 cm^2/s$^{5/2}$) discussed in Section 6.5.2.15; the value is listed in Table 8-2 of this model report. Suzuki developed the mathematical model that underlies the ASHPLUME code, which is used in development of this model report. The underlying two-dimensional partial differential equation relates the change in concentration, ξ, at a point x-y (with x downwind) to wind velocity, *u*, and an eddy diffusivity constant, *C*.

Suzuki (1983 [DIRS 100489], pp. 104 to 107 is one of the two sources for column diffusion constant, β, along with Jarzemba et al. (1997 [DIRS 100987]). Suzuki (1983 [DIRS 100489], pp. 104 to 107) provides the theoretical basis for the use of the column diffusion constant in the Ashplume model and discusses the use of values of 0.01, 0.1, and 0.5.

Extent to which the Data Demonstrate the Properties of Interest—The Ashplume model for Yucca Mountain is based on a mathematical model of Suzuki (1983 [DIRS 100489]) that Jarzemba et al. (1997 [DIRS 100987]) refined to represent violent Strombolian-type eruptions. The code is used to model volcanic ash and waste dispersal during a hypothetical future volcanic eruption through the repository. The eddy diffusivity constant was developed as part of that mathematical model.

Prior Use of the Data—The above-listed reference document provides the basis for ASHPLUME, Version 1.0, a code for contaminated ash dispersal and deposition, prepared by the Center for Nuclear Waste Regulatory Analyses at Southwest Research Institute, San Antonio, Texas, under contract to the NRC. The code was developed for use in evaluation of potential igneous events at Yucca Mountain. The specific value for eddy diffusivity, $400 \text{ cm}^2/\text{s}^{5/2}$, was used as an input value to the code as documented in Tables 5-1 and 5-2 of Jarzemba et al. (1997 [DIRS 100987]). The resultant graph, Figure 5-1b, is identical to the results recorded by Suzuki (1983 [DIRS 100489], Figure 6c).

Based on the foregoing discussion, the data cited from Suzuki (1983 [DIRS 100489]) can be accepted as qualified for use in this AMR.

A4. BACON, C.R. 1977; DRURY, M.J. 1987

References—Bacon, C.R. 1977. "High Temperature Heat Content and Heat Capacity of Silicate Glasses: Experimental Determination and a Model for Calculation." *American Journal of Science, 277,* 109-135. New Haven, Connecticut: Yale University, Kline Geology Laboratory. TIC: 255125. [DIRS 165512]

Drury, M.J. 1987. "Thermal Diffusivity of Some Crystalline Rocks." *Geothermics, 16,* (2), 105-115. New York, New York: Pergamon Press. TIC: 251764. [DIRS 156447]

Description of Use—Bacon (1977 [DIRS 165512]) and Drury (1987 [DIRS 156447]) are used as the basis for the value (1,000 J/(kg-K)) selected for the heat capacity of magma as discussed in Section 6.5.2.10 of this report. The value is rounded from data presented in Figures 1 and 2 in the Bacon article, and from Table 2 in the Drury reference. Heat capacity is one of the variables in the calculation of initial rise velocity, W_0, which is a direct feed to TSPA-LA.

Extent to which the Data Demonstrate the Properties of Interest—Bacon (1977 [DIRS 165512]) documents the results of experimental work to determine the thermodynamic properties of silicate melts. The property of interest, heat capacity, is plotted for different compositions of silicate glasses at different temperatures. Bacon's compositions 1 through 3 bracket the magma compositions (discussed in SNL 2007 [DIRS 174260], Section 6.3.2.1) assumed for this model report. Drury (1987 [DIRS 156447]) also reports thermodynamic data from experimental work on igneous materials of different compositions, including the heat capacity for basalt.

Corroborative Data and Prior Use—The values and ranges for heat capacity for melts of basaltic compositions from these two articles are corroborative. For compositions close to those proposed for this model report, the Bacon reference shows experimental heat capacities ranging from 800 to 1,100 J/(kg-K). Drury (1987 [DIRS 156447]), listed a value of 1,010 J/(kg-K) for the basaltic composition. A value of 1,000 J/(kg-K) for specific heat is also reported in *Characterize Eruptive Processes at Yucca Mountain, Nevada* (SNL 2007 [DIRS 174260], Table 6-5). The similarity of reported values in the two references, combined with the prior use of the specific values in other igneous studies for Yucca Mountain, provide the necessary justification that this value is qualified for the intended use.

A5. JARZEMBA, M.S. 1997

Reference—Jarzemba, M.S. 1997. "Stochastic Radionuclide Distributions After a Basaltic Eruption for Performance Assessments of Yucca Mountain." *Nuclear Technology, 118,* 132-141. [Hinsdale, Illinois]: American Nuclear Society. TIC: 237944. [DIRS 100460]

Description of Use—Section 6.5.2.12 discusses the recommended value for ash particle shape factor (F) used in tephra dispersal calculations. Jarzemba (1997 [DIRS 100460], p. 139) used a value of F = 0.5 (with reference to theoretical considerations in Suzuki 1983 [DIRS 100489], pp. 99 to 100), and, consistent with conclusions in *Characterize Eruptive Processes at Yucca Mountain, Nevada* (SNL 2007 [DIRS 174260], Table 7-1), that value is recommended in this report for TSPA calculations.

Section 6.5.2.1 discusses the recommended range of values for eruptive power used in ASHPLUME tephra dispersal calculations. Jarzemba (1997 [DIRS 100460], p. 136, Table II) presented a table of eruptive power values developed from descriptions of historic eruptions at basaltic volcanoes worldwide. These values are used as the basis for developing the range of values for eruptive power for a potential basaltic eruption in the Yucca Mountain region.

Extent to which the Data Demonstrate the Properties of Interest—Section 6.5.2.12 discusses values for a clast shape factor for use in TSPA calculations of clast dispersal in the atmosphere. Jarzemba (1997 [DIRS 100460], p. 139) used a value of F = 0.5, which is considered to be representative of the range of common clast shapes. The range of values for eruptive power discussed in Section 6.5.2.1 relies on the quantification of eruptive power at historic volcanic eruptions developed by Jarzemba (1997 [DIRS 100460], p. 136).

Qualifications of Personnel or Organizations Generating the Data and Prior Use of the Data—Southwest Research Institute provides technical support for NRC Yucca Mountain programs; thus the Institute can be considered to have the necessary credentials to provide qualified data. This reference publishes some of the work that was conducted by Southwest Research Institute for the NRC. The referenced data have been acquired by Southwest Research Institute under contract to the NRC.

Dr. Jarzemba earned his Ph.D. in 1993 in Nuclear Engineering and an undergraduate degree in Engineering Physics from Ohio State University. Dr. Jarzemba has over 15 years of research and professional experience. At the time of publication, Dr. Jarzemba was a research scientist with Southwest Research Institute. Dr. Jarzemba is the author and coauthor of numerous books and publications. Dr. Jarzemba has established his reputation as a subject matter expert in atmospheric dispersal of tephra as the author of the ASHPLUME code, which he developed from the mathematical relationships originally presented by Suzuki (1983 [DIRS 100489]). His work in developing this code and validating its functionality establish his credentials for developing appropriate ranges of values for input parameters like eruptive power.

Based on the foregoing discussion, the data cited from a report by Jarzemba (1997 [DIRS 100460]), can be accepted as qualified for use in this report.

A6.   WOODS, A.W. 1988

Reference—Woods, A.W. 1988.   "The Fluid Dynamics and Thermodynamics of Eruption Columns."   *Bulletin of Volcanology, 50,* 169-191.   [Berlin, Germany]: Springer-Verlag. TIC: 256689. [DIRS 172081]

Description of Use—This reference provides equations and resulting plots used to estimate the maximum value for the initial rise velocity of the convective-thrust region of an eruptive plume (Section 6.5.2.10).   The report contains a discussion of the development of the equations and results, as well as associated limitations and assumptions.

Extent to which the Data Demonstrate the Properties of Interest—The maximum value specified for initial rise velocity (Section 6.5.2.10) reflects the upper end of possible velocities of the plume as it transitions from the gas-thrust to convective rise portions of the plume.   The velocity of the eruptive mixture decreases markedly from the vent to the base of the convective rise zone.   Results of the multiphase eruption column model developed by Woods (1988 [DIRS 172081], pp. 178 to 179) provide the basis for realistic maximum values.   Woods (1988 [DIRS 172081], Figure 2a) illustrates the variation in vertical plume velocity with height for a simulated eruption (initial column temperature of 1,000 K) for various vent radii.   The curves representing 20- and 50-m vent radii exhibit a rapid decrease in velocity through the gas-thrust region, resulting in a residual upward velocity of about 100 m/s at the base of the convective rise region (≤1,000 m above vent).   Above that velocity transition within the convective rise region, the velocities of the 20- and 50-m curves decrease monotonically, consistent with (and approximated by) the Ashplume model assumption of linear decrease in velocity with height. (Larger vent radii promote increasing mixing with ambient atmosphere, enhanced heat transfer, and superbuoyant convective plumes (Woods 1988 [DIRS 172081], pp. 178 to 179), which are inconsistent with the assumptions of the Ashplume model.)   For the upper end of expected conduit sizes, these 20- and 50-m vent radius curves on Figure 2a of the Woods report (1988 [DIRS 172081]) provide a reasonable upper bound on velocity—100 m/s—at the base of the convective thrust part of the eruption column.

Qualifications of Personnel or Organizations Generating the Data—Dr. Andrew Woods is an internationally recognized scientist in the fields of volcanology and earth and planetary science. Woods is a mathematician with expertise in fluid flow, working on problems in convection and solidification, turbulent buoyant plumes, ocean waves and volcanic eruption processes.   He has authored and coauthored numerous books and professional papers related to their fields of expertise.

Since receiving his BA in Mathematics in Cambridge (1985; St Johns College) and PhD in 1989, from the Department of Applied Mathematics and Theoretical Physics in Cambridge, Woods has worked at the Scripps Institute of Oceanography (La Jolla California: Green Scholar 1989 to 1990), the Institute of Theoretical Geophysics, Lecturer, Cambridge 1990 to 1996; School of Mathematics, Bristol as a Professor of Applied Mathematics, 1996 to 2000; and now he is the BP Professor, Cambridge, 2000 to the present, as well as a Professorial Fellow of St Johns.   He was the recipient of the Marcello Carapezza Prize, 1997; the Italgas Prize, 1997; and the Wager Medal, 2002, as well as being the Bullerwell Lecturer in 2000, the Stewartson Lecturer in 1999, and he presented the GFD Lecture in 2003.

APPENDIX B
YUCCA MOUNTAIN REVIEW PLAN (NUREG-1804)
ACCEPTANCE CRITERIA

B1.   BACKGROUND

Early in 1995, the NRC recognized the need to refocus its prelicensing repository program on resolving issues most significant to repository performance. In 1996, the NRC identified 10 key technical issues (Sagar 1997 [DIRS 145235]) intended to reflect the topics that the NRC considered most important to repository performance. The technical issues included igneous activity, and the status of resolution of each issue and associated open items were described by the NRC in a series of Issue Resolution Status Reports (e.g., Reamer 1999 [DIRS 119693]). In 2002, the NRC consolidated the subissues into a series of integrated subissues and replaced the series of nine issue resolution status reports with an Integrated Issue Resolution Status Report (NRC 2002 [DIRS 159538]). The Integrated Issue Resolution Status Report was based on the realization that the issue resolution process was "mature enough to develop a single Integrated Issue Resolution Status Report that would clearly and consistently reflect the interrelationships among the various key technical issue subissues and the overall resolution status" (NRC 2002 [DIRS 159538], pp. xviii and xix). The Integrated Issue Resolution Status Report and periodic letters from the NRC (e.g., Schlueter 2003 [DIRS 165740]) provide information about the resolution status of the integrated subissues that are described in *Yucca Mountain Review Plan*, *Final Report* (NUREG-1804) (NRC 2003 [DIRS 163274]).

B2.   IGNEOUS ACTIVITY KEY TECHNICAL ISSUE

The key technical issue for igneous activity was defined by the NRC staff as "predicting the consequence and probability of igneous activity affecting the repository in relationship to the overall system performance objective" (NRC 1998 [DIRS 100297], p. 3). Hence, the NRC defined two subissues for the igneous activity key technical issue: probability and consequences (NRC 1998 [DIRS 100297], p. 3). The probability subissue addresses the likelihood that future igneous activity would disrupt a repository at Yucca Mountain. The DOE estimated the probability of future disruption of a repository at Yucca Mountain in *Probabilistic Volcanic Hazard Analysis for Yucca Mountain, Nevada* (CRWMS M&O 1996 [DIRS 100116]). For the TSPA, an analysis based on *Probabilistic Volcanic Hazard Analysis for Yucca Mountain, Nevada* results and consideration of the repository design were updated and documented in *Characterize Framework for Igneous Activity at Yucca Mountain, Nevada* (BSC 2004 [DIRS 169989]).

The consequences subissue examined the effects of igneous activity on various engineered and natural components of the repository system. The consequences subissue comprises four integrated subissues: mechanical disruption of engineered barriers (NRC 2003 [DIRS 163274] Section 2.2.1.3.2); volcanic disruption of waste packages (NRC 2003 [DIRS 163274] Section 2.3.1.3.10); airborne transport of radionuclides (NRC 2003 [DIRS 163274] Section 2.3.1.3.11); and redistribution of radionuclides in soil (NRC 2003 [DIRS 163274] Section 2.3.1.3.13). This model report addresses the integrated subissue of airborne transport of radionuclides (NRC 2003 [DIRS 163274] Section 2.3.1.3.11). Mechanical disruption of engineered barriers and volcanic disruption of waste packages are addressed in *Dike/Drift Interactions* (SNL 2007 [DIRS 177430]), and *Number of Waste Packages Hit by Igneous Intrusion* (SNL 2007 [DIRS 177432]). Redistribution of radionuclides in soil is addressed in *Redistribution of Tephra and Waste by Geomorphic Processes Following a Potential Volcanic Eruption at Yucca Mountain, Nevada* (SNL 2007 [DIRS 179347]).

For the TSPA, two igneous modeling cases have been defined to evaluate the effects of igneous activity on the repository and its contents (SNL 2007 [DIRS 178871], Section 6.5):

- A volcanic eruption or direct-release modeling case featuring penetration of the repository by an ascending basaltic dike followed by eruption of contaminated ash at the surface

- An intrusion or indirect release modeling case featuring penetration of the repository by an ascending basaltic dike without surface eruption, followed by transport of mobilized radionuclides by groundwater flow processes.

For the TSPA, the direct-release model has been described, and documentation is provided in this model report to describe the atmospheric dispersal and subsequent deposition of contaminated tephra that could result from an eruption through the repository. For the igneous intrusion scenario, the potential effects of the repository on the propagation of a basaltic dike, the environmental conditions accompanying intersection of the repository by an ascending dike, and analyses of effects of intrusive igneous activity on repository structures and components are documented in *Dike/Drift Interactions* (SNL 2007 [DIRS 177430]).

A separate model report, *Redistribution of Tephra and Waste by Geomorphic Processes Following a Potential Volcanic Eruption at Yucca Mountain, Nevada* (SNL 2007 [DIRS 179347]), describes the ash redistribution conceptual model and documents the development and validation of that mode. The conceptual model is potentially important to the TSPA because redistribution of contaminated tephra deposits could affect the concentration of radioactive waste material at the RMEI location and, thereby, the dose to the RM EI.

B3.   YUCCA MOUNTAIN REVIEW PLAN ACCEPTANCE CRITERIA

The YMRP (NUREG-1804, NRC 2003 [DIRS 163274]) associates the integrated subissue of airborne transport of radionuclides with the requirements listed in 10 CFR 63.114(a) to (c) and (e) to (g) [DIRS 180319]).   NUREG-1804 (NRC 2003 [DIRS 163274], Sections 2.2.1.3.11) describes the acceptance criteria that the NRC will use to evaluate the adequacy of information addressing the airborne transport of radionuclides in the license application. The acceptance criteria may also be addressed in other analysis model reports that support the license application. The acceptance criteria will be considered fully addressed when this report is considered in conjunction with those reports. The following discussion provides a summary of how the information in this model report addresses those criteria that are associated with the development and use of the Ashplume model.

B4. NUREG-1804, REV 2, SECTION 2.2.1.3.10.3: VOLCANIC DISRUPTION OF WASTE PACKAGES

Acceptance Criterion 1: System Description and Model Integration Are Adequate

(2) *Models used to assess volcanic disruption of waste packages are consistent with physical processes generally interpreted from igneous features in the Yucca Mountain region and/or observed in active igneous systems.*

This model report provides information about the basis for the Ashplume conceptual model (Suzuki 1983 [DIRS 100489]) in Section 6.3. Section 6.3 also describes the consistency of the conceptual model with physical phenomena associated with violent Strombolian eruptions and the development and propagation of an ash cloud downwind of the eruption site followed by deposition of tephra deposits on the ground surface. Base-case model inputs and uncertainties and their consistency with igneous features either observed in the Yucca Mountain region or with features observed at analogue igneous systems are described in Section 6.5.2. The bases for the selection of an appropriate distribution for each uncertain parameter are described in this report (Section 6.5.2). Model inputs that are developed and documented in other analyses or models are appropriately identified, described, and cross-referenced.

Alternative models considered are described in Section 6.4.

(3) *Models account for changes in igneous processes that may occur from interaction with engineered repository systems.*

The Ashplume model does not account for changes in igneous processes that might result from interactions between processes and components of the engineered barrier system. Such interactions are described in other analyses or model reports, as appropriate (e.g., SNL 2007 [DIRS 177430]).

Acceptance Criterion 2: Data Are Sufficient For Model Justification

(1) *Parameter values used in the license application to evaluate volcanic disruption of waste packages are sufficient and adequately justified. Adequate descriptions of how the data were used, interpreted, and appropriately synthesized into the parameters are provided.*

Uses of the parameter values are generally described as part of the mathematical description of the base-case model in Section 6.5.1. The development of all model inputs used for the atmospheric dispersal model is discussed in Section 6.5.2. Subsections describe the individual model input parameters and provide detailed technical bases supporting the use of the numerical value or range for each parameter. Model report outputs for the TSPA are described in Section 8.2.

(2) Data used to model processes affecting volcanic disruption of waste packages are derived from appropriate techniques. These techniques may include site-specific field measurements, natural analog investigations, and laboratory experiments.

The parameter values used as inputs for ASHPLUME V.2.1 dll are described in the model report in Section 4.1, and model outputs are described in Section 8.2. Modeling objectives, the characteristics of the base-case model, consideration of alternative conceptual models, and the basis for the selection of ASHPLUME for modeling airborne transport of radionuclides are discussed in Sections 6.1, 6.3, 6.4, and 6.5, respectively. The formulation of the mathematical model is described in Section 6.5.1, and the base-case model inputs and their appropriateness are described in Section 6.5.2.

This model report describes the conceptual model, formulation of the mathematical model, identification of parameters, selection of appropriate parameter values or distributions, and discusses the consideration of alternative models. All of these considerations are included in the basis for selection of the ASHPLUME model as appropriate for analyzing the airborne transport of radionuclides for the license application. The alternative models considered are described in Section 6.4, and a summary of alternative conceptual models is provided in Section 6.4.7. Section 7 of the report discusses validation of the model and describes how the validation exercises have shown the efficacy of the Ashplume model to represent observed variations in tephra deposit thicknesses at analogue sites. The validation work also shows that the model is internally consistent and produces numerical convergence in simulations. These lines of evidence demonstrate that the Ashplume model is appropriate to analyze the airborne transport of radionuclides.

(3) Sufficient data are available to integrate features, events, and processes, relevant to volcanic disruption of waste packages into process-level models, including determination of appropriate interrelationships and parameter correlations.

Section 6.2 discusses FEPs related to the development and use of the Ashplume model. Table 6-1 identifies the specific FEPs associated with the Ashplume model and provides pointers to relevant sections of this report where these aspects are discussed.

Acceptance Criterion 3: Data Uncertainty Is Characterized and Propagated Through the Model Abstraction

(1) Models use parameter values, assumed ranges, probability distributions, and bounding assumptions that are technically defensible, and reasonably account for uncertainties and variabilities, and do not result in an under-representation of the risk estimate.

The mathematical formulation of the model is described in the model report (Section 6.5.1), and the inputs to the model and assumptions needed to use the Ashplume model for analysis are described in Section 6.5.2. Uncertainties associated with changes in igneous processes are included in Ashplume analyses through the use

of parameter distributions (Section 6.5.2). The bases for the selection of an appropriate distribution for each uncertain parameter are described in the report (Section 6.5.2). The reasonableness of values and distributions for parameters and their suitability for use are described in Section 6.5.2. Assumptions associated with the appropriateness of the Ashplume model are described in Section 5.1, and assumptions associated with specific model parameters are described in Section 5.2. The appropriateness of the base-case model is described in Section 6.3, and the consideration of alternative models is documented in Section 6.4. The screening of an alternative basis for the selection of ASHPLUME is also documented in Section 6.4 (see Table 6-2). Input parameter uncertainty is addressed in Section 4.1.2. These steps ensure that there is no under-representation of risk estimates.

(2) Parameter uncertainty accounts quantitatively for the uncertainty in parameter values observed in site data and the available literature (i.e., data precision), and the uncertainty in abstracting parameter values to process-level models (i.e., data accuracy).

Data precision is addressed in the mathematical description of the base case conceptual model (Section 6.5.1) and in the development of the input parameters (Section 6.5.2 and subsections). Data accuracy is addressed by evaluating uncertainties introduced by model abstraction. These uncertainties are explicitly addressed by the results of the model validation exercise (Sections 7.1, 7.2, 7.3, and 7.5), which shows how well the Ashplume model outputs conform to evaluation criteria, including sensitivity of outputs to variations in input parameters (Section 7.2), comparison of model ash thicknesses with observed thicknesses at analogue sites (Section 7.3), conservation of mass (CRWMS M&O 2000 [DIRS 161492]) (Section 7.3), and sensitivity of the coupled models of ash deposition and redistribution (Section 7.6).

Uncertainties associated with changes in igneous processes are included in Ashplume analyses through the use of parameter distributions (Section 6.5.2). The bases for the selection of an appropriate distribution for each uncertain parameter are described in the report (Section 6.5.2). Parameter uncertainty is addressed in Section 4.1.2.

Acceptance Criterion 4: Model Uncertainty Is Characterized and Propagated Through the Model Abstraction

(1) Alternative modeling approaches to volcanic disruption of the waste package are considered and are consistent with available data and current scientific understandings, and the results and limitations are appropriately considered in the abstraction.

The alternative models that were considered for modeling airborne transport of radionuclides are described in Section 6.4, including the screening of an alternative basis for the selection of ASHPLUME (see Table 6-2). The consistency of the Ashplume model with data and current scientific understanding is described in Sections 6.3 and 6.5.1. Sections 7.1 through 7.6 discuss validation of the model and

show how the validation exercises have demonstrated the efficacy of the Ashplume model to represent observed variations in tephra deposit thicknesses at analogue sites. The validation work shows that the model is internally consistent and produces numerical convergence in simulations. Limitations of the Ashplume model are discussed in Section 1.3.

(2) *Uncertainties in abstracted models are adequately defined and documented, and effects of these uncertainties are assessed in the total system performance.*

Uncertainties associated with Ashplume model outputs are described in Section 8.3; input parameters are described in Section 4.1.1, and parameter uncertainties are described in Section 4.1.2. Section 7.2 describes the sensitivity analyses that were done to evaluate the response of the Ashplume model over the entire range of model input parameter values. The results show that the model is sensitive to variations in eruptive power, wind speed, wind direction, and eruption duration. TSPA sensitivity to parameter variations is beyond the scope of this report.

(3) *Consideration of conceptual model uncertainty is consistent with available site characterization data, laboratory experiments, field measurements, natural analog information and process-level modeling studies; and the treatment of conceptual model uncertainty does not result in an under-representation of the risk estimate.*

The basis of the Ashplume conceptual model is described in Section 6.3, and the mathematical description of the base-case conceptual model is provided in Section 6.5.1. Uncertainties in the model outputs are described in Section 8.3, and conservatisms included to assure that model outputs to the TSPA do not result in an under representation of risk are described as part of the Ashplume model inputs (Section 6.5.2 and subsections).

The alternative models that were considered for modeling airborne transport of radionuclides are described in Section 6.4 and subsections, and are summarized in Section 6.4.7. The screening of an alternative basis for the selection of ASHPLUME is also documented in Section 6.4 (see Table 6-2). The consistency of the Ashplume model with data and current scientific understanding is described in Sections 6.3 and 6.5.1. Sections 7.1 through 7.6 discuss validation of the model and describe how the validation exercises have demonstrated the efficacy of the Ashplume model to represent observed variations in tephra deposit thicknesses at analogue sites. The validation work shows that the model is internally consistent and produces numerical convergence in simulations. Limitations of the Ashplume model are discussed in Section 1.3.

Acceptance Criterion 5: Model Abstraction Output is Supported by Objective Comparisons

(1) *Models implemented in the volcanic disruption of waste packages abstraction provide results consistent with output from detailed process-level models and/or empirical observations (laboratory and field testings and/or natural analogs).*

Section 6.2 lists the specific FEPs that are included in the Ashplume model. Section 6.3 provides a detailed description of the basis for the Ashplume conceptual model and the appropriateness of that model for the analysis of airborne transport of radionuclides. Section 6.5.1 provides a detailed description of the mathematical formulation of the base-case conceptual model and the consistency of that formulation with natural processes. Sections 7.1 through 7.6 discuss validation of the model and show how the validation exercises have shown the efficacy of the Ashplume model to represent observed variations in tephra deposit thicknesses at analogue sites. The validation work also shows that the model is internally consistent and produces numerical convergence in simulations. A comparison between the ASHPLUME and ASHFALL codes (Section 7.5) builds confidence that the Ashplume model is appropriate for its intended purpose.

(2) *Inconsistencies between abstracted models and comparative data are documented, explained, and quantified. The resulting uncertainty is accounted for in the model results.*

The model outputs are described in Section 8.2 and model output uncertainties are described in Section 8.3. Sections 7.1 through 7.5 discuss validation of the model and show how the validation exercises have shown the efficacy of the Ashplume model to represent observed variations in tephra deposit thicknesses at analogue sites (Section 7.3). The validation work also shows that the model is internally consistent and produces numerical convergence in simulations.

B5. NUREG 1804, REV 2, SECTION 2.2.1.3.11.3: INTEGRATED SUBISSUE: AIRBORNE TRANSPORT OF RADIONUCLIDES

Acceptance Criterion 1: System Description and Model Integration Are Adequate

(1) *Total system performance assessment adequately incorporates important design features, physical phenomena, and couplings, and uses consistent and appropriate assumptions throughout the airborne transport of radionuclides abstraction process.*

This model report documents the use of the ASHPLUME code to model the airborne transport of radionuclides. This report provides information about the development of the Ashplume conceptual model by Suzuki (1983 [DIRS 100489]) (Section 6.3) and describes the consistency of the conceptual model with physical phenomena associated with violent Strombolian eruptions and the development and propagation of an ash cloud downwind of the eruption site followed by deposition of tephra deposits on the ground surface (Section 6.3). This report also documents the consistency between the conceptual model and the Ashplume mathematical model used in the

TSPA (Section 6.5). A mathematical description of the base case conceptual model is described in Section 6.5.1. The inputs to the model are described in Section 6.5.2. Model assumptions needed to use the Ashplume model are described in Section 5.1, and parameter assumptions are described in Section 5.2. The TSPA code, GoldSim, includes the ASHPLUME code as a dynamic link library (ASHPLUME_DLL_LA V.2.1). Inclusion of ASHPLUME as a DLL in the TSPA model ensures that physical phenomena and couplings important to the analysis of airborne transport of radionuclides are consistently and appropriately treated in performance assessment.

(2) *Models used to assess airborne transport of radionuclides are consistent with physical processes generally interpreted from igneous features in the Yucca Mountain region and/or observed at active igneous systems.*

This model report provides information about the basis for the Ashplume conceptual model (Suzuki 1983 [DIRS 100489]) in Section 6.3. Section 6.3 also describes the consistency of the conceptual model with physical phenomena associated with violent Strombolian eruptions and the development and propagation of an ash cloud downwind of the eruption site followed by deposition of tephra deposits on the ground surface. Base-case model inputs and uncertainties and their consistency with igneous features either observed in the Yucca Mountain region or with features observed at analogue igneous systems are described in Section 6.5.2. The bases for the selection of an appropriate distribution for each uncertain parameter are described in this report (Section 6.5.2). Model inputs that are developed and documented in other analyses or models are appropriately identified, described, and cross-referenced.

Alternative models considered are described in Section 6.4.1 through 6.4.7.

(3) *Models account for changes in igneous processes that may occur from interactions with engineered repository systems.*

The Ashplume model does not account for changes in igneous processes that might result from interactions between processes and components of the engineered barrier system. Such interactions are described in other analyses or model reports, as appropriate (e.g., *Dike/Drift Interactions* (SNL 2007 [DIRS 177430]) and *Number of Waste Packages Hit by Igneous Intrusion* (SNL 2007 [DIRS 177432]).

(4) *Guidance in NUREG-1297 and NUREG-1298 (Altman et al. 1988; Altman et al. 1988), or in other acceptable approaches for peer review and data qualification is followed.*

Quality assurance considerations for modeling activities associated with development of the ASHPLUME_DLL_LA V.2.1 software [DIRS 178870] are described in Section 3. Data, parameters, and other model inputs are described in Section 4.1.

NUREG-1297 describes the generic technical position with respect to the use of peer reviews on high-level waste repository programs. The independent peer review of the Ashplume model is described in Section 7.4. Additional documentation is provided in Appendix E. The review was done in accordance with the Project procedure, *Peer*

Review (AP-2.21Q), in effect at the time of the review. NUREG-1298 describes the generic technical position with respect to qualification of existing data. External sources have provided unqualified data that have been used as direct input to this document. The inputs from these sources are qualified for intended use within the document using the criteria found in SCI-PRO-006, *Models* (Appendix A). These criteria represent a subset of the methods and attributes required for qualification of data per SCI-PRO-001, *Qualification of Unqualified Data.* These methods and attributes are based on those that are presented in NUREG-1298, which are meant to provide "the level of confidence in the data … commensurate with their intended use." The quality assurance status of the inputs for the Ashplume model is described in Section 4.1.1.

Acceptance Criterion 2: Data Are Sufficient for Model Justification

(1) *Parameter values used in the license application to evaluate airborne transport of radionuclides are sufficient and adequately justified. Adequate descriptions of how the data were used, interpreted, and appropriately synthesized into the parameters are provided.*

Uses of the parameter values are generally described as part of the mathematical description of the base-case model in Section 6.5.1. The development of all model inputs used for the atmospheric dispersal model is discussed in Section 6.5.2. Subsections describe the individual model input parameters and provide detailed technical bases supporting the use of the numerical value or range for each parameter. Model report outputs for the TSPA are described in Section 8.2.

(2) *Data used to model processes affecting airborne transport of radionuclides are derived from appropriate techniques. These techniques may include site-specific field measurements, natural analog investigations, and laboratory experiments.*

The parameter values used as inputs for ASHPLUME_DLL_LA V.2.1 are described in the model report in Section 4.1.1, and model outputs are described in Section 8.2. Modeling objectives, the characteristics of the base-case model, consideration of alternative conceptual models, and the basis for the selection of ASHPLUME for modeling airborne transport of radionuclides are discussed in Sections 6.1, 6.3, 6.4, and 6.5 respectively. The formulation of the mathematical model is described in Section 6.5.1, and the base-case model inputs and their appropriateness are described in Section 6.5.2.

This model report describes the conceptual model, formulation of the mathematical model, identification of parameters, selection of appropriate parameter values or distributions, and discusses the consideration of alternative models. All of these considerations are included in the basis for selection of the ASHPLUME model as appropriate for analyzing the airborne transport of radionuclides for the license application. The alternative models considered are described in Section 6.4, and a summary of alternative conceptual models is provided in Section 6.4.7. Section 7 of the report discusses validation of the model and shows how the validation exercises

have shown the efficacy of the Ashplume model to represent observed variations in tephra deposit thicknesses at analogue sites. The validation work also shows that the model is internally consistent and produces numerical convergence in simulations. These lines of evidence demonstrate that the Ashplume model is appropriate to analyze the airborne transport of radionuclides.

(3) Sufficient data are available to integrate features, events, and processes, relevant to airborne transport of radionuclides into process-level models, including site-specific determination of appropriate interrelationships and parameter correlations.

FEPs related to the development and use of the Ashplume model are discussed in Section 6.2. Table 6-1 identifies the specific FEPs associated with the Ashplume model and provides pointers to relevant sections of this report where these aspects are discussed.

Acceptance Criterion 3: Data Uncertainty is Characterized and Propagated Through the Model Abstraction

(1) Models use parameter values, assumed ranges, probability distributions, and bounding assumptions that are technically defensible, reasonably account for uncertainties and variabilities, and do not result in an under-representation of the risk estimate.

The development of the individual mathematical formulations for the model is described in the model report (Section 6.5.1) as are the inputs to the model and assumptions needed to use the Ashplume model for analysis (Section 6.5.2). Uncertainties associated with changes in igneous processes are included in Ashplume analyses through the use of parameter distributions (Section 6.5.2). The bases for the selection of an appropriate distribution for each uncertain parameter are described in the report (Section 6.5.2). The reasonableness of values and distributions for parameters and their suitability for use are described in Section 6.5.2. Assumptions associated with the appropriateness of the Ashplume model are described in Section 5.1, and assumptions associated with specific model parameters are described in Section 5.2. The appropriateness of the base-case model is described in Section 6.3, and the consideration of alternative models is documented in Section 6.4. The screening of an alternative basis for the selection of ASHPLUME is also documented in Section 6.4.7 (see Table 6-2). Input parameter uncertainty is addressed in Section 4.1.2.

(2) Parameter uncertainty accounts quantitatively for the uncertainty in parameter values derived from site data and the available literature (i.e., data precision) and the uncertainty introduced by model abstraction (i.e., data accuracy).

Data precision is addressed in the mathematical description of the base case conceptual model (Section 6.5.1) and in the development of the input parameters (Section 6.5.2 and subsections). Data accuracy is addressed by evaluating uncertainties introduced by model abstraction. These uncertainties are explicitly addressed by the results of the model validation exercise (Sections 7.2 through 7.6),

which shows how well the Ashplume model outputs conform to evaluation criteria, including sensitivity of outputs to variations in input parameters (Section 7.2), comparison of model ash thicknesses with observed thicknesses at analogue sites (Section 7.3), and conservation of mass (CRWMS M&O 2000 [DIRS 161492]) (Section 7.3).

Uncertainties associated with changes in igneous processes are included in Ashplume analyses through the use of parameter distributions (Section 6.5.2). The bases for the selection of an appropriate distribution for each uncertain parameter are described in the report (Section 6.5.2). Parameter uncertainty is addressed in Section 4.1.2.

(3) Where sufficient data do not exist, the definition of parameter values and associated uncertainty is based on appropriate use of expert elicitation conducted in accordance with NUREG-1563 (Kotra et al. 1996). If other approaches are used, the U.S. Department of Energy adequately justifies their use.

Sufficient data exist to define the parameter values and associated conceptual models needed to model the atmospheric dispersal and deposition of tephra (Section 6.5.2). Expert elicitation has not been used in the definition of parameter values and associated conceptual models.

Acceptance Criterion 4: Model Uncertainty is Characterized and Propagated Through the Model Abstraction

(1) Alternative modeling approaches to airborne transport of radionuclides are considered and are consistent with the available data and current scientific understandings, and the results and limitations are appropriately considered in the abstraction.

The alternative models that were considered for modeling airborne transport of radionuclides are described in Section 6.4, including the screening of an alternative basis for the selection of ASHPLUME (see Table 6-2). The consistency of the Ashplume model with data and current scientific understanding is described in Sections 6.3 and 6.5.1. Sections 7.2 through 7.6 discuss validation of the model and show how the validation exercises have demonstrated the efficacy of the Ashplume model to represent observed variations in tephra deposit thicknesses at analogue sites (Section 7.3). The validation work shows that the model is internally consistent and produces numerical convergence in simulations. Limitations of the Ashplume model are discussed in Section 1.3.

(2) Uncertainties in abstracted models are adequately defined and documented, and effects of these uncertainties are assessed in the total system performance assessment.

Uncertainties associated with Ashplume model outputs are described in Section 8.3, and input parameters and parameter uncertainties are described in Section 4.1.2. Section 7.2 describes the sensitivity analyses that were done to evaluate the response of the Ashplume model over the entire range of model input parameter values. The results show that the model is sensitive to variations in eruptive power, wind speed,

wind direction, and eruption duration. TSPA sensitivity to parameter variations is beyond the scope of this report.

(3) Consideration of conceptual model uncertainty is consistent with available site characterization data, laboratory experiments, field measurements, natural analog information, and process-level modeling studies; and the treatment of conceptual model uncertainty does not result in an under representation of the risk estimate.

The basis of the Ashplume conceptual model is described in Section 6.3, and the mathematical description of the base-case conceptual model is provided in Section 6.5.1. Uncertainties in the model outputs are described in Section 8.3, and conservatisms included to assure that model outputs to the TSPA do not result in an under representation of risk are described as part of the conceptual model (Section 6.5.2 and subsections).

The alternative models that were considered for modeling airborne transport of radionuclides are described in Section 6.4 and are summarized in Section 6.4.7. The screening of an alternative basis for the selection of ASHPLUME is also documented in Section 6.4.7 (see Table 6-2). The consistency of the Ashplume model with data and current scientific understanding is described in Sections 6.3 and 6.5.1. Sections 7.1 through 7.5 discuss validation of the model and show how the validation exercises have demonstrated the efficacy of the Ashplume model to represent observed variations in tephra deposit thicknesses at analogue sites. The validation work shows that the model is internally consistent and produces numerical convergence in simulations. Limitations of the Ashplume model are discussed in Section 1.3.

Acceptance Criterion 5:   Model Abstraction Output is Supported by Objective Comparisons

(1) Models implemented in the airborne transport of radionuclides abstraction provide results consistent with output from detailed process-level models and/or empirical observations (laboratory and field testings and/or natural analogs).

Section 6.2 lists the specific FEPs that are included in the Ashplume model. Section 6.3.1 provides a detailed description of the basis for the Ashplume conceptual model and the appropriateness of that model for the analysis of airborne transport of radionuclides. Section 6.5.1 provides a detailed description of the mathematical formulation of the base-case conceptual model and the consistency of that formulation with natural processes. Sections 7.1 through 7.6 discuss validation of the model and show how the validation exercises have shown the efficacy of the Ashplume model to represent observed variations in tephra deposit thicknesses at analogue sites. The validation work also shows that the model is internally consistent and produces numerical convergence in simulations.

(2) Inconsistencies between abstracted models and comparative data are documented, explained, and quantified. The resulting uncertainty is accounted for in the model results.

The model outputs are described in Section 8.2 and model output uncertainties are described in Section 8.3. Sections 7.1 through 7.6 discuss validation of the model and show how the validation exercises have shown the efficacy of the Ashplume model to represent observed variations in tephra deposit thicknesses at analogue sites (Section 7.3). The validation work also shows that the model is internally consistent and produces numerical convergence in simulations.

INTENTIONALLY LEFT BLANK

APPENDIX C
SENSITIVITY STUDIES

APPENDIX C
SENSITIVITY STUDIES

Sensitivity analyses were performed both to ensure that the Ashplume model operated over the parameter ranges selected and to demonstrate that there were not limitations in model validity due to numerical constraints. The sensitivity analyses were performed by varying the value of the following input parameters: eruptive power, mean ash particle diameter, ash particle diameter standard deviation, column diffusion constant (beta), initial rise velocity, wind speed, wind direction, eruption duration, waste incorporation ratio, and waste particle size statistics (minimum, mode, maximum). The range for each of these parameters is provided in Table 8-2. Values were chosen for the sensitivity analyses based on scientific judgment to evaluate the entire range of each parameter, and values for non-varying parameters were set at base-case values (Table C-1). This sensitivity analysis was performed using ASHPLUME_DLL_LA V.2.1 [DIRS 178870]. Sample input and output files are included at the end of this appendix. The sensitivity factors resulting from these analyses may differ from those resulting from a full Monte Carlo analysis, which considers all of the uncertain parameters together.

Sensitivity analyses were performed by executing a series of Ashplume model runs in which values for a single parameter were sequentially varied over its expected range, while the other input values were held constant. The values of other stochastic parameters were set to midrange values, and the values of non-varying parameters were set to base-case values (Table C-1). The model calculated ash and waste concentrations for a single point, the RMEI area, which is located 18 km south of the vent (assumed to be in the center of the repository footprint). Analysis results are presented in this appendix in the form of tables and graphs that display the varying parameter values and calculated values for tephra and fuel deposition (g/cm^2) at the RMEI location.

Figure C-1 demonstrates the moderate sensitivity of tephra and fuel concentration to **eruptive power**. Total eruptive volume is held constant for this series of runs by varying the eruptive duration. Wind speed is held constant despite the variation in column height. As power increases, the tephra deposition 18 km downwind eventually decreases as the center of mass passes beyond the observation point, consistent with the results of Suzuki (1983 [DIRS 100489], Figure 9c). Fuel concentration follows a similar trend. Variation over three orders of magnitude in power produces a factor of 2 to 3 in fuel and tephra concentration at the RMEI location.

Tephra concentrations show strong sensitivity (factor of 35) to **mean ash particle diameter,** and fuel concentrations show small sensitivity (factor of 2) to two orders of magnitude variation in mean ash particle diameter. Figure C-2 shows the sensitivity of tephra and fuel concentration. Increasing mean tephra particle size results in mass diffusion at a lower level in the eruptive column and greater deposition proximal to the vent. Similar to the effect of eruptive power, for an observation point at the RMEI location, increasing mean ash particle diameter initially results in an increase in tephra and fuel concentration, a maximum, and eventually decreasing concentrations as the center of mass passes toward the vent.

Table C-1. Input Parameter Values for ASHPLUME Sensitivity Studies

	Base Case (Total Range)	Base Case (Representative)	Sensitivity Analysis									
			Power	Dmean	Dsigma	Beta	Initial Rise Velocity	Wind Speed	Wind Direction	Eruption Duration	Waste Incorporation Ratio	Waste Particle Size
Beta	0.01 to 0.5	0.3	0.3	0.3	0.3	0.01 to 0.5	0.3	0.3	0.3	0.3	0.3	0.3
Ash particle mean (dmean) (cm)	0.001 to 0.01 to 0.1	0.01	0.01	0.001 to 0.1	0.01	0.01	0.01	0.01	0.01	0.01	0.01	0.01
Dsigma (log (cm))	0.301 to 0.903	0.602	0.602	0.602	0.301 to 0.903	0.602	0.602	0.602	0.602	0.602	0.602	0.602
Minimum waste particle size (fdmin) (cm)	0.0001	0.0001	0.0001	0.0001	0.0001	0.0001	0.0001	0.0001	0.0001	0.0001	0.0001	0.0001
Mode waste particle size (fdmean) (cm)	0.0013	0.0013	0.0013	0.0013	0.0013	0.0013	0.0013	0.0013	0.0013	0.0013	0.0013	0.0010, 0.0013, 0.0016
Max. waste particle size (fdmax) (cm)	0.2	0.2	0.2	0.2	0.2	0.2	0.2	0.2	0.2	0.2	0.2	0.0050, 0.0500, 0.2000
Wind dir (Ashplume degrees)	−180 to +180	−90	−90	−90	−90	−90	−90	−90	−180 to +180	−90	−90	−90
Wind speed (cm/s)	0 to 14,100	1,215	1,215	1,215	1,215	1,215	1,215	1 to 14,100	1,215	1,215	1,215	1,215
Initial rise velocity (cm/s)	1.0 to 10,000	5,000	5,000	5,000	5,000	5,000	1.0 to 10,000	5,000	5,000	5,000	5,000	5,000
Power (W)	10^9 to 10^{12}	5×10^{10}	10^9 to 10^{12}	5×10^{10}	5×10^{10}	5×10^{10}	5×10^{10}	5×10^{10}	5×10^{10}	1.06×10^{12} to 1.06×10^{10}	5×10^{10}	5×10^{10}
Duration (s)	6.48×10^4 to 6.48×10^6	1.38×10^6	6.9×10^7 to 6.9×10^4	1.38×10^6	1.38×10^6	1.38×10^6	1.38×10^6	1.38×10^6	1.38×10^6	6.48×10^4 to 6.48×10^6	1.38×10^6	1.38×10^6

Table C-1. Input Parameter Values for ASHPLUME Sensitivity Studies (Continued)

	Base Case (Total Range)	Base Case (Representative)	Sensitivity Analysis									
			Power	Dmean	Dsigma	Beta	Initial Rise Velocity	Wind Speed	Wind Direction	Eruption Duration	Waste Incorporation Ratio	Waste Particle Size
Waste incorporation ratio	0.0 to 1.0	0.0	0.0	0.0	0.0	0.0	0.0	0.0	0.0	0.0	0.0 to 1.0	0.0
Parameters with Constant Values												
Ashdenmin (g/cm³)		1.04		Iscrn	0		Airden		0.001734		Rmin	0
Ashdenmax (g/cm³)		2.08		Xmin, xmax	0, 0		Airvis		0.000185		Rfactor	0
Ashrholow (log(cm))		−3		Ymin, ymax	0, 0		Dmax		10		Nr	0
Ashrhohi (log(cm))		0		Nx, ny	1, 1		Hmin		0.001		Nthet	0
Fshape		0.5		C	400		Acutoff		10^{-10}		Numapts	
Mass of waste (g)		1×10^8										

NOTE: Parameter values from base-case values in Table 8-2. Total range for wind speed represents 0 to 13 km altitude; midrange value represents average velocity for 3 to 4 km height (appropriate for base case power value). Wind speed is held constant for the variable-power runs despite the variable column height. Wind direction is held due south (−90 degrees, in direction of RMEI location) for all runs except wind direction analysis. Expected value for ash density of 1.0 g/cm³ was assumed for calculation of range limits of range of eruption duration. In the power sensitivity analysis, eruption duration is calculated separately for each model run by Equation 8-2 (as power varies) in order to hold total erupted volume constant for the analysis; base case volume=0.069 km³ for P = 5.0 × 10^{10}, Td = 1.38 × 10^6, ash settled density (ψ_s) = 1,000 kg/m³, assume (CpT) = 1 × 10^6 from Eqs. 6-7b and 6-7c. In the eruption duration analysis, eruptive power is calculated separately for each model run by Equation 8-2 (as duration varies) in order to hold total erupted volume constant for the analysis. Waste particle size distributions analyzed represent 1) fine-grained waste, 2) former base-case, and 3) current base-case distributions.

Analysis results demonstrate moderate sensitivity to **mean ash particle diameter standard deviation**, which produces a factor-of-two (or less) variation in concentration of tephra and fuel at the RMEI location (Figure C-3). The curving, peaked trend is the result of the changing shape of the deposition pattern from one emphasizing a local thickness maximum downwind from the vent at low to moderate dsigma values to a monotonic decrease in downwind thickness for higher values of dsigma (e.g., Suzuki 1983 [DIRS 100489], Figure 9b).

Variation in **column diffusion constant (β)** produces very little change in either tephra (10%) or fuel concentration (30%) at the RMEI location (Figure C-4). The observed concentration variation is due to the upward shift in mass diffusion within the eruption column with increasing β and the resulting downwind shift in center of mass of the deposit.

Variation in **initial rise velocity** has little effect on tephra/fuel deposition (20% to 30%, Figure C-5). The shapes of the concentration trends are similar to those caused by variation in the parameter, β; both parameters affect the retention of mass with height in the eruption column.

Ashplume results demonstrate strong sensitivity to variation in **wind speed** (Figure C-6). Increasing wind speed causes the center of mass of the tephra deposit to shift downwind, producing a local maximum in observed tephra and fuel concentration at a point 18 km south of the vent. Four orders of magnitude variation in wind speed results in a factor of 25 variation in tephra concentration and a factor of 60 variation in fuel concentration.

The model shows a similar strong sensitivity to variation in **wind direction**, with tephra and fuel concentrations varying over seven orders of magnitude for wind directions spanning the compass rose (Figure C-7). Variation in wind direction results in increased tephra/fuel deposition at the RMEI location when the plume is directed toward due south (−90°) and results in decreased deposition at the RMEI location with other wind directions.

Analysis results indicate a moderate sensitivity to **eruption duration** (Figure C-8). Erupted volume is held constant by decreasing eruptive power as eruption duration increases. The observed factor-of-three increase in tephra concentration with increasing duration is caused by the associated reduction in power (and column height), the consequent ventward migration of the center of mass of the deposit, and the accompanying moderate increase in tephra (and fuel) concentrations at this relatively proximal observation location (18 km from the vent).

Variation in **waste incorporation ratio** causes only minor (<10%) variation in waste concentration at the RMEI location (Figure C-9). Tephra concentration is constant since erupted tephra mass is a function of eruption duration. Fuel concentration exhibits small variation in this case since the waste particle size distribution is significantly smaller than the base-case tephra particle size distribution and the range of values for waste incorporation ratio allows most of the waste to be transported.

Variations in values for statistics describing the **waste particle size distribution** (minimum, mode, maximum) produce minor change in calculated fuel deposition at the RMEI location (Figure C-10). Calculated tephra concentration is constant because it is not affected by the waste particle size parameters. The range of variation analyzed does not produce significant variation in model results.

Table C-2. Sensitivity of Calculated Tephra and Fuel Concentration to Eruptive Power

Eruptive Power (W)	Eruption Column Height (km)	Eruption Duration (s)	Calculated Tephra Deposition (g/cm^2)	Calculated Fuel Deposition (g/cm^2)
1×10^9	1.5	6.90×10^7	2.43×10^1	2.79×10^{-5}
2.00×10^9	1.7	3.46×10^7	2.47×10^1	3.04×10^{-5}
3.98×10^9	2.1	1.73×10^7	2.48×10^1	3.14×10^{-5}
7.94×10^9	2.4	8.69×10^6	2.45×10^1	3.28×10^{-5}
1.58×10^{10}	2.9	4.35×10^6	2.35×10^1	3.35×10^{-5}
3.16×10^{10}	3.5	2.18×10^6	2.20×10^1	3.33×10^{-5}
6.31×10^{10}	4.1	1.09×10^6	1.97×10^1	3.19×10^{-5}
1.26×10^{11}	4.9	5.48×10^5	1.70×10^1	2.94×10^{-5}
2.51×10^{11}	5.8	2.75×10^5	1.40×10^1	2.61×10^{-5}
5.01×10^{11}	6.9	1.38×10^5	1.13×10^1	2.23×10^{-5}
1×10^{12}	8.2	6.90×10^4	8.75	1.84×10^{-5}

NOTE: Total erupted volume is held constant for all runs by varying eruption duration along with erupted power. Column height is calculated by Equation 6-7a.
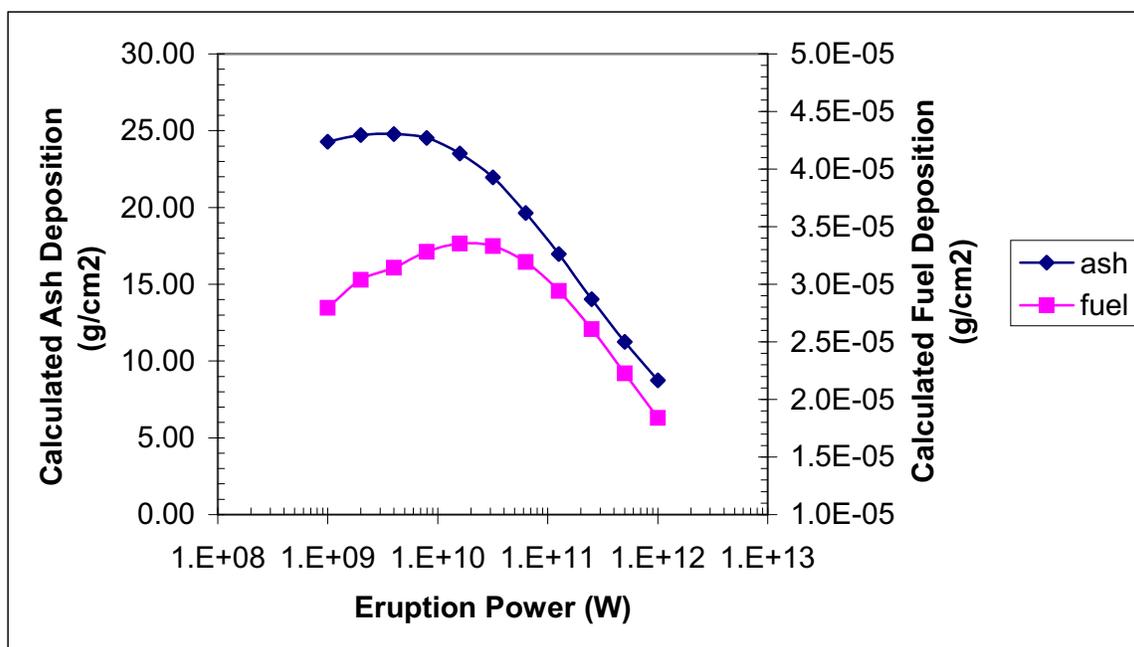
NOTE: With total erupted volume (and mass) held constant in this series of Ashplume runs, the primary effect of increased power is increased column height of the eruption. The fixed observation point (18 km south of the repository) receives the maximum ash and waste in the 10^9 to 10^{10} W range; as the power increases, the center of mass of the deposit moves downwind, beyond the observation point. Wind speed is held constant for these runs, despite the variation in column height. Variation in power over three orders of magnitude has a factor-of-three effect on deposited concentration of tephra (factor-of-two effect on fuel).

Figure C-1. Sensitivity of Calculated Tephra and Fuel Concentration to Eruptive Power

Table C-3. Sensitivity of Calculated Tephra and Fuel Concentration to Mean Ash Particle Diameter

Mean Ash Particle Diameter (cm)	Calculated Tephra Deposition (g/cm^2)	Calculated Fuel Deposition (g/cm^2)
0.00100	1.01	1.72×10^{-5}
0.00158	2.28	1.89×10^{-5}
0.00251	4.65	2.13×10^{-5}
0.00398	8.50	2.44×10^{-5}
0.00631	13.9	2.83×10^{-5}
0.01000	20.5	3.25×10^{-5}
0.01585	27.2	3.63×10^{-5}
0.02512	32.4	3.85×10^{-5}
0.03981	34.6	3.83×10^{-5}
0.06310	33.2	3.52×10^{-5}
0.10000	28.7	2.96×10^{-5}
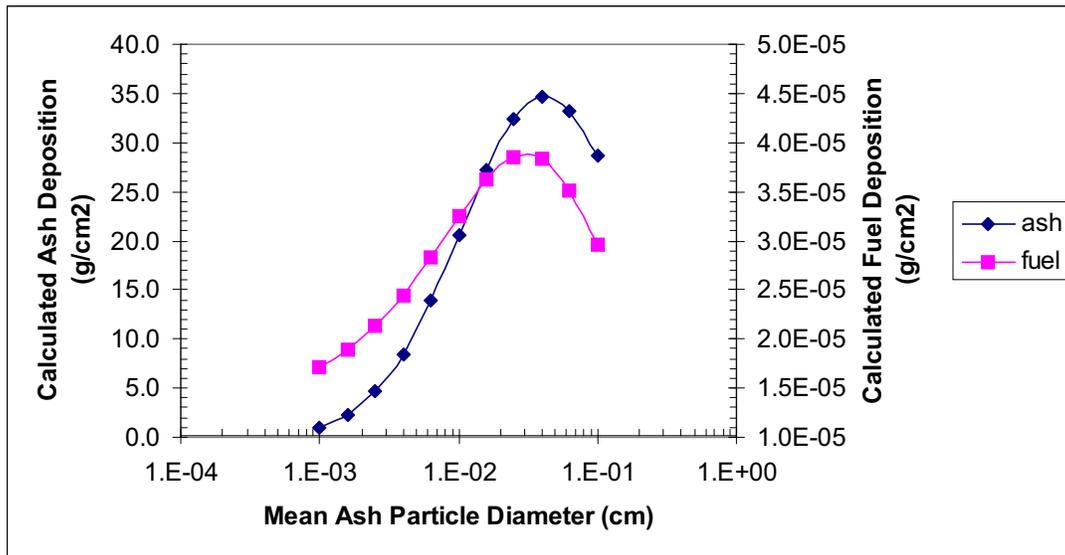
NOTE: The variation in tephra/fuel concentration with vari ation in mean ash particle diameter is smooth, with an order of magnitude increase in tephra concentration and a factor-of-two increase in fuel concentration for three orders of magnitude variation in mean ash particle diameter. As mean tephra size increases, mass diffusion occurs lower in the plume, and the center of mass of the tephra deposit migrates backward toward the vent. For this fixed observation point, the tephra concentration initially increases with increasing particle size and then decreases as the center of mass passes as it moves uprange toward the vent.

Figure C-2. Sensitivity of Calculated Tephra and Fuel Concentration to Mean Ash Particle Diameter

Table C-4. Sensitivity of Calculated Tephra and Fuel Concentration to Ash Particle Diameter Standard Deviation

Ash Particle Diameter Standard Deviation (log (cm))	Calculated Tephra Deposition (g/cm^2)	Calculated Fuel Deposition (g/cm^2)
0.301	9.80	2.36×10^{-5}
0.3612	14.2	2.79×10^{-5}
0.4214	17.4	3.07×10^{-5}
0.4816	19.3	3.21×10^{-5}
0.5418	20.2	3.26×10^{-5}
0.602	20.5	3.25×10^{-5}
0.6622	20.5	3.20×10^{-5}
0.7224	20.1	3.13×10^{-5}
0.7826	19.6	3.04×10^{-5}
0.8428	19.0	2.95×10^{-5}
0.903	18.4	2.86×10^{-5}
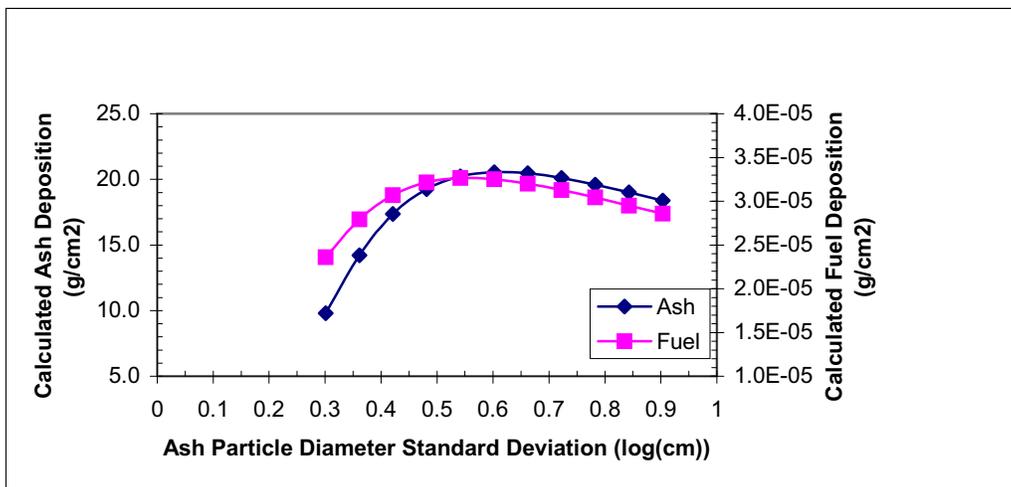
NOTES: Variation in the standard deviation of (log) particle diameter of nearly one log cycle produces a factor-of-two (or less) variation in tephra and fuel deposition at the RMEI location. The curving trend is the result of the changing shape of the deposition pattern from one emphasizing a local thickness maximum downwind from the vent at low to moderate dsigma values to a monotonic decrease in downwind thickness for higher values of dsigma.

Figure C-3. Sensitivity of Calculated Tephra and Fuel Concentration to Ash Particle Diameter Standard Deviation

Table C-5. Sensitivity of Calculated Tephra and Fuel Concentration to Column Diffusion Constant (beta)

Column Diffusion Constant (Beta)	Calculated Tephra Deposition (g/cm^2)	Calculated Fuel Deposition (g/cm^2)
0.0100	20.3	2.50×10^{-5}
0.0148	20.1	2.51×10^{-5}
0.0219	19.3	2.47×10^{-5}
0.0323	18.8	2.46×10^{-5}
0.0478	18.4	2.48×10^{-5}
0.0707	18.4	2.56×10^{-5}
0.1046	18.6	2.69×10^{-5}
0.1546	19.3	2.88×10^{-5}
0.2287	20.1	3.11×10^{-5}
0.3381	20.7	3.31×10^{-5}
0.5000	21.1	3.45×10^{-5}
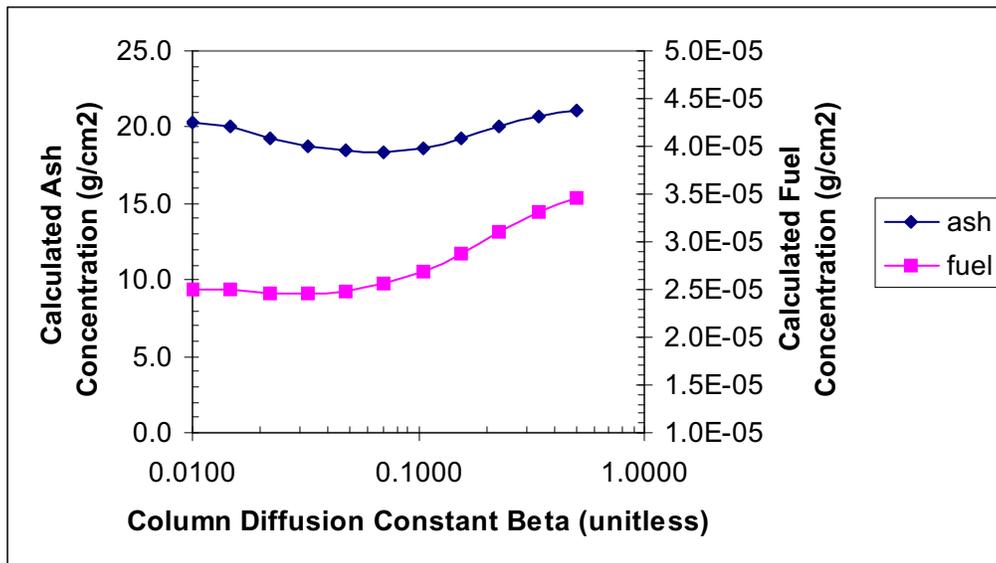
NOTE: Variation in β produces a very little change in either tephra or fuel concentration at the RMEI location. The observed concentration variation is due to upward shift in mass diffusion within the eruption column with increasing β and resulting downwind shift in center of mass of the deposit.

Figure C-4. Sensitivity of Calculated Tephra and Fuel Concentration to Column Diffusion Constant (Beta)

Table C-6.   Sensitivity of Calculated Tephra and Fuel Concentration to Initial Rise Velocity

Initial Rise Velocity (cm/s)	Calculated Tephra Deposition (g/cm²)	Calculated Fuel Deposition (g/cm²)
1	23.8	2.81×10^{-5}
3	23.7	2.80×10^{-5}
6	23.6	2.79×10^{-5}
16	23.2	2.69×10^{-5}
40	22.4	2.57×10^{-5}
100	21.4	2.57×10^{-5}
251	20.1	2.50×10^{-5}
631	18.6	2.46×10^{-5}
1,585	18.5	2.65×10^{-5}
3,981	20.2	3.13×10^{-5}
10,000	21.2	3.50×10^{-5}
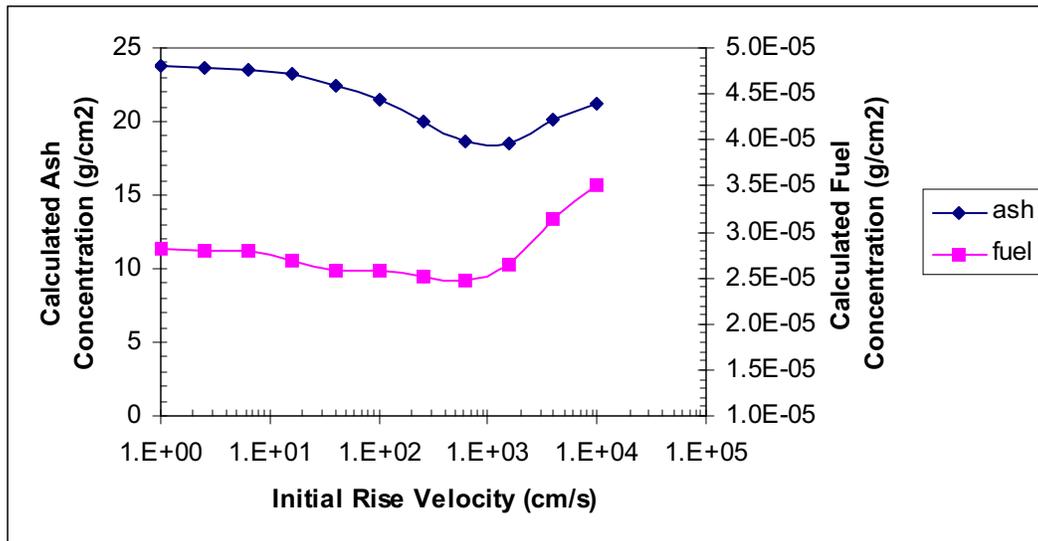
NOTES: Variation in initial rise velocity has little effect on tephra/fuel deposition (20% to 30%). The shapes of the trends are similar to those caused by variation in the parameter, β; both parameters affect the retention of mass with height in the eruption column.

Figure C-5. Sensitivity of Calculated Tephra and Fuel Concentration to Initial Rise Velocity

Table C-7. Sensitivity of Calculated Tephra and Fuel Concentration to Wind Speed

Wind Speed (cm/s)	Calculated Tephra Deposition (g/cm^2)	Calculated Fuel Deposition (g/cm^2)
1	7.11×10^{-1}	6.64×10^{-7}
3	7.22×10^{-1}	6.74×10^{-7}
7	7.44×10^{-1}	6.96×10^{-7}
18	8.07×10^{-1}	7.59×10^{-7}
46	9.88×10^{-1}	9.40×10^{-7}
119	1.60	1.57×10^{-6}
309	4.25	4.56×10^{-6}
803	14.7	1.96×10^{-5}
2,086	19.2	3.96×10^{-5}
5,424	7.40	1.80×10^{-5}
14,100	4.14	1.02×10^{-5}
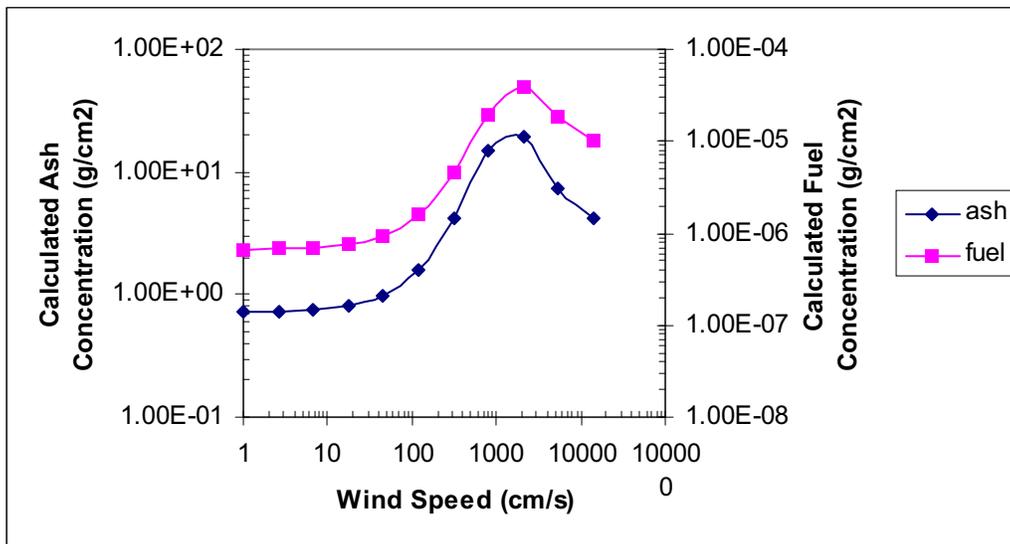
NOTES: Increasing wind speed causes the center of mass of the tephra deposit to shift downwind, producing a local maximum in observed tephra and fuel concentration at a point 18 km south of the vent. Four orders of magnitude variation in wind speed results in a factor-of-25 variation in tephra concentration and a factor-of-60 variation in fuel concentration.

Figure C-6. Sensitivity of Calculated Tephra and Fuel Concentration to Wind Speed

Table C-8. Sensitivity of Calculated Tephra and Fuel Concentration to Wind Direction

Wind Direction (degrees)	Calculated Tephra Deposition (g/cm^2)	Calculated Fuel Deposition (g/cm^2)
−150	2.20×10^{-6}	1.07×10^{-12}
−117	3.68×10^{-2}	5.61×10^{-8}
−84	14.7	2.32×10^{-5}
−51	1.19×10^{-4}	1.67×10^{-10}
−18	2.07×10^{-6}	9.88×10^{-13}
15	1.80×10^{-6}	8.35×10^{-10}
48	1.63×10^{-6}	7.41×10^{-10}
81	1.55×10^{-6}	7.02×10^{-10}
114	1.58×10^{-6}	7.13×10^{-10}
147	$1.70E \times 10^{-6}$	7.77×10^{-10}
180	1.92×10^{-6}	8.97×10^{-10}
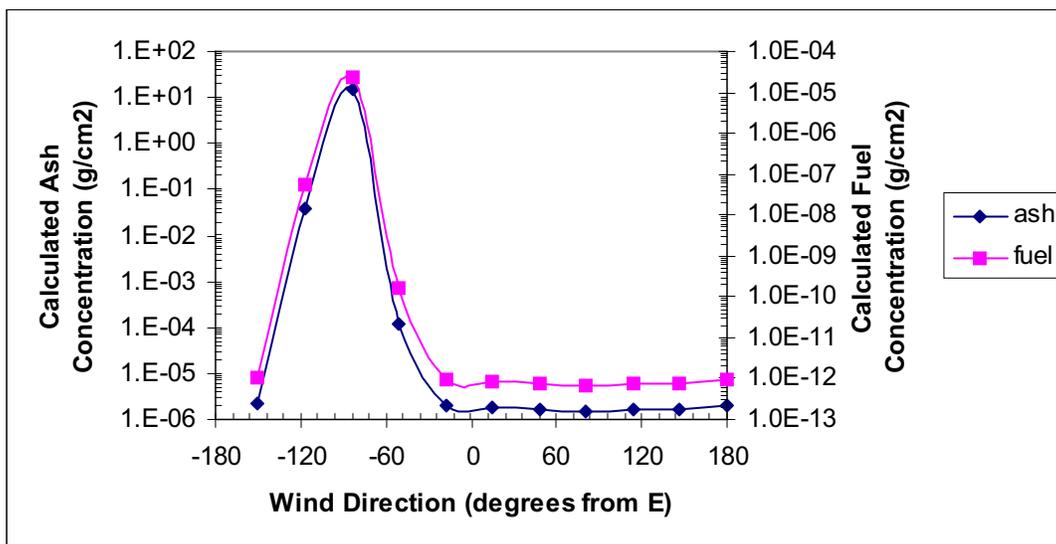
NOTES: Variation in wind direction results in increased tephra/fuel deposition at the RMEI location when the plume is directed toward due south (−90°) and results in decreased deposition at the RMEI location with other wind directions. The small but nonzero values in tephra and fuel concentrations when the wind is blowing directly away from the RMEI location (e.g., north, or +90°) is a result of diffusion back through the atmosphere (upwind).

Figure C-7. Sensitivity of Calculated Tephra and Fuel Concentration to Wind Direction

Table C-9.   Sensitivity of Calculated Tephra and Fuel Concentration to Eruption Duration

Eruption Duration (s)	Eruptive Power (W)	Calculated Tephra Deposition (g/cm^2)	Calculated Fuel Deposition (g/cm^2)
6.48×10^4	1.06×10^{12}	8.52	1.81×10^{-5}
1.03×10^5	6.72×10^{11}	10.2	2.06×10^{-5}
1.63×10^5	4.24×10^{11}	11.9	2.32×10^{-5}
2.58×10^5	2.67×10^{11}	13.8	2.57×10^{-5}
4.09×10^5	1.69×10^{11}	15.7	2.81×10^{-5}
6.48×10^5	1.06×10^{11}	17.6	3.01×10^{-5}
1.03×10^6	6.72×10^{10}	19.5	3.17×10^{-5}
1.63×10^6	4.24×10^{10}	21.1	3.29×10^{-5}
2.58×10^6	2.67×10^{10}	22.4	3.35×10^{-5}
4.09×10^6	1.69×10^{10}	23.5	3.36×10^{-5}
6.48×10^6	1.06×10^{10}	24.1	3.32×10^{-5}

NOTE: Total erupted volume is held constant for all runs by varying eruption power along with erupted duration.
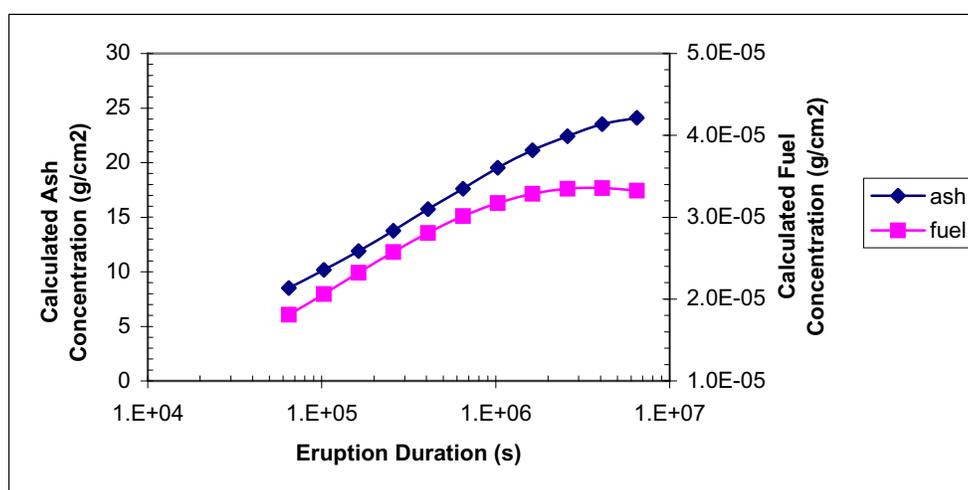
NOTES: Erupted volume is held constant by decreasing eruptive power as eruption duration increases. The observed moderate (factor of three) increase in tephra concentration with increasing duration is caused by the associated reduction in power (and column height), the consequent ventward migration of the center of mass of the deposit, and the accompanying increase in tephra (and fuel) concentrations at this relatively proximal observation location (18 km from the vent).

Figure C-8. Sensitivity of Calculated Tephra and Fuel Concentration to Eruption Duration

Table C-10. Sensitivity of Calculated Tephra and Fuel Concentration to Waste Incorporation Ratio

Waste Incorporation Ratio	Calculated Tephra Deposition (g/cm^2)	Calculated Fuel Deposition (g/cm^2)
0.0	20.5	3.25×10^{-5}
0.1	20.5	3.32×10^{-5}
0.2	20.5	3.38×10^{-5}
0.3	20.5	3.44×10^{-5}
0.4	20.5	3.48×10^{-5}
0.5	20.5	3.52×10^{-5}
0.6	20.5	3.54×10^{-5}
0.7	20.5	3.55×10^{-5}
0.8	20.5	3.53×10^{-5}
0.9	20.5	3.50×10^{-5}
1.0	20.5	3.45×10^{-5}
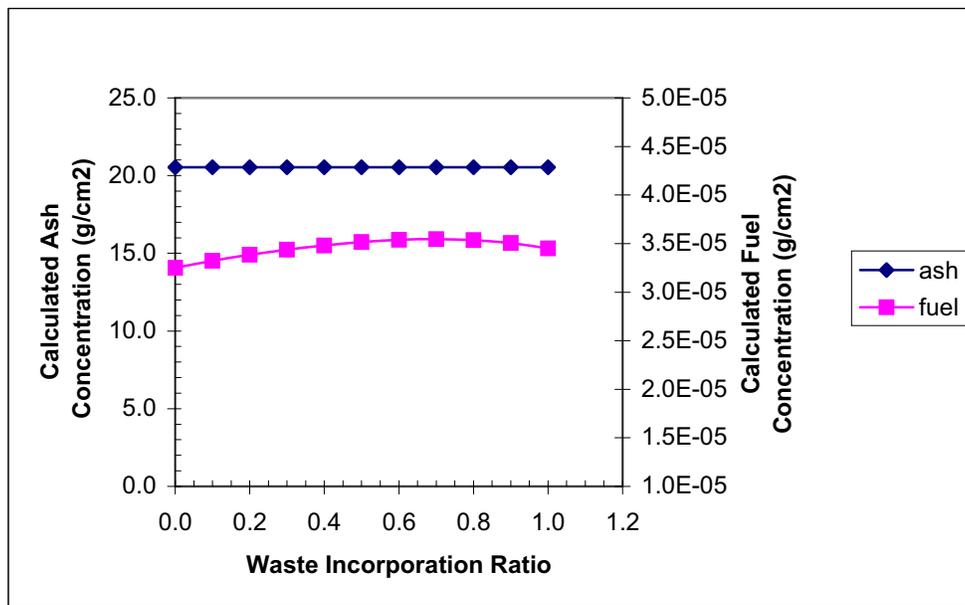
NOTES: With increasing waste incorporation ratio, tephra concentration is unaffected since erupted tephra mass is a function of eruption duration. Fuel concentration exhibits small (<10%) variation in this case, since the waste particle size distribution is significantly smaller than the base-case tephra particle size distribution and the range of values for waste incorporation ratio allows most of the waste to be transported.

Figure C-9. Sensitivity of Calculated Tephra and Fuel Concentration to Waste Incorporation Ratio

Table C-11. Sensitivity of Calculated Tephra and Fuel Concentration to Waste Particle Size

Run #	Waste Particle Size (cm) fdmin, fdmean, fdmax	Calculated Tephra Deposition (g/cm^2)	Calculated Fuel Deposition (g/cm^2)
1	0.0001, 0.0010 0.0050[1]	20.5	2.32×10^{-5}
2	0.0001, 0.0016, 0.05[2]	20.5	3.06×10^{-5}
3	0.0001, 0.0013, 0.2[3]	20.5	3.25×10^{-5}

NOTES: [1] Fine-grained waste: minimum 1 micron, maximum 50 micron; this run provides context for extremely fine-grained waste, below the size range used for the base case.
[2] Former base-case (BSC 2005 [DIRS 174067], Table 8-2): minimum 1 micron, mode 16 micron, maximum 500 micron.
[3] Current case-case waste particle distribution (Appendix F, Table 8-2): minimum 1 micron, mode 13 micron, maximum 2,000 micron (0.2 cm).
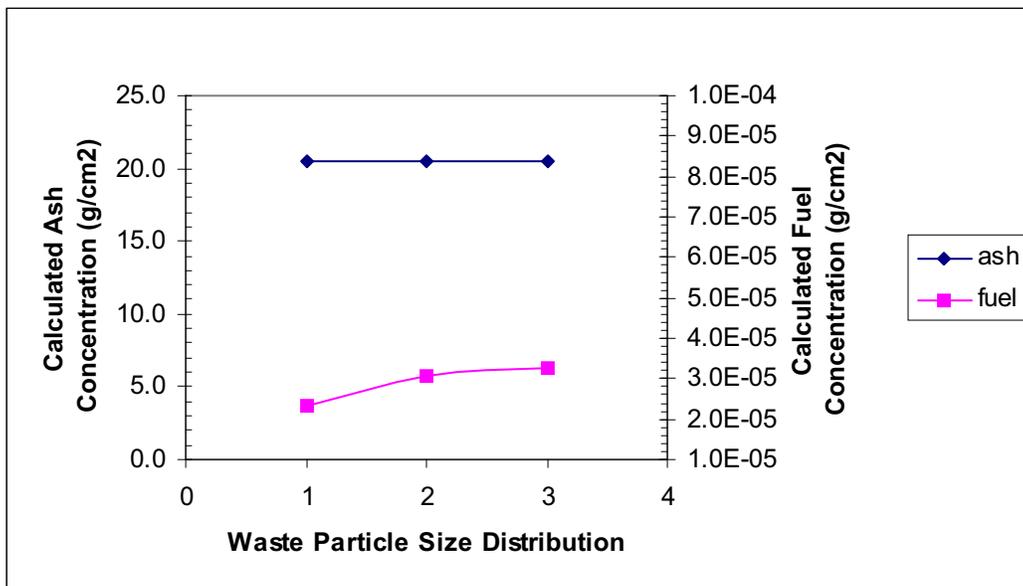
NOTE: Fuel deposition is observed to vary slightly as the coarseness of the waste particle size distribution increases. Calculated tephra concentration is constant because it is not affected by the waste particle size parameters. The range of variation analyzed does not produce significant variation in model results.

Figure C-10.   Sensitivity of Calculated Tephra and Fuel Concentration to Waste Particle Size

Sample input file for power sensitivity analyis:

```
ASHPLUME v2.1 Sensitivity Analysis: Power1
1                              ! iscrn, 0 = no screen output, 1 = yes
0    0                         ! xmin, xmax in km
-18  -18.0                     ! ymin, ymax in km
1                              ! numptsx
1                              ! numptsy
1.04    2.08                   ! ashdenmin, ashdenmax in g/cm3
-3.0    0.0                    ! ashrholow, ashrhohi
0.5                            ! fshape
0.001734  0.000185             ! airden in g/cm3, airvis in g/cm-s
400.0                          ! c in cm2/s to the 5/2
10.0                           ! dmax in cm
0.0001  0.0013  0.2            ! fdmin, fdmean, fdmax all in cm
0.001                          ! hmin in km
1.0e-10                        ! acutoff in g/cm2
0.3                    ***     ! the constant beta (unitless)
0.01                   ***     ! the mean ash particle diameter (cm)
0.602                  ***     ! sigma for the ash lognormal dist.
0.0                            ! the incorporation ratio (unitless)
1.0e+08                ***     ! the mass of fuel to incorporate (g)
-90.0                  ***     ! the wind direction- relation to due east
(deg)
1215.                  ***     ! the wind speed (cm/s)
5000.                  ***     ! the initial eruption velocity (cm/s)
1.0e+9                 ***     ! the power (watts)
6.90e+07               ***     ! the event duration (s)
0.0                            ! rmin,  minimum radius
0.0                            ! rfactor, radial grid multiplier
0                              ! nr,  number of radial divisions
0                              ! nthet, number of theta (angle) grid

                                 divisions
0                              ! numapts, number of points in histograms
```

*** Parameters sampled in TSPA model

Sample output file for the power sensitivity analysis:

```
ASHPLUME_DLL_LA version 2.1
***********************************************************************
      Input Parameters (From vin vector):
          Minimum x location (km)...............      0.0000
          Maximum x location (km)...............      0.0000
          Minimum y location (km)...............    -18.0000
          Maximum y location (km)...............    -18.0000
          Number of grid points in x............          1
          Number of grid points in y............          1
          Minimum ash density (g/cm^3)..........      1.0400
          Maximum ash density (g/cm^3)..........      2.0800
          Minimum particle size [log(cm)].......     -3.0000
          Maximum particle size [log(cm)].......      0.0000
          Particle shape parameter..............      0.5000
          Air density (g/cc)....................  1.7340E-03
          Air viscosity (g/cm-s)................  1.8500E-04
          Eddy diff. constant (cm^2/s^[5/2])....    400.0000
          Size cutoff (cm)......................     10.0000
          Minimum waste particle diameter (cm)..      0.0001
          Mode waste particle diameter (cm).....      0.0013
          Maximum waste particle diameter (cm)..      0.2000
          Minimum height of column (km).........      0.0010
          Lower limit for ash deposits (g/cm^2).  1.0000E-10
          Dispersion constant, beta.............      0.3000
          Mean particle diameter (cm)...........      0.0100
          Log particle standard deviation.......      0.6020
          Incorporation ratio...................      0.0000
          Total fuel mass available (g)......... 1.0000E+08
          Wind direction (deg)..................    -90.0000
          Wind speed (cm/s).....................  1215.0000
          Vent exit velocity (cm/s).............  5000.0000
          Event power (w).......................  1.0000E+09
          Event duration (s)....................  6.9000E+07
          minimum radial distance (km)..........      0.0000
          radial multiplier.....................      0.0000
          number of radial points...............          0
          number of theta (angle) points........          0
          number of histogram points...........          0
***********************************************************************
      Derived Parameters:
          Ash particle minimum log-diameter.....     -5.0100
          Ash particle mean log-diameter........     -2.0000
          Ash particle maximum log-diameter.....      1.0100
          Fuel particle minimum log-diameter....     -4.0000
          Fuel particle mode log-diameter.......     -2.8861
          Fuel particle maximum log-diameter....     -0.6990
          Column height (km)....................      1.4582
          Ash mass (g)..........................  9.4029E+13
***********************************************************************
      Results (To vout vector):
      Note: If more than one location is specified here, only the last
            one will be returned in vout.
       x(km)       y(km)      xash(g/cm^2)      xfuel(g/cm^2)
       0.000     -18.000       2.4272E+01        2.7942E-05
```

APPENDIX D
DESERT ROCK WIND DATA ANALYSIS METHODS

APPENDIX D
DESERT ROCK WIND DATA ANALYSIS METHODS

Parameter distributions for atmospheric data inputs to the TSPA model were developed in 2003 (and revised in 2004) according to LP-SV.1Q-BSC, *Control of the Electronic Management of Information*, in effect at the time the work was performed. Statistical analyses, including cumulative distribution functions (CDFs) and probability distribution functions (PDFs), were performed on a qualified data set to develop these parameter distributions. The parameter distributions developed from these data account for uncertainty in the observed data. The parameters under consideration are wind speed and wind direction. Both the data and the methods used to develop these parameter distributions are also contained in the associated Output DTN: MO0408SPADRWSD.002. A discussion of the methods and sample data tables are included in this appendix, but the full data set is not reproduced here. These data are technical product output from this model report.

The first step in analyzing Desert Rock wind data involved importing a usable data file into Microsoft Access, *desertrock.zip* (NOAA 2004 [DIRS 171035]), provided through an FTP site (ftp.ncdc.noaa.gov) by Scott Stephens of the National Climatic Data Center in Asheville, North Carolina, on August 3, 2004. A total of 1,619,404 data lines were imported.

Column headers followed by blank lines were present within the data file received. To remove these involved deletion of 48,321 header and blank rows. In addition, one wind speed column data value with a ".0" in the cell that had an associated direction reading was deleted. Then, three data lines having a wind speed reading without an associated direction were deleted. Next, a search for "999.9" and "999" (i.e., the designators for blank data fields) was completed for the wind speed and direction columns, respectively. In all, there were 124,253 lines of data deleted as a result of the blank field data search, leaving a total of 1,446,826 data lines for analysis.

D1. HEIGHT GROUPINGS

At the repository site, the crest of Yucca Mountain is approximately 4,905 ft (1,495 m) above sea level (DTN: MO9912GSC99492.000 [DIRS 165922], boring SD-6). Using this datum, heights in meters above mean sea level in the wind data file were sorted by height in meters above Yucca Mountain. This was accomplished by setting the query field under the height column to the text shown in Table D-1. This process was repeated for each height interval, from 0 to 13 km, resulting in thirteen tables used for further data analyses as described later in this appendix.

The resulting datasets were saved as tables containing four columns including: height in meters (HEIGHT MTR), wind speed in meters per second (WNDSP MS), direction in degrees (DIR), and the id number (ID) assigned to each line by Microsoft Access, the program used for these initial activities. These tables were then exported from Microsoft Access to Microsoft Excel for further analyses of wind direction and speed. Prior to being imported into Excel, all fields were changed from text to number format in the table design view. Table D-2 provides the format of the data tables used for the CDF and PDF analyses.

For the 1 to 2, 2 to 3, and 3 to 4 data groupings, the number of data lines exceeded the number able to be stored (65,536) per worksheet in Excel. To accommodate the additional data lines, the first 65,536 lines were exported automatically by Access, while the remaining lines for each grouping were copied and pasted manually into an additional worksheet. Therefore, the CDFs and PDFs for these groupings were done separately for each worksheet, and then combined at the end.

Table D-1. Height Grouping Query Results

Query Name (Number of Data Lines Resulting)	Query Field Contents Under Height Column
0 to 1 (64,002)	>=" 1495" And <" 2495"
1 to 2 (72,498)	>=" 2495" And <" 3495"
2 to 3 (82,192)	>=" 3495" And <" 4495"
3 to 4 (70,748)	>=" 4495" And <" 5495"
4 to 5 (65,494)	>=" 5495" And <" 6495"
5 to 6 (62,169)	>=" 6495" And <" 7495"
6 to 7 (57,505)	>=" 7495" And <" 8495"
7 to 8 (51,434)	>=" 8495" And <" 9495"
8 to 9 (47,373)	>=" 9495" And <" 10495"
9 to 10 (49,869)	>=" 10495" And <" 11495"
10 to 11 (53,635)	>=" 11495" And <" 12495"
11 to 12 (56,917)	>=" 12495" And <" 13495"
12 to 13 (51,774)	>=" 13495" And <" 14495"

Table D-2. Example of Table Exported from Access to Excel

0 to 1 Table			
HEIGHT MTR	WINDSP MS	DIR	ID
1927	16	192	8

NOTES: HEIGHT MTR = height in meters; WINDSP MD = wind speed in meters per second;
DIR = direction in degrees; ID = ID number.

D2. WIND DIRECTION

The wind directions given in the raw data were in compass degrees *from* the indicated direction (e.g., wind from the west) and needed to be converted to ASHPLUME degrees *toward* the indicated direction (e.g., wind toward the east). For each of the heights indicated above, data were initially grouped into bins using the Histogram function under the Data Analysis selection under the Tools menu in Excel. Degree bins were entered manually into column E of the spreadsheet. After choosing tools, data analyses, and then histograms, a popup menu appeared and requested choices regarding input and output options. For the input, the wind direction data were entered (column C in the spreadsheet) in the input range cell similar to the following for the 0- to 1-km data table, "$C$2:$C$64003." Column E (bin degrees) was then chosen as the input for the bin range and typed in as: "$E$2:$E$15" under the Histogram function. This process was repeated for each of the remaining height groupings.

Table D-3 provides the histogram function analysis output.

Bins 0, 14, and 360 were combined to represent the 345- to 15-degree interval on the compass. The remaining bins represent the degree intervals as indicated in Table D-4.

Table D-3. 0 to 1 Histogram Function Output

Bin (in Compass Degrees)	Frequency
0	125
14	1,931
44	5,411
74	5,225
104	3,596
134	2,411
164	2,363
194	8,336
224	18,290
254	6,633
284	2,910
314	2,407
344	2,670
360	1,694

Source: Output DTN: MO0408SPADRWSD.002.

Table D-4. Bins Converted to Compass Degree Intervals

Compass Degree Intervals	Representative Bins
345 to 15	0, 14, and 360
15 to 45	44
45 to 75	74
75 to 105	104
105 to 135	134
135 to 165	164
165 to 195	194
195 to 225	224
225 to 255	254
255 to 285	284
285 to 315	314
15 to 345	344

NOTE: This table summarizes the histogram bins used to represent compass degree intervals.

Converting compass degrees to ASHPLUME degrees is depicted by Figure D-1. ASHPLUME degrees (Figure D-1, ASHPLUME degrees are around the perimeter, compass degrees are inside) *toward* the indicated direction were determined by selecting the ASHPLUME direction exactly opposite of the indicated compass-degree interval and recording the midpoint of the degree interval (Table D-5).
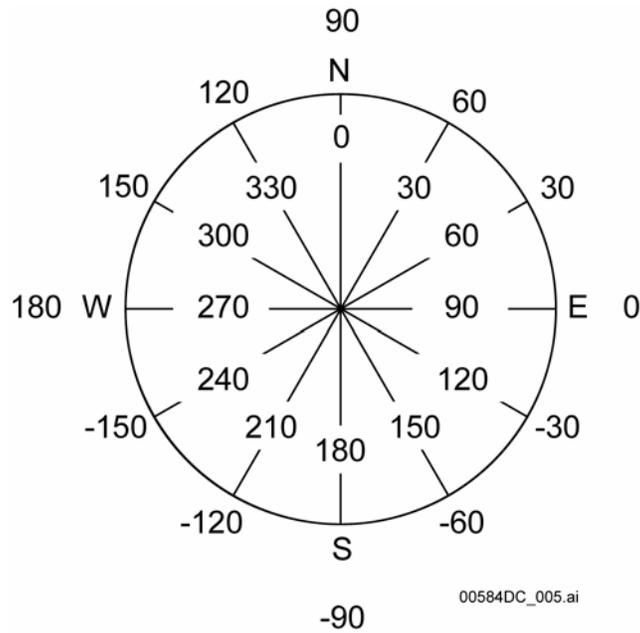
Figure D-1. Compass (Inside Numbers) and ASHPLUME (Outside Numbers) Degree Comparison

Table D-5. Compass Degrees (from Direction) Converted to ASHPLUME Degrees (toward Direction)

Compass Degrees	ASHPLUME Degrees
165 to 195	90 (North)
195 to 225	60
225 to 255	30
255 to 285	0 (East)
285 to 315	−30
315 to 345	−60
345 to 15	−90 (South)
15 to 45	−120
45 to 75	−150
75 to 105	180 (West)
105 to 135	150
135 to 165	120

NOTE: This table summarizes the conversion of compass direction to
ASHPLUME direction using the relationship depicted in
Figure D-1.

Table D-6. Example PDF Results

	A	B	C	D*	D
1	Compass Degrees	ASHPLUME Degrees	Count/ Frequency	PDF	PDF
2	165 to 195	90 (North)	8,336	=C2/(sumC2:C13)	0.1303
3	195 to 225	60	18,290	=C3/(sumC2:C13)	0.2858
4	225 to 255	30	6,633	=C4/(sumC2:C13)	0.1036

Table D-6. Example PDF Results (Continued)

1	Compass Degrees	ASHPLUME Degrees	Count/ Frequency	PDF	PDF
5	255 to 285	0 (East)	2,910	=C5/(sumC2:C13)	0.0455
6	285 to 315	−30	2,407	=C6/(sumC2:C13)	0.0376
7	315 to 345	−60	2,670	=C7/(sumC2:C13)	0.0417
8	345 to 15	−90 (South)	3,750	=C8/(sumC2:C13)	0.0586
9	15 to 45	−120	5,411	=C9/(sumC2:C13)	0.0845
10	45 to 75	−150	5,225	=C10/(sumC2:C13)	0.0816
11	75 to 105	180 (West)	3,596	=C11/(sumC2:C13)	0.0562
12	105 to 135	150	2,411	=C12/(sumC2:C13)	0.0377
13	135 to 165	120	2,363	=C13/(sumC2:C13)	0.0369

NOTES: This spreadsheet excerpt illustrates the method used to create wind direction PDFs for the 0 to 1 km interval.

    * = visible cell calculation.

Next, a PDF was completed using Microsoft Excel for each data grouping. This was performed by taking the sample count for each interval and dividing by the total number of samples for that particular height interval. The ASHPLUME degrees and count were then plotted against one another using the radar-type graph under Excel's Chart function to produce a "wind rose" diagram like Figure D-2.

Table D-6 was constructed for the 0 to 1 km interval in Excel. For final insertion into the TSPA model, four decimal places were used for the PDF values, and adjustments (+/- 0.0001) were made to ensure the sum of the distribution equaled exactly 1. ASHPLUME degrees were arranged sequentially, and the "Frequency" and "Compass Degrees" columns were deleted as shown in Output DTN: MO0408SPADRWSD.002.

Under the Excel Insert pull-down menu, Chart was selected, Radar was selected, and then the last example of radar graphs was chosen. Next, Columns B and C were plotted against each other to form the Figure D-2 for the 0 to 1 km interval. An example table containing all 13 intervals is displayed later in this appendix (Table D-11). For TSPA, these tables were formatted to contain only the PDF value and ASHPLUME degrees columns organized in ascending order (Output DTN: MO0408SPADRWSD.002).

Wind Rose Frequency of Occurrences (wind toward designation) at 0 to 1 km above YM
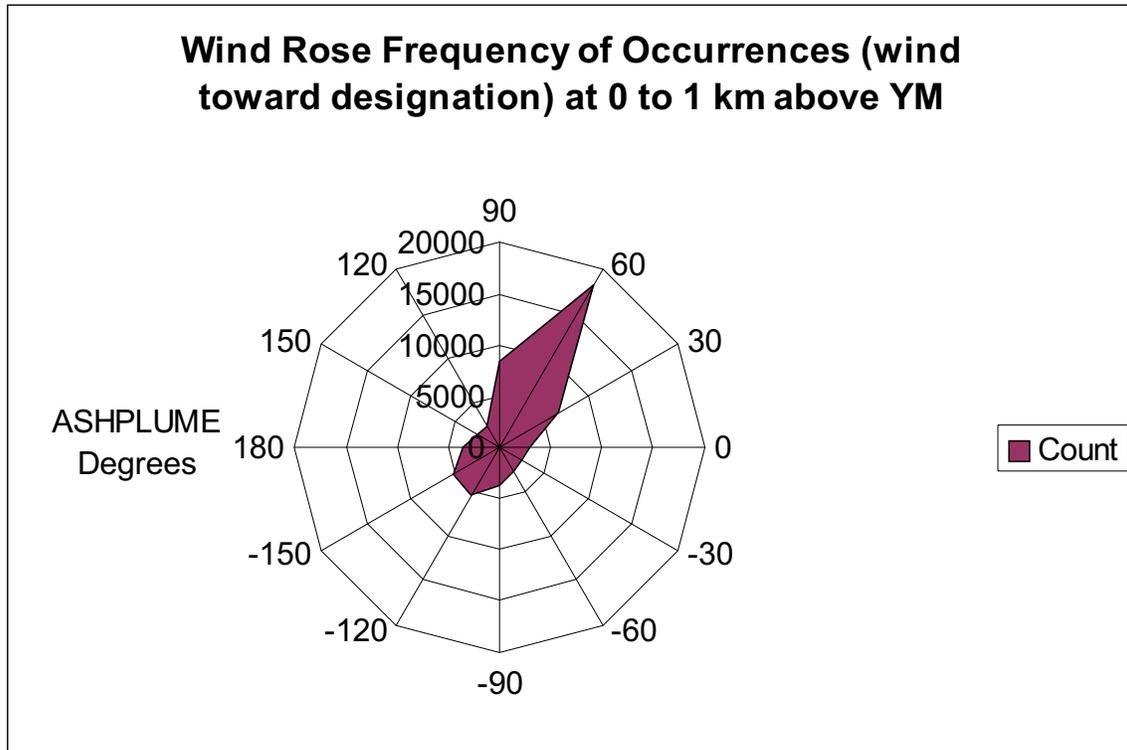
Source: Output DTN: MO0408SPADRWSD.002.

NOTE: This figure illustrates the method used to present information graphically using a radar-type graph.

Figure D-2. Wind Rose Diagram for 0 to 1 km above Yucca Mountain

D3. WIND SPEED

A CDF was calculated for each height grouping also using the Histogram function under the Data Analysis menu in Microsoft Excel. The wind speed column from table "0_to_1_Table" was copied and pasted into column A of a new worksheet, named "0 to 1 windspeed." Next, the wind speeds in meters per second were converted to centimeters per second in column B by multiplying each cell by 100. Table D-7 below shows the conversion. After choosing Tools, Data Analysis, and then Histogram, a popup menu appeared and asked for input and output options. For the input, the wind-speed data were entered in the input range cell, "$B$2:$B$64003," for the 0- to 1-km example. Wind-speed bin intervals consisting of 100 cm/s each, up to the highest wind speed recorded (14,100 cm/s) for all applicable heights (0 to 13 km), were then pasted into Column C in each Excel table (Table D-7). This column was then chosen as the input for the bin range cell and typed in as: "$C$2:$C$143" under the Histogram function.

Table D-7. Format of Tables Used to Calculate Wind Speed CDFs

A	B*	B	C
WNDSP MS	WNDSP CONV	WNDSP CMS	BINS CMS
16	= A2 × 100	1,600	0
15	= A3 ×100	1,500	100
9	= A4 ×100	900	200
7	= A5 ×100	700	300
8	= A6 ×100	800	400
7	= A7 ×100	700	500
8	= A8 ×100	800	600
7	= A9 ×100	700	700
6	= A10 ×100	600	800
6	= A11 ×100	600	900
1	= A12 ×100	100	1,000
3	= A13 ×100	300	1,100
2	= A14 ×100	200	1,200
3	= A15 ×100	300	1,300
2	= A16 ×100	200	1,400
1	= A17 ×100	100	1,500
2	= A18 ×100	200	1,600
4	= A19 ×100	400	1,700
4	= A20 ×100	400	1,800
3	= A21 ×100	300	1,900
3	= A22 ×100	300	2,000
9	= A23 ×100	900	2,100
13	= A24 ×100	1,300	2,200

NOTES: This spreadsheet excerpt illustrates the method used to bin the wind speed data.
* = visible cell calculation.

Additionally, the cumulative percentage (converted to decimal format in example Table D-8, below, by simply formatting the cell) and chart output boxes in the output menu were selected, which resulted in a table similar to Table D-8.

Table D-8. 0 to 1 km CDF Table

Bin (cm/s)	Frequency	CDF
0	125	0.00195
100	2624	0.04295
200	3,326	0.09492
300	6,156	0.19110
400	8,571	0.32502
500	6,873	0.43241
600	4,840	0.50803
700	6,045	0.60248

Table D-8. 0 to 1 km CDF Table (Continued)

Bin (cm/s)	Frequency	CDF
800	5,301	0.68531
900	4,661	0.75813
1,000	3,916	0.81932
1,100	2,907	0.86474
1,200	2,252	0.89993
1,300	1,743	0.92716
1,400	1,271	0.94702
1,500	908	0.96120
1,600	695	0.97206
1,700	480	0.97956
1,800	382	0.98553
1,900	259	0.98958
2,000	135	0.99169
2,100	193	0.99470
2,200	121	0.99659
2,300	71	0.99770
2,400	48	0.99845
2,500	32	0.99895
2,600	22	0.99930
2,700	16	0.99955
2,800	12	0.99973
2,900	8	0.99986
3,000	5	0.99994
3,100	0	0.99994
3,200	1	0.99995
3,300	0	0.99995
3,400	0	0.99995
3,500	0	0.99995
3,600	0	0.99995
3,700	0	0.99995
3,800	1	0.99997
3,900	0	0.99997
4,000	0	0.99997
4,100	0	0.99997
4,200	0	0.99997
4,300	0	0.99997
4,400	0	0.99997
4,500	1	0.99998
4,600	0	0.99998
4,700	1	1.00000
4,800	0	1.00000

Table D-8. 0 to 1 km CDF Table (Continued)

Bin (cm/s)	Frequency	CDF
4,900	0	1.00000
5,000	0	1.00000
5,100	0	1.00000
5,200	0	1.00000
5,300	0	1.00000
5,400	0	1.00000
5,500	0	1.00000
5,600	0	1.00000
5,700	0	1.00000
5,800	0	1.00000
5,900	0	1.00000
6,000	0	1.00000
6,100	0	1.00000
6,200	0	1.00000
6,300	0	1.00000
6,400	0	1.00000
6,500	0	1.00000
6,600	0	1.00000
6,700	0	1.00000
6,800	0	1.00000
6,900	0	1.00000
7,000	0	1.00000
7,100	0	1.00000
7,200	0	1.00000
7,300	0	1.00000
7,400	0	1.00000
7,500	0	1.00000
7,600	0	1.00000
7,700	0	1.00000
7,800	0	1.00000
7,900	0	1.00000
8,000	0	1.00000
8,100	0	1.00000
8,200	0	1.00000
8,300	0	1.00000
8,400	0	1.00000
8,500	0	1.00000
8,600	0	1.00000
8,700	0	1.00000
8,800	0	1.00000
8,900	0	1.00000
9,000	0	1.00000

Table D-8. 0 to 1 km CDF Table (Continued)

Bin (cm/s)	Frequency	CDF
9,100	0	1.00000
9,200	0	1.00000
9,300	0	1.00000
9,400	0	1.00000
9,500	0	1.00000
9,600	0	1.00000
9,700	0	1.00000
9,800	0	1.00000
9,900	0	1.00000
10,000	0	1.00000
10,100	0	1.00000
10,200	0	1.00000
10,300	0	1.00000
10,400	0	1.00000
10,500	0	1.00000
10,600	0	1.00000
10,800	0	1.00000
10,900	0	1.00000
11,000	0	1.00000
11,100	0	1.00000
11,200	0	1.00000
11,300	0	1.00000
11,400	0	1.00000
11,500	0	1.00000
11,600	0	1.00000
11,700	0	1.00000
11,800	0	1.00000
11,900	0	1.00000
12,000	0	1.00000
12,100	0	1.00000
12,200	0	1.00000
12,300	0	1.00000
12,400	0	1.00000
12,500	0	1.00000
12,600	0	1.00000
12,700	0	1.00000
12,800	0	1.00000
12,900	0	1.00000
13,000	0	1.00000
13,100	0	1.00000
13,200	0	1.00000
13,300	0	1.00000

Table D-8.   0 to 1 km CDF Table (Continued)

Bin (cm/s)	Frequency	CDF
13,400	0	1.00000
13,500	0	1.00000
13,600	0	1.00000
13,700	0	1.00000
13,800	0	1.00000
13,900	0	1.00000
14,000	0	1.00000
14,100	0	1.00000

Source: Output DTN: MO0408SPADRWSD.002.

This same procedure was followed for the remaining 12 tables (1 to 2 km, 2 to 3 km, 3 to 4 km, 4 to 5 km, 5 to 6 km, 6 to 7 km, 7 to 8 km, 8 to 9 km, 9 to 10 km, 10 to 11 km, 11 to 12 km, and 12 to 13 km) (see Output DTN: MO0408SPADRWSD.002).

For correct insertion into the TSPA model, the formatting of these tables was modified further. Specifically, all bins without samples (Frequency = 0) were deleted from the tables, the "Frequency" column was deleted, and only five decimal places were used for the CDF values. Additionally, the TSPA model requires the first bin CDF value to equal zero. As such, the zero wind speed bin was replaced with 1E-30 to account for data having a wind speed of zero, and the first bin was added which equaled zero. Table D-9 is the result of the minimum, maximum, and average wind speeds (in cm/s) calculated for each height interval in Access and then imported into one table in Excel. An example of the wind speed CDF tables formatted for TSPA is shown below (Table D-10). Table D-11 is an example of the wind direction PDF tables, and Figure D-2 displays a sample wind rose. The full wind speed and direction tables and figures are included in Output DTN: MO0408SPADRWSD.002 in individual Excel worksheets, following a consistent file-naming scheme. For instance, the wind speed data for the 0 to 1 km elevation range are listed in worksheet "0 to 1 CDF for TSPA" within the *0 to 1 CDF.xls* workbook; the wind direction data for the 0 to 1 km elevation range are listed in worksheet "0 to 1 PDF for TSPA" within the *0 to 1 PDF.xls* workbook.

Table D-9.   Minimum, Maximum, and Average Wind Speed

Height (km)	Minimum (cm/s)	Maximum (cm/s)	Average (cm/s)
0 to 1	0	4,670	668
1 to 2	0	4,480	817
2 to 3	0	5,000	1,007
3 to 4	0	6,400	1,215
4 to 5	0	10,500	1,486
5 to 6	0	14,100	1,695
6 to 7	0	10,300	1,949
7 to 8	0	11,000	2,160

Table D-9. Minimum, Maximum, and Average Wind Speed (Continued)

Height (km)	Minimum (cm/s)	Maximum (cm/s)	Average (cm/s)
8 to 9	0	8,700	2,294
9 to 10	0	8,640	2,416
10 to 11	0	8,900	2,437
11 to 12	0	9,900	2,311
12 to 13	0	7,300	2,064

Source: Output DTN: MO0408SPADRWSD.002.

Table D-10. 0 to 1 km CDF

CDF	Bin (cm/s)
0.00000	0
0.00195	1.00E–30
0.04295	100
0.09492	200
0.19110	300
0.32502	400
0.43241	500
0.50803	600
0.60248	700
0.68531	800
0.75813	900
0.81932	1,000
0.86474	1,100
0.89993	1,200
0.92716	1,300
0.94702	1,400
0.96120	1,500
0.97206	1,600
0.97956	1,700
0.98553	1,800
0.98958	1,900
0.99169	2,000
0.99470	2,100
0.99659	2,200
0.99770	2,300
0.99845	2,400
0.99895	2,500

Table D-10. 0 to 1 km CDF (Continued)

CDF	Bin (cm/s)
0.99930	2,600
0.99955	2,700
0.99973	2,800
0.99986	2,900
0.99994	3,000
0.99995	3,200
0.99997	3,800
0.99998	4,500
1.00000	4,700

Source: Output DTN: MO0408SPADRWSD.002.

Table D-11. 0 to 1 km PDF

Compass Degrees	ASHPLUME Degrees	Count	PDF
165 to 195	90	8,336	0.1303
195 to 225	60	18,290	0.2858
225 to 255	30	6,633	0.1036
255 to 285	0	2,910	0.0455
285 to 315	−30	2,407	0.0376
315 to 345	−60	2,670	0.0417
345 to 15	−90	3,750	0.0586
15 to 45	−120	5,411	0.0845
45 to 75	−150	5,225	0.0816
75 to 105	180	3,596	0.0562
105 to 135	150	2,411	0.0377
135 to 165	120	2,363	0.0369
	Totals	64,002	1.0000

INTENTIONALLY LEFT BLANK

APPENDIX E
INDEPENDENT TECHNICAL REVIEW OF MDL-MGR-GS-000002 REV 00B
CONDUCTED BY DR. FRANK SPERA,
UNIVERSITY OF CALIFORNIA, SANTA BARBARA

APPENDIX E
INDEPENDENT TECHNICAL REVIEW OF
MDL-MGR-GS-000002 REV 00B

This appendix presents an independent technical review of a Yucca Mountain Project (YMP) document conducted by F.J. Spera from March 24 to April 10, 2003 (Pfeifle 2007 [DIRS 182321]). The structure of this review is based on six review criteria set out in "Exhibit D Amended Scope of Work: Independent Review for Model Validation." The review criteria are listed below as a series of questions. The analysis provided below addresses each of these issues.

1. *Is the mathematical model (ASHPLUME) appropriate for representing the conceptual model (i.e., is this model appropriate for its intended use?)*

2. *Are the inputs sufficient?*

3. *Were all reasonable alternative models identified and adequately treated? If not, what are they, what are their capabilities, and what are their limitations?*

4. *Are the assumptions appropriate for use in the model?*

5. *Do the outputs of the model represent the inputs, or are the limitations to the model such that the outputs are not representative of possible future states?*

6. *Are the outputs of the model a reasonable representation of what may be expected from a volcanic eruption at Yucca Mountain?*

No computer codes were run during the course of this review. The review focuses on the conceptual and technical bases of YMP work regarding the dispersal of volcanic ash using the computer code ASHPLUME. Results from ASHPLUME are used as input for the TSPA.

Is the mathematical model (ASHPLUME) appropriate for representing the conceptual model, i.e., is this model appropriate for its intended use?

Introduction—There are a number of ash dispersal mathematical models of differing sophistication. It is beyond the scope of this report to review the history of ash dispersal modeling. ASHPLUME traces its origin back to the Suzuki model (1983 [DIRS 100489]), which applies to a steady eruption (constant eruptive mass flow rate, $\dot{M}$) from a circular cross-sectional vent. The fundamental factors governing the fallout distribution of volcanic tephra include the height of the steady state volcanic column (H), which is a function of the eruptive mass flow rate, $\dot{M}$, the total eruptive volume (V) and the spatial and temporal structure of the winds aloft during the eruptive event of duration t_d. The relationship between the total eruptive volume (V) and the volumetric eruptive rate ($\dot{V}$) for a steady eruption is simply $V=\dot{V}t_d$.

Because the density of ash (ρ_e) is essentially constant, there is a simple relationship between the eruptive mass flow rate, $\dot{M}$, and the volumetric eruption rate $\dot{V}$. The relationship is $\dot{V}=\dot{M}/\rho_e$ where ρ_e is the density of tephra particles at the vent. The size distribution of tephra also plays a role in ash dispersal. The distribution of ash particle size is relatively well known based on

granulometric studies of tephra from Strombolian eruptions and varies between reasonably well-defined bounds.

Plume Height (H), Mass Flow ($\dot{M}$), and Eruptive Volume(V)

Volcanic plume height (H) scales with the eruptive mass flow rate, $\dot{M}$, according to:

$$H \propto \dot{M}^{1/4} \qquad \text{(Eq. E-1)}$$

An example of a quantitative parameterization is the expression:

$$H = 0.24 \dot{M}^{1/4} \qquad \text{(Eq. E-2)}$$

with H measured in kilometers and the eruptive mass flow measured in kg/s. The scaling relation (1) comes from momentum-buoyancy plume theory and rests on a solid fluid dynamical footing. The determination of the constant in Equation 2 comes from an empirical calibration using data from a small number (~ 10 to 20) of volcanic eruptions for which column height is independently known. Its value may be uncertain by $\pm 20\%$ due to unsteadiness of column height and the intrinsic difficulty of measuring column height during an eruption. Note that Equation 2 is strictly valid for steady eruptions where $\dot{M}$ (or $\dot{V}$) is constant. In fact, no volcanic eruption is truly steady. Variations in mass flow during eruptions give rise to time-varying column heights. For example, during the 1980 eruption at Mount Saint Helens, the mass flow (and hence column height) varied significantly in non-monotonic fashion during the ~ 10 hour Plinian phase of the eruption. Although the expected eruptive style at Yucca Mountain is Strombolian and not Plinian, eruptive unsteadiness is typical of all styles of eruption, even eruptive events dominated by lava flows. One way of incorporating unsteadiness into ash dispersal is to model a single eruption as a sequence of smaller eruptive phases each with its own characteristic parameters. In effect one could use the ASHPLUME steady state model serially to evaluate the effects of eruption unsteadiness at least to a first approximation. Whether or not this is important depends on the timescale associated with wind and magma discharge unsteadiness. For example, if the timescale for changes in wind direction are comparable to or shorter than eruptive duration (t_d) then unsteady winds could have a marked effect on the distribution of ash at the surface.

In the model used by the Project, critical input comes from two relations expressed as Equations (7a) and (7b) on p. 39 of MDL-MGR-GS-000002 REV 00B. The first is an assumed relationship between the eruptive volume of ash (V) and the duration of the eruption (t_d). This essentially defines the eruptive volume flow rate (and the eruptive mass flow rate) as a function of total eruptive volume (V). That is, Equation 7a may be recast as:

$$V/t_d = e^{-a} V^{1-b} \qquad \text{(Eq. E-3)}$$

with a = 15.29 and b = 0.527 and the units of V in km^3 and t_d in seconds. Because

$$\dot{V} = \dot{M} / \rho_e \qquad \text{(Eq. E-4)}$$

it follows from the Project model that the eruptive mass flow rate is a function of eruptive volume:

$$\dot{M} = k \rho_e V^{1-b}$$ (Eq. E-5)

with $k = 229$, V in km^3, ρ_e in kg/m^3 and $\dot{M}$ in kg/s. On p. 44 of MDL-MGR-GS-000002 REV 00B the bounds on V are set between 0.004 km^3 and 0.08 km^3. This gives limits for $\dot{M}$ between 2.5×10^4 kg/s and 1.1×10^5 kg/s assuming an ash density of 1,500 kg/m^3. These values define bounds that vary by ~ one order of magnitude which seems somewhat on the small side of its potential range. Eruptive mass flow rates in the range 10^4 kg/s to 10^6 kg/s have been cited for Strombolian eruptions by some volcanologists (e.g., see Mastin 2002; Mastin and Ghiorso 2000; Mastin and Ghiorso 2001).

On what grounds can eruptions with mass flows ~ 10^6 kg/s be excluded?

According to Equation 7b on p. 39 of MDL-MGR-GS-000002 REV 00B, column heights corresponding to volumes of 0.004 km^3 and 0.08 km^3 are 2.2 km and 3.8 km, respectively. Again this is a rather small range and at the low to intermediate end for Strombolian eruptions. According to Equation 2, the aforementioned limits (2.5×10^4 kg/s and 1.1×10^5 kg/s) for $\dot{M}$ correspond to column heights between 3 km and 4.3 km in good agreement with Project calculations.

The main point is that eruptive mass flow rates up to 10^6 kg/s should not be excluded. At $\dot{M} = 10^6$ kg/s, a column height H = 7.6 km is predicted from Equation 2. Because the a priori assumption in Project ash dispersal calculations is the relationship between eruptive duration and eruptive volume, the range of corresponding eruptive mass flow rates is uniquely defined. It is the opinion of this reviewer that starting off by bounding eruptive mass flow rates ($\dot{M}$) rather than volume (V) might be advantageous partly because it is the correlation between $\dot{M}$ and H that has some fluid dynamical basis (i.e., unlike the V-t$_d$ correlation which is entirely empirical) and partly because the limits on $\dot{M}$ between ~ 10^4 kg/ to 10^6 kg/s encompass the range for normal Strombolian eruptions. Violent Strombolian eruption can attain even greater eruptive mass flow rates, up to 10^7 kg/s. According to Equation 2, a violent Strombolian eruption with $\dot{M} = 10^7$ kg/s would generate a column height H = 13 km. It is not argued here that such a value is 'typical.' However, the range 2 to 4 km considered by the Project seems unduly restrictive. Should the Project wish to consider additional higher mass flow eruptions, it would not be difficult to perform the simulations using Project models.

Structure and Variability of Winds Aloft—In addition to plume column height, the structure of prevailing winds during an eruption is critical to determination of ash dispersal. In the most detailed model, one can imagine wind velocity (direction and magnitude) prescribed on a three-dimensional grid of specified spatial resolution. Because upper atmosphere winds are often different from low level winds, it is important to get a complete profile of wind versus height from the vent up to the top of the eruption column. The wind velocity (speed and direction) can also vary temporally. Indeed, the eruption used by the Project (see Section 7.4 Natural Analogue Study on p. 56 in MDL-MGR-GS-000002 REV 00B) to "ground test" ASHPLUME shows how variations in winds aloft *during* an eruption influence ash distribution.

In the simplest ash dispersal model, the wind speed and direction is spatially constant (speed and direction) with no temporal variability during the eruptive interval (t_d). ASHPLUME implements a simple model of constant wind speed and direction and uses the wind vector from a height equal to "upper elevations to which the ash plume reaches." Presumably this corresponds to the height of the eruption column (H) derived from the relationship between eruptive volume (V) and column height (H).

Summary—ASHPLUME is applicable to steady volcanic eruptions (constant mass flow, $\dot{M}$) characterized by eruption columns of fixed height (H). Although no volcanic eruption is truly steady, the state-of-the-art in volcanic plume modeling is not sufficiently advanced to consider eruptions with unsteady discharge. ASHPLUME can be used serially to approximately model discharge unsteadiness and/or variable winds.

Two critical factors affecting ash dispersal are the column height and structure of winds aloft. ASHPLUME uses an empirically calibrated correlation between eruptive volume (V) and column height, H. In fluid dynamical terms, the height of an eruption column (H) scales with the mass flow, $\dot{M}$ according to H ~ $\dot{M}^{1/4}$. The eruptive volume (V) as given in Equation 3 correlates to H provided the plume-generating eruption is steady (i.e., $\dot{M}$ is constant) and the density of ash is constant. Regarding the issue of the winds aloft, any single ASHPLUME realization of ash dispersal assumes a constant wind speed and direction. Clearly this is a gross approximation; the vertical structure of the winds will generally depend on height above the vent. On the other hand, predicting the structure of the winds aloft at some time in the future 10,000 years is not easily accomplished. The Monte Carlo method of drawing a constant wind velocity from a meteorologically-based distribution and performing many realizations and then sampled for TSPA purposes is sound.

The range of eruptive volumes leads to a range of eruptive mass flows that are in the low to intermediate range for Strombolian eruptions. Eruptive mass flow rates of 10^6 kg/s cannot be precluded and should be computed.

Are the Inputs Sufficient?–discussion is keyed to numbered sections in MDL-MGR-GS-000002 REV 00B.

4.1.1 DATA

The variation of volcanic ash size distributions for Strombolian eruptions based on granulometric studies of G.P.L. Walker and coworkers beginning in the early 1970s and continuing to the present today is well known. Although the precise distribution of particle size is unique to a given eruption, the variations are not large. Similarly, waste particle size distributions are adequately known for the purposes of the TSPA given other limitations of the ASHPLUME model.

4.1.2 PARAMETERS AND PARAMETER UNCERTAINTY

The method of developing probability distributions for compatibility with MC methods used in the TSPA is a sound practice.

4.1.3 OTHER MODEL INPUTS

Items in Table 4, p. 20 of MDL-MGR-GS-000002 REV 00B are needed to perform ASHPLUME simulations and are commented on here.

The mathematical model of Suzuki (1983 [DIRS 100489]) is the starting point. The Suzuki model was used by Jarzemba (1997) with an important correction (see Equation 2 in Jarzemba) in order to achieve mass conservation, a constraint that must be incorporated in any ash dispersal model. However, the paper by Jarzemba has at least two errors. The first is that Equation 1 in Jarzemba (1997) is missing a negative sign in front of the numerator in the exponential term. The second is that there is a missing factor of g in the third term in the denominator of Equation 3 in Jarzemba. I note that these errors have been corrected in the Project work; that is, Equation 2 and Equation 4 on p. 37 and p. 38 in MDL-MGR-GS-000002 REV 00B are correct unlike the analogous equations in Jarzemba (1997).

The physical properties used for air (viscosity and density) from Lide (1994) are adequate for the purposes of the TSPA.

Are the Assumptions Justified?–discussion is keyed to numbered sections in MDL-MGR-GS-000002 REV 00B.

5.1.1 TWO-DIMENSIONAL DIFFUSION

The two-dimensional model may be sufficient for the purposes of the TSPA. It is hard to determine the level of confidence one should assign to ASHPLUME results without making a direct comparison between ASHPLUME and a three-dimensional code such as the one by G. Macedonio and co-workers (Armienti et al. 1988; Macedonia et al. 1988; 1990). Approximations are made in contracting a three-dimensional model to a two-dimensional model. The neglect of vertical diffusion is probably justified because vertical advection is many orders-of-magnitude larger than vertical diffusion. In the two-dimensional models one can increase the two-dimensional eddy diffusivity to roughly account for three-dimensional effects. The only way to evaluate the quality of the two-dimensional approximations is to carry out the full three-dimensional calculation and compare results. This reviewer has not made this comparison. Presumably, if the Project felt this was important, they could contact the Italian volcanologists mentioned and explore this possibility. Alternatively, the Project can generate two-dimensional ASHPLUME results and compare these to published three-dimensional forward models relevant to eruptions at Mount Vesuvius, Italy. My own guess is that for the purposes of the TSPA the two-dimensional model would suffice. Even with a sophisticated three-dimensional model, the lack of knowledge of the winds aloft at some time in the future 10,000 years may translate into a larger uncertainty in ash thickness at a specific location than that associated with a two-dimensional rather than three-dimensional model. But this is speculation on my part.

5.1.2 ASHPLUME REPRESENTATION OF THE CONCEPTUAL MODEL

This is a very conservative assumption. Inspection of volcanological data suggests the ratio of lava to proximate tephra (cone-building deposits) to distal ash (the deposition that ASHPLUME and like models compute) is of order 1:1:<<1. That is, for the sort of eruption 'expected' at

Yucca Mountain, the distal ash will make up only a small portion of the total. Hence the assumption made by the Project, that the entire eruptive volume is processed through a Strombolian column, is conservative. For Lathrop Wells, if the entire eruptive volume of $0.06 \, km^3$ is identified with the ash volume (it clearly is not!), then according to expressions used by the Project, the eruptive duration was ~ 11.5 days, the eruptive mass flow was $6 \times 10^4 \, kg/s$ and the column height was $H \sim 3.6 \, km$.

5.1.3 WASTE-PARTICLE VALUES BELOW INCORPORATION RATIO

Small ash particles cannot host large fuel waste particles. This seems to be a very reasonable assumption in no further need of documentation or explanation.

5.2.1 FUTURE WIND SPEED AND DIRECTION

Even if one knew the future climate, predicting winds aloft and their variation in time and space is most difficult. The present winds aloft structure is as good as any other and is consistent with the level of approximation in ASHPLUME.

5.2.2 WASTE PARTICLE SIZE

Waste is assumed to be unaltered spent commercial fuel. This is an adequate approximation given other uncertainties.

5.2.3 ERUPTION VELOCITY AT VENT

The Project adopts a relationship from Wilson and Head (1981) between vent exit radius (r_e) and eruptive velocity (u_e), as input for ASHPLUME. Neither the derivation of this relationship nor a discussion of the assumptions upon which it is based is given in MDL-MGR-GS-000002 REV 00B. It is noted here that this "correlation" is based on incompressible flow and assumes specific pressure gradients (based on a density differences between magma and host crust) and magma viscosities. *The conditions assumed to generate the values in Table 3 in Wilson and Head (1981) are not generally applicable to the highly compressible high-speed eruption of volatile-charged magma in the inertial regime.* Jarzemba (1997) also cites a relationship from Wilson and Head (1981) that provides a correlation amongst vent exit radius (r_e), mean density of ash particles (ρ_p) and eruption mass flow rate ($\dot{M}$) to determine the eruption velocity at the vent exit (u_e). It is important to insure that the Wilson and Head (WH) scaling relation does not implicitly or explicitly involve assumptions inconsistent with other assumed relations (e.g., Equation (7a) on p. 39 of MDL-MGR-GS-000002 REV 00B). In particular, the last few sentences of Section 5.2.3 on p. 26 of MDL-MGR-GS-000002 REV 00B are puzzling. *Results plotted on fig. 6a in WH (1981) pertain to specific exsolved magma water contents which are less than those expected for basaltic volcanism at Yucca Mountain (see Final Report of the Igneous Consequences Peer Review Panel, February 2003).*

From review of the documentation, it appears that the Project develops the input needed for ASHPLUME according to the following scheme. First, a value for the eruptive ash volume (V) is picked from a uniform distribution. Then using Equation 7a on p. 39 of MDL-MGR-GS-000002 REV 00B, the eruptive duration, t_d is calculated (project literature calls this T_d; to

avoid confusion with the thermodynamic temperature used in some volcanic plume models, although not in ASHPLUME, use is made of the symbol t_d here). Once t_d and V are known, then Equation 7b on p. 39 of MDL-MGR-GS-000002 REV 00B is used to compute the column height, H. Once V and t_d are known, $\dot{M}$ and M (eruptive mass) are easily computed given a density (based on particle size) of ash particles using $\dot{V}=\dot{M}/\rho_e$ and V=M/ρ_e, respectively. (Project uses symbol ψ_p for particle density). Then the Project uses the Wilson and Head (WH) scaling relation (discussed above) amongst r_e, $\dot{M}$ and ρ_e to obtain the vent exit radius, r_e and finally, from the continuity expression $\dot{M}=\rho_e\pi r_e^2 u_e$, the eruption velocity at vent exit (labeled W_0 by Project and u_e in this review).

It seems, unless this reviewer is mistaken, that this procedure is redundant. That is, once V and hence t_d are determined, then indeed H is easily determined. However, implicit in the correlation between V and t_d is the value of $\dot{M}$ and hence M, for an assumed ash density. It seems the vent exit velocity is uniquely determined once a value for r_e is chosen using the expression $\dot{M}=\rho_e\pi r_e^2 u_e$. In other words, why does the Project resort to the use of the WH correlation, presumably identical to or a closely related to the one given as Equation 14 in Jarzemba (1997)?

First of all, it is not clear that Equations 7a and 7b on p. 39 of MDL-MGR-GS-000002 REV 00B are consistent with the WH relationship used by the Project. The density of the magmatic mixture depends on the pressure at the vent exit, which in turn depends on the volatile content. Do these considerations affect the r_e-u_e scaling relationship assumed to obtain input parameters for ASHPLUME? *Secondly, and most importantly, it is not clear why the WH scaling correlation is needed at all.* Straightforward manipulation of Equation 7a on p. 39 of MDL-MGR-GS-000002 REV 00B gives:

$$\frac{V}{t_d}=e^{-a}\,V^{1-b}$$

(Eq. E-6)

where a and b are constants. Hence Equation 6 combined with continuity ($\dot{M}=\rho_e\pi r_e^2 u_e$) implies that

$$\pi r_e^2\,u_e=e^{-a}\,V^{1-b}$$

(Eq. E-7)

From Equation 7 it appears that given V, a unique relationship between r_e and u_e exists. A selected value for r_e completely determines u_e without need for an additional WH correlation.

Were all reasonable alternative models identified and adequately treated? If not, what are they, what are their capabilities, and what are their limitations?

The short answer to this question is "No." The Project uses the ASHPLUME model. There has been no systematic comparison of results generated by ASHPLUME with other models. On p. 34 in MDL-MGR-GS-000002 REV 00B there is discussion of other models although no detailed comparisons have been made. The models briefly mentioned in MDL-MGR-GS-000002 REV 00B (Gaussian-Plume, PUFF and Gas-Thrust code) suffer

limitations and cannot generate the quantitative output needed for the TSPA without modification. A model not mentioned in MDL-MGR-GS-000002 REV 00B called VAFTAD (Hefter and Stunder 1993) has been found to accurately model the dispersion of volcanic ash in the atmosphere. That is, to predict the motion of airborne ash clouds. Unfortunately, VAFTAD like PUFF offers no prediction of ground-level ash accumulation and therefore unsuitable in its present form for TSPA purposes.

Fortunately, other volcanological ash dispersal models that provide quantitative results for ground-level ash accumulation exist and may be utilized by the Project to build confidence and discover the limitations of ASHPLUME. Perhaps the most cogent model is one developed by Hurst and co-workers (Hurst 1994) based on the earlier model of G. Macedonio and co-workers (Armienti et al. 1988; Macedonio et al. 1988, 1990). The code developed by the Italian group implements a three-dimensional particle diffusion model with allowance for wind direction and speed as a function of height. The original code was somewhat unwieldy requiring large three-dimensional arrays and long run times. Motivated by the need for an easy-to-implement Civil Defense tool, Hurst and co-workers developed a code called ASHFALL. This is a two-dimensional imensional code that accounts for variations in wind speed and direction as a function of altitude and time. Vertical diffusion of ash is neglected (as in ASHPLUME). The output of ASHFALL is the ash thickness at points on a rectangular grid centered on the vent. Details of the model can be found in the report and users guide entitled "ASHFALL-A Computer Program for estimating Volcanic Ash Fallout" by T. Hurst (1994). The characteristics and performance of ASHFALL are documented in the studies of Hurst and Turner (1999). A comparison of ASHFALL predictions with observed ash distributions of three ash-producing events from Ruapehu volcano in the North Island of New Zealand shows that actual ash thickness at any location are generally within a factor of two of that forecast by ASHFALL. The accuracy of the forecast wind direction is the main factor affecting quality of ASHFALL predicted tephra isopachs according to the study by Hurst and Turner (1999).

Finally, mention should be made of the Hybrid Particle and Concentration Transport Model (HYPACT) of Walko and Tremback (1985). HYPACT simulates the motion of atmospheric tracers under the influence of winds and turbulence. Its Lagrangian formulation enables representation of sources of any size and the maintenance of concentrated, narrow plumes until atmospheric dispersion dictates they should broaden. The Lagrangian particle plume can then be converted into a concentration field and advected using a Eulerian formulation. The Lagrangian particles are moved through space and time based on interpolated wind velocities plus a superimposed random motion scaled to the intensity of local turbulence. A spectrum of gravitational settling velocities related to particle size can be specified. The velocity field (all three components), the potential temperature and information regarding the scale of turbulence are necessary input for implementation of HYPACT. HYPACT is the most sophisticated model for following the trajectory of airborne particles known to this reviewer.

In the study of Turner and Hurst (2001) a comparison is made between HYPACT and ASHFALL using the Regional Atmospheric Modeling System (RAMS) for the winds aloft structure as input for both models (see Pielke et al. 1992 for details pertaining to RAMS). Comparison of the performance of RAMS/HYPACT with ASHFALL shows that RAMS/HYPACT provides more accurate spatial and temporal forecasts of ash transport. Although the HYPACT model is superior in reproducing the temporal and spatial movement of

the ash cloud, it is not suitable in its current form for quantifying the depth of ash. The code would need to be modified in order to determine the distribution of isopachs.

In summary, a detailed comparison should be made between ASHFALL and ASHPLUME. This can be done in two ways. First, one can select representative eruption and winds aloft parameters and compare predictions made by ASHPLUME and ASHFALL. Secondly, one can apply ASHPLUME to the 1995 and 1996 Mount Ruapehu, New Zealand eruptions. These have already been modeled using ASHFALL and results are readily available in the literature. Based on the results of such comparisons, one will be able to develop confidence in the results from ASHPLUME. Because the ASHFALL code is not freely available, Project geoscientists may want to work with Dr. Tony Hurst (*T.Hurst@gns.cri.nz*). Hurst is the developer of ASHFALL and may be available to run some models in coordination with Project geologists. ASHFALL unlike ASHPLUME can handle a time-varying vertical profile of wind speed and direction perhaps more appropriate to conditions during an eruption. It can also be used in the simpler ASHPLUME-like mode with constant wind speed and direction.

Do the outputs of the model represent the inputs, or are the limitations to the model such that the outputs are not representative of possible future states?

In general, the output of an ash dispersal model provides the type of information needed for the TSPA. The real issue is the quality of the forward model. Ash dispersal in all its complexity is a problem that has not been fully solved. However, for the purposes of the TSPA and given the state-of-the-art, a two-dimensional model such as ASHPLUME may suffice. However, further work should be accomplished to increase the confidence in ASHPLUME results. One way of doing this is to make a detailed comparison between ASHFALL and ASHPLUME. Another is to apply ASHPLUME to the 1995 and 1996 eruptions at Mount Ruapehu. Typically, these eruptions exhibit column heights H ~ 10 km consistent with eruptive mass flow $\dot{M} \sim 3 \times 10^6$ kg/s, eruptive volume V~ 0.08 km^3 and ~ 10-hr eruption duration. This is within the range of possibility for Strombolian eruptions at Yucca Mountain. Recall that Strombolian mass flows are generally in the range 10^4-10^6 kg/s with very strong so-called 'violent' Strombolian eruptions having $\dot{M}$ up to ~ 10^7 kg/s. The main need is to compare ASHPLUME results to results from another method. This task can probably be accomplished by 3-5 weeks or less if outside expertise (e.g., Dr. Tony Hurst for ASHFALL) contributes to the effort.

Are the outputs of the model a reasonable representation of what may be expected from a volcanic eruption at Yucca Mountain?–Tentatively the answer to this question is "probably yes." Comparison of ASHPLUME results with other codes would enable one to more definitively answer this question. *An explanation of the issue raised in section labeled 5.2.3 in this review should be provided to insure self-consistency is maintained in application of ASHPLUME.*

Other Comments on MDL-MGR-GS-000002, REV 00B–p. 41 reference to 'Suzuki et al.' should be to 'Jarzemba et al. (1997)'.

REFERENCES CITED*

NOTE: These references were used at part of the technical review and are not reflected in the document input reference system as part of this report.

Armienti, P., Macedonio, G., and Pareschi, M.T. A numerical model for the distribution of tephra transport and deposition: applications to May 18, 1980 Mt. St. Helens eruption, *Jour. Geophys. Res.,* **93**, 6463-6476, 1988.

Hefter, J.L. and B.J. Stunder, Volcanic ash forecast and dispersion (VAFTAD) model, *Weather and Forecasting*, **8**, 533-541, 1993.

Hurst, T.W. and R.W. Turner, Performance of a program for volcanic ashfall forecasting, *N.Z. J. Geol. Geophys.,* **42**, 615-622, 1999.

Hurst, T.W., ASHFALL- a computer program for estimating volcanic ash fallout. Report and user guide. *Institute of* Geological *and Nuclear Sciences Science Report 94/23.* 22p., 1994.

Jarzemba, M.S., Stochastic radionuclide distributions after a basaltic eruption for Performance Assessments of Yucca Mountain, *Nucl. Tech.,* **118**, 132-142, 1997

Lide, D.R., ed. 1994. *CRC Handbook of Chemistry and Physics, A Ready-Reference Book of Chemical and Physical Data.* 75th Edition. Boca Raton, Florida: CRC Press. TIC: 102972.

Macedonio, G., Pareschi, M.T. and Santacroce, R., A numerical simulation of the plinian fall phase of 79 A.D. eruption of Vesuvius, *Jour. Geophys. Res*, **93**, 14817-14827, 1988.

Macedonio, G., Pareschi, M.T. and Santacroce, R., Renewal of explosive activity at Vesuvius: models for the expected tephra fallout, *Jour Volcanol. Geother. Res.*, **40**, 327-342, 1990.

Mastin, L.G., Insights into volcanic conduit flow from an open-source numerical model, *Geochem. Geophys. Geosys.*, *3*(7), 10.1029, 2002.

Mastin, L.G., and M.S. Ghiorso, *A Numerical Program for Steady-State Flow of Magma-Gas Mixtures Through Vertical Eruptive Conduits, U.S. Geological Survey,* Open-File Report 00-209, 2000.

Mastin, L.G., and M.S. Ghiorso, Adiabatic temperature changes of magma-gas mixtures during ascent and eruption, Contributions to *Mineralogy & Petrology,* **141**, 307-321, 2001.

Pielke, R.A., W.R. Cotton, C.J. Tremback, M.E. Nicholls, M.D. Moran, D.A. Wesley, T.J. Lee and J.H. Copeland, A comprehensive meteorological modeling system-RAMS, *Meteor. Atmos. Phys*., **49**, 69-91, 1992.

Suzuki, T., A theoretical model for dispersion of tephra, *In*: Shimozuru, D. and I. Yokohama (*eds*) Arc volcanism: physics and tectonics, p. 95-113, 1983.

Turner, R and T.W. Hurst, Factors influencing volcanic ash dispersal from 1995 and 1996 eruptions of Mount Ruapehu, New Zealand, *J. Appl. Meteorol.,* **40**, 56-69, 2001.

Walko, R.L. and C.J. Tremback, HYPACT: The Hybrid Particle and Concentration Transport Model. User's guide, 13pp, 1995. Available from ASTER Division, Mission Research Corporation, P.O. Box 466, Fort Collins, CO 80522.

Wilson, L. and J.W. Head, Ascent and eruption of basaltic magma on the Earth and Moon, *Jour. Geophys. Res*., **86**, 2971-3001, 1981.

INTENTIONALLY LEFT BLANK

APPENDIX F
DEVELOPMENT OF WASTE PARTICLE SIZE DISTRIBUTION

APPENDIX F
DEVELOPMENT OF WASTE PARTICLE SIZE DISTRIBUTION

F1.   METHOD

This analysis of the assumption and rationale for defining the waste particle size criteria is based on literature review. The minimum, maximum, and mode for waste particle size resulting from magma-waste interaction are defined via comparisons of the results of studies of physical, chemical, and thermal waste degradation.

F2.   POTENTIAL INFLUENCE ON WASTE PARTICLE SIZE

Two eruptive scenarios can be described, based on different potential effects on waste particle size and incorporation in the dispersed volcanic ash. These two scenarios are dependent on whether the rising magma flux is effusive or explosive at the point of interaction with the repository drifts. The preeruptive and eruptive stage steps and potential effects on the waste interaction are shown in Figure F-1.

Scenario 1 of Figure F-1 shows that an effusive magma flux interaction with the failed waste packages could result in physical mixing of the waste particles within the molten magma. This interaction and physical incorporation might include some degree of waste-magma eutectic formation. However, independent of this and of the degree to which the waste fragments are altered through the effects of oxidation, the considered potential overall effect is a distribution of the waste into the magma as a mixed mass fraction. The waste would then distribute, disperse and deposit as a mass fraction of the lava, scoria, and tephra.

Scenario 2 involves an explosive magma flux through the repository resulting in the disaggregation of waste to the assumed particle size distribution and incorporation with ash particles during the plume formation. The description in Figure F-1 revises this process to include mixing of the waste with the magma during transport through the conduit and subsequent distribution, dispersal, and deposition of the waste as a mass fraction of the lava, scoria, and tephra.
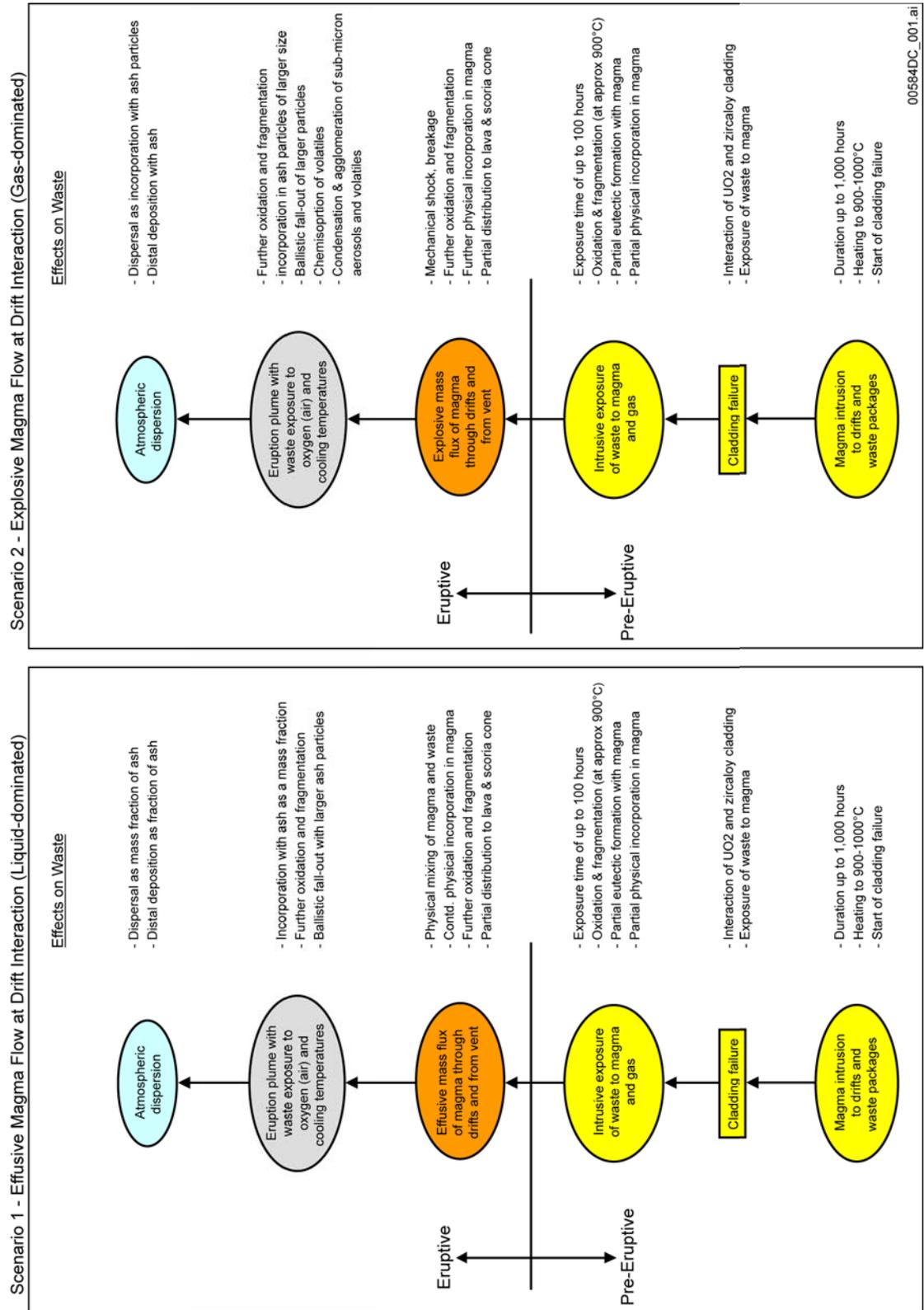
Figure F-1. Extrusive Event Sequence of Potential Influences on Waste and Waste Particle Size

F3. SUMMARY OBSERVATIONS AND COMMENTS

From the literature survey, a number of summary observations have been made; these are discussed below.

F3.1 SPENT FUEL CHARACTERIZATION

Extensive investigations have been conducted by Pacific Northwest National Laboratory (PNNL) for the DOE OCRWM Program to characterize spent fuel and the physico-chemical effects that can occur under long-term storage conditions.   The investigations include inter- and intra-granular physical and chemical effects; however spent fuel particle-size distribution has not been addressed in a manner directly applicable to this model report. Approved testing materials (ATM) test report photomacrographs (Guenther et al. 1991 [DIRS 109207]; Guenther et al. 1991 [DIRS 127061]) show significant fragmentation of irradiated fuel while the upper-end fuel particle size (in both dimensions) is visually gauged to be approximately equivalent to half pellet diameter (i.e., approximately 4.5 to 5 mm).   Example fuel pellet fragmentation is shown in Figure F-2. The fuel form pellet in this case was 9.56 mm dia. × 11.4 mm long.
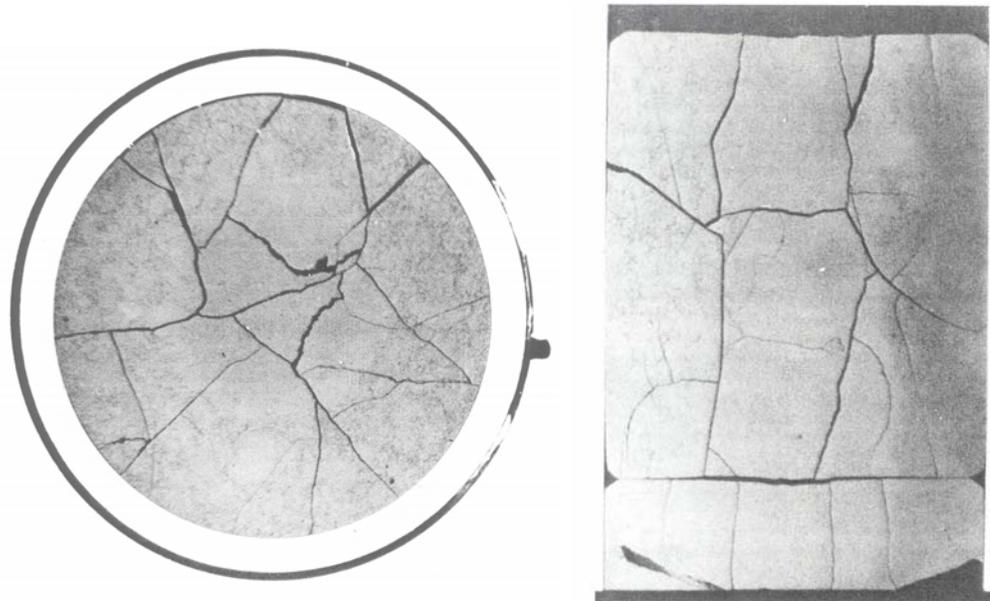
Source: Guenther et al. 1991 [DIRS 127061], Figures E.1.g and E.1.h.

NOTES: (Left) Photomacrograph of as-polished transverse sample 105-ADD2966-J (~10×) (Neg. No. 8802836-1)
      (Right) Photomacrograph of as-polished transverse sample 105-ADD2996-1 (~10×) (Neg. No. 8803473-6).

Figure F-2. Photomacrographs Illustrating Spent Fuel Fragmentation Under Long-Term Storage Conditions

F3.2   FUEL FORM

The primary grain size for fuel form is proprietary to the source and application, with a typical assessment being that average grain size generally ranges from 7 to 12 μm, with good reproducibility around 9 μm (Guenther et al. 1991 [DIRS 109207], p. 3.4). It is not consistently clear whether this relates to the attainable grain size through disaggregation processes (see below).

"Oxidation of Spent Fuel in Air at 175 to 195°C" (Einziger et al. 1992 [DIRS 101607], Table 2) lists the grain size for the ATM fuels and a Turkey Point fuel as shown in Table F-1.

Table F-1.   Spent Fuel Grain Size

Spent Fuel	Grain Size, μm
ATM-103	18.5
ATM-104	5–15
ATM-105	11–15
ATM-106	10–13
Turkey Point	20–30

Source: Einziger et al. 1992 [DIRS 101607], Table 2.

F3.3   OXIDATION OF UO2

Extensive studies have investigated the oxidation effects on irradiated and non-irradiated UO_2 fuel (DOE 2003 [DIRS 166027], p. 19). Mostly these have been for temperature ranges up to about 400°C, presumably pertaining to spent fuel handling and storage. The chemistry of the uranium oxide system is complex because of the existence of hyperstochiometric oxides (DOE 2003 [DIRS 166027], p. 20). U_3O_8 is cited as being well known as the crystalline phase responsible for fuel swelling and disaggregation when oxidized (Dehaudt 2001 [DIRS 164019], p. 13). At lower temperatures, the progressive oxidation of UO_2 to the higher valence state involves an incubation time, which ranges from 23 to 80 minutes at 400°C and tends towards 0 at 500°C (Dehaudt 2001 [DIRS 164019]; Einziger et al. (1992 [DIRS 101607], p. 55) report that oxidation up to $UO_{2.4}$ leads to volume reduction of the UO_2 matrix, thereby opening grain boundaries that can result in disaggregation of fuel into single fuel grains. Further oxidation to U_3O_8 and related oxides results in a large volume expansion and potentially extreme degradation of the fuel into a powder (DOE 2003 [DIRS 166027], p. 23).

For high temperatures (magma interaction is ~1,100°C), and somewhat countering the foregoing perspective, other work reports that above ~350°C, the intermediate U_3O_7/U_4O_9 is generally not observed in major quantities; instead, the bulk oxidation appears to proceed directly to U_3O_8. Above ~500°C the rate of U_3O_8 formation on sintered UO_2 pellets does not display Arrhenius behavior, but rather, the rate declines with increasing temperature. This behavior has been attributed to the increased plasticity of U_3O_8 above 500°C; thus the U_3O_8 formed does not readily spall from the UO_2 surface but instead forms a barrier to retard further oxidation. The particle size of U_3O_8 powder generated by air oxidation of UO_2 pellets increases with oxidation temperature, perhaps because of increasing U_3O_8 plasticity between 400°C and 700°C. The major product of UO_2 oxidation remains U_3O_8 up to ~1,100°C, above which U_3O_8 decomposes

to a series of oxides with slightly lower O:U ratios (McEachern and Taylor 1997 [DIRS 101726], Section 2.1).

F3.4 MECHANICAL SHOCK

Sandia National Laboratories performed sub-scale and full-scale tests to evaluate the capability of high-energy devices to breach spent fuel truck casks and disperse cask contents (Sandoval et al. 1993 [DIRS 156313]). This work is one of few that report particle size distribution for the outcome. The reported mass median particle diameter in this case is 210 μm. However, this test represents mechanical shock at ambient temperatures and may not be a most appropriate analogue for an eruptive event in which fuel is pre-heated to elevated temperature (resulting in plasticity) and is subjected to shock forces from molten magma and expanding gas.

F3.5 ARGONNE NATIONAL LABORATORY FUEL DISAGGREGATION EXPERIMENTS[1]

The following discussion is based largely on laboratory examinations of commercial spent nuclear fuels performed at Argonne National Laboratory (ANL), but conducted for purposes outside the realm of understanding particle size. The aim of the sample preparation, from which much of the discussed information was obtained, was to disaggregate spent-fuel fragments in order to maximize the fuel's surface area before using it in "accelerated" aqueous-corrosion tests. There is no statistical information available for the distribution of particle sizes caused by the disaggregation and grinding of spent UO_2 fuels in the laboratory. There is a similar paucity of data for oxidized and corroded fuels. Particle-size estimates reported here, as well as estimates for mean sizes and ranges, are based on a combination of data obtained from intentional crushing and grinding of "unaltered" spent fuel, as well as the author's experience with handling and examining spent commercial fuel in various states of degradation. These observations are augmented by citations to selected open-literature reports on the physical condition of spent commercial fuel, as well as naturally occurring UO_2 (the later being considered a useful natural analogue for severely corroded spent commercial fuel). It is emphasized that no formal statistical treatment was performed to justify the mean sizes and ranges reported here. The following discussion concerns commercial spent UO_2-based fuels. Three states of fuel degradation can be defined: (1) unaltered fuel (i.e., uncorroded and unoxidized); (2) dry-air oxidized fuel; and (3) aqueous-corroded fuel. Particle sizes are estimated for each below.

F3.5.1 Unaltered Fuel (Uncorroded And Unoxidized)

When crushing spent UO_2 fuel during the preparation of samples for aqueous-corrosion studies on fuel being conducted at ANL, it was found that reducing the particle sizes of a fuel of moderate burnup [approved testing material (ATM) 103: ~ 30 MW-d/kg-U] was readily achieved by using a two-step crushing and grinding process. Fuel fragments that had been removed from the cladding (with fragment sizes of several millimeters across) were initially crushed by using a stainless-steel impact tool, followed by sieving the resulting pieces through

---

[1] This work was completed in 1999 by Dr. R.J. Finch, ANL. This text was updated by R.J. Finch for BSC 2004 [DIRS 170026], Appendix H in May through August 2004. This summary of ANL work was included in BSC 2005 [DIRS 174067], Appendix H, and it has been included here as a stand-alone analysis in this broader survey of nuclear waste particle sizes under a variety of environments.

two stacked sieves with nominal openings of 0.015 cm and 0.0045 cm (i.e., 200 and 325 mesh, respectively). The largest size fraction (> 0.015 cm) was then placed into a stainless-steel-ball mill [an ANL-designed and built vibratory roller mill cylinder] and ground for a total of 31 minutes. After each grinding step, the fuel was emptied from the ball mill into the stack of three sieves, with the largest size fraction (> 0.015 cm) being returned to the ball mill for re-grinding (Finch and Fortner 2002 [DIRS 179323], p. 9). The distribution of particles sizes obtained after crushing and milling was approximately bimodal, with numerous large (>0.015 cm diameter) fragments and material less than 0.0045 cm, which subsequent examination by a scanning electron microscope (SEM) revealed to be approximately single fuel grains (approximately 0.020-mm diameter). A relatively small number (~11%) of fuel particles were between ~ 0.0045 cm and 0.015 cm in diameter. No attempt was made to estimate the relative distribution of these three particle sizes during the initial grinding; however, following the sample preparation procedure, in which the largest fragments (>0.0075 cm) were crushed and milled a second time, the final distribution of particle sizes obtained after preparation for the ANL tests given in Table F-2 was achieved.

Table F-2. Final Distribution of Fuel Particle Sizes After All Grinding Cycles (ANL Tests)

Size Fraction (Particle Diameter)	Mass (Gram)	Relative Amount*
<0.0045 cm (ave. ~0.0020 cm) (mostly single fuel grains)	2.3252	81%
0.0045 to 0.015 cm	0.3063	11%
>0.015 cm	0.2520	9%

Source: DTN: LL001104412241.019 [DIRS 155224].

NOTE: * Total relative amounts may exceed 100% due to rounding.

A second grinding was performed as part of the same sample preparation for additional tests at ANL (Finch and Fortner 2002 [DIRS 179323]). The procedure followed was similar to that followed for the first grinding described above; however, the fuel was ground in the ball mill for a total of 55 minutes, nearly twice as long as for Trial 1. Also, masses were determined for only two size fractions following the second grinding procedure: that fraction with particles less than 0.0045 cm, which was 76% of the total mass, and that with particles larger than 0.0045 cm, which was 24% of the total mass. The distribution for this second grinding differs slightly from, but is nevertheless consistent with, that reported after the first grinding. That is, most of the crushed and ground fuel was reduced to less than 0.0045 cm grain sizes (76%), much of which consisted of single fuel grains (Finch and Fortner 2002 [DIRS 179323], page 20).

Several powders of spent UO_2 fuels were prepared for flow-through dissolution studies conducted at Pacific Northwest National Laboratory by crushing and grinding declad segments, and the results are reported by Gray and Wilson (1995 [DIRS 100758]), who reproduce SEM micrographs of the prepared powders. Gray and Wilson (1995 [DIRS 100758]) do not discuss what fraction of the crushed fuel had a size fraction exceeding that used in the flow-through studies, and it is assumed here that the distribution is similar to that given in Table F-2. The most important factor illustrated by Gray and Wilson (1995 [DIRS 100758]), in terms of understanding the potential distribution of particle sizes produced during a disruptive volcanic event, is that not all fuels prepared by them show identical particle size distributions. Several fuels display very small particles—on the order of 0.001 cm or less. Although SEM

examinations of the ANL fuel grains revealed relatively few particles of ATM103 fuel with sizes less than single grains, the PNNL results from a wider variety of fuel types necessitates shifting the potential distribution of grain sizes to smaller particle sizes than that estimated from the ATM103 results alone. From these laboratory experiments, 0.0001-cm-diameter particles represent a reasonable lower limit on particle sizes for all unaltered fuels exposed to mechanical disaggregation.

F3.5.2 Dry-Air Oxidized Fuel

Spent UO_2 fuel that has been oxidized in the absence of moisture may form a series of oxides, with concomitant degradation of the integrity of the fuel meat (i.e., the UO_2 pellets only, but not the cladding, stainless steel spacers, and other components that make up a complete fuel bundle). Oxidation up to a stoichiometry of $UO_{2.4}$ leads to volume reduction of the UO_2 matrix. This can open grain boundaries and may result in the disaggregation of the fuel into single fuel grains (Einziger et al. 1992). Further oxidation to U_3O_8 and related oxides results in a large volume expansion and potentially extreme degradation of the fuel into a powder with particle sizes less than one micrometer in diameter. SEM examination of spent fuel oxidized to approximately U_3O_8 indicates particle sizes of approximately 2.5 µm (0.00025 cm dia.) with lower limits of approximately 0.5 µm (0.00005 cm dia.) (Gray and Wilson 1995 [DIRS 100758]), with larger particles ranging up to approximately 50 µm diameter (0.005 cm) (Table F-3). An estimate of the larger limit on the range of particle sizes is more difficult to make with much certainty. Based on qualitative observations of ATM103 fuel following preparation for the ANL corrosion studies, an upper limit of 0.05 cm diameter is chosen (Table F-3).

F3.5.3 Aqueous-Corroded Fuel

SEM examinations of corroded spent fuel following interaction with simulated groundwater at 90°C are reported by Finch et al. (1999 [DIRS 127332]). The grain sizes of uranium(VI) alteration products on corroded fuel commonly reach 0.01 cm (Finch et al. 1999 [DIRS 127332]); however, based on the understanding of the physical properties of uranium(VI) compounds, these phases are similar to gypsum or calcite in terms of hardness and fracture toughness. Therefore, a volcanic eruptive event would probably fragment nearly all of the larger crystals of secondary U phases, which is why a smaller upper limit of 0.001 cm diameter is chosen for the range of particle sizes for aqueous-corroded fuel (Table F-3). The lower value for the particle-size range is based on the SEM examinations reported by Finch et al. (1999 [DIRS 127332]), who demonstrate the extremely fine-grained nature of many alteration products, with crystal dimensions as small as 0.5 µm or less (≤0.00005 cm).

Table F-3 provides particle-size ranges and average values for particle sizes (based on light-water-reactor fuels) for modeling disaggregation effects, such as those resulting from a volcanic eruption through the repository. These values represent professional judgment, developed on the basis of the foregoing data, cited sources, and experience of the authors (Finch et al. 1999 [DIRS 127332]). No firm statistical foundation underlies the averages or ranges listed in Table F-3; however, based on observation experience with fuels and literature sources, the listed averages are considered reasonable. Limiting values for the ranges are perhaps less well-constrained, but a reasonable estimate is that 80% to 90% of the fuel particles will fall within the ranges reported in Table F-3.

Table F-3.   Estimated Fuel-Particle Sizes from ANL Studies

Degradation State	Mean (cm dia.)	Range (cm dia.)
Unaltered fuel	0.0020	0.0001 to 0.050
Oxidized in dry air	0.00025	0.00005 to 0.0005
Corroded fuel	0.0002	0.00005 to 0.001

Based on the current level of understanding, it seems reasonable to treat both categories of altered fuel (dry-air oxidized and aqueous corroded) as identical, since their estimated particle sizes are similar. The altered fuel is substantially more friable than (most) unaltered fuel, with size distributions that may be skewed to quite small sizes.

F3.6   CHERNOBYL ACCIDENT AS AN ANALOGUE

There have been numerous international scientific studies on various aspects of the Chernobyl Nuclear Power Plant (CNPP) accident on April 26, 1986. The major coverage in those studies has been the radiological and health impacts.

The incident was not a volcanic event; however, there are some aspects that support the use as an analogue for an igneous event at Yucca Mountain. The initial phase included two explosions. This was followed by days of elevated thermal exposure in which it has been estimated that temperatures greater than 1,900°C were reached in the core melt (Ushakov et al. 1997 [DIRS 174141]). In contrast to a volcanic event, the fuel dispersal was more as a discrete material without the proportionately massive volcanic ash component.

While there are numerous references to particulate and aerosol sizes in the reported work, only one reference was found with a quantification of particle size range in a form that might apply as an analogue for an extrusive event at Yucca Mountain. The referenced quantification listed in Table F-4 was provided as the product of a personal communication with a Russian worker, but unfortunately without elaboration of the methodology for sampling or measurement.   The quantification also lacks specificity of the numerical data basis, though it has been considered reasonable to assume, for the purpose of data interpretation, that mass fraction representation was intended.

Table F-4.   Fraction of Hot Particles of a Given Particle Size Depending on Distance from CNPP

Distance from CNPP (km)	Fraction of Hot Particles with a Given Particle Size			
	0 to 20μm	20 to 50 μm	50 to 100 μm	100 to 200 μm
4	—	12.5%	75%	12.5%
10	—	65%	35%	—
20	8%	87%	5%	—
37	40%	60%	—	—
55	65%	35%	—	—

Source: Mück et al. 2002 [DIRS 170378], Table 5.

These data were extrapolated to obtain the maximum near-source waste particle size. The histogram-type data from the literature (Table F-4) were converted to cumulative size distributions (Table F-5) and transformed to a log-probability plot for log-normal distributions for the distal values. For analysis, the 10- and 37-km data (two data points per location) were adjusted to reflect log-probability size distribution slopes similar to those of the other distal data. From the log-probability size distribution lines (Figure F-3), including the adjusted lines for 10-and 37-km, intersect values are read and tabulated (Table F-6) to provide minimum, median (50% cumulative) and maximum particle diameters for each of the distal plot lines.

Table F-5.   Transformation of CNPP Histogram Data to Cumulative Size Distributions

Distance from ChNPP (km)	Cumluative Size Distribution of Hot Particles (mass %)			
	20 μm	50 μm	100 μm	200 μm
4	—	12.5	87.5	100
10	—	65	100	—
20	8	95	100	—
37	40	100	—	—
55	65	100	—	—

Source: Developed DTN: MO0506SPACHERN.000 [DIRS 174126].
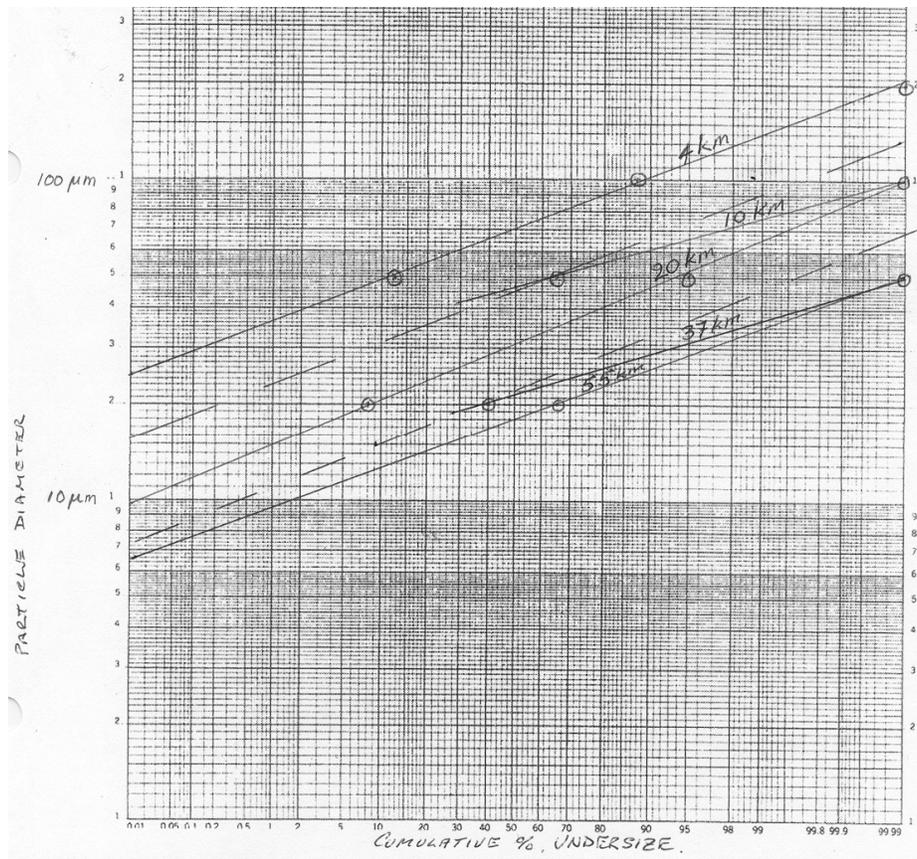
Source: Developed DTN: MO0506SPACHERN.000 [DIRS 174126].

NOTES: Labels on trend lines refer to distance from the CNPP. It is observed that the best-fit lines (solid) for the distal data sets have similar slopes, with the exception of the 10- and 37-km data sets (dashed). Those two data sets have only two values; a mid size point and a top size point. Since the midsize points are in somewhat interpolative positions relative to the other distal line plots, it is assumed that for the statistically weak representation, the top size sampling may be more suspect. With this assumption, hand drawn plot lines (dashed) are made through the 10- and 37-km midsize data such that the lines are approximate interpolations from the other distal plot lines.

Figure F-3. Plot of CNPP Hot Particle Cumulative Size Data

Table F-6.   Estimated CNPP Hot Particle Size Statistics by Distance

Distance (km)	Maximum Diameter (µm)	Median Diameter (µm)	Minimum Diameter (µm)
4	210	70	25
10	140	45	15
20	100	31	10
37	70	22	7.2
55	50	18	6.5

Source: Developed DTN: MO0506SPACHERN.000 [DIRS 174126].

A trend line of maximum particle size by distance was then generated in Excel 2003 and extrapolated to estimate the maximum size at the emission source (Figure F-4). The distal size data (Table F-6) were plotted using the standard charting functions of the Excel spreadsheet (Figure F-4). The best-fit trendline for the maximum particle size plot line in this Excel chart was produced by the standard Excel charting function "Add Trendline." A logarithmic type trendline was selected for this purpose. The logarithmic equation derived by Excel for the trendline was used to extrapolate for near source-term maximum hot particle diameters (Table F-7).
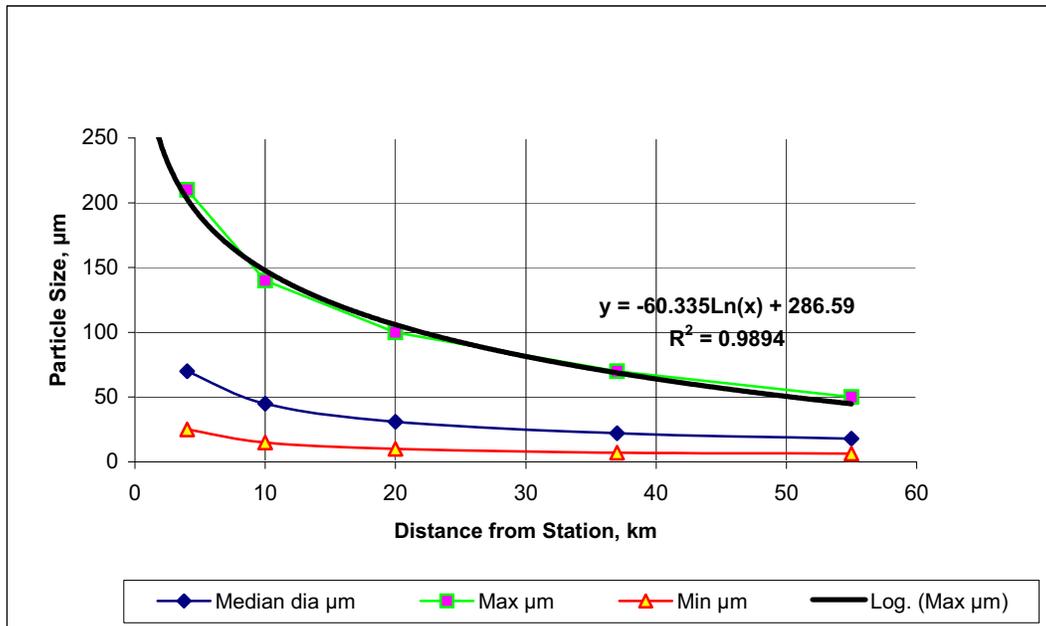
Source: Developed DTN: MO0506SPACHERN.000 [DIRS 174126].

NOTE: Data are from Table F-6. Trend line for Y-intercept (Figure F-4) is approximately 1 mm maximum diameter. This extrapolation (to source) of maximum airborne particles may exclude larger particles that have behaved ballistically at short range and are therefore not represented in the distal field data.

Figure F-4. Extrapolation of CNPP Hot Particle Size by Distance

Table F-7. Best-Fit Estimate of Maximum Near-Source CNPP Hot Particle Size

Distance (km)	Extrapolated Maximum Particle Diameter (μm)
0.001	703
0.01	564
0.1	426
1	287
2	245
4	203

Source: Developed DTN: MO0506SPACHERN.000 [DIRS 174126].

NOTE: Based on equation for logarithmic trend line developed in Figure F-4).

The most highly contaminated area was the 30-km zone surrounding the Chernobyl reactor. The principal physico-chemical forms of the deposited radionuclides were dispersed fuel particles, condensation-generated particles, and mixed-type particles. The distribution in the nearby contaminated zone (<100 km) reflected the radionuclide composition of the fuel and differs from that in the far zone (>100 km to 2,000 km) (NEA 2002 [DIRS 174224], pp. 39 and 44).

Submicron size particulate emission is reported (NEA 2002 [DIRS 174224], p. 38); however, it is also noted by Harrison (1993 [DIRS 173851], Chapter 3) that since nuclei mode aerosol (c.a. 0.01 μm diameter) is inherently unstable with respect to growth mechanisms such as coagulation and condensation, there is a tendency for growth, leading to formation of accumulation mode particles (c.a. 0.1 up to 1 or 2 μm).

In the concentrates of hot particles obtained (at distances of 1 to 12 km), the zirconium-uranium-containing particles accounted for 10% to 45% of the total amount of hot particles. The remaining part is represented by fuel particles with block morphology characteristic of irradiated fuel. The size of the examined particles (from 10 to 200 μm) and their distance from the fourth unit (power station accident source) allow for the conclusion that the given particles were thrown out as a result of the explosions and, hence did not undergo possible changes connected with interaction with structural materials after the accident (Ushakov 1997 [DIRS 174141]).

F3.7   EPRI REPORT

The Electrical Power Research Institute (EPRI) report (EPRI 2004 [DIRS 171915]) identifies two sources of information for the determination of waste particle size in an extrusive event. The first is the crushing and milling techniques used by ANL in preparation for fuel dissolution experiments (Section F3.6). EPRI questions the relevance of this with respect to the disaggregation of fuel under an impact of magma.

The second source of information to which EPRI refers is from studies on the consequences of transportation accidents involving shipping casks and the used fuel inside. This is the basis that EPRI preferred, and it selects a conservative (low energy/low fragmentation) energy density to determine a particle size distribution for the volcanic scenarios. Based on this, the EPRI-recommended particle size distribution for the disaggregation of used fuel following impact of a rock projectile on the waste package is a log-normal distribution having a mass median particle size of 900 μm and a standard deviation of 19 μm.

F4.   REVISED WASTE PARTICLE SIZE

F4.1   DISCUSSION

It is convenient to present possible interpretations of waste particle size in a consistent manner to compare size distributions from different sources and to illustrate the significance of a selected recommendation. This is done in Figure F-5, in which some selected log-normal particle size distributions are plotted on a single log-probability graph. The following notes are in reference to the plotted size-distribution lines.
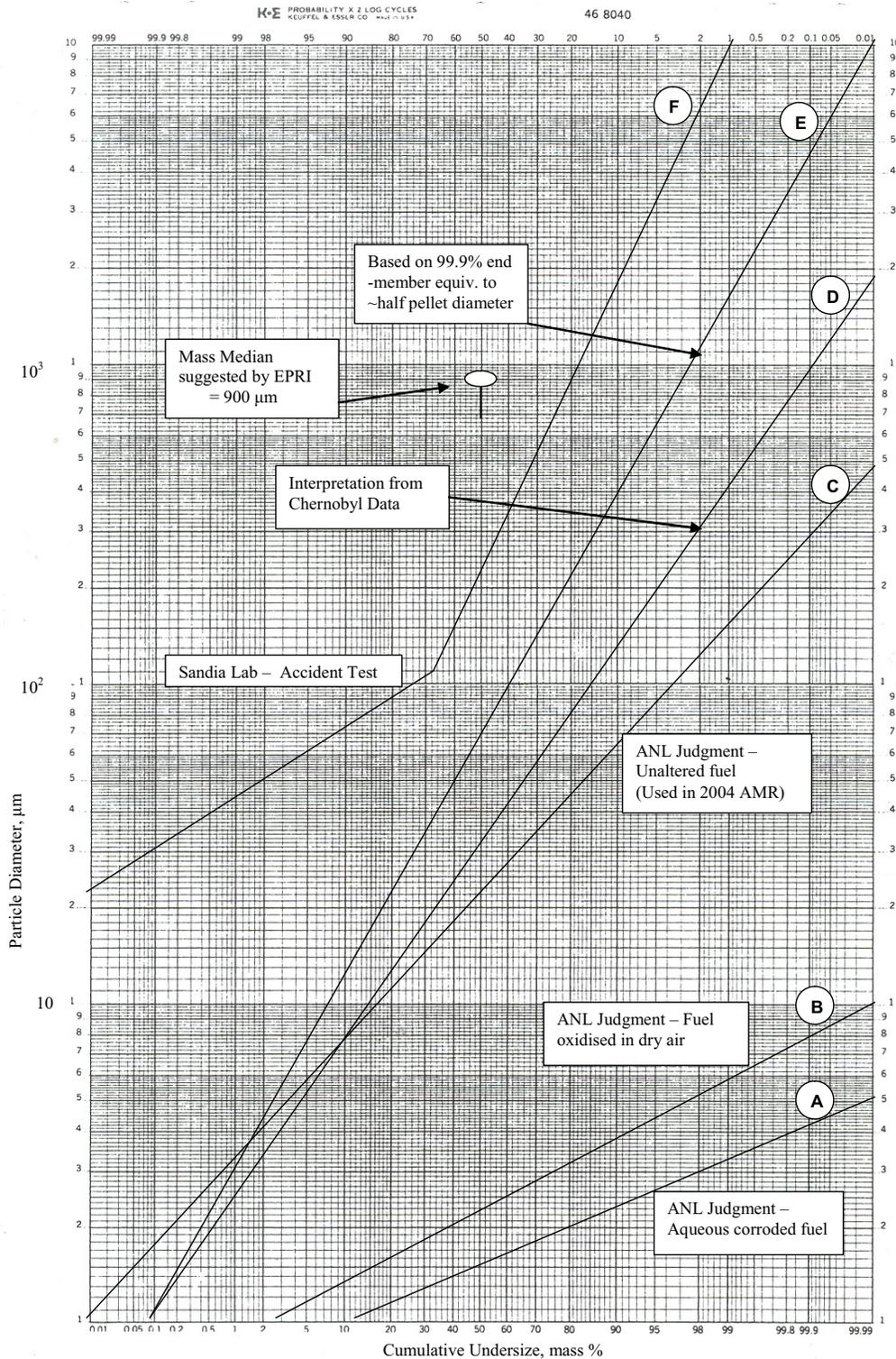
Figure F-5. Plot of Various Waste Particle Size Distributions, Single Log-Probability versus Log Particle Diameter

Lines A, B and C represent size distributions provided by ANL as professional judgments for suggested use in modeling fuel disaggregation effects from events such as a volcanic eruption through the repository (Table F-3). No firm statistical foundation underlies the ranges; however, they are based on fuel observation experience and literature sources. The limiting values were less well-constrained but were estimated to apply to 80% to 90% of the fuel. The judgments were partly based on crushing and grinding of fuels in preparation for wet dissolution tests.

Line D is derived from an analysis of the CNPP data tabulated in Table F-7. This estimated maximum was then applied (as a judgment) to the 99.9% probability to conceptually allow an end-member "tail" of larger ballistic size that would likely be omitted from the more distant field data. Drawing upon the observation (noted in Section F3.6) that submicron particles have a tendency to grow (to 0.1 and up to 1 or 2 μm), Line D is plotted with 0.1 mass percent at one μm in recognition of a 'tail' of submicron size.

Line E is a log-normal interpretation of distribution where the upper end-member represents a particle approximating half the diameter of a fuel pellet. This speculation is based on the possible ejection of some spent fuel in size fractions relatively unaffected by the magma. The half-pellet diameter is based on some of the ATM test photomacrographs of the type shown in Figure F-2 (also see Guenther et al. 1991 [DIRS 109207], Figure 8.3). The speculated scenario for survival of such pieces also includes the case of core-ends that have not been fully exposed to the magma or fuel pieces that have formed $Zr(O)$-UO_2 complexes and which then may not fragment in a manner similar to UO_2. The lower-end member for Line E is derived in the same manner as for Line D.

Line F is reproduced from work reported by Sandoval et al. (1983 [DIRS 156313]). The full-scale test subjected a 25.45-tonne generic truck cask containing a section of a single surrogate pressurized water reactor spent fuel assembly. The use of different instruments for capturing and measuring applicable size ranges, plus a limitation of mass accountability (estimated error ± 10%), might explain the distribution slope change at around 100 μm, otherwise it might represent bimodality. The mass median Stokes diameter for the collected particle range is reported as 210 μm.

The accident test represents mechanical shock at ambient temperatures and is not necessarily an appropriate analogue for an eruptive event in which fuel has been pre-heated to elevated temperature (resulting in plasticity) and experiences shock forces from molten magma and gas. However it is a useful comparative plot line since, with the relative exclusion of high temperature and time for oxidation-caused fragmentation, Line F might represent a reasonable upper limit of the range of possibilities considered for the igneous event.

The mass median value from the EPRI report is also plotted for reference. The low-energy / low-fragmentation case resulted in a coarser grain size than the other tests, and it provides an upper bound on possible grain size.

F5. SUMMARY

For the purpose of the Ashplume model, it is reasonable to base the waste particle size distribution criteria on Line D, the line in Figure F-5 that is derived from CNPP data. For the purposes of the Ashplume model, it is also considered reasonable to modify the minimum end of the log distribution such that the minimum particle diameter is one micrometer but that the mass median particle diameter is based on the distribution as shown in Line D, which recognizes submicron sizes. This results in the following:

Minimum particle diameter	1 μm (0.0001 cm)
Maximum particle diameter	2,000 μm (0.2 cm)
Mass median diameter	30 μm (0.0030 cm).

These size criteria would be applied to either the effusive or explosive magma flux scenarios depicted in Figure F-1.

Some considerations in support of selecting the CNPP-derived data as a basis include:

- It is a full-scale analogue in which irradiated fuel was exposed to explosive forces, temperature, and UO_2 oxidation. The dispersal may differ from an igneous case in which massive ash volumes are available for particle incorporation; however that does not invalidate the extrapolation of the CNPP distal particle depositions to estimate source term maximum particle size.

- The log-normal size distribution derived from the CNPP data is comparable to that of the judgment-based sizing criteria provided by ANL for unaltered fuel, which lacked specific supporting data. Line D also represents a mid-range distribution for the entire scope of available tests.

The assumptions upon which Line E is based do not seem unreasonable but lack data support. Line E is more conservative than the log-normal size distribution from CNPP, in that it would provide a greater proportion of short-range deposition; however it would be tenuous to apply the more conservative interpretation without supporting data.

INTENTIONALLY LEFT BLANK

APPENDIX G
CALCULATION OF MAGMA RISE VELOCITY

APPENDIX G
CALCULATION OF MAGMA RISE VELOCITY

The initial rise velocity of the eruptive column (Section 6.5.2.10) is assumed to be the minimum velocity required to provide the modeled power to the plume (Section 5.2.5). This velocity is related to, but typically much lower than, vent velocity. Vent velocities are related to magma volatile content (SNL 2007 [DIRS 174260], Section 6.3.4.3) and acceleration due to volatile exsolution, and these values do not reflect the deceleration of the tephra particles that occurs near the top of the gas thrust portion of the eruptive column before their entry into the convectively rising plume, which must be assumed for application of the Ashplume model. The function of the initial rise velocity parameter is to deliver the thermal mass (power) to the eruption column, and the velocity of the material entering the plume must only be that required to deliver the necessary power (i.e., without additional momentum due to volatile exsolution). Neglecting the gas-thrust part of the eruption column and given that the heat flux is directly proportional to the mass flux of magma at the vent, the simplest approach to developing the initial rise velocity is to calculate the mass flux of magma below the vent. This calculation follows a discussion in *Characterize Eruptive Processes at Yucca Mountain, Nevada* (SNL 2007 [DIRS 174260], Section 6.3.4.1) and supports the development of the range in values for the initial rise velocity parameter in Section 6.5.2.10 of the current report.

Wilson and Head (1981 [DIRS 101034], Equation 12) provide the following equation for magma velocity, u, below the fragmentation depth:

$$u = \frac{A\eta}{4K\rho_m r}\left[\left(1 + \frac{64g_c r^3\left(\rho_c - \rho_m\right)K\rho_m}{A^2\eta^2}\right)^{1/2} - 1\right]$$

(Eq. G-1)

where

u = magma rise velocity below fragmentation depth

A = 64 (circular conduit) or 24 (dike)

η = magma viscosity

K = 0.01

ρ_m = melt density (no bubbles)

ρ_c = wall rock density

r = conduit radius or dike half width

g_c = gravitational acceleration.

Important variables include magma density and viscosity and wall rock density. The flow of magma is driven by the difference in density between the magma and host (wall) rock; in order to investigate minimal magma ascent velocity, a 10% difference in magma and wall rock densities is assumed. Figure G-1 presents a spreadsheet that incorporates Equation G-1 to calculate magma ascent velocity for a variety of magma density and viscosity values (depending on initial water content) and dike/conduit radius. Values for magma properties as a function of initial water content are provided in *Characterize Eruptive Processes at Yucca Mountain,*

Nevada (SNL 2007 [DIRS 174260], Table 6-5), and values for conduit/dike radii are provided in the output from that report (DTN: LA0612DK831811.001 [DIRS 179987]).

	G	H	I	J	K	L	M	N	O	P	Q	R	S	T	U
on depth, based on Wilson and Head (1981), Equation 12															
						Initial water content (%) for basaltic magma, values from ANL-MGR-GS-2, Rev3, Table 6-5									
A=	64					0	1	2	3	4					
K=	0.01		rhom	(kg/m3)		2663	2605	2556	2512	2474					
g=	9.81	m/s2	rhoc	(kg/m3)		2929	2866	2812	2763	2721	<-- assume wall rock density = magma density+10%				
al calculations]			viscosity	(Pa s)		4764	2965	1920	1294	906					
inner frx			Initial H2O	---->											
9.5375			content			0	1	2	3	4					
ble 3}			radius	0.5		1.712	2.699	4.087	5.946	8.357					
			(m)	1		6.847	10.794	16.349	23.782	33.421	Magma Rise Velocity, (cm/s)				
			I	2		27.385	43.167	65.364	95.034	133.420	Assuming bouyancy driven by minimal				
			I	5		170.915	268.865	405.333	584.291	807.922	density contrast (rhoc = rhom + 10%)				
			V	8		435.545	680.660	1012.295	1423.897	1894.545					
−1				10		676.683	1049.207	1536.753	2108.805	2714.366					
				12		966.366	1482.017	2128.276	2838.589	3534.666					

Source: Wilson and Head 1981 [DIRS 101034], Equation 12.

NOTES: Magma ascent velocity is given in cm/s and occupies the largest shaded area, columns L through P. Magma ascent velocity is calculated based on variations in magma density (rhom) and viscosity as a function of initial magma water content, wall-rock density (rhoc), and conduit radius.

Figure G-1. Spreadsheet Used for Calculating Magma Ascent Velocity

The results of this calculation are plotted in Figure G-2.
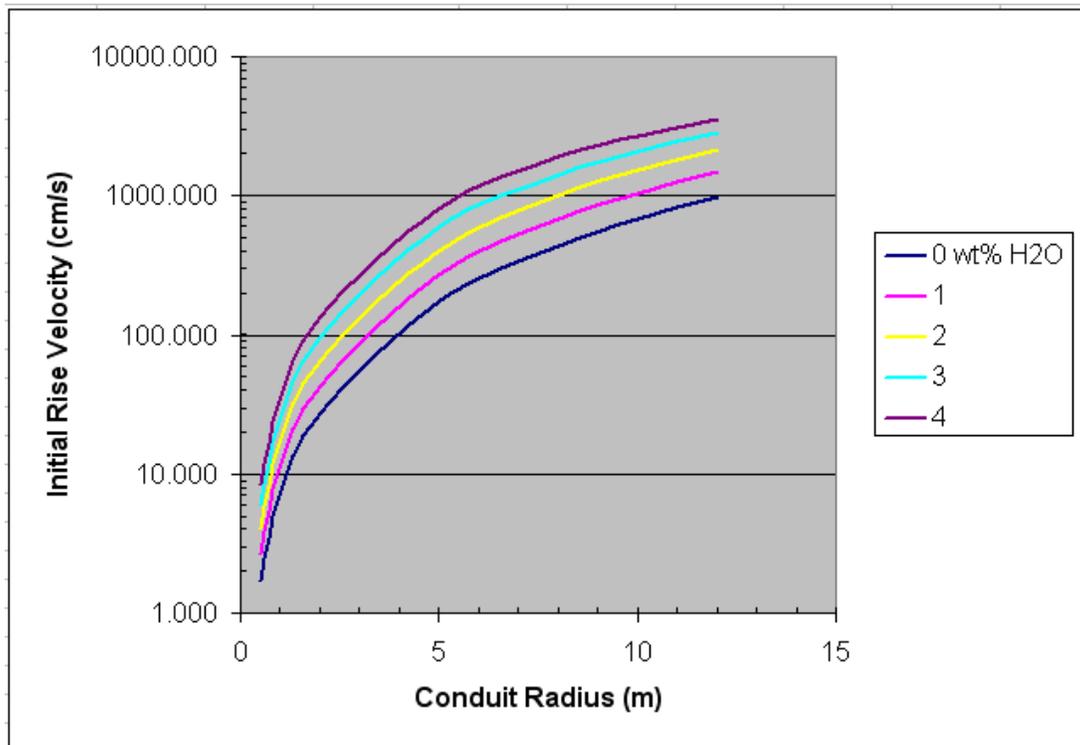
Source: Wilson and Head 1981 [DIRS 101034], Equation 12.

Figure G-2. Plot of Magma Ascent Velocity (Initial Rise Velocity) versus Conduit Radius for Five Initial Magma Water Contents, as Calculated in the Spreadsheet Shown in Figure G-1

For basalt magma properties appropriate for the Yucca Mountain region (SNL 2007 [DIRS 174260], Section 6.3.2), magma rise velocity ranges from about 1 to 3,500 cm/s.

Spreadsheet formulas are provided in Figure G-3.

	H	I	J	K	L
1					Initial water content (%) for basaltic magma, values from ANL-MGR-GS-2, Rev3, Table 6-5
2					
3					
4					
5	64				0
6	0.01		rhom	(kg/m3)	2663
7	9.81	m/s2	rhoc	(kg/m3)	2929
8			viscosity	(Pa s)	4764
9			Initial H2O	---->	
10			content		0
11			radius	0.5	=(($I$8*L$11)/(4*$I$9*L$9*$L11))*(((1+((64*$I$10*($L11^3)*(L$10-L$9)*$I$9*L$9)/($I8^2*L11^2)))^0.5)-1)*100
12			(m)	1	=(($I$8*L$11)/(4*$I$9*L$9*$L12))*(((1+((64*$I$10*($L12^3)*(L$10-L$9)*$I$9*L$9)/($I8^2*L11^2)))^0.5)-1)*100
13				2	=(($I$8*L$11)/(4*$I$9*L$9*$L13))*(((1+((64*$I$10*($L13^3)*(L$10-L$9)*$I$9*L$9)/($I8^2*L11^2)))^0.5)-1)*100
14				5	=(($I$8*L$11)/(4*$I$9*L$9*$L14))*(((1+((64*$I$10*($L14^3)*(L$10-L$9)*$I$9*L$9)/($I8^2*L11^2)))^0.5)-1)*100
15			V	8	=(($I$8*L$11)/(4*$I$9*L$9*$L15))*(((1+((64*$I$10*($L15^3)*(L$10-L$9)*$I$9*L$9)/($I8^2*L11^2)))^0.5)-1)*100
16				10	=(($I$8*L$11)/(4*$I$9*L$9*$L16))*(((1+((64*$I$10*($L16^3)*(L$10-L$9)*$I$9*L$9)/($I8^2*L11^2)))^0.5)-1)*100
17				12	=(($I$8*L$11)/(4*$I$9*L$9*$L17))*(((1+((64*$I$10*($L17^3)*(L$10-L$9)*$I$9*L$9)/($I8^2*L11^2)))^0.5)-1)*100
18					

Source: Wilson and Head 1981 [DIRS 101034], Equation 12.

Figure G-3. Spreadsheet Formulas for the Calculation Illustrated in Figure G-1

INTENTIONALLY LEFT BLANK

APPENDIX H
DEVELOPMENT OF QUANTITATIVE ACCURACY CRITERIA FOR ASHPLUME
MODEL VALIDATION

APPENDIX H
DEVELOPMENT OF QUANTITATIVE ACCURACY CRITERIA FOR ASHPLUME MODEL VALIDATION

H1. INTRODUCTION

Natural analogue studies addressed the adequacy and accuracy of the Ashplume model by comparing model results to observed tephra fall thickness distributions at Cerro Negro volcano, Nicaragua, Lathrop Wells volcano, Nevada, and Cinder Cone, California (Section 7.3). Criteria for acceptable accuracy in these studies are established by summarizing acceptance criteria used in published tephra dispersal model studies.

H2. LITERATURE REVIEW FOR ESTABLISHING QUANTITATIVE VALIDATION ACCURACY CRITERIA

A review of major journal articles indicates that quantitative acceptance criteria for studies involving comparison of model output to measured tephra thickness are rare (Table H-1). In most cases, investigators visually compared the model-predicted distribution of tephra thickness (isopachs) or concentration (isopleths) with distributions developed from ground measurements or with satellite imagery and made a subjective, qualitative evaluation of goodness of fit. Examples of such qualitative criteria include a) predicted presence/absence of ashfall in particular locations (e.g., cities) where ash was observed (Tanaka and Yamamoto 2002 [DIRS 179741]), b) satellite image eruption cloud boundaries contained within modeled cloud boundaries (Hefftner and Stunder 1993 [DIRS 179744]), or c) attempts to match the location of a particular isopach or isopleth with measured values or a general reproduction of the pattern of the deposit (e.g., Macedonio et al. 1988 [DIRS 179745], Hill et al. 1998 [DIRS 151040], Barberi et al. (1992 [DIRS 179747], Pfeiffer et al. 2005 [DIRS 174826]).

Published studies that quantify the accuracy of a model validation/verification exercise have done so in terms of

1. Error in match between computed and measured tephra thickness at specific locations: within a factor of two (or 0.5) (Hurst and Turner 1999 [DIRS 176897], Glaze and Self 1991 [DIRS 110277]), chi-squared values of 1.1 to 3.5 (Pfeiffer et al. 2005 [DIRS 174826]);

2. Calculation of a "misfit function" during sensitivity analyses, a quantity that can be minimized for best model calibration (Bonadonna et al. 2005 [DIRS 179753]); or

3. Statistical goodness of fit—correlation coefficient (R^2) $\geq$ 0.9 and slope of the regression line 0.72 – 0.87 (95th percent confidence) (Connor and Connor 2006 [DIRS 179760]).

For use in the ASHPLUME validation exercises (e.g., Cinder Cone and Lathrop Wells cases), useful measures of accuracy are #1 and #3, quantified as:

I. **Error in match between computed and measured tephra thickness at specific locations within a factor of two, or**

II. **Statistical goodness of fit—correlation coefficient (R) $\geq$ 0.9 and slope of the regression line within 30% of unity (B statistic = 0.7 to 1.3)**

A third qualitative criteria is added (e.g., Cerro Negro case):

III. **Reasonable match between computed and observed pattern of the tephra deposit, in terms of two-dimensional profile or three-dimensional tephra sheet shape.**

While the published studies do not put forth "accuracy acceptance criteria" per se, the peer review process for these journal articles provides a vetting process for the methodologies they described, and the summary of the pertinent literature provides a basis for establishing such accuracy acceptance criteria for the Ashplume model validation effort.

H3.   A NOTE ON MATCHING OBSERVED TEPHRA THICKNESS

Tephra-dispersal models, such as Ashplume and others based on the Suzuki (1983 [DIRS 100489]) mathematical model, simplify the eruption column as a vertical line source, rather than explicitly modeling eruption column physics. As a result, the computed tephra concentrations are valid only for distances sufficiently far from the source that the tephra dispersal processes can be described by advection-dispersion and particle settling processes (Pfeiffer et al. 2005 [DIRS 174826], pp. 273 to 274). In practice, this means that, in model validation comparisons of computed vs. observed tephra thicknesses, greater weight should be given to matching distal data. For example, modeling studies that fitted proximal data in order to reconstruct tephra distributions resulted in extreme underestimation of total erupted mass (Pfeiffer et al. 2005 [DIRS 174826], pp. 291 to 292). In the modeling studies of analogue cases (Section 7.3), fits to the distal data have been emphasized in the evaluation of the performance of the model relative to accuracy criteria.

Table H-1. Summary of Ash Dispersal Modeling Literature and Basis for Establishing ASHPLUME Validation Accuracy Acceptance Criteria

Reference	Description of Work	Model	Comparison Case Study	Method of Validation	Accepted Accuracy	Location in Reference
Aloisi et al. 2002 [DIRS 179761]	Model application to evaluate eruption parameters	PUFF	Etna 22 July 1998	Subjective, visual comparison of model output with satellite imagery	Qualitative (no criteria)	pp. ECU 9-9 through 9-11; Figures 7 to 8
Armienti et al. 1988 [DIRS 179762]	Development of mathematical model, comparison to observed data	Armienti et al. 1988 [DIRS 179762]	Mount St. Helens	Visual comparison of calculated versus observed isopachs and dispersion axes	Qualitative (no criteria)	pp. 6,472 to 6,475, Figures 7b, 9, 10, 13
Barberi et al. 1992 [DIRS 179747]	Development of hazard model based on maximum expected eruption; used model to predict ash fall; calibrated to historic eruption	Armienti et al. 1988 [DIRS 179762]	Guagua Pichincha 1660 A.D.	Visual comparison of computed isopachs with observed (point) ash thicknesses	Qualitative (no criteria)	pp. 61 to 64; Figures 10 to 11
Bonadonna et al. 2005 [DIRS 179753]	Hazards prediction maps, evaluate code by comparison to observed eruptions	TEPHRA	Kaharoa (Tarawera, NZ), 1315; Ruapehu 1996	Misfit function for sensitivity analyses, visual calculated versus observed mass correlation, visual comparison of calculated versus observed isopachs	Minimized misfit function	pp. 7 to 8, 10 to 13
Connor and Connor 2006 [DIRS 179760]	Inversion techniques for model validation	TEPHRA	Cerro Negro 1992	Correlation coefficient; linear regression	0.9; 0.72 to 0.87 (95% confidence)	p. 238
Glaze and Self 1991 [DIRS 110277]	Application of Suzuki 1983 model to Lascar eruption	Suzuki 1983 [DIRS 100489]	Hekla 1980, Mt. St. Helens July 1980, Lascar 1986	Visual comparison of calculated versus observed isopachs and isopleths; computed/measured ash thickness at single location	Qualitative (isopach/isopleths); within a factor of 0.5 for computed/measured thickness	pp. 1,238 to 1,240; Figures 2 to 4.
Heffter 1996 [DIRS 179763]	Verification of model vs. observed eruption	VAFTAD	Klyuchevskoi 1994	Comparison of model results with ash cloud outlines derived from satellite images	Qualitative (no criteria)	pp. 1,490 to 1,492; Figure 3

Table H-1. Summary of Ash Dispersal Modeling Literature and Basis for Establishing ASHPLUME Validation Accuracy Acceptance Criteria (Continued)

Reference	Description of Work	Model	Comparison Case Study	Method of Validation	Accepted Accuracy	Location in Reference
Heffter and Stunder 1993 [DIRS 179744]	Development of model, preliminary validation	VAFTAD	Mt. Spurr, 1992	Subjective, visual comparison of model output with visual and infrared satellite imagery	Qualitative: image eruption cloud boundaries contained within model cloud boundaries	pp. 538 to 541; Figure 5
Hill et al. 1998 [DIRS 151040]	Hazard analysis, risk assessment	Ashplume ("modified Suzuki model")	Cerro Negro 1995	Visual comparison of calculated versus observed isopachs; sensitivity analyses of parameters versus profile plots	Qualitative (no criteria)	pp. 1,236 to 1,238, Figures 5 to 6
Hopkins and Bridgman 1985 [DIRS 110280]	Development of model for tephra dispersal along centerline of plume with variable winds; code verification	Hopkins	Mt. St. Helens May 18, 1980	Comparison of model results to observed particle sizes along plume; observed/computed isopachs	Qualitative (no criteria)	pp. 10,623 to 10,630; Figures 4, 8, 9, 10, 11, 13, 14
Hurst and Turner 1999 [DIRS 176897]	Comparison of code to eruption to evaluate forecasting capability	ASHFALL	Ruapehu 1995, 1996	Visual comparison of calculated versus observed isopachs	Factor of 2	pp. 618 to 620
Macedonio et al. 1988 [DIRS 179745]	Evaluation of capability of model to accurately reproduce eruption as first step toward probabilistic hazard analysis	Macedonio et al. 1988	Vesuvius 79 A.D.	Visual comparison of calculated isopachs versus observed point thickness (map and profiles); comparison of calculated/observed grain sizes	Shape of deposit, thickness; grain size distributions; qualitative (no criteria)	Figures 5 to 8
Pfeiffer et al. 2005 [DIRS 174826]	Model verification, 2D version of Armiento/Macedonio model	HAZMAP	Vesuvius AD 79	Comparison of computed isopachs with point tephra thickness observations; comparison of computed to measured grain size; use combination of thickness, and granulometric assessment for validation-- (chi squared)	Reduced chi-squared 1.08 to 3.54 (+ higher values)	pp. 283 to 293; Figures 7 to 10, Table 2.

Table H-1. Summary of Ash Dispersal Modeling Literature and Basis for Establishing ASHPLUME Validation Accuracy Acceptance Criteria (Continued)

Reference	Description of Work	Model	Comparison Case Study	Method of Validation	Accepted Accuracy	Location in Reference
Searcy et al. 1998 [DIRS 101015]	Model development, preliminary validation	PUFF	Mt. Spurr, 1992, Klyuchevskoi 1994, Rabaul 1994	Subjective, visual comparison of model output with visual and infrared satellite imagery	Qualitative (no criteria)	pp. 7 to 15, Figures 4, 8, 9, 10, 12
Tanaka and Yamamoto 2002 [DIRS 179741]	Model verification	PUFF	Usu 2002	Visual comparison of calculated versus observed isopleths (concentration)	Qualitative (no criteria)	p. 751; Figures 2 and 9
Turner and Hurst 2001 [DIRS 179765]	Development of RAMS atmospheric model to drive HYPACT and ASHFALL; comparison to observed data	ASHFALL, RAMS/HYPACT	Ruapehu 1995, 1996	Visual comparison of calculated isopachs with satellite image of plume and observed isopachs	Qualitative (no criteria)	pp. 57, 61, 64 to 68 ; Figures 1, 4, 6, 8, 10 to 16

INTENTIONALLY LEFT BLANK

APPENDIX I
SENSITIVITY OF FAR MODEL RESULTS ON RESOLUTION FOR CARTESIAN AND POLAR GRIDS

APPENDIX I
SENSITIVITY OF FAR MODEL RESULTS ON RESOLUTION FOR CARTESIAN AND POLAR GRIDS

I1.   INTRODUCTION

The FAR model requires that tephra and waste be sampled within the entire Fortymile Wash drainage basin by running the Ashplume model sequentially for each point on the grid. This requirement potentially poses a computational challenge due to the size of the basin, the strong spatial variation in tephra close to the vent, and the requirement that TSPA sample 1000 or more hypothetical eruptions within a Monte Carlo framework. If strong spatial variations in tephra thickness close to the vent require sampling at 500 m, for example, then a Cartesian grid with uniform resolution would require nearly 4,000 ASHPLUME samples for each eruption. In order to improve the efficiency of the coupled Ashplume/FAR system, additional capability was provided to run ASHPLUME with a polar grid in which the radial sampling interval increases with distance from the vent. This approach focuses computational resources close to the vent where tephra thickness is most rapidly varying.

This appendix presents model results performed at a range of ASHPLUME resolutions for both Cartesian and polar grids. The purpose of this work is to identify the minimum grid resolution necessary to obtain accurate results and to provide guidance on which grid type to choose for optimum results. While the type and resolution of the grid refers to the sampling within the Ashplume model, the key issue is how those results are propagated through the FAR model. FAR performs a bilinear interpolation on the ASHPLUME samples and models the mobilization of tephra and waste through the landscape. In these sensitivity studies, therefore, computations are done to determine the sensitivity of: 1) the total mass of primary fallout tephra, 2) the fraction of tephra mobilized from the Fortymile Wash drainage basin, 3) the dilution factor at the Fortymile Wash outlet, and 4) the surface waste concentration in channels. As the grid resolution increases and the drainage basin more finely sampled, each of these parameters should converge asymptotically to the mathematically accurate answer. Convergence of the first parameter (total fallout tephra) indicates that the ASHPLUME grid is being sampled finely enough that the bilinear interpolation within FAR produces an accurate representation of the plume deposit. More important, however, is whether the FAR outputs (mobilized mass, dilution factor, and tephra concentration in channels) have converged, because these parameters more directly affect the concentration of waste at the location of the RMEI and, thus, the annual dose to the RMEI calculated in the TSPA model.

I2.   RESULTS FOR CARTESIAN GRID

Table I-1 and Figure I-1 present the results for the Cartesian grid using a representative output of ASHPLUME with southerly winds. A sample FAR output file that echoes input parameter values is included at the end of this Appendix. As the resolution grid size decreases from 4 km to 0.5 km, these results show that each of the key output parameters varies greatly and does not clearly converge to a single value. Total tephra (in g), for example, varies by 10% between 500 m and 1 km and hence has not converged. The fraction of tephra mobilized and the dilution factor show improved convergence relative to total tephra (i.e., approximately 3% difference between 500 m and 1 km). These results suggest that a resolution of at least 250 m is required to

obtain results within 1% of the asymptotic solution. This would require approximately 16,000 ASHPLUME samples per eruption and would pose a serious computational challenge to the TSPA model.

Table I-1   Sensitivity of Key FAR Output Parameters for Different Spatial Resolutions of ASHPLUME with a Cartesian Grid.

Resolution (km)	N_x, N_y	Total Fallout Tephra (g)	Fraction of Tephra Mobilized	Dilution Factor	Surface Channel Concentration (g/cm^3) at t = 10 years
4	11,21	1.83×10^{12}	0.0087	0.000089	7.067×10^{-13}
2	21,41	3.02×10^{12}	0.0307	0.001110	2.040×10^{-10}
1	41,81	2.75×10^{12}	0.0253	0.000834	8.980×10^{-10}
0.5	81,161	2.55×10^{12}	0.0260	0.000809	8.200×10^{-11}
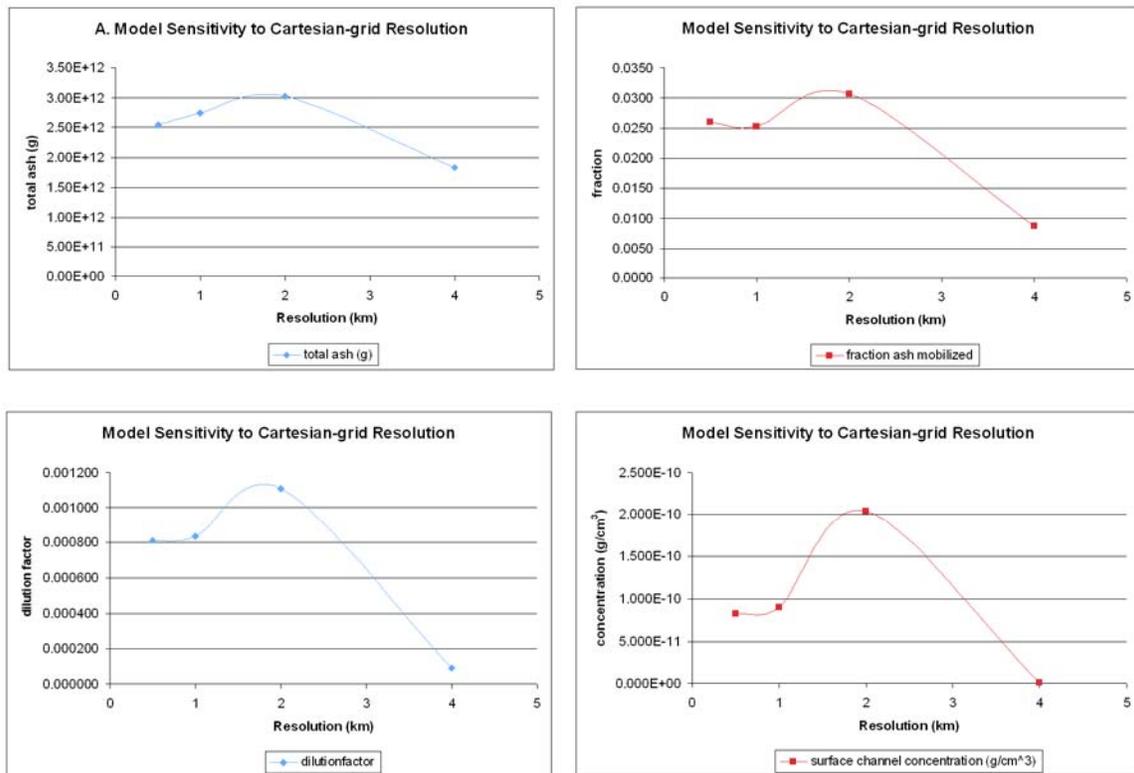
Figure I-1. Sensitivity of Key FAR Output Parameters for Different Spatial Resolutions of ASHPLUME with a Cartesian Grid.

Figure I-2 presents color maps of the primary fallout tephra thickness (as interpolated by the FAR model) for 500-m to 4-km resolution. This figure helps to illustrate the limitations of the uniform Cartesian grid framework. As the figure shows, the tephra thickness varies strongly in the immediate vicinity of the vent. As a result, resolutions of 2 km to 4 km do a very poor job of resolving the fallout pattern near the plume. These results suggest that a framework that samples more finely close to the vent might be a better approach.
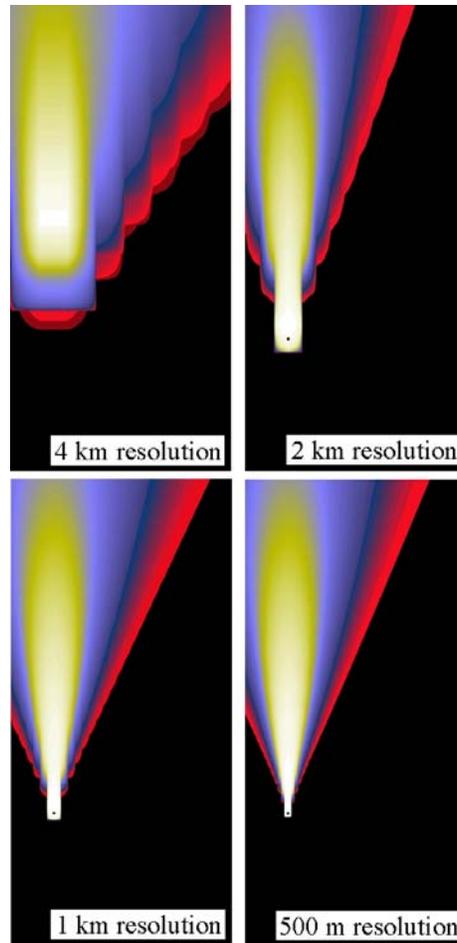
Figure I-2. Color Maps of Fallout Tephra as Interpolated by the FAR Model for ASHPLUME Resolutions of 500 m to 4 km for a Uniform Cartesian Grid.

I3. RESULTS FOR POLAR GRID

Results for the nonuniform polar grid are presented in Table I-2 and Figure I-3. In this case, a synthetic ASHPLUME grid was used because the version of Ashplume that works with the polar grid was not qualified at the time this work was performed. The synthetic grid was created within Matlab according to the following function:

Concentration

$$(r, \theta) = 100.0 \exp(-r^2/50000000.0)\left|\sin(4\theta)\right| \quad \text{if} \quad \pi/4 <= \theta <= \pi/2$$

$$= 0.0 \quad \text{if} \quad \theta < \pi/4 \text{ or } \theta > \pi/2 \qquad \text{(Eq. I-1)}$$

This function was chosen to be broadly representative of plume shapes, and it is expected that sensitivity studies performed with this synthetic function can be applied to the results of the Ashplume model generally. (Compare the synthetic plumes in Figure I-2 to those generated by ASHPLUME in Figure K-4.) The results are presented in terms of the number of grid cells in the radial and azimuthal directions rather than the resolution due to the nonuniformity of the grid in this case. The distance of the radial sample from the vent starts at 200 m from the vent in each of these runs and increases geometrically with the value of *rfactor*. The value of N_r is the smallest number required to ensure complete coverage of the drainage basin.

Table I-2. Sensitivity of Key FAR Output Parameters for Different Spatial Resolutions of ASHPLUME Using a Polar Grid with Geometrically Increasing Radius

N_r	*rfactor*	N_θ	Total Fallout Tephra (g)	Fraction of Tephra Mobilized	Dilution Factor	Surface Channel Concentration (g/cm³)
59	1.1	18	1.3217×10^{13}	0.2224	0.0326	4.359×10^{-6}
31	1.2	18	1.3380×10^{13}	0.2222	0.0330	4.450×10^{-6}
21	1.3	18	1.3617×10^{13}	0.2218	0.0335	4.570×10^{-6}
14	1.5	18	1.4270×10^{13}	0.2218	0.0352	4.941×10^{-6}
9	1.7	18	1.4190×10^{13}	0.2224	0.0347	4.900×10^{-6}
59	1.1	36	1.2420×10^{13}	0.2362	0.0300	4.189×10^{-6}
31	1.2	36	1.2570×10^{13}	0.2360	0.0304	4.284×10^{-6}
21	1.3	36	1.2790×10^{13}	0.2356	0.0308	4.410×10^{-6}
14	1.5	36	1.3410×10^{13}	0.2356	0.0324	4.800×10^{-6}
9	1.7	36	1.3330×10^{13}	0.2362	0.0319	4.750×10^{-6}
59	1.1	72	1.2420×10^{13}	0.2366	0.0291	4.140×10^{-6}
31	1.2	72	1.2570×10^{13}	0.2364	0.0295	4.236×10^{-6}
21	1.3	72	1.2793×10^{13}	0.2360	0.0299	4.360×10^{-6}
14	1.5	72	1.3410×10^{13}	0.2360	0.0315	4.760×10^{-6}
9	1.7	72	1.3330×10^{13}	0.2360	0.0309	4.700×10^{-6}
59	1.1	144	1.2514×10^{13}	0.2366	0.0293	4.204×10^{-6}
31	1.2	144	1.2670×10^{13}	0.2365	0.0297	4.300×10^{-6}
21	1.3	144	1.2890×10^{13}	0.2360	0.0301	4.426×10^{-6}
14	1.5	144	1.3500×10^{13}	0.2360	0.0317	4.825×10^{-6}
9	1.7	144	1.3400×10^{13}	0.2360	0.0311	4.763×10^{-6}

Results for the nonuniform polar grid illustrate rapid convergence relative to the uniform Cartesian grid. The asymptotic solution for this example can be taken to be the results for $N_r = 59$ and $N_\theta = 144$, since these parameters result from the grid with the finest resolution. The results of Table I-2 show that model results for $N_\theta \geq 36$ and $N_r \geq 31$ provide results generally to within less than 1% of the asymptotic values. The total fallout tephra for $N_\theta = 36$ and $N_r = 31$, for example, is less than 0.5% from the asymptotic value. The waste concentration in channels for $N_\theta = 36$ and $N_r = 31$ is within 2% of the asymptotic value of 4.204×10^{-6}. Importantly, the modeled values using $N_\theta \geq 36$ and $N_r \geq 21$ all slightly overestimate the waste concentration and its related parameters. Therefore, the model does not underestimate tephra concentrations on its approach to the asymptotic value.
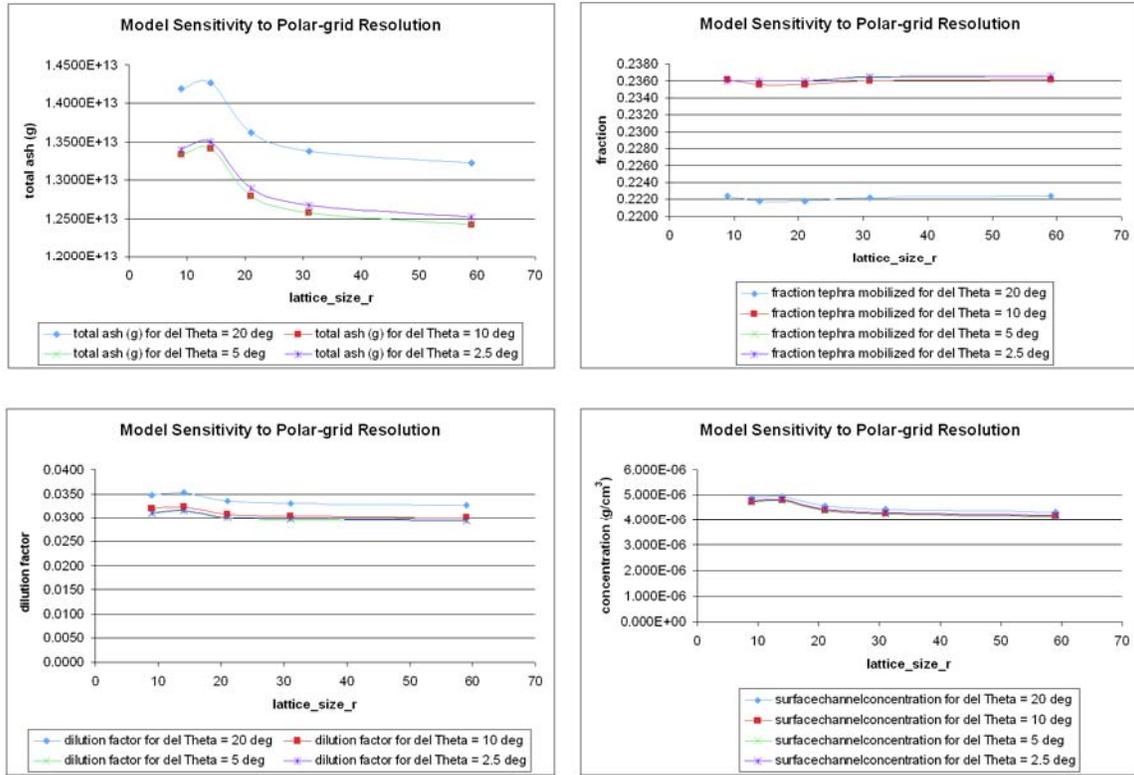
Figure I-3. Sensitivity of Key FAR Output Parameters for Different Spatial Resolutions of ASHPLUME with a Nonuniform Polar Grid
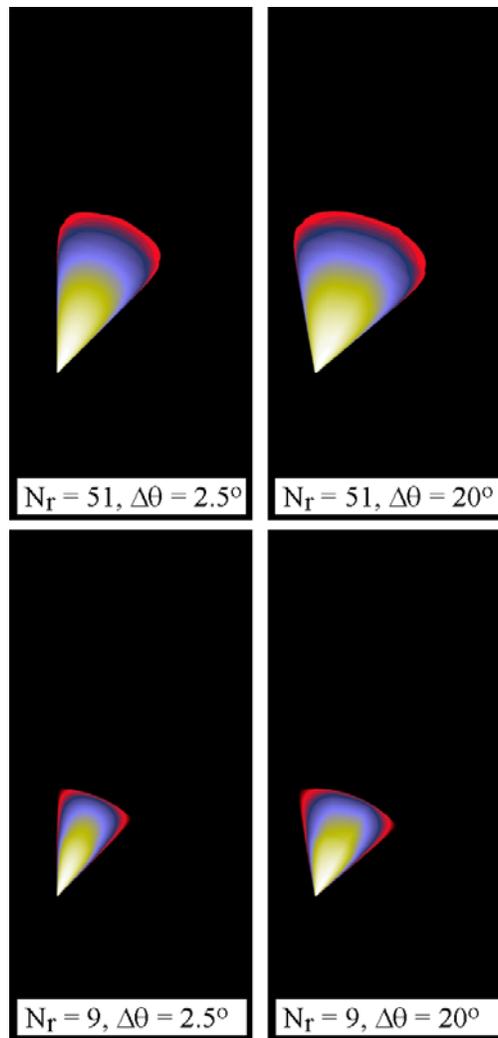
Figure I-4. Color Maps of Synthetic Fallout Tephra as Interpolated by the FAR Model for a Range of ASHPLUME Resolutions for a Nonuniform Polar Grid

I4.   SUMMARY

Sensitivity studies illustrate that the non-uniform polar grid is superior to the uniform Cartesian grid in its convergence properties. The nonuniform polar grid converges faster and requires fewer samples to achieve model accuracy because it samples more finely where the tephra thickness is rapidlyvarying. For the representative synthetic plume considered in this appendix, accurate results (within 4% to 5%) were obtained for minimum values of $N_r = 21$ and $N_\theta = 36$, and better results (within 1% to 2%) were obtained using minimum values of $N_r = 31$and $N_\theta = 36$. Recommended values are $N_r = 31$and $N_\theta = 36$. Using these values, each eruption requires $31 \times 36 = 1,116$ ASHPLUME samples. This required number of samples does not pose a computational challenge to TSPA even when considering 1,000 or more hypothetical eruptions.

Sample output file (partial) for FAR resolution study (echoes input parameter values):

```
OUTPUT FILE for FAR V1.0, TIME and DATE: Thu Nov 30 11:12:38 2006

INPUT PARAMETERS
  criticalslope =                      0.300000 (m/m)
  drainagedensityupperbasin =         30.000000 (km^-1)
  scourdepthoutlet =                 100.000000 (cm)
  RMEIarea =                          30.000000 (km^2)
  fractionchannel =                    0.200000
  Ldivide =                          100.000000 (cm)
  Lchannel =                         200.000000 (cm)
  Ddivide =                            0.010000 (cm^2/yr)
  Dchannel =                           0.050000 (cm^2/yr)
  ashsettleddensity =                  1.000000 (g/cm^3)
  xvent =                         548510.000000 (m)
  yvent =                        4078760.000000 (m)
  gridflag =                                  1
  minx =                             -10.000000 (km)
  maxx =                              30.000000 (km)
  miny =                             -20.000000 (km)
  maxy =                              60.000000 (km)
  lattice_size_x =                           21
  lattice_size_y =                           41
  minrad =                           200.000000 (m)
  rfactor =                            1.200000
  lattice_size_r =                           31
  rvent =                            200.000000
  lattice_size_theta =                       18
  timestep =                          10.000000 (yr)
  simulationlength =               10000.000000 (yr)
  Bdepth =                            20.000000 (cm)
  oflag =                                     1
  ashdepositionRMEI =             6.743070e-004 (g/cm^2)
  fueldepositionRMEI =            3.070000e-010 (g/cm^2)

INTERMEDIATE OUTPUT PARAMETERS
  totalash:                       1.337672e+013 (g)
  totalfuel:                      1.337682e+008 (g)
  ashmobilized:                   2.973097e+012 (g)
  fuelmobilized:                  2.971972e+007 (g)
  ashmobilized (fraction total):  2.222590e-001
  fuelmobilized (fraction total): 2.221733e-001
  dilutionfactoroutlet:           3.302986e-002
  fueldivideinit:                 4.552822e-007 (g/cm^3)
  primaryashthickness:            6.743070e-004 (cm)
  fuelchannelinit:                4.953290e-006 (g/cm^3)
  depthfuelchannel:               1.636683e+000 (cm)

TIME SERIES OF RADIONUCLIDE CONCENTRATIONS AT RMEI LOCATION
time   fuelsurfacedivide   fueldepthBdivide fuelsurfacechannel   fueldepthBchannel
10.0      5.477255e-010       3.070000e-010      4.449557e-006       8.106969e-006
20.0      3.873007e-010       3.070001e-010      3.729104e-006       8.106970e-006
30.0      3.162296e-010       3.070001e-010      3.245942e-006       8.106968e-006
40.0      2.738630e-010       3.069999e-010      2.906776e-006       8.106966e-006
50.0      2.449505e-010       3.070001e-010      2.653969e-006       8.106962e-006
60.0      2.236082e-010       3.069999e-010      2.456718e-006       8.106970e-006
70.0      2.070210e-010       3.070000e-010      2.297461e-006       8.106966e-006
80.0      1.936503e-010       3.070000e-010      2.165469e-006       8.106966e-006
90.0      1.825754e-010       3.070001e-010      2.053793e-006       8.106968e-006
......
```

INTENTIONALLY LEFT BLANK

APPENDIX J
ASHPLUME – ASHFALL CODE COMPARISON SUMMARY

APPENDIX J
ASHPLUME – ASHFALL CODE COMPARISON SUMMARY

J1. INTRODUCTION

In his 2003 independent technical review of the Ashplume model, Dr. Frank Spera recommended a comparison of the ASHPLUME and ASHFALL codes for modeling atmospheric dispersal and deposition of tephra in order to strengthen the validation of the Ashplume model (Appendix E). This model validation exercise satisfies that recommendation and enhances confidence in the use of the ASHPLUME code for its intended purpose by comparing the mathematics of the ASHPLUME and ASHFALL codes and developing Ashplume input parameter values for simulations to match the published results of the ASHFALL simulation of the 1996 Ruapehu (New Zealand) eruption. This ASHFALL study was performed by Dr. Tony Hurst and is published in a journal article by Hurst and Turner (1999 [DIRS 176897]). Related information is published in a journal article by Turner and Hurst (2001 [DIRS 179765]). For this activity an SCM-controlled copy of ASHPLUME_DLL_LA V.2.1 [DIRS 178870] was used.

J2. DESCRIPTION OF THE ASHFALL AND ASHPLUME CODES

ASHFALL is based on a 3-dimensional model of tephra dispersal by Armienti et al. (1988 [DIRS 179762]). Like ASHPLUME, ASHFALL is based on the method of Suzuki (1983 [DIRS 100489]), but Hurst added time- and altitude-dependent wind conditions while retaining the two-dimensional dispersion downwind (Hurst and Turner 1999 [DIRS 176897], p. 615). ASHFALL also uses a set of prescribed settling velocities for ash particles rather than the mean and standard deviation of particle size used in ASHPLUME. The transport methods differ in that ASHFALL incorporates variations in wind conditions in time and space, while ASHPLUME assumes a single, constant value for wind speed and direction based on conditions at the top of the plume. Both codes use the method of Suzuki (1983 [DIRS 100489]) to prescribe the initial conditions of tephra mass distribution with height in the eruption column. This distribution is specified as a probability distribution with height for lateral diffusion of tephra out of the column; that is, the greater the value of the probability for diffusion out of the column, the greater the equivalent mass of tephra at that height in the column. From Suzuki (1983 [DIRS 100489], p. 103) and modified (corrected) by Jarzemba et al. (1997 [DIRS 100987], pp. 2-3 to 2-4), the probability density distribution function for particle diffusion out of the eruption column $p(z)$ is given by:

$$p(z) = \frac{\beta W_0 Y e^{-Y}}{V_0 H \left\{ 1 - (1 + Y_0) e^{-Y_0} \right\}}$$ (Eq. J-1)

where

$$Y = \frac{\beta W(z)}{V_0}$$

$$Y_0 = \frac{\beta W_0}{V_0}$$

β = a constant controlling diffusion of particles in the eruption column (dimensionless)

W_0 = initial particle rise velocity in cm/s, that represents initial rise velocity of the convective part of the plume.

V_0 = particle terminal velocity at mean sea level in cm/s

$W(z)$ = particle velocity as a function of height = $W_0\left(1 - \dfrac{z}{H}\right)$ in cm/s (Section 6.5.2.10).

Armienti et al. (1988 [DIRS 179762], p. 6466) distributed mass in the eruption column, $\theta(z)$, by multiplying the right-hand side of Equation J-1 by the amount of material brought into the column per unit time, Q, and introducing:

$$A \propto \frac{\beta W_0}{V_0}, \tag{Eq. J-2}$$

$$\theta(z) = Q * \frac{A^2\left(1 - \dfrac{z}{H}\right)e^{-A\left(1 - \frac{z}{H}\right)}}{H\left(1 - (1+A)e^{-A}\right)} * \delta(x - x_v)\delta(y - y_v) \tag{Eq. J-3}$$

for $W_0 >> V_0$; $\delta(x - x_v)\delta(y - y_v)$ is the Dirac delta function for mass input at the vent.

According to Armienti et al. (1988 [DIRS 179762], p. 6,467), the parameter, A, has geometrical significance as the height at which the column reaches maximum enlargement or the location of the maximum source concentration:

$$z_b = H - \frac{H}{A}; \tag{Eq. J-4}$$

for a typical value of $A=4$ (Section J8.1), $z_b = 0.8H$ for an anvil cloud.

J3. THE HURST AND TURNER (ASHFALL) STUDY OF RUAPEHU ERUPTIONS

The purpose of the Hurst and Turner study was to test the ASHFALL model for use in civil defense to accurately predict where ash was likely to fall, with secondary concerns for precisely how much ash falls in a particular location (Hurst and Turner 1999 [DIRS 176897], p. 617). Hurst and Turner chose the 1995 to 1996 eruptions of Ruapehu in New Zealand to test their model's capability to use routinely available information about an eruption (meteorological data, location, generalized ash particle size distribution, etc.) to make rapid predictions during the eruption about what areas could expect to receive significant ash deposition. In doing so, Hurst and Turner (1999 [DIRS 176897]) summarized available observational data on three small to moderate volume eruptions of Ruapehu in 1995 and 1996 (0.005 to 0.025 km³; Hurst and Turner 1999 [DIRS 176897], p. 617), along with their model input and results. Combined with the ASHFALL input files obtained from Dr. Tony Hurst (Section J8.1), Hurst and Turner (1999

[DIRS 176897]) provide sufficient information to compare the performance of ASHFALL and ASHPLUME and to assess the latter code's capabilities and limitations in light of a more sophisticated approach used in ASHFALL.

ASHFALL requires two input files (Section J8.1): one file ending in *.VOL* and a second file ending in *.WIN*. The *.VOL* file (Figure J-1) contains eruption parameters, including grid coordinates (in New Zealand Map Grid), horizontal diffusion coefficient (CDIFF, m^2s^{-1}), and a "Suzuki constant" (Asuz); then, for each eruption period, eruption time (Ehr, hr NZDT), coordinates of the eruption, height of the eruption column (Zmax, m), eruption volume (Totvol, km^3), and followed by a list of particle settling velocities that comprise a CDF of particle size equivalents. The *.WIN* file contains wind speed and direction information from meteorological sources, in the form of bins of wind speed and direction with altitude at various times during the eruption (Figure J-2).

```
[File OCT11E.VOL]
2700000.  3000000.  6170000.  6400000.    XI   XF   YI   YF
 500.   1000.     6000.    4.              DX   DZ   Cdiff    Asuz
[Eruption Period 1]
22.  2731300.  6210600.  10000.  0.006    Ehr   X    Y    Zmax    Totvol
37                                        Number of Ash sizes
  0.3    .001                             Settling Velocity
  0.32   .002                                & Fraction with Velocity
  0.34   .003
  0.36   .004          [Eruption Period 2]
  0.38   .005           25.  2731300.  6210600.  10000.  0.015    Ehr   X    Y    Zmax    Totvol
  0.4    .006           37                                        Number of Ash sizes
  0.43   .006             0.3    .001                             Settling Velocity
  0.46   .007             0.32   .002                                & Fraction with Velocity
  0.49   .008             0.34   .003
  0.52   .009             0.36   .004      [Eruption Period 3]
  0.55   .010             0.38   .005       28.  2731300.  6210600.  10000.  0.009
  0.58   .011             0.4    .006       37
  0.61   .012             0.43   .006         0.3    .001
  0.65   .013             0.46   .007         0.32   .002
  0.69   .013             0.49   .008         0.34   .003
  0.73   .013             0.52   .009         0.36   .004
  0.77   .014             0.55   .010         0.38   .005
  0.81   .014             0.58   .011         0.4    .006
  0.85   .014             0.61   .012         0.43   .006
  0.90   .015             0.65   .013         0.46   .007
  0.95   .015             0.69   .013         0.49   .008
  1.0    .025             0.73   .013         0.52   .009
  1.1    .03              0.77   .014         0.55   .010
  1.2    .04              0.81   .014         0.58   .011
  1.4    .04              0.85   .014         0.61   .012
  1.55   .04              0.90   .015         0.65   .013
  1.7    .04              0.95   .015         0.69   .013
  1.85   .04              1.0    .025         0.73   .013
  2.0    .05              1.1    .03          0.77   .014
  2.2    .05              1.2    .04          0.81   .014
  2.4    .05              1.4    .04          0.85   .014
  2.7    .05              1.55   .04          0.90   .015
  3.0    .05              1.7    .04          0.95   .015
  4.0    .11              1.85   .04          1.0    .025
  5.0    .07              2.0    .05          1.1    .03
  7.0    .04              2.2    .05          1.2    .04
  9.0    .08              2.4    .05          1.4    .04
                         2.7    .05          1.55   .04
                         3.0    .05          1.7    .04
                         4.0    .11          1.85   .04
                         5.0    .07          2.0    .05
                         7.0    .04          2.2    .05
                         9.0    .08          2.4    .05
                                             2.7    .05
                                             3.0    .05
                                             4.0    .11
                                             5.0    .07
                                             7.0    .04
                                             9.0    .08
```

NOTE: Input values for three eruption periods are shown. Identification information for each value in the header rows is given on the right end of the line. Refer to Table J-1 for descriptions.

Figure J-1. ASHFALL Input File for Eruption Parameters

```
[File R1012F1.WIN]
20.   14  1000  6211  2731
24. 245
26. 250
28. 255
29. 250
30. 245
33. 240
38. 235
41. 232
44. 230
42. 232
40. 235
40. 235
40. 235
40. 235
48.   14  1000  6211  2731
24. 245
26. 250
28. 255
29. 250
30. 245
33. 240
38. 235
41. 232
44. 230
42. 232
40. 235
40. 235
40. 235
40. 235
END
from Met Forecast at 951011 01:08 for Ruapehu @ 1012 0000
then repeated
```

NOTE: Header lines for each forecast period include the following information: wind time (hrs from start of eruption), number of levels at which wind speed and direction are given, vertical increment, and coordinates of wind profile (NZMG, km). This header is followed by multiple rows containing wind velocity (m/s) and direction (compass degrees).

Figure J-2. ASHFALL Input File for Wind Information

Consider the 11.Oct.1995 eruption of Mt. Ruapehu as documented in Hurst and Turner (1999 [DIRS 176897] pp. 617 to 618). The volume is estimated at 0.025 km^3 with an observed eruption height of about 10 km. The observed tephra spread widely, indicating that the wind may have shifted during the ca. 8-hour eruption. Hurst and Turner (1999 [DIRS 176897]) initially used discrete wind fields to the NE and to the E in separate model runs, producing narrow tephra distributions covering part of the observed tephra sheet. Their final model for this eruption involved variable wind conditions and resulted in a better overall fit to the observed isopachs. For this model comparison, an ASHPLUME match to ASHFALL results for the single, NE-directed wind field was developed to assess the comparability of model input parameters. An ASHPLUME match to the variable-wind ASHFALL results was developed by superimposing the several ASHPLUME sub-eruptions to assess the capabilities and limitations of ASHPLUME to handle variable winds. Copies of the ASHFALL input files used to create the model results published in a journal article by Hurst and Turner (1999 [DIRS 176897]) were obtained directly from Tony Hurst for the purposes of this code comparison (Section J8.1).

J4. ESTABLISHING EQUIVALENT INPUT VALUES FOR ASHPLUME AND ASHFALL

A comparison of input parameters used by the ASHPLUME and ASHFALL models is presented in Table J-1. The development of specific values for these input parameters is discussed in the following sections.

Table J-1.   Comparison of Input Parameters for the ASHPLUME v2.1 and ASHFALL v1.0 Codes

Parameter Description (comments)	ASHPLUME V2.1 Input Parameters	units	ASHFALL v1.0 Input Parameters	units	Parameter Description (comments)
screen display flag	Iscrn (iscrn)	none	--		not used in ASHFALL
computational grid	X_{min} (xmin)	km	XI	m	computational grid
	X_{max} (xmax)	km	XF	m	
	Y_{min} (ymin)	km	YI	m	
	Y_{max} (ymax)	km	YF	m	
	N_x (numptsx)	$none$	DX	m	horizontal spatial step
	N_y (numptsy)	$none$	DX	m	
particle size-density relationship	Y_p^{low} (ashdenmin)	g/cm^3	--		included in settling velocity formulation
	Y_p^{high} (ashdenmax)	g/cm^3	--		
	r_a^{low} (ashrholow)	log (cm)	--		
	r_a^{high} (ashrhohi)	log (cm)	--		
particle shape factor	F (fshape)	none	--		included in settling velocity formulation
air density	Y_a (airden)	g/cm^3	--		included in settling velocity formulation
air viscosity	h_a (airvis)	g/m/s	--		included in settling velocity formulation
horizontal eddy diffusion coefficient	C (C)	cm^2/s$^{5/2}$	CDIFF	m^2/s	horizontal diffusion coefficient
maximum size for transport	d_{max} (dmax)	cm	--		not used in ASHFALL
waste particle size stats	r_{min}^f (fdmin)	cm	--		waste not transported in ASHFALL
	r_{mode}^f (fdmean)	cm	--		
	r_{max}^f (fdmax)	cm	--		
minimum height of eruption column	H_{min} (hmin)	km	--		not used in ASHFALL
minimum threshold for ash accumulation	Ash Cutoff (acutoff)	g/cm^2	--		not used in ASHFALL
column diffusion coefficient	b (beta)	none	ASUZ	none	Suzuki constant
ash particle size stats	d (dmean)	cm	VJ[I], NVJ[I]	m/s, %	settling velocity CDF
	s_d (dsigma)	log (cm)	--		
waste incorporation ratio	r_c (rhocut)	none	--		no waste transported in ASHFALL
mass of waste to transport	U (uran)	g	--		

Table J-1.   Comparison of Input Parameters for the ASHPLUME v2.1 and ASHFALL v1.0 Codes
(Continued)

Parameter Description	ASHPLUME V2.1 Input Parameters	units	ASHFALL v1.0 Input Parameters	units	Parameter Description
(comments)					(comments)
wind direction	Wind Direction (udir)	degrees	VENTD[j]	degrees	defined for multiple [j] levels
wind speed	U (u)	cm/s	VENTO[j]	m/s	for multiple times
initial rise velocity	W_0 (werupt0)	cm/s	--		included in Suzuki constant
eruption power	P (power)	W	Zmax	m	height of eruption column (power calculates height in ASHPLUME)
eruption duration	T_d (tdur)	s	Ehr Totvol	Hrs km3	eruption time, volume (volume calculates duration in ASHPLUME)
Polar grid description	$rmin$ (rmin)	km	--		polar grid not used in ASHFALL
	$rfactor$ (rfactor)	none	--		
	nr (nr)	none	--		
	$nthet$ (nthet)	none	--		
Particle size output flag	$numapts$ (numapts)	none	--		not provided in ASHFALL
Not used in ASHPLUME	--		DZ	m	vertical transport step
Assumed to be (0,0) in ASHPLUME	--		X, Y	m	coordinates of eruption (NZMG)
Only one wind speed used in ASHPLUME	--		Whr	hrs	time of wind data (for each
	--		NW	none	# levels at which wind data are defined
	--		DZ	none	vertical step (spatial interval of wind data)
	--		WX, WY	km	coordinates of wind data measurements

J4.1   MODEL GRID

Both models calculate tephra accumulation at user-defined points in a two-dimensional array corresponding to the earth's surface. The calculational grid for ASHFALL is defined in meters in New Zealand Map Grid (NZMG) coordinates. In contrast, the ASHPLUME calculational grid is independent of geographic coordinates and is given in km relative to the eruptive vent, which is assumed to have (0, 0) coordinates. ASHPLUME was run using Cartesian coordinates for this modeling activity. In order to compare the results of the two models, ASHPLUME results were translated and viewed in a geographical information system (GIS) containing ASHFALL results in a NZMG framework (using ArcGIS V.9.1 Desktop software [DIRS 176015]). The translation was performed by mapping the ASHPLUME vent (0, 0 km) to the Ruapehu vent (2731300, 6210600 m; Hurst and Turner 1999 [DIRS 176897], Figure 1) and converting the regular ASHPLUME grid to these NZMG coordinates.

J4.2 ERUPTION POWER, COLUMN HEIGHT, AND DURATION

The column height for the October 11, 1995 eruption of Ruapehu was assigned at 10 km on the basis of observations (Hurst and Turner 1999 [DIRS 176897], p. 618). Using the column height – power relationship provided by Jarzemba et al. (1997 [DIRS 100987], p. 4-4) for height in km and power in W:

$$H = 0.0082P^{1/4}, \text{ or } P = \left(\frac{H}{0.0082}\right)^4 \qquad \text{(Eq. J-5)}$$

For $H = 10$ km, $\underline{P = 2.2 \text{x} 10^{12} \text{ W}}$.

The mass flux (kg/s) is related to the eruption power via the thermal energy contained in the erupted material, characterized by the product of specific heat of the erupted mixture and the temperature difference with the ambient atmosphere. Values for each of these variables are assigned as discussed in Section 6.5.2.1, and the resulting product is 1×10^6 J/kg. Using Equation 6-7b, mass flux = 2.2×10^6 kg/s. The relationship between mass flux and duration is given by (Section 6.5.1):

$$\dot{Q} = \frac{V\psi_s}{T_d} \qquad \text{(Eq. J-6)}$$

where $\dot{Q}$ is mass flux (kg/s)

V is volume (m³)

ψ_s is tephra settled density

T_d is eruption duration (s).

For $V = 3\text{x}10^7$ m³ (sum of the three eruptive periods, Figure J-1), $\psi_s = 1000$ kg/m³ (mean from SNL 2007 [DIRS 174260], Table 7-1), and $\dot{Q}=2.2\text{x}10^6$ kg/s, $\underline{T_d = 1.3\text{x}10^4 \text{ s}}$, or about 4 hours. This duration is half of the observed ca. 8-hour eruption duration, but the model assumes that the entire eruption is at peak mass flux, while the actual October 11, 1995 Ruapehu eruption exhibited a wide variability in mass flux, as interpreted from seismic power levels (Hurst and Turner, 1999 [DIRS 176897], Figure 2).

J4.3 EDDY DIFFUSIVITY

From Suzuki (1983 [DIRS 100489], p. 98), the solution to the basic advection-dispersion equation for atmospheric transport is:

$$\chi = \frac{5q}{8\pi Ct^{5/2}} \exp\left[\frac{-5\left((x-ut)^2 + y^2\right)}{8Ct^{5/2}}\right], \qquad \text{(Eq. J-7)}$$

where q is mass of ash transported and C is a constant relating eddy diffusivity and particle fall time ($cm^2/s^{5/2}$). In order to determine the value of C, Suzuki (1983 [DIRS 100489], p. 98) gives the relationship between the apparent eddy diffusivity, A_L, and the eddy length scale, L, as:

$$A_L = 0.08073 C^{2/5} L^{6/5},$$

(Eq. J-8)

for A_L in cm^2/s, L in cm, and C in $cm^2/S^{5/2}$. Suzuki's (1983 [DIRS 100489]) Figure 2 provides observed $A_L - L$ data to calculate a regression:

$$A_L = 0.887 L^{6/5},$$

(Eq. J-9)

and hence $C = 400$ $cm^2/s^{5/2}$ (Section 6.5.2.15). ASHPLUME uses the parameter C as direct input, while ASHFALL uses a value for the horizontal diffusion coefficient (*CDIFF*), in units of m^2/s, from the original two-dimensional advection-dispersion equation (Suzuki 1983 [DIRS 100489], p. 98):

$$\frac{\partial \chi}{\partial t} = -u \frac{\partial \chi}{\partial x} - \frac{\partial}{\partial x}\left(K \frac{\partial \chi}{\partial x}\right) - \frac{\partial}{\partial y}\left(K \frac{\partial \chi}{\partial y}\right).$$

(Eq. J-10)

Suzuki (1983 [DIRS 100489], p. 98) defines $K = Ct^{3/2}$, so

$$CDIFF \approx Ct^{3/2}.$$

(Eq. J-11)

Armienti et al. (1988 [DIRS 179762], p. 6,466) describe the scale dependency of horizontal diffusion coefficient:

For 10s of km, $K \sim 0$ to 250 m^2/s
For 100s of km, $K \sim 10^3$ to 10^4 m^2/s
For >100's of km, $K \sim 10^4$ m^2/s.

For length scales of about 100 km, as in the Ruapehu case, K should be about 10^3 m^2/s, consistent with the value of 6,000 m^2/s for *CDIFF* used by Hurst and Turner 1999 [DIRS 176897] p. 621). Solving for time using the input values used in the two models ($C = 400$ $cm^2/s^{5/2}$, *CDIFF* = 6,000 m^2/s) yields a time scale of about 2,800 s. Given the wind speed of about 3,000 to 4,200 cm/s used in the ASHFALL input for the October 11 eruption (Figure J-2), this time scale corresponds to a horizontal advective transport scale of 80 to 120 km. This is roughly the area of interest for the comparison of tephra deposition from the 1995-1996 eruptions of Ruapehu, and therefore the values discussed above for these two model inputs are considered comparable.

J4.4   TEPHRA PARTICLE SIZE DISTRIBUTION

ASHFALL used a single set of particle settling velocities (defined as a probability distribution) for all eruption periods in the October 11, 1995 model (Hurst and Turner 1999 [DIRS 176897], p. 616; Figure J-1). The probability distribution of particle settling velocities must be converted to mean and standard deviation of the corresponding particle size distribution for use in

ASHPLUME. This conversion was accomplished using the grain size—settling velocity relationship for cylinders of Walker et al. (1971 [DIRS 181319], Fig. 2) using the settling velocity data in ASHFALL input file *OCT11E.VOL* (Table J-2). The resulting grain size data were plotted so that standard granulometric parameters (i.e., mean and standard deviation) could be developed (Figure J-3).

Table J-2. Calculation of Grain Size Information from ASHFALL Particle Settling Velocity Distribution

ASHFALL	Calculated	Calculated	ASHFALL	Calculated	Calculated
Settling Velocity (m/s)	Grain Size[1] (mm)	Grain Size (phi)	Fraction per Settling Velocity	Cumulative (frx)	Cumulative (%)
9	5.5	−2.45943	0.08	0.08	8
7	3	−1.58496	0.04	0.12	12
5	1.3	−0.37851	0.07	0.19	19
4	1	0	0.11	0.3	30
3	0.7	0.51457	0.05	0.35	35
2.7		—	0.05	0.4	40
2.4		—	0.05	0.45	45
2.2		—	0.05	0.5	50
2	0.4	1.32193	0.05	0.55	55
1.85		—	0.04	0.59	59
1.7		—	0.04	0.63	63
1.55		—	0.04	0.67	67
1.4		—	0.04	0.71	71
1.2		—	0.04	0.75	75
1.1		—	0.03	0.78	78
1	0.18	2.47393	0.025	0.805	80.5
0.95		—	0.015	0.82	82
0.9	0.15	2.73697	0.015	0.835	83.5
0.85		—	0.014	0.849	84.9
0.81	0.14	2.8365	0.014	0.863	86.3
0.77		—	0.014	0.877	87.7
0.73		—	0.013	0.89	89
0.69	0.1	3.32193	0.013	0.903	90.3
0.65		—	0.013	0.916	91.6
0.61	0.095	3.39593	0.012	0.928	92.8
0.58		—	0.011	0.939	93.9
0.55		—	0.01	0.949	94.9
0.52		—	0.009	0.958	95.8
0.49	0.08	3.64386	0.008	0.966	96.6
0.46		—	0.007	0.973	97.3
0.43		—	0.006	0.979	97.9
0.4	0.06	4.05889	0.006	0.985	98.5
0.38		—	0.005	0.99	99
0.36		—	0.004	0.994	99.4
0.34		—	0.003	0.997	99.7
0.32		—	0.002	0.999	99.9
0.3	0.05	4.32193	1×10^{-3}	1	100

NOTE: [1] Determined visually from Walker et al. 1971 [DIRS 181319], Figure 2 using a variable particle density (Section 6.5.2.11).
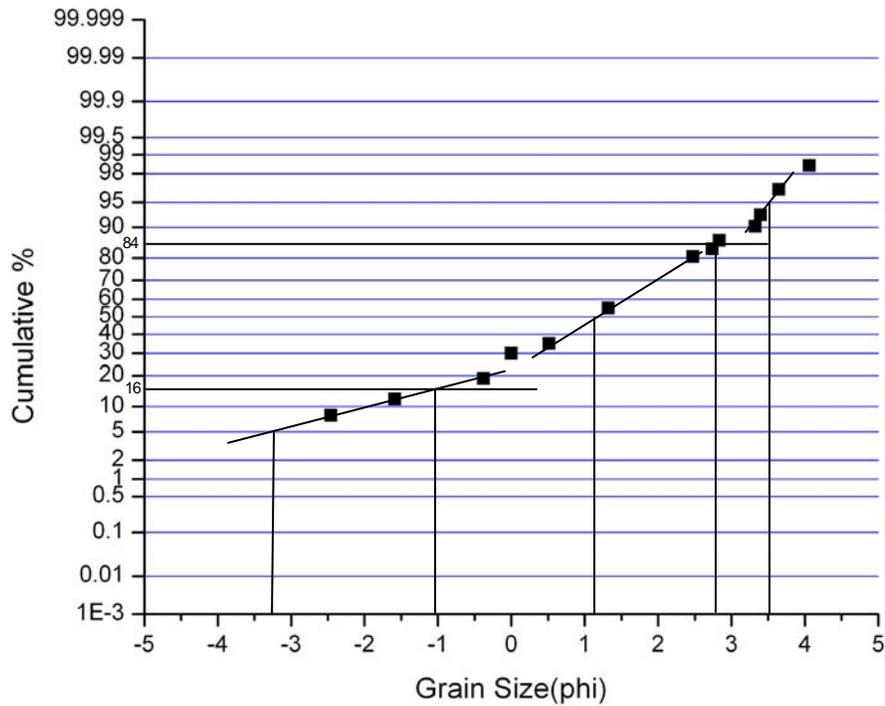
Figure J-3. Grain Size Frequency Distribution Derived from ASHFALL Particle Settling Velocity Distribution

The mean and standard deviation of the particle size distribution was developed from the grain size – cumulative percent coarser values presented in Figure J-3. Using the method of Folk, the mean is $\bar{x} = (\phi_{84} + \phi_{50} + \phi_{16})/3$ and standard deviation is $\sigma_\phi = (\phi_{84} - \phi_{16})/4 + (\phi_{95} - \phi_5)/6.6$ (Swan and Sandilands 1998 [DIRS 153441], p. 126). As developed in Figure J-3, $\phi_{95} = 3.5$, $\phi_{84} = 2.8$, $\phi_{50} = 1.1$, $\phi_{16} = -1.0$, $\phi_5 = -3.3$,

and the mean is 0.93ϕ. Given that $\phi = -\log_2(grainsize(mm))$, the mean can be converted to 0.087 cm. The standard deviation is 2.0ϕ.[2] Ashplume requires a value for particle size standard deviation ("dsigma", or σ_d) in units of log(cm). Utilizing identities of logarithms (as summarized in Section 6.5.2.5), $\sigma_d = 0.301\sigma_\phi$ and therefore $\sigma_d = 0.602$ log(cm).

J4.5   COLUMN DIFFUSION COEFFICIENT

As introduced in Section J2, the column diffusion coefficient, β, is related to the Suzuki constant, A, by

---

[2] Another common method is that of Inman, described by Fischer and Schmincke (1984 [DIRS 162806], p. 118): $\sigma_\phi = (\phi_{84} - \phi_{16})/2$, which yields $\sigma_\phi = 1.95\phi$, an equivalent value when rounded to two significant digits.

$$A \propto \frac{\beta W_0}{V_s} \quad \text{or}$$

$$W_0 \propto \frac{A V_s}{\beta}, \quad \text{(Eq. J-12)}$$

Where V_s is the particle settling velocity (cm/s). For the 1995-96 Ruapehu simulations, a value of $A = 4$ was used (see Addendum, Section J8.1). Applying the relationship above, initial values for A, β, and V_s were used to approximate W_o as a check for consistency within the sets of the former three parameters (Table J-3).

Table J-3.   Sample Sets of Related Values for Particle Transport Parameters

A	V_s (cm/s)	β	W_0 (cm/s)
4	400 (~ 1-mm diameter)[1]	0.5	3,200
4	30 (~0.05-mm diameter)	0.5	240
4	300 (~0.7-mm diameter)	0.5	2,400
4	900 (~5.5-mm diameter)	0.5	7,200
4	900	0.3	12,000
4	900	0.25	14,400

NOTE: [1] See Table J-2 for example grain size—settling velocity equivalencies.

These values cover the range in settling velocities included in ASHFALL input file *OCT11E.VOL* and a typical range in values for β as described in Section 6.5.2.3. The resulting values of W_0 are within the range described in Section 6.5.2.10, except the last value (14,400 cm/s). Therefore, the for input value of the Suzuki constant, $A = 4$ and for settling velocities covering the range used in ASHFALL input file *OCT11E.VOL*, values for the ASHPLUME input parameter, β, should be in the range of $\beta = 0.3$ to 0.5.

J5.   COMPARISON OF SINGLE-PLUME MODELS

The 11.Oct.1995 (2100 hours NZDT) eruption of Ruapehu provided a well-documented case study for Hurst and Turner (1999 [DIRS 176897], p. 618) to investigate the effects of constant vs. varying wind fields during a single eruption. The ASHFALL analysis used constant wind conditions based on a 12-hour forecast given the previous afternoon (Hurst and Turner 1999 [DIRS 176897], p. 618, Figure 1b). The plume resulting from the constant-windfield ASHFALL simulation was relatively simple and suitable for comparison to ASHPLUME results. Sample input and output files are provided in Section J8.2. All input and output files from this code comparison are included in validation DTN: LA0706GK150308.001. A qualified version of ASHPLUME_DLL_LA V2.1 [DIRS 178870] was obtained from Software Configuration Management for use in this modeling exercise.

Results of ASHPLUME model runs were superimposed on published ASHFALL results (tephra thickness isopachs) for visual and quantitative comparison. Tephra thickness (cm) was calculated from ASHPLUME areal concentrations (g/cm^2) by assuming a tephra deposit density value of 1.0 g/cm^3 consistent with the development of equivalent model parameter values in Section J4.2. ASHPLUME output files were converted to two-dimensional matrices using

built-in functions of the OriginPro 7.5 plotting software. Since ASHPLUME does not calculate results at the vent (location 0, 0 km), an artificial vent concentration value was generated by copying the tephra concentration value at a neighboring point (0, 2 km) to the vent point (0, 0 km) prior to creating the matrix; however, this was only done for data visualization purposes and does not affect the calculation of total mass transported or other model output. The matrix was inverted (flipped) about its horizontal axis to transform the origin from the upper left corner to the lower left corner for visualization in a geographical information system (GIS). Once the matrix was flipped, it was exported from OriginPro 7.5 as an ASCII raster. A header was added based on model grid properties and coordinates provided in the journal article by Hurst and Turner (1999 [DIRS 176897], Figure 1).

The GIS (ArcGIS 9.1 [DIRS 176015]) provides a common geographical framework for visualizing published model results, geographic landmarks, and results of ASHPLUME modeling. ArcGIS 9.1 was used to geo-rectify a scanned image of ASHFALL results (Hurst and Turner 1999 [DIRS 176897], Figure 1b) and to project it into New Zealand Map Grid coordinates (Hurst and Turner 1999 [DIRS 176897], Figure 3). The ASHPLUME raster (with header) was converted to an ArcGIS floating-point grid using built-in tools in ArcGIS 9.1 and brought into a common geographical framework with the scanned results of ASHFALL (Figure J-4). Points were established for comparing model results, recorded along with their distances downwind along the axis of the plume as measured using the built-in measurement tool in ArcGIS 9.1 (Figure J-4).
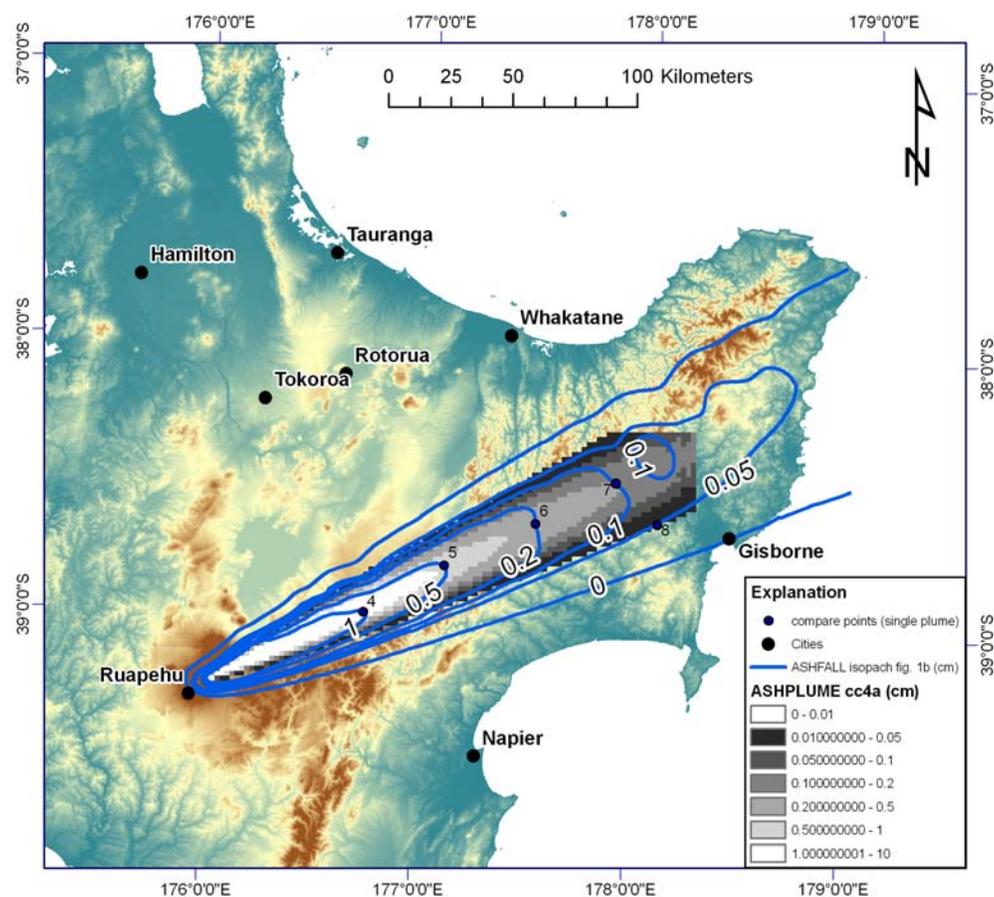
Sources: Hurst and Turner 1999 [DIRS 176897], Figure 1b (ASHFALL results); U.S. Geological Survey (digital
elevation model), for illustration purposes only.

NOTE: ASHPLUME run cc4a (base case for single plume) is shown with ASHFALL results superimposed.

Figure J-4. Sample Plot of Results of ASHFALL and Single-Plume ASHPLUME Models in Geographic
Framework

Single-plume ASHPLUME model runs are summarized in Table J-4. The base-case model run
(cc4a) used input parameter values based on the model equivalencies described in the preceding
sections. Parameters that control the distribution of tephra in both models include wind speed
and direction, eruptive power and duration (which define total erupted volume), β and A
(parameters related to the Suzuki constant for initial particle distribution in the eruptive column),
W_0 (initial eruptive rise velocity), and C (eddy diffusion constant). Values for these parameters
were adjusted to achieve the best possible agreement between the results of the two models. The
wind direction was established by best fit to the axis of the observed tephra fall (and fine tuned
during modeling). Wind speed was varied within the limits of meteorological forecasts at all
altitudes containing tephra above Mt. Ruapehu (Figure J-2). The eddy diffusion constant, C, was
varied to evaluate its effect on the pattern of tephra deposition. Values of β and W_0 were varied
in the context of the related ASHFALL parameter, Suzuki constant, A, in order to understand the
effects of varying the initial mass loading in the eruption column.

Table J-4. Summary of Input Parameters Varied in Single-Plume Code Comparison

Parameter	Base-case Value	Range Varied	Model Runs	Comment
β	0.5	0.1 to 5.0	cc4a, 6a, 8b, 8c, 9b	Higher values result in too much ash downrange
Wind speed (cm/s)	4,200	2,000 to 4,200	cc4a, 6a, 6b, 9b, 9e, 9f, 9g, 9h	Primary effect on results
Wind direction (degrees north of east)	+38°	+25°	cc3d, 4a	Good match at +25°
W_0 (cm/s)	2,000	1,000 to 10,000	cc4a, 8a, 8c, 9b, 9e	Higher values yield broader plume, more transport downrange
C ($cm^2/s^{5/2}$)	400	400 to 1,600	cc4a, 7, 7a	Higher values yield broader plume
P (W)	2.2×10^{12}	n/a	All	Not varied; value determined by assumed eruptive volume, column height
T_d (s)	1.36×10^4 s	n/a	All	Not varied; value determined by assumed eruptive volume, column height
A^1	3.3	0.33 to 33	Cc4a, 8a, 8b, 8c, 9b	Parameter provides control on initial mass loading in column; primary effect on results

NOTE: [1] The parameter *A* (Suzuki constant) is not a primary input to ASHPLUME; rather, it is a combination of two ASHPLUME input parameters (Eq. J-2).

Comparison of the ASHPLUME results to published results of ASHFALL was made by means of plan-view maps (e.g., Figure J-4) and profiles. Profiles of results of ASHFALL (Hurst and Turner 1999 [DIRS 176897], Figure 1b) and ASHPLUME were developed based on values at the comparison points (Figure J-4) and are presented in groups according to variations in individual parameters in Figure J-5. Variation in tephra deposition pattern was most strongly controlled by variation in wind speed (Figure J-5b) and the combination of β and W_0 in the Suzuki constant, *A* (Figure J-5c). Variation in values of the eddy diffusivity constant (*C*, Figure J-5d) increased the lateral transport of tephra, but its value was returned to the default due to lack of technical basis for varying it from the original value developed by Suzuki (1983 [DIRS 100489], p. 98). While variations in wind speed within the range of meteorological observations (Figure J-5b) provide tephra thickness profiles that bracket the ASHFALL results shown by Hurst and Turner (1999 [DIRS 176897], Figure 1b), the shape of the deposition is not consistent with the ASHFALL model results: generally too much proximal deposition and too little distal deposition. For most model runs, an appropriate wind speed was chosen from the meteorological observations relevant for the elevation of the center of mass of the tephra particles in the eruption column, based on values of β and W_0 (given by proxy as the maximum value of $P(z)$, Figure J-6). Final matching of the two codes was done using values of β and W_0 such that $A=4$ (e.g., β=0.5 and W_0=2400 cm/s) (i.e, runs cc9e, 9f, 9g, 9h).
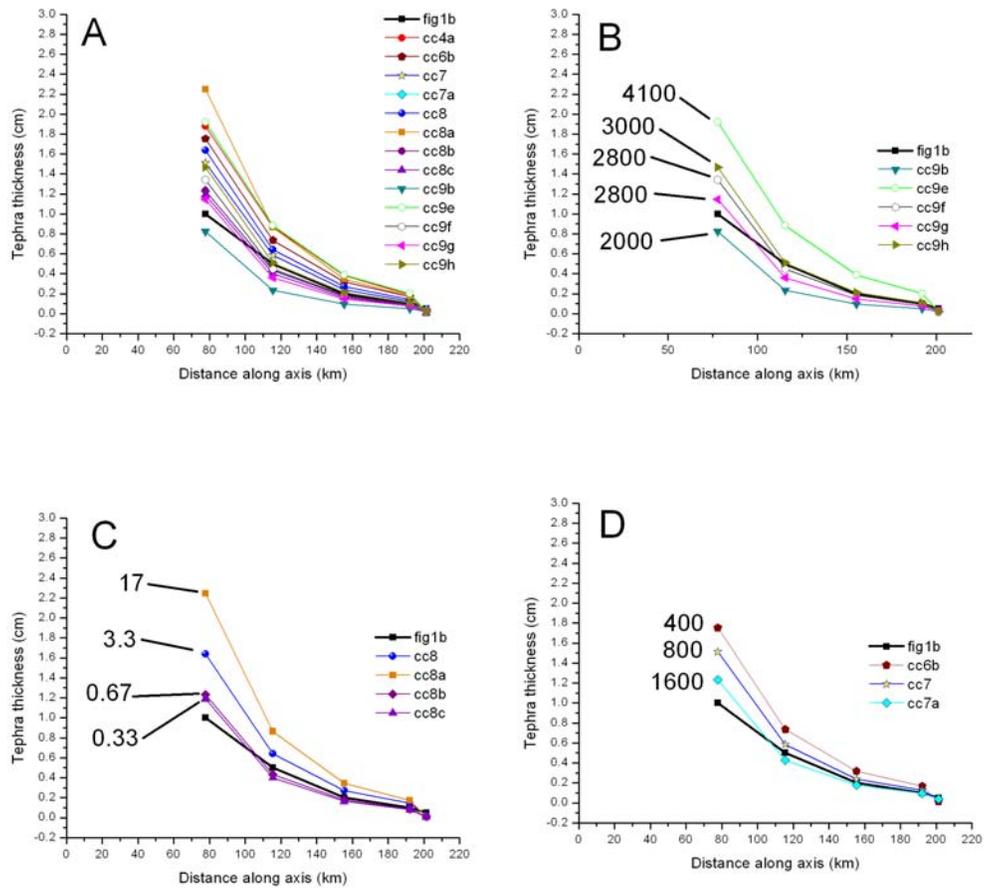
Source: Hurst and Turner 1999 [DIRS 176897], Figure 1b; heavy black line and black squares.

NOTE: Values for each named parameter are shown next to each profile. A) All model runs; B) variation in wind speed (*u*, cm/s); C) variation in Suzuki constant (*A*); D) Variation in eddy diffusion constant (*C*, cm^2/s$^{5/2}$).

Figure J-5. Summary of Single-plume ASHPLUME Model Runs Compared to ASHFALL Results at Points Along a Profile on the Longitudinal Axis of the Tephra Sheet
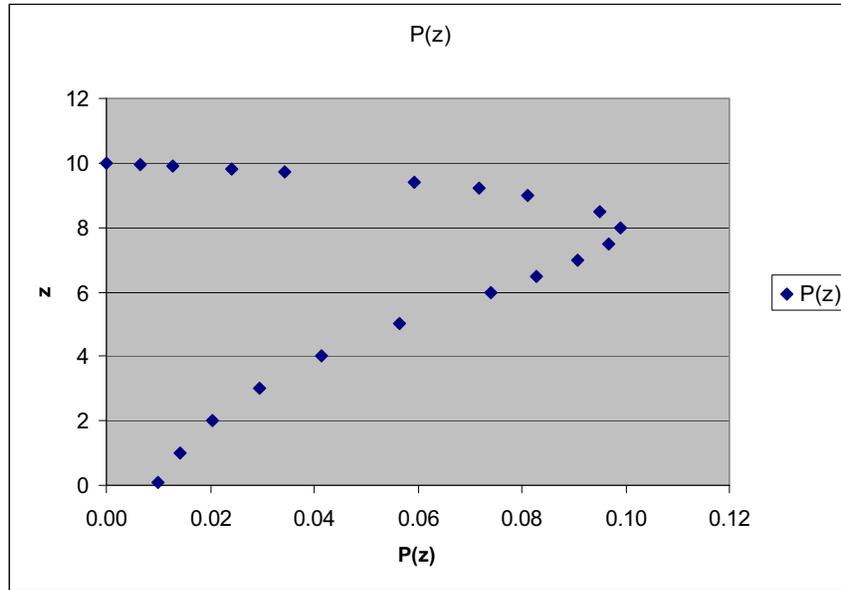
NOTE: β=0.5, W_0=2400 cm/s, mean particle diameter = 0.087 cm, particle shape factor=0.5, and particle density = 1.5 g/cm^3. For these parameter values, the center of mass of the column is at 8,000 feet. See Figure J-14 for spreadsheet calculation.

Figure J-6. Calculated Distribution of Values of *P(z)*

ASHPLUME tephra distributions from the base-case single-plume simulations were narrower than those produced by ASHFALL for compatible input parameter values that produce similar thicknesses along the axis (e.g., runs cc4a and cc8, Figure J-7). This is most likely due to the slight fanning of the ASHFALL deposit even in the case where only a single set of meteorological observations are used throughout the eruption; there is a 25° variation in wind direction and speed with height among the 1-km wind bins used by ASHFALL (Figure J-2). More narrow ASHPLUME tephra distributions result from the use of a single wind speed value (at the top of the eruptive column). Runs in which the ASHPLUME wind speed was decreased (e.g., cc9b, Figure J-5b) produced wider deposits (closer to the width of ASHFALL deposits) but were too short compared to the ASHFALL results. Good matches to ASHFALL results were achieved for ASHPLUME runs with *A*=4 and wind speeds in the range of 2,800 to 3,000 cm/s. The difference between tephra thicknesses estimated by ASHPLUME and ASHFALL for the best matching runs (e.g., cc8, cc9f) was a factor of two or less (Table J-5, Figure J-8).

As pointed out by Hurst and Turner (1999 [DIRS 176897], p. 616), the fraction of tephra in different size ranges strongly affects transport. The equivalency between the two models' formulations of settling velocity is focused primarily on the translation of a probability distribution of settling velocities to a mean and standard deviation of particle size (Section J4.4). Therefore, small variations in the distribution of settling velocities (and therefore grain size) can be made by adjusting the particle size statistics for ASHPLUME. A simple evaluation of the effect of grain size on transport was made by varying mean ash particle size parameter, dmean, from its base-case value of 0.052 to 0.087 cm. The results of this change are illustrated in Figure J-9. Using the smaller mean particle size value, tephra thickness (and hence transport) increased by 10% to 20% proximally and up to 50% distally.
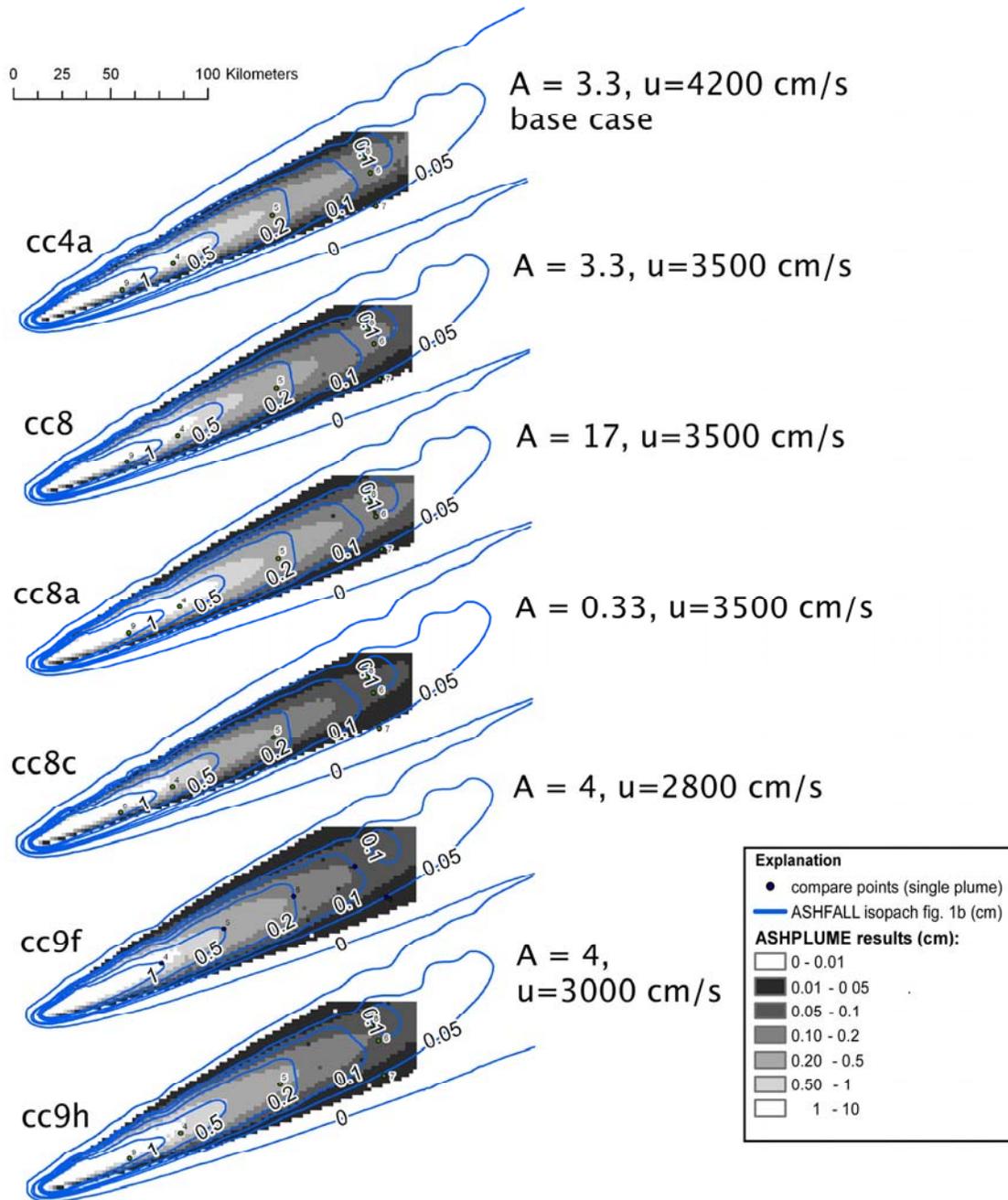
NOTE: Model run designators are given on left side of plume maps; values for parameters Suzuki constant, *A*, and wind speed (*u*, cm/s) are given on the right. See Figure J-4 for geographical context.

Figure J-7. Comparison of Single-plume Results of ASHPLUME (Grayscale) versus Results of ASHFALL (Contours)

Table J-5. Differences[1] between Tephra Thicknesses Calculated by ASHPLUME (single plume) and ASHFALL at Selected Comparison Points

ASHPLUME Run	Comparison Point Number[2] (Distance from Vent, km)				
	4 (77.8)	5 (115.5)	6 (155.3)	7 (192.1)	8 (201.3)
Cc4a	1.9	1.7	1.9	1.9	0.2
Cc6b	1.8	1.5	1.6	1.7	0.3
Cc7	1.5	1.2	1.2	1.3	0.6
Cc7a	1.2	0.9	0.9	0.9	0.8
Cc8	1.6	1.3	1.4	1.5	0.4
Cc8a	2.2	1.7	1.7	1.8	0.1
Cc8b	1.2	0.9	0.9	0.9	0.2
Cc8c	1.2	0.8	0.8	0.8	0.2
Cc9b	0.8	0.5	0.5	0.5	0.5
Cc9e	1.9	1.8	1.9	2.0	0.3
Cc9f	1.3	0.9	0.9	0.9	0.5
Cc9g	1.1	0.7	0.7	0.8	0.5
Cc9h	1.5	1.0	1.1	1.1	0.5

NOTES: [1] Difference values are calculated as the quotient of results of ASHPLUME and ASHFALL; no difference = 1.0.

[2] See Figure J-4 for location of comparison points. Points 4-7 are located along the longitudinal axis of the plume on the 1, 0.5, 0.2, and 0.1 cm tephra isopachs; point 8 is located off-axis at the outer edge of the 0.05-cm isopach.
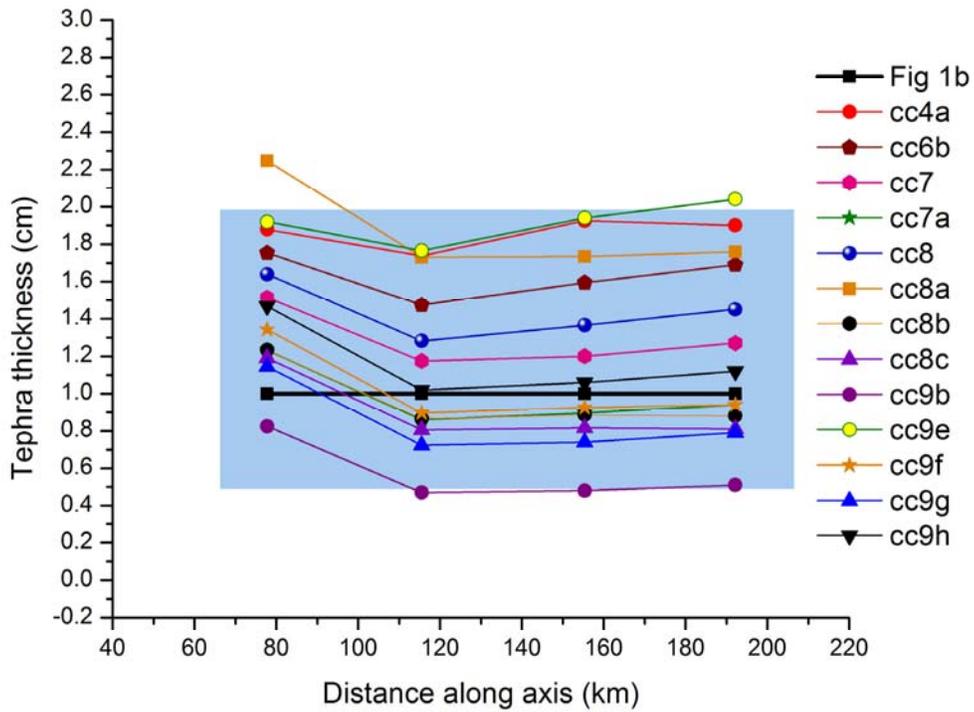
NOTE: Values are plotted at comparison points along plume centerline presented in Figure J-4. See Table J-5 for values and note on method of calculation. Shaded box denotes values within a factor of two of ASHFALL runs ("Fig 1b" line).

Figure J-8. Difference between Tephra Thickness Estimated by ASHPLUME and ASHFALL for Single-plume Runs
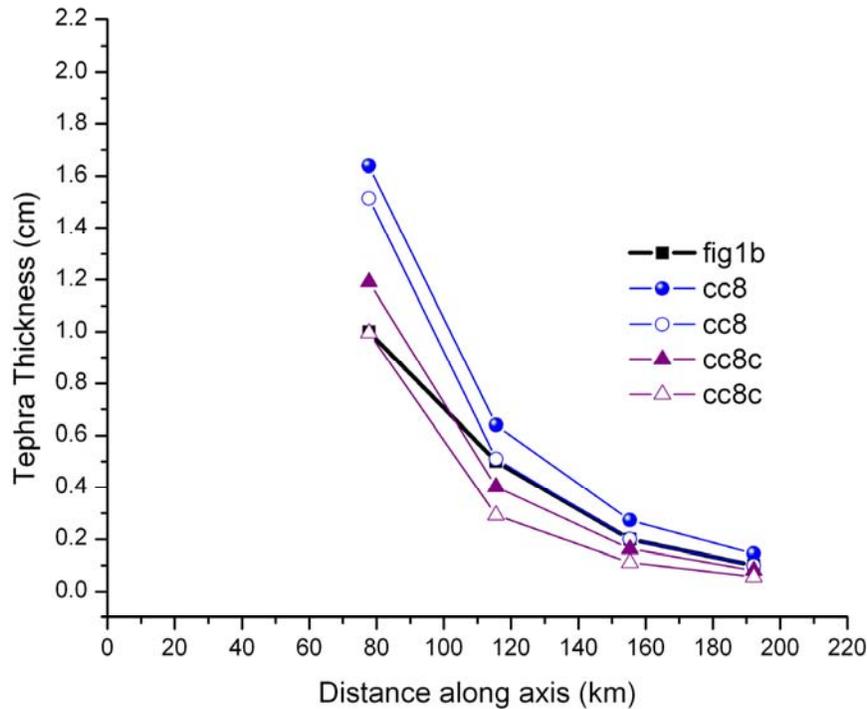
NOTE: Variations in tephra thickness for two ASHPLUME runs are shown, using mean ash particle diameter
          (dmean) values of 0.052 (base case, solid symbols) and 0.087 (open symbols).

Figure J-9. Tephra Thickness Variations as a Result of Value of Mean Ash Particle Diameter

J6.   COMPARISON OF COMPOSITE (MULTI-LOBED) PLUME MODELS

The best match of observed tephra fall from the October 11, 1995 Ruapehu eruption was obtained with ASHFALL based on a wind field that shifted direction during the eight-hour eruption (Hurst and Turner 1999 [DIRS 176897], Figure 1d). Hurst and Turner (1999 [DIRS 176897], p. 618) used observed wind conditions at New Plymouth, NZ (130 km west of Ruapehu), which included a 35° clockwise shift in wind direction during the eruption period. The resulting pattern of tephra deposition calculated by ASHFALL includes two distinct lobes (Figure J-10). In order to match this complex tephra distribution pattern using ASHPLUME, the total eruption volume (0.03 km^3) was divided into two equal subsets (0.015 km^3 each) and was erupted over the course of two separate model runs. The input files for these separate component runs ("sub-eruptions") were identical except for the azimuth of the wind, which was established by inspection of the plot of ASHFALL model output (Hurst and Turner 1999 [DIRS 176897], Figure 1d).
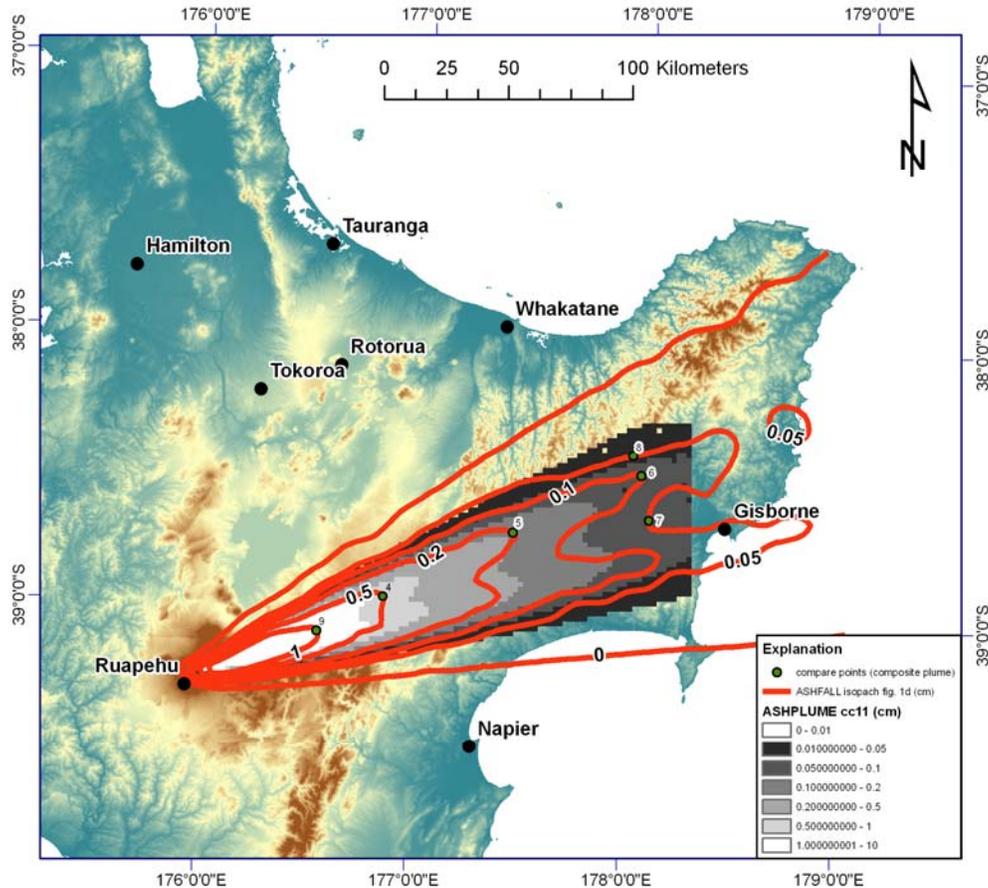
Sources: Hurst and Turner 1999 [DIRS 176897], Figure 1d (ASHFALL results); U.S. Geological Survey (digital elevation model); for illustration purposes only.

NOTE: ASHPLUME run cc11 (base case for composite plume) is shown in grey levels with ASHFALL results superimposed as contours.

Figure J-10. Sample Plot of Results of ASHFALL and Composite-plume ASHPLUME Models in Geographic Framework

As was done with the single-plume model results, ASHPLUME results for each sub-eruption were imported into OriginPro 7.5 and converted to a two-dimensional matrix. A new, empty matrix was created and assigned dimensions equivalent to those of the model results (106 columns, 56 rows; x coordinates –10, 200; y coordinates –10, 100). Values for the new matrix were assigned as the sum of the two suberuptions to produce a composite ash thickness matrix for the entire eruptive volume. This matrix was then flipped, exported to an ASCII raster, and brought into GIS for visualization (e.g., Figure J-10).

The variation in parameter values in the composite plume ASHPLUME runs is summarized in Table J-6. Based on experience in the single-plume runs (Section J5), analysis for the composite-plume runs focused on the effects of values of the Suzuki constant, A (incorporating β and W_0; Eq. J-2), total eruption volume (varied by adjusting power and duration), and impulsiveness of the eruption (i.e., short, high eruption versus longer, lower eruption). In total,

the tephra thickness profiles from the ASHPLUME composite-plume runs over-estimated the ASHFALL thickness profile in the proximal and median areas, while distal deposits estimated by ASHPLUME were consistently thin (Figure J-11a, b). Variations in erupted volume (Figure J-11c) and in the Suzuki constant, *A*, (Figure J-11d) provided close approach to the ASHFALL profile. Increasing values for parameters W_0, *β*, power, and wind speed increased overall transport downwind but did not change the slope of the axial thickness profile (Figure J-11). The value of the Suzuki constant, *A*, provided a good tool for approaching the ASHFALL thickness distribution (Figure J-11d). A higher, shorter eruption (more impulsive, column height 13 km – run cc14) resulted in greater overall tephra transport but did not provide a better match than the base case value of 12 km (run cc13, Figure J-11a).

Table J-6. Summary of Input Parameters Varied in Composite-plume Code Comparison

Parameter	Base-case Value	Range Varied	Model Runs	Comment
β	0.5	0.5 to 1.0	cc11, 18	Higher values enhance transport; analyzed together with W_0 as part of Suzuki constant, A
Wind speed (cm/s)	3500	3,500 to 4,000	cc11, 15, 19, 22	Decreasing transport with decreasing wind speed
Wind direction (degrees north of east)	+32° / +15°	+32° to +23° / +15°	cc10, 11, 20	Good match at +23° / +15°
W_0 (cm/s)	2,000	2,000 to 10,000	cc11, 17, 18, 19	Higher values yield more transport downrange; analyzed together with β as part of Suzuki constant, A
C (cm^2/s$^{5/2}$)	400	N/a	cc11	Not varied
P (W)	4.6×10^{12}	4.6×10^{12} to 6.3×10^{12}	cc13, 14	Column height varied between 12 and 13 km; higher column yielded greater tephra transport
T_d[1] (s)	3,260	2,200 to 3,260	cc11, 13, 14, 15, 17	Varied to adjust total volume (0.01 to 0.02 km^3 per sub-eruption) and to balance variable eruption height (power); tephra thickness proportional to erupted volume
A[2]	3.3	3.3 to 33	cc11, 17, 18, 19	ASHFALL results bracketed by trial range

NOTES: [1] Duration per suberuption.
       [2] The parameter *A* (Suzuki constant) is not a primary input to ASHPLUME; rather, it is a combination of two ASHPLUME input parameters (Equation J-2).
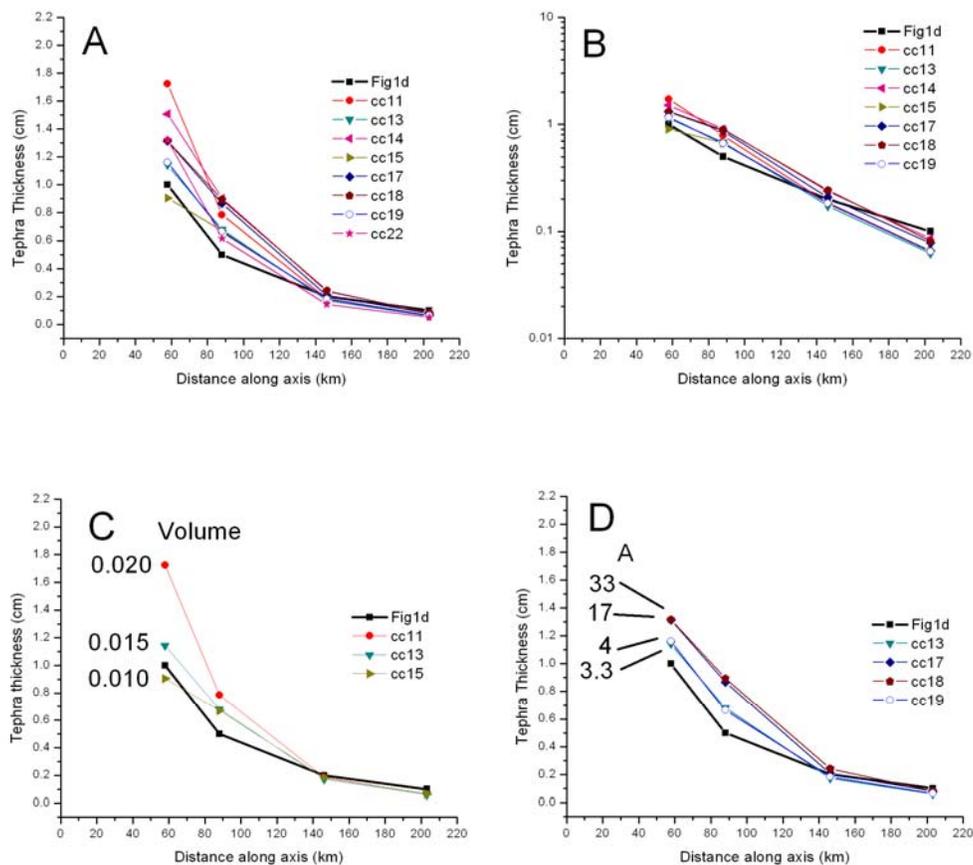
Source: Hurst and Turner 1999 [DIRS 176897], Figure 1d (heavy black line and black squares).

NOTE: Values for each named parameter are shown next to each profile. A) All model runs; B) all model runs, logarithmic tephra thickness scale; C) variation in erupted volume per sub-eruption (km^3); D) variation in Suzuki constant, *A* (Equation J-2).

Figure J-11. Summary of Composite-Plume ASHPLUME Model Runs Compared to ASHFALL Results at Points along a Profile on the Longitudinal Axis of the Tephra Sheet

Plan-view comparisons of estimates of tephra thickness from ASHPLUME and ASHFALL illustrate the general match between the two models (Figure J-12). The general agreement is evident between the ASHFALL simulation using a variable wind field (wind speed and direction vs. height and vs. time) and the ASHPLUME simulation using a composite of two distinct sub-eruptions, each with different constant wind conditions. The use of wind speeds appropriate for 7 to 8 km elevation (4,000 cm/s; Figure J-7) and a value of 4 for the Suzuki constant, *A*, produced the best fit (run cc19, Figure J-12). ASHPLUME tends to produce greater tephra thickness in the proximal (<100 km) area and relatively less in the distal (>150 km) areas. However, as shown in Table J-7 and Figure J-13, the ASHPLUME runs showing the best match to ASHFALL results (Hurst and Turner 1999 [DIRS 176897], Figure 1d) are well within a factor of two of the ASHFALL results (consistent with the results of the single-plume simulation).
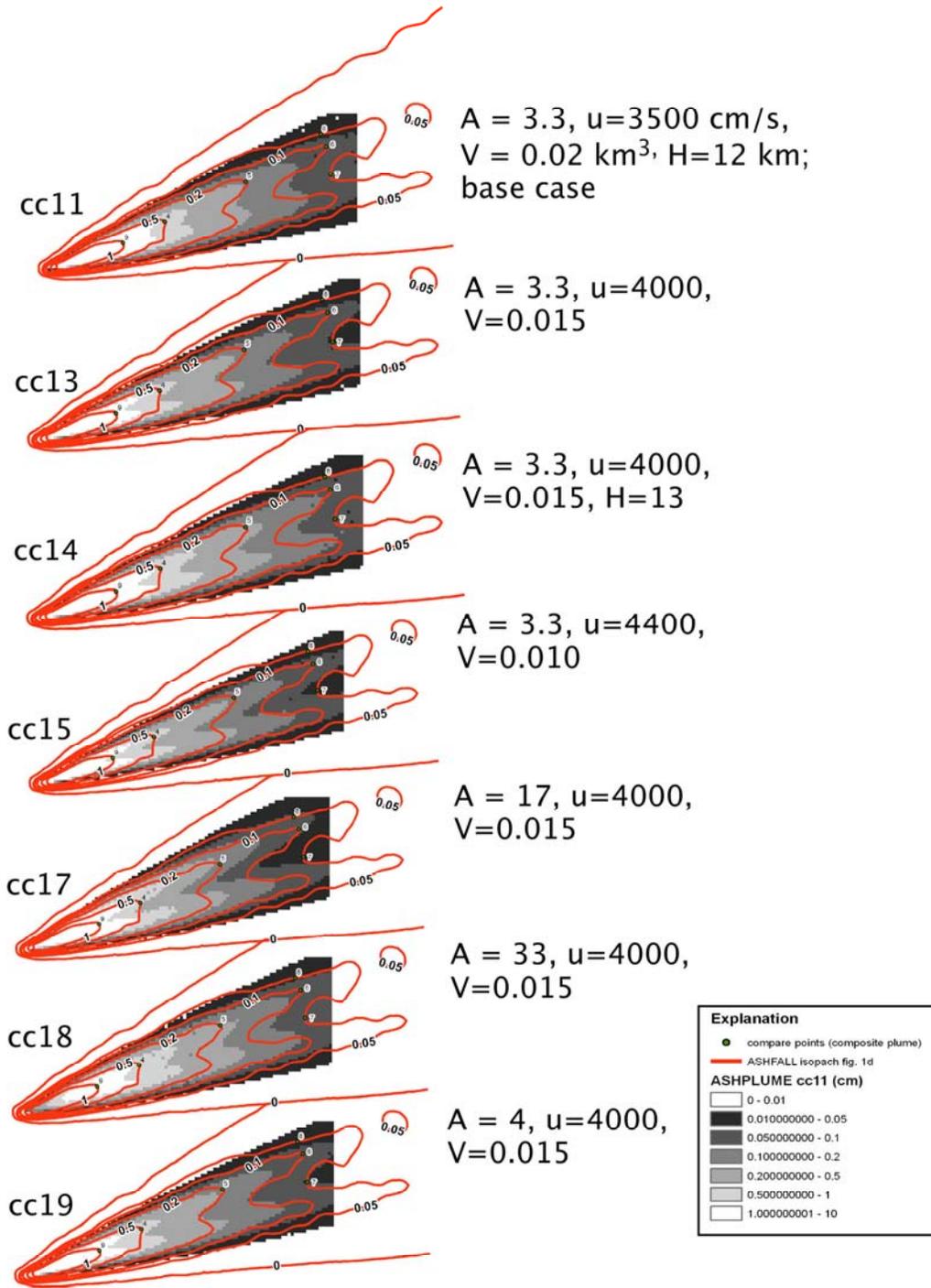
NOTE: Model run designators are given on left side of plume maps; values for parameters Suzuki constant, *A,* wind speed (*u*, cm/s), erupted volume (V, km^3), and column height (H, km) are given on the right. When not listed, parameter values are identical to base case run (cc11). See Figure J-10 for geographical context.

Figure J-12. Comparison of Selected Composite-Plume Results of ASHPLUME (grayscale) versus Results of ASHFALL (contours)

Table J-7. Difference[1] Between Tephra Thicknesses Calculated by ASHPLUME (composite plume) and ASHFALL at Selected Comparison Points

ASHPLUME Run	Comparison Point Number[2] (distance from vent, km)					
	9 (57.8)	4 (88.0)	5 (146.2)	6 (203.1)	7 (199.2)	8 (203.6)
Cc11	1.7	1.6	0.9	0.7	1.3	0.8
Cc13	1.1	1.4	0.9	0.6	1.0	0.6
Cc14	1.5	1.8	1.2	0.9	1.4	0.8
Cc15	0.9	1.3	0.9	0.7	0.8	0.6
Cc17	1.3	1.7	1.0	0.8	1.3	0.8
Cc18	1.3	1.8	1.2	0.8	1.4	0.9
Cc19	1.2	1.3	0.9	0.7	1.0	0.6
Cc22	1.3	1.2	0.7	0.4	1.0	0.6

NOTES: [1] Difference values are calculated as the quotient of results of ASHPLUME and ASHFALL; no difference = 1.0.

[2] See Figure J-10 for location of comparison points. Points 9 and 4 to 6 are located along the longitudinal axis of the plume on the 1, 0.5, 0.2, and 0.1 cm tephra isopachs, respectively; points 7 and 8 are located at the outer edges of the 0.05-cm isopach for one lobe of the tephra deposit.
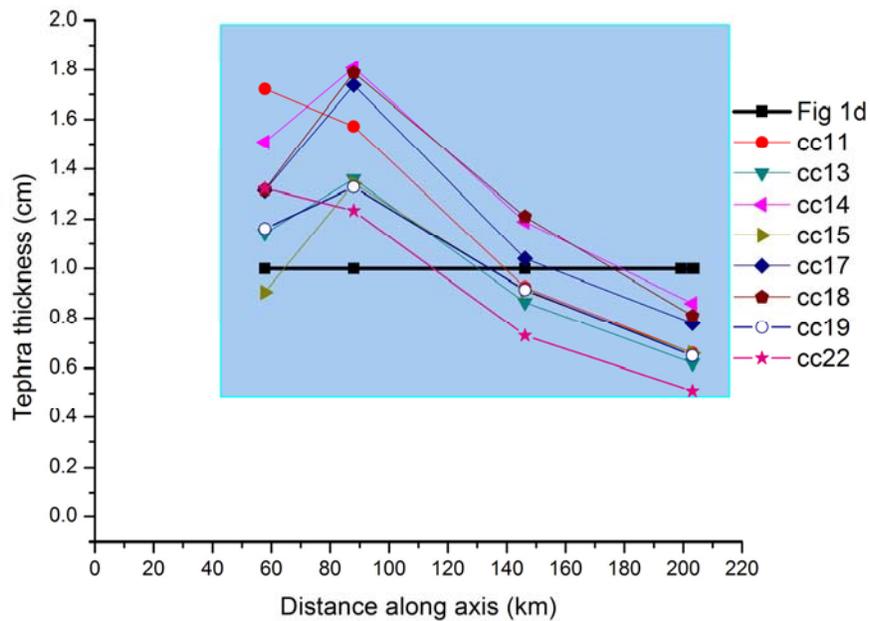
NOTE: Values are plotted at comparison points along plume centerline presented in Figure J-10. See Table J-7 for values and note on method of calculation. Shaded box denotes values within a factor of two of ASHFALL runs ("Fig 1d" line).

Figure J-13. Difference Between Tephra Thickness Estimated by ASHPLUME and ASHFALL for Composite Plume Runs

J7. SUMMARY

The ASHPLUME code was used in two sets of model runs to attempt to match published output from the ASHFALL code for constant wind conditions and a variable wind field (Hurst and Turner 1999 [DIRS 176897], Figures 1b and 1d). In both cases the results of the ASHPLUME code were similar to ASHFALL in terms of the shape and distribution of the tephra deposit. ASHPLUME input parameter values were adjusted within reasonable ranges to fine-tune the match between the two models. In both cases the best fits were obtained using base-case parameter values (those derived from direct equivalencies between the two mathematical models) with adjustment to wind speeds appropriate for the center of mass of the eruptive column and to values of the Suzuki constant to match the usage of a journal article by Hurst and Turner (1999 [DIRS 176897]).

A consistent difference occurred in the shape of the axial profiles of the results of the two models: the ASHPLUME model typically resulted in greater proximal (<80 km) tephra thickness and less distal (>140 km) deposition. The distribution of tephra from the ASHFALL model was generally wider than that of ASHPLUME, most likely due to the slight variation in wind speed and direction at the 13 altitude bins used by the former model vs. the single wind condition at the top of the eruption column used by the latter. The 25° spread in ASHFALL wind directions with elevation resulted in a slight fanning of the eruption plume.

Composite-plume tephra distributions were created from two separate ASHPLUME model runs that were identical except for varying wind direction. The distribution of tephra from this combination was compared to the results of an ASHFALL run that used a wind field that shifted in direction during the eruption. Similar to the single-plume runs, the ASHFALL tephra deposit was more diffuse than that of ASHPLUME due to the variation of wind conditions with height. ASHPLUME wind speeds for the model runs that compared most favorably to ASHFALL were slightly slower than what would be expected from the meteorological data appropriate for the altitude of greatest ash concentration in the eruptive column. This may result from the need to match ASHFALL, which transports tephra using a combination of lower wind speeds near the ground and higher speed winds that exist near the top of the eruption column.

The consistent difference in downwind tephra thickness profile shape between ASHPLUME and ASHFALL may result from a fundamental difference between the codes, perhaps as a result of differences in the way fall velocities are defined for the tephra particles. ASHPLUME calculates particle settling and deposition by the use of a mean and standard deviation for particle size, together with values for particle density, shape factor, and properties of air. In contrast, ASHFALL uses direct input of a probability distribution of particle settling velocities, which may produce a more complex tephra distribution pattern. A 60% increase in mean particle size in ASHPLUME resulted in a 10% to 50% decrease in transport (tephra thickness), but it did not change the shape of the ASHPLUME tephra profile.

The single- and composite-plume simulation exercises both provided results that were close to the results of ASHFALL, indicating that, while the exact shape of the plume was not reproduced, the overall distribution of tephra could be reproduced within a factor of two. This level of precision is consistent with acceptance criteria for other ASHPLUME model validation exercises, as defined in Section 7.3.1. As a result of this code comparison activity, it has been

demonstrated that the ASHPLUME code can use reasonable input parameter values to produce results comparable to the ASHFALL code, which uses more complex treatments of tephra particle settling velocities and variable wind conditions with height and with time.

J8.   ADDENDUM

J8.1   EMAIL CORRESPONDENCE

Below is an email received from Dr. Tony Hurst in January, 2004 which accompanied several files that provided sample inputs for the ASHFALL code (see Figures J-1 and J-2).

```
To: Gordon Keating <gkea@lanl.gov>
Subject: Re: Ash dispersal code comparison
From: "Tony Hurst" <T.Hurst@gns.cri.nz>
Date: Fri, 16 Jan 2004 09:58:19 +1300

Dear Dr Keating,

I've attached a WORD file of the report, but please don't pass it outside
your laboratory.

I can also give you the parameters of some of the models I used in the
1999 paper.  As explained in the manual each model uses a .VOL file
describing the eruption, and a WIN file describing the wind.  Because
ASHPLUME can't cope with variable winds, you really can only compare the
times when the wind was comparatively uniform over the height range and
not changing much with time.

Fig 1b was produced with the the files OCT11E.VOL and R1012F1.WIN

Fig 3b was produced with the file OCT14U.VOL and  a wind file very like
R1014F4.WIN

Fig 5b was produced with the files JUN17U7.VOL and JUN17A.VOL

The volcano positions, map boundaries etc. are all in the New Zealand Map
Grid, in metres (sometimes km) N and E.

The vertical distribution of the ash in the eruption column was given by
the Suzuki distribution, (see report), normally with a Suzuki coefficient of
4.

I hope this explains my models, you can contact me again if something
isn't clear.

I understand that your time constraints give a problem on setting up
contracting, so I am open to other suggestions of how we might work together.

Regards

Tony Hurst

Attachments Converted: Ashfall.doc, JUN17A.WIN, JUN17U7.VOL, OCT11E.VOL,
OCT14U.VOL, R1012F1.WIN, R1014F4.WIN
```

J8.2   SAMPLE ASHPLUME INPUT AND OUTPUT FILES

Below are a sample ASHPLUME input file and an abbreviated output files for the single-plume base-case run cc4a.

```
ASHPLUME v2.1 Code Comparison v. ASHFALL, run cc4anew
1                                ! iscrn, 0 = no screen output, 1 = yes
-10.    200.                     ! xmin, xmax in km
-10.    100.                     ! ymin, ymax in km
106                               ! numptsx
56                               ! numptsy
1.04  2.08                       ! ashdenmin, ashdenmax in g/cm3
-3.0    0.0                      ! ashrholow, ashrhohi
0.5                              ! fshape
0.001117  0.0001758              ! airden in g/cm3, airvis in g/cm-s
400.0                            ! c in cm2/s to the 5/2
10.0                             ! dmax in cm
0.0001  0.002  0.05              ! fdmin, fdmean, fdmax all in cm
0.001                            ! hmin in km
1.0e-30                          ! acutoff in g/cm2
0.5                        ***   ! the constant beta (unitless)
0.052                      ***   ! the mean ash particle diameter (cm)
0.602                      ***   ! sigma for the ash lognormal dist.
0.5                              ! the incorporation ratio (unitless)
0.                         ***   ! the mass of fuel to incorporate (g)
25.0                       ***   ! the wind direction- relation to due east (deg)
4200.                      ***   ! the wind speed (cm/s)
2000.                      ***   ! the initial eruption velocity (cm/s)
2.2e+12                    ***   ! the power (watts)
1.36e+04                   ***   ! the event duration (s)
0.0                              ! rmin,  minimum radius
0.0                              ! rfactor, radial grid multiplier
0                                ! nr,  number of radial divisions
0                                ! nthet, number of theta (angle) grid divisions
0                                ! numapts, number of points in histograms


ASHPLUME_DLL_LA version 2.1
*************************************************************************
     Input Parameters (From vin vector):
        Minimum x location (km)...............  -10.0000
        Maximum x location (km)...............  200.0000
        Minimum y location (km)...............  -10.0000
        Maximum y location (km)...............  100.0000
        Number of grid points in x............      106
        Number of grid points in y............       56
        Minimum ash density (g/cm^3)..........    1.0400
        Maximum ash density (g/cm^3)..........    2.0800
        Minimum particle size [log(cm)].......   -3.0000
        Maximum particle size [log(cm)].......    0.0000
        Particle shape parameter..............    0.5000
        Air density (g/cc)....................  1.1170E-03
        Air viscosity (g/cm-s)................  1.7580E-04
        Eddy diff. constant (cm^2/s^[5/2])....  400.0000
        Size cutoff (cm)......................   10.0000
        Minimum waste particle diameter (cm)..    0.0001
        Mode waste particle diameter (cm).....    0.0020
        Maximum waste particle diameter (cm)..    0.0500
        Minimum height of column (km).........    0.0010
        Lower limit for ash deposits (g/cm^2).  1.0000E-30
        Dispersion constant, beta.............    0.5000
        Mean particle diameter (cm)...........    0.0520
```

```
      Log particle standard deviation.......      0.6020
      Incorporation ratio...................      0.5000
      Total fuel mass available (g)......... 0.0000E+00
      Wind direction (deg)..................     25.0000
      Wind speed (cm/s).....................   4200.0000
      Vent exit velocity (cm/s).............   2000.0000
      Event power (w).......................  2.2000E+12
      Event duration (s)....................  1.3600E+04
      minimum radial distance (km)..........      0.0000
      radial multiplier.....................      0.0000
      number of radial points...............           0
      number of theta (angle) points........           0
      number of histogram points............           0
**********************************************************************
     Derived Parameters:
      Ash particle minimum log-diameter.....     -4.2940
      Ash particle mean log-diameter........     -1.2840
      Ash particle maximum log-diameter.....      1.7260
      Fuel particle minimum log-diameter....     -4.0000
      Fuel particle mode log-diameter.......     -2.6990
      Fuel particle maximum log-diameter....     -1.3010
      Column height (km)....................      9.9866
      Ash mass (g).......................... 4.0773E+13
**********************************************************************
     Results (To vout vector):
     Note: If more than one location is specified here, only the last
           one will be returned in vout.


      x(km)        y(km)      xash(g/cm^2)     xfuel(g/cm^2)

     -10.000     -10.000       5.7566E-20       0.0000E+00
     -10.000      -8.000       5.7600E-20       0.0000E+00
     -10.000      -6.000       5.7634E-20       0.0000E+00
     -10.000      -4.000       5.7668E-20       0.0000E+00
     -10.000      -2.000       5.7702E-20       0.0000E+00
     -10.000       0.000       5.7736E-20       0.0000E+00
     -10.000       2.000       5.7770E-20       0.0000E+00
     -10.000       4.000       5.7805E-20       0.0000E+00
     -10.000       6.000       5.7839E-20       0.0000E+00
     -10.000       8.000       5.7873E-20       0.0000E+00
     -10.000      10.000       5.7907E-20       0.0000E+00
     -10.000      12.000       5.7941E-20       0.0000E+00
     -10.000      14.000       5.7975E-20       0.0000E+00
     -10.000      16.000       5.8010E-20       0.0000E+00
     -10.000      18.000       5.8044E-20       0.0000E+00
     -10.000      20.000       5.8078E-20       0.0000E+00
     -10.000      22.000       5.8113E-20       0.0000E+00
     -10.000      24.000       5.8147E-20       0.0000E+00
     -10.000      26.000       5.8181E-20       0.0000E+00
     -10.000      28.000       5.8216E-20       0.0000E+00
     -10.000      30.000       5.8250E-20       0.0000E+00
     -10.000      32.000       5.8284E-20       0.0000E+00
     -10.000      34.000       5.8319E-20       0.0000E+00
```

J8.3   CALCULATION OF DISTRIBUTION OF VALUES OF P(Z).

Spreadsheet (top), showing Ashplume CGS terms and the P(z) distribution table and chart:

part. diam	part. dens.	shape F	Beta	Wo	Vo	Yo
0.087	1.5	0.5	0.5	2400	243.3231	4.9317

air density = 0.001734
air visosity = 0.000185

H (z)	W(z)	Y	P(z)	P(z) normalized	t (s)
10.0000	0.0000	0.0000	0.0000	0.0000	2.2827E+03
9.9500	12.0000	0.0247	0.0124	0.0065	2.2751E+03
9.9000	24.0000	0.0493	0.0242	0.0126	2.2674E+03
9.8000	48.0000	0.0986	0.0460	0.0241	2.2521E+03
9.7000	72.0000	0.1480	0.0657	0.0344	2.2366E+03
9.4000	144.0000	0.2959	0.1134	0.0593	2.1895E+03
9.2000	192.0000	0.3945	0.1370	0.0716	2.1576E+03
9.0000	240.0000	0.4932	0.1552	0.0811	2.1252E+03
8.5000	360.0000	0.7398	0.1819	0.0951	2.0424E+03
8.0000	480.0000	0.9863	0.1895	0.0991	1.9566E+03
7.5000	600.0000	1.2329	0.1851	0.0968	1.8678E+03
7.0000	720.0000	1.4795	0.1736	0.0908	1.7758E+03
6.5000	840.0000	1.7261	0.1583	0.0828	1.6805E+03
6.0000	960.0000	1.9727	0.1414	0.0739	1.5817E+03
5.0000	1200.0000	2.4659	0.1079	0.0564	1.3729E+03
4.0000	1440.0000	2.9590	0.0791	0.0413	1.1478E+03
3.0000	1680.0000	3.4522	0.0563	0.0295	9.0427E+02
2.0000	1920.0000	3.9454	0.0393	0.0206	6.3897E+02
1.0000	2160.0000	4.4385	0.0270	0.0141	3.4602E+02
0.1000	2376.0000	4.8824	0.0191	0.0100	4.2106E+01
			1.9125		

$$Y = \frac{\beta W(z)}{V_0}$$

$$t = 0.752 \times 10^6 \left[\frac{1 - e^{-0.0625z}}{V_0} \right]^{0.926}$$

$$Yo = \frac{\beta W_0}{V_0}$$

$$W(z) = W_0 \left(1 - \frac{z}{H} \right)$$

$$p(z) = \frac{\beta W_0 Y e^{-Y}}{V_0 H \left\{ 1 - (1 + Y_0) e^{-Y_0} \right\}}$$

$$V_0 = \frac{\psi_p g_c d^2}{9\eta_a F^{-0.32} + \sqrt{81\eta_a^2 F^{-0.64} + \frac{3}{2}\psi_p \psi_a g_c d^3 \sqrt{1.07 - F}}}$$

Spreadsheet (center), formulas for calculating columns A–G:

part. diam	part. dens.	shape F	Beta	Wo	Vo
0.087	1.5	0.5	0.5	2000	=$B$4*980*($A$4^2)/((9*$B$10*$C$4^-0.32)+SQRT(81*$B$10^2*$C$4^-0.64+1.5*$B$4*$B$9*980*$A$4^3*SQRT(1.07-$C$4)))

air density 0.001117
air visosity 0.0001758

Spreadsheet (bottom), formulas for calculating columns H to N:

Yo	H (z)	W(z)	Y	P(z)	P(z) normalized	t (s)
=$D$4*$E$4/$G$4	10	=($E$4)*(1-($I4/$I$4))	=$D$4*$J4/$G$4	=$D$4*$E$4*$K4*EXP(-$K4)/($G$4*$I$4*(1-(1+$H$4)*EXP(-$H$4)))	=$L4/$L$24	=752000*((1-EXP(-0.0625*$I4))/$G$4)^0.926
	9.95	=($E$4)*(1-($I5/$I$4))	=$D$4*$J5/$G$4	=$D$4*$E$4*$K5*EXP(-$K5)/($G$4*$I$4*(1-(1+$H$4)*EXP(-$H$4)))	=$L5/$L$24	=752000*((1-EXP(-0.0625*$I5))/$G$4)^0.926
	9.9	=($E$4)*(1-($I6/$I$4))	=$D$4*$J6/$G$4	=$D$4*$E$4*$K6*EXP(-$K6)/($G$4*$I$4*(1-(1+$H$4)*EXP(-$H$4)))	=$L6/$L$24	=752000*((1-EXP(-0.0625*$I6))/$G$4)^0.926
	9.8	=($E$4)*(1-($I7/$I$4))	=$D$4*$J7/$G$4	=$D$4*$E$4*$K7*EXP(-$K7)/($G$4*$I$4*(1-(1+$H$4)*EXP(-$H$4)))	=$L7/$L$24	=752000*((1-EXP(-0.0625*$I7))/$G$4)^0.926
	9.7	=($E$4)*(1-($I8/$I$4))	=$D$4*$J8/$G$4	=$D$4*$E$4*$K8*EXP(-$K8)/($G$4*$I$4*(1-(1+$H$4)*EXP(-$H$4)))	=$L8/$L$24	=752000*((1-EXP(-0.0625*$I8))/$G$4)^0.926
	9.4	=($E$4)*(1-($I9/$I$4))	=$D$4*$J9/$G$4	=$D$4*$E$4*$K9*EXP(-$K9)/($G$4*$I$4*(1-(1+$H$4)*EXP(-$H$4)))	=$L9/$L$24	=752000*((1-EXP(-0.0625*$I9))/$G$4)^0.926
	9.2	=($E$4)*(1-($I10/$I$4))	=$D$4*$J10/$G$4	=$D$4*$E$4*$K10*EXP(-$K10)/($G$4*$I$4*(1-(1+$H$4)*EXP(-$H$4)))	=$L10/$L$24	=752000*((1-EXP(-0.0625*$I10))/$G$4)^0.926
	9	=($E$4)*(1-($I11/$I$4))	=$D$4*$J11/$G$4	=$D$4*$E$4*$K11*EXP(-$K11)/($G$4*$I$4*(1-(1+$H$4)*EXP(-$H$4)))	=$L11/$L$24	=752000*((1-EXP(-0.0625*$I11))/$G$4)^0.926
	8.5	=($E$4)*(1-($I12/$I$4))	=$D$4*$J12/$G$4	=$D$4*$E$4*$K12*EXP(-$K12)/($G$4*$I$4*(1-(1+$H$4)*EXP(-$H$4)))	=$L12/$L$24	=752000*((1-EXP(-0.0625*$I12))/$G$4)^0.926
	8	=($E$4)*(1-($I13/$I$4))	=$D$4*$J13/$G$4	=$D$4*$E$4*$K13*EXP(-$K13)/($G$4*$I$4*(1-(1+$H$4)*EXP(-$H$4)))	=$L13/$L$24	=752000*((1-EXP(-0.0625*$I13))/$G$4)^0.926
	7.5	=($E$4)*(1-($I14/$I$4))	=$D$4*$J14/$G$4	=$D$4*$E$4*$K14*EXP(-$K14)/($G$4*$I$4*(1-(1+$H$4)*EXP(-$H$4)))	=$L14/$L$24	=752000*((1-EXP(-0.0625*$I14))/$G$4)^0.926
	7	=($E$4)*(1-($I15/$I$4))	=$D$4*$J15/$G$4	=$D$4*$E$4*$K15*EXP(-$K15)/($G$4*$I$4*(1-(1+$H$4)*EXP(-$H$4)))	=$L15/$L$24	=752000*((1-EXP(-0.0625*$I15))/$G$4)^0.926
	6.5	=($E$4)*(1-($I16/$I$4))	=$D$4*$J16/$G$4	=$D$4*$E$4*$K16*EXP(-$K16)/($G$4*$I$4*(1-(1+$H$4)*EXP(-$H$4)))	=$L16/$L$24	=752000*((1-EXP(-0.0625*$I16))/$G$4)^0.926
	6	=($E$4)*(1-($I17/$I$4))	=$D$4*$J17/$G$4	=$D$4*$E$4*$K17*EXP(-$K17)/($G$4*$I$4*(1-(1+$H$4)*EXP(-$H$4)))	=$L17/$L$24	=752000*((1-EXP(-0.0625*$I17))/$G$4)^0.926
	5	=($E$4)*(1-($I18/$I$4))	=$D$4*$J18/$G$4	=$D$4*$E$4*$K18*EXP(-$K18)/($G$4*$I$4*(1-(1+$H$4)*EXP(-$H$4)))	=$L18/$L$24	=752000*((1-EXP(-0.0625*$I18))/$G$4)^0.926
	4	=($E$4)*(1-($I19/$I$4))	=$D$4*$J19/$G$4	=$D$4*$E$4*$K19*EXP(-$K19)/($G$4*$I$4*(1-(1+$H$4)*EXP(-$H$4)))	=$L19/$L$24	=752000*((1-EXP(-0.0625*$I19))/$G$4)^0.926
	3	=($E$4)*(1-($I20/$I$4))	=$D$4*$J20/$G$4	=$D$4*$E$4*$K20*EXP(-$K20)/($G$4*$I$4*(1-(1+$H$4)*EXP(-$H$4)))	=$L20/$L$24	=752000*((1-EXP(-0.0625*$I20))/$G$4)^0.926
	2	=($E$4)*(1-($I21/$I$4))	=$D$4*$J21/$G$4	=$D$4*$E$4*$K21*EXP(-$K21)/($G$4*$I$4*(1-(1+$H$4)*EXP(-$H$4)))	=$L21/$L$24	=752000*((1-EXP(-0.0625*$I21))/$G$4)^0.926
	1	=($E$4)*(1-($I22/$I$4))	=$D$4*$J22/$G$4	=$D$4*$E$4*$K22*EXP(-$K22)/($G$4*$I$4*(1-(1+$H$4)*EXP(-$H$4)))	=$L22/$L$24	=752000*((1-EXP(-0.0625*$I22))/$G$4)^0.926
	0.1	=($E$4)*(1-($I23/$I$4))	=$D$4*$J23/$G$4	=$D$4*$E$4*$K23*EXP(-$K23)/($G$4*$I$4*(1-(1+$H$4)*EXP(-$H$4)))	=$L23/$L$24	=752000*((1-EXP(-0.0625*$I23))/$G$4)^0.926
		=SUM(L4:L23)				

NOTE: This spreadsheet was used to produce Figure J- 6 for typical values used in ASHPLUME model runs. Top: spreadsheet; Center: formulas for calculating columns A-G; Bottom: formulas for calculating columns H to N.

Figure J-14. Spreadsheet Used to Calculate the Distribution of Values of P(z) with Height

INTENTIONALLY LEFT BLANK

APPENDIX K
INVESTIGATION OF SENSITIVITY OF COUPLED ASHPLUME-FAR MODELS

APPENDIX K
INVESTIGATION OF SENSITIVITY OF COUPLED
ASHPLUME-FAR MODELS

K1.   INTRODUCTION

ASHPLUME_DLL_LA V.2.1 [DIRS 178870] simulates the dispersal of volcanic tephra and incorporated waste by assuming that volcanic activity during an eruption is consistently energetic (violent Strombolian), with constant eruptive power for the duration of the eruption. According to the algorithm used in the code, this translates into a constant eruption column height (Section 6.5.1).   Additionally, ASHPLUME calculates advective transport utilizing a single value each for wind speed and direction, which remain constant during the eruption. These values are assigned based on conditions at the maximum column height. These code limitations have recently been set aside in other tephra dispersal models that utilize time- and altitude-dependent wind conditions or unsteady column height (Section 6.5.4). However, given that the ASHPLUME code is coupled to the tephra redistribution model (FAR; SNL 2007 [DIRS 179347]), the effects of these code limitations on the tephra/waste concentration at the RMEI location after atmospheric dispersal and fluvial redistribution are not obvious.   This appendix describes an analysis of the effects of 1) unsteady column height, and 2) variable wind conditions on the concentration of waste-containing tephra in sediment at the outlet of Fortymile Wash (or "Fortymile Wash fan apex"), prior to distribution to the RMEI location and subsequent soil migration. The observed effects of variations in these individual eruption parameters are placed in context of effects due to variations in terrain within the watershed.

Eruptive facies in the Quaternary volcanoes in the Yucca Mountain region indicate that explosive eruptions include substantial components of the violent Strombolian style, consisting of sustained eruption columns of well-fragmented basaltic clasts rising up to several km altitude (SNL 2007 [DIRS 174260], Section 6.3.1).   From a risk assessment perspective (within the regulatory time frame) these eruptions are most important because they could disperse contaminated fallout tephra over areas of 10s of km^2. Such tephra could impact the control population by either: 1) direct deposition by fallout under certain wind and eruption conditions, 2) deposition upstream in the Fortymile Wash drainage basin and subsequent transport to the control population by surficial processes, or 3) a combination of both (Figure K-1). Given the dominant southwesterly winds in the Yucca Mountain region in the 1 to 13 km altitude range (Appendix D), the dominant direction for a wind-driven eruptive plume is to the northeast. Therefore, the risk due to redistribution of waste-contaminated tephra across the landscape by fluvial processes should be evaluated relative to the risk from primary fallout of waste-contaminated tephra on the RMEI location.
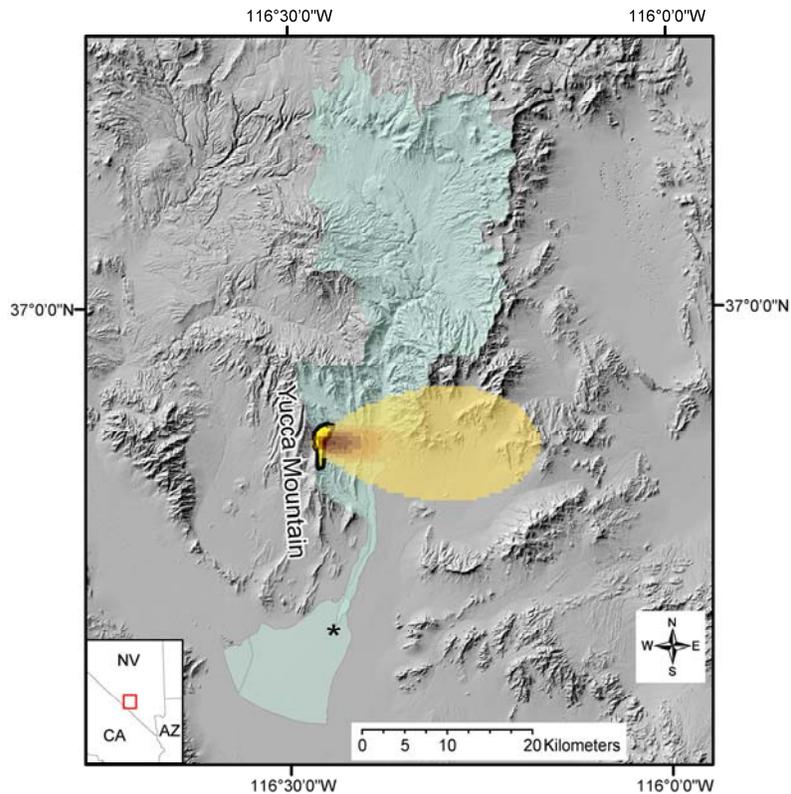
Source: DTN: MO0605SPAFORTY.000 [DIRS 179527] (Fortymile wash watershed).

NOTE: The map includes the proposed high-level nuclear waste repository (yellow), Fortymile Wash watershed (light blue), the approximate location of the RMEI (*), and a typical ASHPLUME tephra distribution (yellow-brown; >1 mm depth). For illustration purposes only.

Figure K-1. Schematic Illustration of Sample Tephra Deposit in Relation to the Fortymile Wash Watershed

K2.   ASHPLUME AND FAR MODELS

The coupled component models for these processes use ASHPLUME_DLL_LA V2.1 [DIRS 178870] and FAR V1.2 (2007 [DIRS 182225]), respectively. The output from ASHPLUME, a two-dimensional distribution of waste-contaminated tephra, provides the initial conditions for FAR, a scour-dilution-mixing model (SNL 2007 [DIRS 179347]). FAR calculates the fluvial (bedload) transport of tephra that is mobilized from steep hillslopes and deposited on active channels, and then routed through the drainage system to the RMEI area, located in the upper areas of the Fortymile Wash alluvial fan. Areal concentrations of tephra and waste (g/cm^2) are passed from FAR to the final TSPA component model, which converts these mass concentrations to activity concentrations and uses BDCFs to calculate radiological dose to the RMEI for each Monte Carlo model realization.

K3. ANALYSIS

The tephra deposit calculated by ASHPLUME is filtered by the underlying landscape within the coupled tephra redistribution model, FAR. The FAR model uses a digital elevation model (DEM) of the terrain in Fortymile Wash watershed to determine contributing areas for streams and slopes greater than a threshold value, from which tephra is mobilized. The tephra blanket from ASHPLUME is processed in FAR to exclude tephra deposited outside the watershed and to accumulate the tephra mass that was deposited on steep slopes and in active channels. This bedload-transported tephra is mixed with sediment to the scour depth and routed through channels to the apex of the alluvial fan. This tephra concentration in channel sediment is determined by contributing area and scour depth and defines initial concentrations within active alluvial channels in the RMEI area for the purposes of calculating migration of tephra and waste within the soil column (SNL 2007 [DIRS 179347], Section 6.2.2).

Parameter values that produce a representative eruption for the Yucca Mountain region are based on values presented in Table 8-2. Midrange values were chosen for parameters that are defined by stochastic ranges. An example ASHPLUME input file for the "base-case" model run (run W1) is included at the end of this appendix. Parameters that varied from run to run (e.g., eruptive power, duration, wind speed, and wind direction) are listed in Table K-1. Input and output files for the ASHPLUME and FAR codes are included in validation DTN: LA0708GK150308.001.

Output files from ASHPLUME_DLL_LA V2.1 [DIRS 178870] runs provided input to FAR V1.2 (2007 [DIRS 182225]). Results from FAR were postprocessed via two scientific visualization software packages. Initial visualization was performed using Tecplot 360, in which the large (22 Mb) concentration grids for the Fortymile Wash watershed were inverted (to change the origin to the lower left corner for subsequent plotting) and trimmed to remove the upper half of the watershed (for smaller file size that focused on the area between Yucca Mountain and the Fortymile Wash outlet). Subsequently these revised grids were imported into Origin Pro V7.5 for analysis and visualization. The tephra concentration in sediment at the outlet of Fortymile Wash was compared by recording the maximum value in grid cells with coordinates x = 283, 284, or 285, and y = 0. (The origin for these transformed grids is in the lower left corner.)

For a typical eruption plume (e.g., run W1), the east-directed, base-case 0.035 km^3 tephra deposit results in a tephra concentration (fraction of tephra) of 0.062 in the stream sediment at the fan apex (Figure K-2).
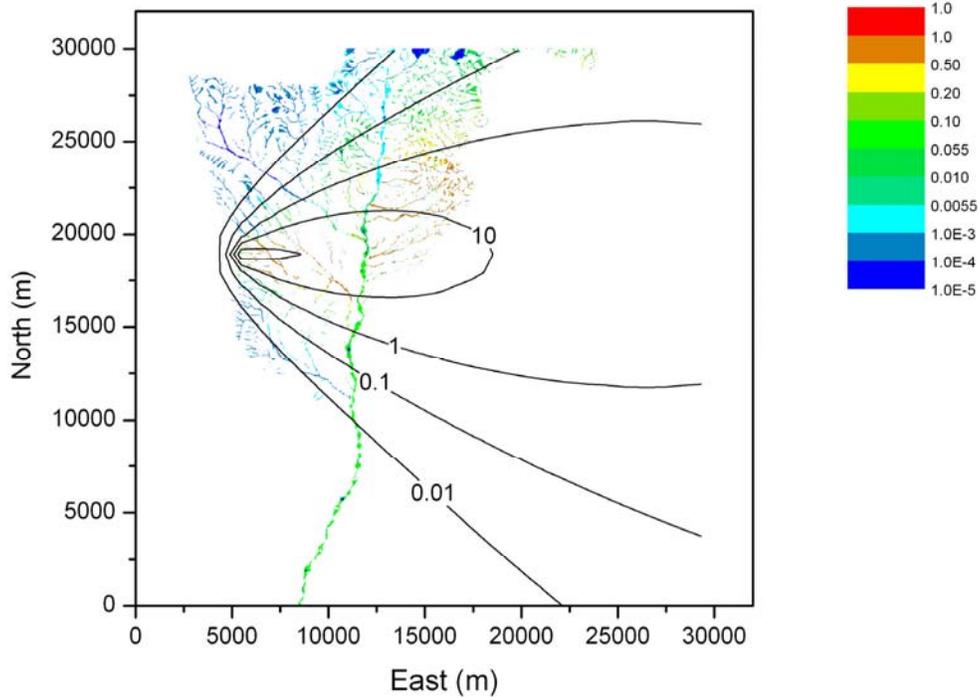
NOTE: Isopach contours are 0.01, 0.1, 1.0, 10, and 100 cm. Background colors represent tephra concentration (fraction of tephra) in stream channel sediment. The point of the comparison of tephra concentrations in sediment at the outlet of Fortymile Wash is located at the bottom of the plot, at approximately 7,500 m east and 0 m north. In this Base Case (run W1), the concentration of tephra in channel sediment is 0.062.

Figure K-2. Tephra Isopachs (cm) for the Base-Case Eruption Modeled by ASHPLUME Overlaid on Results of FAR Tephra Redistribution Model Results

The effect of variable column height during an eruption was assessed by dividing the base-case eruption volume among three small eruptions, each with constant wind direction but variable power, column height, wind speed, and duration (runs H2, H3; Table K-1, Figure K-3). The sets of small-volume model runs were combined to form composite tephra sheets for comparison to other model cases. The results were very close to the instantaneous, constant-column-height base case (W1), despite varying the component eruption volume by an order of magnitude, the column height by a factor of 2, and the wind speed by 30%. After routing through FAR, the tephra concentrations in sediment at the outlet of Fortymile Wash were within 15% of the base case (Table K-1).

Table K-1. Summary of ASHPLUME Model Runs to Evaluate the Effect of Constant Column Height and Variable Wind Conditions on Concentration of Tephra in Sediment at the Outlet of Fortymile Wash

ASHPLUME Run Number	Representative Input Values					Composite Model Run Characteristics	Fraction of Tephra in Sediment at Wash Outlet	Concentration Change vs. Base Case
	Volume (km³)	Duration (days)	Power (W)	Column Height (km)	Wind Speed (m/s)			
Base Case (W1)	0.035	1.5	2.7×10^{11}	5.9	7	—	0.062	—
H2	0.002	1	2.5×10^{10}	3.3	5	Variable column height	0.058	0.94
	0.010	1	1.3×10^{11}	4.9	6.5			
	0.023	1	2.9×10^{11}	6.0	9			
H3	0.023	10	2.5×10^{10}	3.3	5	Variable column height	0.071	1.15
	0.010	1	1.3×10^{11}	4.9	6.5			
	0.002	0.1	2.9×10^{11}	6.0	9			
W4[†]	0.012	1	1.5×10^{11}	5.1	7	30° wind direction spread	0.063	1.02
W3[†]	0.012	1	1.5×10^{11}	5.1	7	60° spread	0.065	1.05
W5[†]	0.012	1	1.5×10^{11}	5.1	7	90° spread	0.051	0.82
W6[‡]	0.0175	1	2.2×10^{11}	5.6	7	90° wind direction divergence	0.139	2.24
W7[‡]	0.0175	1	2.2×10^{11}	5.6	7	120° divergence	0.125	2.02
W8[‡]	0.0175	1	2.2×10^{11}	5.6	7	150° divergence	0.078	1.26
W9[‡]	0.0175	1	2.2×10^{11}	5.6	7	180° divergence	0.034	0.55
W1N[*]	0.035	1.5	2.7×10^{11}	5.9	7	90° N rotation[§]	0.045	0.73
W1N30E[*]	0.035	1.5	2.7×10^{11}	5.9	7	60° N rotation[§]	0.160	2.58
W1N60E[*]	0.035	1.5	2.7×10^{11}	5.9	7	30° N rotation[§]	0.114	1.84
W1S60E[*]	0.035	1.5	2.7×10^{11}	5.9	7	30° S rotation[§]	0.057	0.92
W1S30E[*]	0.035	1.5	2.7×10^{11}	5.9	7	60° S rotation[§]	0.055	0.89
W1S[*]	0.035	1.5	2.7×10^{11}	5.9	7	90° S rotation[§]	0.012	0.19

† Runs W3, W4, W5 included three individual model runs with identical input parameter values except wind direction.

‡ Runs W6, W7, W8, W9 included two individual model runs with identical input parameter values except wind direction.

* Base case, single-eruption plume rotated across the landscape in 30° increments.

§Angles of rotation are relative to due east.

The effect of variation in wind direction during an eruption was assessed in two separate cases: 1) *spread*, caused by minor variations in wind direction throughout an eruption, and 2) *divergence*, caused by two distinct wind directions during the eruptive period. Sets of three small component eruptions simulated varying wind direction (spread) over 30°, 60°, and 90° compared to the base-case, east-directed run (Figure K-3, Table K-1). The concentrations of tephra in sediment at the watershed outlet resulting from mobilization of these tephra sheets were normalized vs. the base case value. As the degree of spread in the plume increased from due east toward the southeast quadrant, the outlet concentration increased slightly as a greater proportion of the tephra fell in the active channel area just upstream of the watershed outlet; however, at 90° spread the concentration dropped off, as a significant portion of the tephra was deposited due south, outside the Fortymile Wash watershed (Figures K-1 and K-4a). Bi-lobate composite tephra sheets resulted from sets of two small eruptions used to evaluate the effect of diverging wind directions during eruption (Table K-1, Figure K-3). The effect of divergence in wind direction was assessed for 90°, 120°, 150°, and 180° separation (Figure K-4b). The local maximum in normalized tephra concentration at 90° divergence indicates that this is an optimal plume orientation for depositing tephra on steep slopes and active channels, with one lobe directed into the heart of the watershed to the northeast and one onto the large active channel to the southeast. The normalized tephra concentration decreases with increasing divergence of the plume, so that by 180° much of the tephra is deposited outside the watershed.
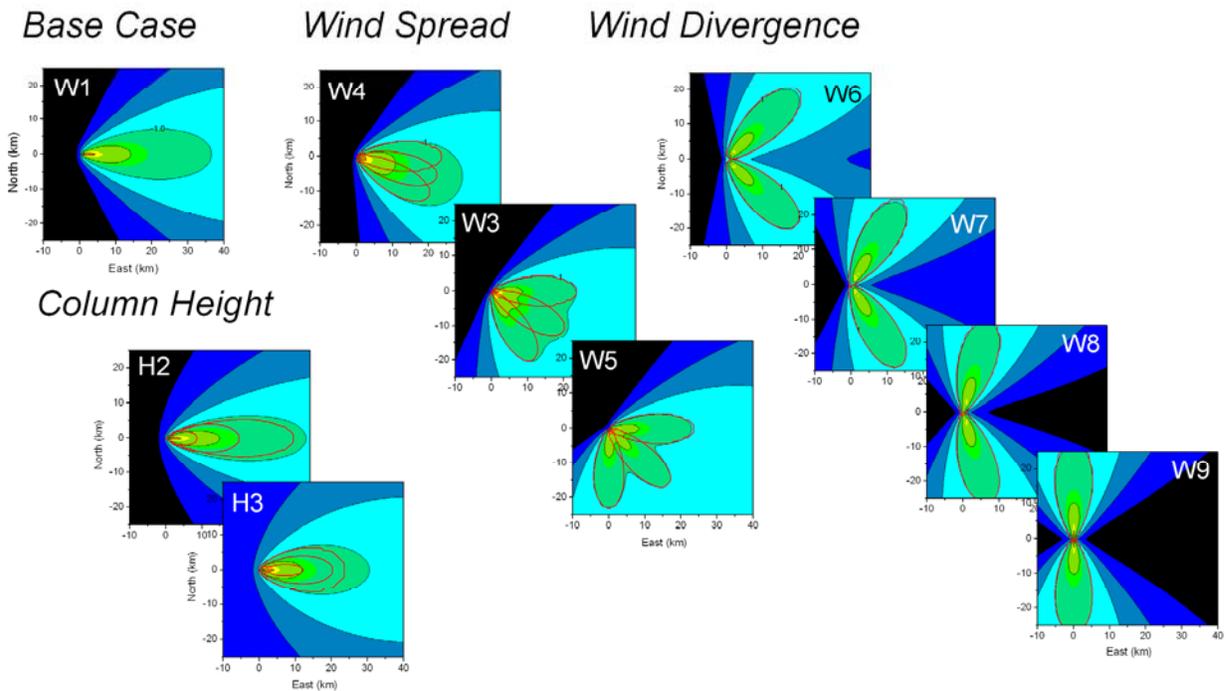
NOTE: Model results showing column height variation and wind spread and divergence are compared to the base-case simple plume (upper left). Red outlines denote the 1-cm isopach for the component tephra sheets. Contour spacing (black lines) is logarithmic: 0.001, 0.01, 0.1, 1, 10, and 100 cm.

Figure K-3. Composite Tephra Sheets Produced by Column Height Variation and Wind Spread and Divergence during Eruption
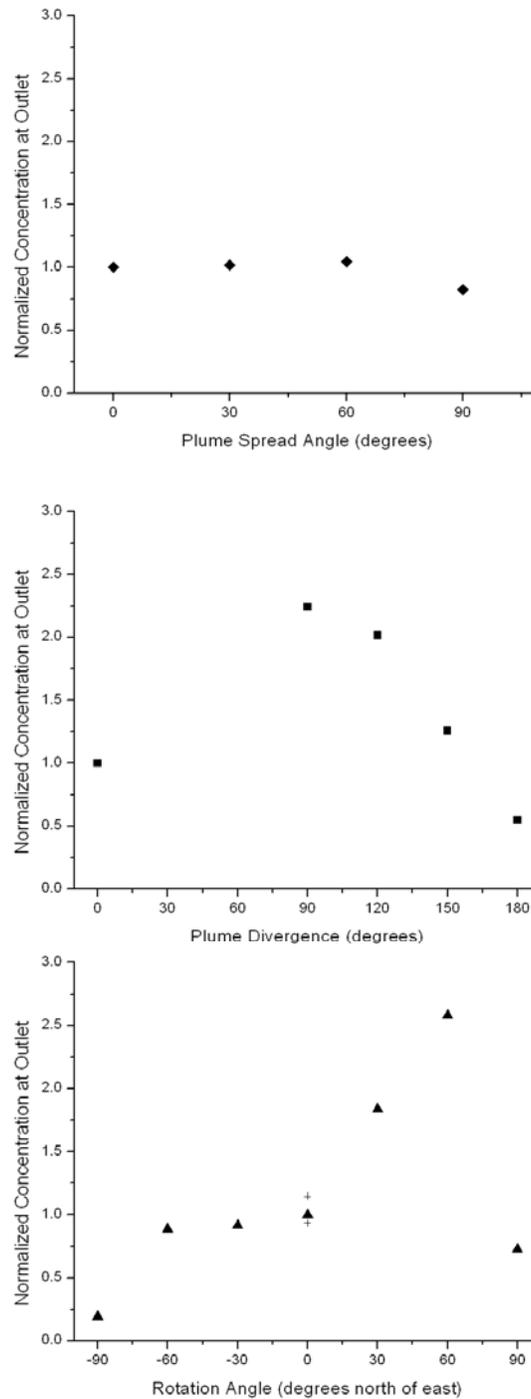
NOTE: Plots illustrate effects of variation in wind during an eruption that produces A) spread in the tephra sheet, B) divergence of tephra sheet lobes, and C) rotation of the plume through the range of likely downwind direction. Variation due to unsteady column height denoted by (+). Concentrations are normalized to the base-case value of a simple plume directed due east (Figure K-3).

Figure K-4. Summary Plot of Tephra Concentration Variation in Sediment at the Outlet of Fortymile Wash Due to Variation in Column Height and Wind Direction

These studies indicate that the geometry and terrain of a watershed play a significant role in the outcome of the coupled tephra dispersal—redistribution model system. In order to investigate the control of watershed geometry and terrain alone, the base-case tephra plume was rotated over the landscape in 30° increments from north to south and then the resulting tephra sheet was routed through the FAR model. This 180° band captures 95% of the wind directions for the 3- to 13-km altitude (see wind rose diagrams in DTN: MO0408SPADRWSD.002). The effect of the simple change in azimuth for the base-case plume (constant column height, constant wind conditions) is greater than the effects from the other, more complex variations (Figure K-4c). As the plume is rotated from east to south, the normalized tephra concentration at the watershed outlet decreases as the tephra deposits fall increasingly on gentle slopes or outside the watershed. As in the *spread* and *divergence* cases, the increase in azimuth north of east produces initial increases in transported tephra concentration as more of the tephra mass is deposited in the center of the watershed. With a due north azimuth, however, much of the tephra mass is deposited outside the watershed or experiences increased dilution due to its long travel times in the channels.

K4. SUMMARY

Unsteady eruption column height simulated in a series of ASHPLUME model runs produced only slight change in the distribution of tephra deposited in the Fortymile Wash watershed. The aspect ratio for the composite tephra sheet changed by $\pm20\%$ versus the simple diffusive plume base case. When the composite tephra mass from these variable column height eruptions was routed through the FAR sediment-transport model, the concentration of tephra in sediment at the outlet of Fortymile Wash varied by $\pm15\%$ or less compared to the base case. The effect of wind variation during an eruption (spread or divergence of the eruptive plume) produced a maximum increase in sediment tephra concentration 2.24 times that of the base case. The variation in amount of tephra mobilized off steep slopes and through active channels varied non-monotonically with azimuth in these studies, suggesting that factors other than unsteady eruption or variable wind conditions were controlling tephra remobilization efficiency.

The controlling effect of watershed geometry and terrain was identified in an exercise in which the simple single-eruption, constant-wind tephra sheet was rotated in 30° increments within an 180° azimuthal band downwind of the vent area. Notably, the span of tephra concentrations in sediment at the Fortymile watershed outlet calculated for the simple azimuthal rotation case (0.2 to 2.6 times the base case) encompasses all variation resulting from the more complex eruptive cases involving variation in column height and wind conditions during an eruption (Table K-1, Figure K-4).

The significance of this variation in tephra sediment concentration at the watershed outlet is determined by considering the overall uncertainty of the system of component models. The overall tephra concentration varied by less than a factor of three in these studies. In contrast, the uncertainty is much higher in other risk parameters used to develop the inputs to the Ashplume model; for instance, the range of likely values for eruptive conduit size (which directly determines the quantity of radioactive waste entrained into the eruption), eruptive volume, and eruption duration range over one to two orders of magnitude (SNL 2007 [DIRS 174260], Table 7-1). Monte Carlo modeling techniques (e.g., those used in TSPA) are necessary to capture the range in uncertainty of model inputs derived from these data. Therefore, from a

tephra dispersal and deposition modeling perspective, variations in tephra concentration at the Fortymile Wash outlet due to unsteady eruption or variable winds during an eruption are not significant in the context of the uncertainty in other eruption parameters.

Despite its simplification relative to recent tephra dispersal models, we consider the Ashplume model to be adequate for its intended purpose within the YMP TSPA risk assessment framework. The analysis of risk due to tephra remobilization is highly dependent on the nature of the specific geometry and terrain in the study area, and these effects outweigh sensitivities to eruption parameters in the coupled-model risk assessment. The use of more sophisticated tephra dispersal models that incorporate more complex physics would arguably not provide a more meaningful result once the details of the tephra thickness distributions on the landscape had been diffused by the tephra redistribution model.

Example ASHPLUME_DLL_LA V.2.1 input file (run W1):

```
ASHPLUME v2.1 Sensitivity Analysis: w1new
1                                  ! iscrn, 0 = no screen output, 1 = yes
-10    40                          ! xmin, xmax in km
-25    25                          ! ymin, ymax in km
51                                 ! numptsx
51                                 ! numptsy
1.04    2.08                       ! ashdenmin, ashdenmax in g/cm3
-3.0    0.0                        ! ashrholow, ashrhohi
0.5                                ! fshape
0.001134  0.000185                 ! airden in g/cm3, airvis in g/cm-s
400.0                              ! c in cm2/s to the 5/2
10.0                               ! dmax in cm
0.0001  0.0013  0.20               ! fdmin, fdmean, fdmax all in cm
0.001                              ! hmin in km
1.0e-10                            ! acutoff in g/cm2
0.3                        ***     ! the constant beta (unitless)
0.0100                     ***     ! the mean ash particle diameter (cm)
0.602                      ***     ! sigma for the ash lognormal dist.
0.0                                ! the incorporation ratio (unitless)
4.01E+07                   ***     ! the mass of fuel to incorporate (g)
0.0                        ***     ! the wind direction- relation to due east (deg)
713.                       ***     ! the wind speed (cm/s)
10.1540                    ***     ! the initial eruption velocity (cm/s)
2.715e+11                  ***     ! the power (watts)
1.3048e+05                 ***     ! the event duration (s)  (3 days)
0.0                                ! rmin,  minimum radius
0.0                                ! rfactor, radial grid multiplier
0                                  ! nr,  number of radial divisions
0                                  ! nthet, number of theta (angle) grid divisions
0                                  ! numapts, number of points in histograms


*** Parameters sampled in TSPA model
```

Example ASHPLUME_DLL_LA V.2.1 output file (run W1), partial listing:

```
ASHPLUME_DLL_LA version 2.1
************************************************************************
      Input Parameters (From vin vector):
          Minimum x location (km)...............  -10.0000
          Maximum x location (km)...............   40.0000
          Minimum y location (km)...............  -25.0000
          Maximum y location (km)...............   25.0000
          Number of grid points in x...........         51
          Number of grid points in y...........         51
          Minimum ash density (g/cm^3)..........    1.0400
          Maximum ash density (g/cm^3)..........    2.0800
          Minimum particle size [log(cm)].......   -3.0000
          Maximum particle size [log(cm)].......    0.0000
          Particle shape parameter..............    0.5000
          Air density (g/cc)....................  1.1340E-03
          Air viscosity (g/cm-s)................  1.8500E-04
          Eddy diff. constant (cm^2/s^[5/2])....   400.0000
          Size cutoff (cm)......................    10.0000
          Minimum waste particle diameter (cm)..     0.0001
          Mode waste particle diameter (cm).....     0.0013
          Maximum waste particle diameter (cm)..     0.2000
          Minimum height of column (km).........     0.0010
          Lower limit for ash deposits (g/cm^2).  1.0000E-10
          Dispersion constant, beta.............     0.3000
```

```
        Mean particle diameter (cm)...........       0.0100
        Log particle standard deviation.......       0.6020
        Incorporation ratio...................       0.0000
        Total fuel mass available (g)........ 4.0100E+07
        Wind direction (deg).................       0.0000
        Wind speed (cm/s)....................     713.0000
        Vent exit velocity (cm/s)............      10.1540
        Event power (w)...................... 2.7150E+11
        Event duration (s)................... 1.3048E+05
        minimum radial distance (km).........       0.0000
        radial multiplier....................       0.0000
        number of radial points..............            0
        number of theta (angle) points.......            0
        number of histogram points...........            0
**********************************************************************
    Derived Parameters:
        Ash particle minimum log-diameter.....      -5.0100
        Ash particle mean log-diameter........      -2.0000
        Ash particle maximum log-diameter.....       1.0100
        Fuel particle minimum log-diameter....      -4.0000
        Fuel particle mode log-diameter.......      -2.8861
        Fuel particle maximum log-diameter....      -0.6990
        Column height (km)...................       5.9191
        Ash mass (g)......................... 4.8275E+13
**********************************************************************
    Results (To vout vector):
    Note: If more than one location is specified here, only the last
          one will be returned in vout.


      x(km)        y(km)       xash(g/cm^2)      xfuel(g/cm^2)

    -10.000      -25.000        1.6410E-04         7.7365E-11
    -10.000      -24.000        1.6544E-04         7.8121E-11
    -10.000      -23.000        1.6676E-04         7.8871E-11
    -10.000      -22.000        1.6806E-04         7.9614E-11
    -10.000      -21.000        1.6934E-04         8.0344E-11
    -10.000      -20.000        1.7061E-04         8.1068E-11
    -10.000      -19.000        1.7185E-04         8.1779E-11
    -10.000      -18.000        1.7306E-04         8.2475E-11
    -10.000      -17.000        1.7423E-04         8.3156E-11
    -10.000      -16.000        1.7537E-04         8.3856E-11
    -10.000      -15.000        1.7647E-04         8.4497E-11
    -10.000      -14.000        1.7753E-04         8.5114E-11
    -10.000      -13.000        1.7854E-04         8.5705E-11
    -10.000      -12.000        1.7950E-04         8.6267E-11
    -10.000      -11.000        1.8040E-04         8.6787E-11
    -10.000      -10.000        1.8125E-04         8.7283E-11
    -10.000       -9.000        1.8203E-04         8.7743E-11
    -10.000       -8.000        1.8274E-04         8.8163E-11
    -10.000       -7.000        1.8337E-04         8.8521E-11
    -10.000       -6.000        1.8393E-04         8.8854E-11
    -10.000       -5.000        1.8441E-04         8.9141E-11
    -10.000       -4.000        1.8481E-04         8.9379E-11
    -10.000       -3.000        1.8512E-04         8.9565E-11
    -10.000       -2.000        1.8535E-04         8.9700E-11
    -10.000       -1.000        1.8548E-04         8.9781E-11
    -10.000        0.000        1.8553E-04         8.9808E-11
    -10.000        1.000        1.8548E-04         8.9781E-11
    -10.000        2.000        1.8535E-04         8.9700E-11
    -10.000        3.000        1.8512E-04         8.9565E-11
    -10.000        4.000        1.8481E-04         8.9379E-11
```

INTENTIONALLY LEFT BLANK

APPENDIX L
COMPARISON OF ASHPLUME MODEL RESULTS TO REPRESENTATIVE TEPHRA FALL DEPOSITS

L1.   PURPOSE

The ASHPLUME computer code implements the mathematical model of Suzuki (1983 [DIRS 100489]) for estimation of the areal density of tephra deposits on the surface of the earth following a volcanic eruption. The code, developed by Jarzemba et al. (1997 [DIRS 100987]), includes estimation of the areal density of spent fuel particles incorporated into tephra particles due to a volcanic event that intersects the repository. ASHPLUME is used as a component of the Total Systems Performance Assessment (TSPA) model to assess hazards from possible volcanic activity at the Yucca Mountain site.

The purpose of this calculation is to compare the ASHPLUME estimate of ash (tephra) deposits with an actual eruptive event at the Cerro Negro volcano in 1995. Cerro Negro is a basaltic cinder cone volcano located 20 km northeast of the city of Leon in northwestern Nicaragua (Figure L-1). Ash deposit thickness measurements were taken immediately after a Cerro Negro eruption in November 1995 (Hill et al. 1998 [DIRS 151040]). These data provide an opportunity to compare the ash deposition calculation in the ASHPLUME code with a representative ashfall event.

The ash deposition calculation was conducted using two different versions of the ASHPLUME code, Version 1.4LV [DIRS 154748] and Version 2.0 [DIRS 152844]. The two versions are similar with the only differences being in how they employ different methods of calculating certain eruption parameters. The mathematical differences between the two versions in terms of the eruption models used are given in Section L2. As discussed in Section 1.2.1, the latest version of the code is ASHPLUME_DLL_LA V2.1 [DIRS 178870]. The code was modified to provide the capability for computing on a radial (polar) grid. Since the code modification as part of ASHPLUME_DLL_LA V2.1 affected only the routines that define the grid and did not affect the numerical solver routines, the validation activities using Version 2.0 remain valid and current for Version 2.1. An additional objective of this calculation was to provide a comparison of how these differences within the two versions affect calculated results.

Ash thickness measurements downwind are the only measured data available from the 1995 Cerro Negro event. The scope of this comparison will consider ash layers only. The spent fuel distribution within ASHPLUME will not be examined in this calculation.

L2.   METHOD

A detailed mathematical development of the ASHPLUME mathematical model is given in Section 6.5.1. The two versions of the ASHPLUME code (i.e., V1.4LV and V2.0) that were compared in this calculation differ in the definition of the total mass of the erupted material (Q) and the height of the eruption column (H). In version 1.4LV of the code, H and Q are calculated using (CRWMS M&O 1999 [DIRS 132547], pg. B-3):

$$T_d = e^{(15.29 + 0.527\,lnV)} \qquad\qquad \text{(Eq. L-1a)}$$

$$H = e^{\left[7.83 + 0.394\,ln\left(\frac{V}{T_d}\right)\right]} \qquad\qquad \text{(Eq. L-1b)}$$

and

$$Q = \overline{\rho} \, V \times 10^{15} \qquad\qquad \text{(Eq. L-2)}$$

where T_d is the event duration in seconds and the parameters $\overline{\rho}$ and V are user inputs and are defined as

$\overline{\rho}$ = the average density of erupted material, g/cm^3

V = the total volume of erupted material, km^3.

In version 2.0 of the code, H and Q are calculated using (Jarzemba et al. 1997 [DIRS 100987], pp. 4-4 and 4-5):

$$H = 0.0082 \, P^{1/4} \qquad\qquad \text{(Eq. L-3)}$$

and

$$Q = 1000 \, T_d \left(\frac{H}{0.24} \right)^4 \qquad\qquad \text{(Eq. L-4)}$$

where P and T_d are input by the user and are defined as:

P = the eruption power in Watts

T_d = the event duration in seconds.

As stated in Section L1, one objective of this calculation is to compare the effects on the results of using equations L-3 and L-4 instead of equations L-1 and L-2.

L3.   ASSUMPTIONS

The underlying assumptions used in the ASHPLUME mathematical model are discussed by Suzuki (1983 [DIRS 100489]) and Jarzemba et al. (1997 [DIRS 100987]). In addition to those assumptions, several assumptions were made in developing the input data for this calculation. The following paragraphs discuss these assumptions.

L3.1   USE OF INFORMATION FROM HILL ET AL. 1998 [DIRS 151040]

Assumption: The scope of the calculation is to reproduce within the ASHPLUME model as closely as possible the input parameters and their associated values as reported by Hill et al. (1998 [DIRS 151040]). The assumption is made that these parameters and the associated values and the field data documented in the article are reported accurately. It is further assumed that by running the ASHPLUME mathematical models utilizing these input parameters and the associated values when compared to the actual measured field data under the same conditions represents a meaningful comparison of the ASHPLUME code to this specific set of field measurement data.

Rationale: The measured parameters and associated values are presented in a manner that allows direct mapping to the ASHPLUME code parameters. The paper reports a comparison of the field data to a modified version of the Suzuki (1983 [DIRS 100489]) model. ASHPLUME is also a modified version of the Suzuki model and the comparison done in the paper along with the comparison in this calculation utilize the same field data, similar mathematical models, and the same parameters and associated values. Thus, the conclusion is made that the work documented in this calculation is a valid use of the information presented by Hill et al. (1998 [DIRS 151040]).

L3.2   WIND SPEED AND DIRECTION

Assumption: Constant wind speed and wind direction were assumed for this calculation.

Rationale: Hill et al. (1998 [DIRS 151040]) state that the wind speed ranged from 8 to 10 m/s. Hill et al. (1998 [DIRS 151040], Table 3) also list the eruption parameters and list the wind speed as a constant 9 m/s. Thus, this constant value is utilized for wind speed. It is almost certain that the wind direction was not constant during the actual Cerro Negro eruption. However, from the actual ash thickness data it appears that the primary wind direction was towards the city of Leon. In addition, no data were available to document changes in wind direction. Therefore, the wind direction was assumed to be constant and blowing towards the city of Leon.

L3.3   CONSTANT DENSITY

Assumption: A constant ash particle density was assumed for this calculation.

Rationale: The ASHPLUME code contains a feature that allows particle density to be a linear function of particle size. Hill et al. (1998 [DIRS 151040], Table 3) present the measured average ash density as 1.2 g/cm^3. This value is utilized as a constant as presented.

L3.4   TOTAL ASH MASS BASIS OF COMPARISON

Assumption: Because the two versions of the ASHPLUME code being compared have slightly different input parameter sets, a basis for maintaining consistency between the data set for one version and the data set for the other version needed to be established. Thus, the assumption was made to have the same total mass of ash being ejected from the volcano.

Rationale: A different basis could have been used, such as assuming the same column height for each version. However, it was decided that the most consistent treatment would be matching the masses because ASHPLUME results are given in mass based units and by utilizing the same total mass the codes would each be dispersing the same amount of material. Also, this mass erupted would then compare directly with the actual measured mass from the volcano.

L3.5   UPPER LIMIT OF PARTICLE DIAMETER

Assumption: The volcanic ash mass is represented within the ASHPLUME code by a log-normal distribution defined as a function of particle size (Jarzemba et al. 1997 [DIRS 100987], Sec. 2.2). The mean particle diameter, ρ_{mean}, and standard deviation, σ, of the

distribution are specified by the user in the input file. The integration limits, ρ_{min} and ρ_{max}, of the outer integral in Equation 6-2 are then defined in terms of these parameters as follows:

$$_{min} = \log(\rho_{mean}) - 5.0\ \sigma$$

and   (Eq. L-5)

$$\rho_{max} = \log(\rho_{mean}) + 5.0\ \sigma$$

The upper limit of the integration, ρ_{max}, may be limited by using the input parameter *dmax*. The code will use the smaller of ρ_{max} from Equation L-5 and $\log(dmax)$ from the input file. It is assumed in this calculation that the upper integration limit specified according to Equation L-5 is appropriate and no limitation will be applied with parameter *dmax*.

Rationale: Jarzemba et al. (1997 [DIRS 100987], pg. 2-2) indicate that the Suzuki (1983 [DIRS 100489]) model is suitable for eruptions with particle sizes greater than 15 - 30 micrometers.

L4.   COMPUTER SOFTWARE AND MODELS

ASHPLUME V.1.4LV [DIRS 154748] and ASHPLUME V.2.0 [DIRS 152844] of the code were compared to the Cerro Negro ash thickness data (Wunderman et al. 1995 [DIRS 152504]) in this calculation. The inputs and outputs for each version are identified in Sections L5 and L6. Each version of the software is appropriate for its intended use in this calculation. The "intended use" within the context of this calculation, as stated in Section L1, is to determine how results from the two versions compare given matched inputs and to compare the results of each version to data from an observed eruption. In version 1.4LV the ash volume and ash density are used to determine column height and total mass of ash in the eruption column. In version 2.0 the eruption power and event duration are used to determine column height and total mass of ejecta. A description of the mathematical differences between the two versions is given in Section L2. Each version of the code was used within the range in which it is valid for this calculation.

In addition to the two versions of the ASHPLUME code, several commercial software programs were utilized in this calculation. They are:

- Microsoft Excel 97 SR-2
- Microsoft PowerPoint 97 SR-2
- Golden Software's Surfer Version 6.01.

All software used in this calculation was executed on a Dell Dimension XPS pro 180n running under the Microsoft Windows NT Version 4.0 SP3 operating system.

L5.   CALCULATION

The Suzuki (1983 [DIRS 100489]) model was used by Hill et al. (1998 [DIRS 151040]) to analyze the 1995 Cerro Negro eruption. The Hill analysis was used as the basis of this comparison and the physical parameters and model constants required by ASHPLUME for this calculation are taken from the Hill analysis. Each version of the code was executed using inputs

appropriate for that version and the results from each version were compared to the Cerro Negro ash thickness data by graphically overlaying ash thickness contours. The graphical overlay of results provides a concise mechanism for satisfying the two objectives of this calculation discussed in Section L1 (i.e., the comparison of results from the two versions with each other and with the Cerro Negro data).

The following paragraphs contain a description of the input data sets used with each version of the code and describe the steps used to run the codes. Version 2.0 of the ASHPLUME code was executed first. The program was executed in a MSDOS window using the MSDOS batch file shown in Figure L-2. The following command was used to execute the program:

>**runashp20 cn_2_0**

The file *cn_2_0.in* was the input file and is shown in Figure L-3. The output files produced by the above command were *cn_2_0.out* and *cn_2_0.log*. The file *cn_2_0.out* is discussed in the next section. The file *cn_2_0.log* is a diagnostic file and indicates that no errors were encountered.

The following list provides the source of the data or provides an explanation of why a particular value was used. The line numbers in the list refer to the line numbers in the input file shown in Figure L-3.

Line 1)   The run title.

Line 2)   Iscrn equal to a value of 1 enables ASHPLUME output to the screen in addition to the output file.

Line 3)   Xmin and xmax are the receptor grid limits in the x direction in km. The coordinate x=0,y=0 is coded within ASHPLUME to be at the volcano vent. These limits were chosen to provide receptor points on each side of the vent out to a distance sufficient to include the 0.1-cm ash contour.

Line 4)   Ymin and ymax are the receptor grid limits in the y direction in km. These limits in the y direction were chosen to provide receptor points downwind from the vent to a distance sufficient to include the 0.1-cm ash contour.

Line 5)   Numptsx is the number of receptor points in the x direction. The receptor grid spacing, dx, is determined by dx = (xmax – xmin)/(numptsx – 1).

Line 6)   Numptsy is the number of receptor points in the y direction. The receptor grid spacing, dy, is determined by dy = (ymax – ymin)/(numptsy – 1).

Line 7)   Ashdenmin and ashdenmax are the ash densities corresponding to particle diameters of ashrholow and ashrhohi on the following line. ASHPLUME provides for allowing ash density to vary linearly with ash particle diameter. Because ash density variation with particle size data was not available for the Cerro Negro event, ash density was assumed (Section L3.3) for this calculation to be a constant at the average clast density of 1.2 g/cm^3 provided by the article by Hill et al. (1998 [DIRS 151040], Table 3).

Line 8)   Ashrholow and ashrhohi are the logs of the particle diameters corresponding to the ash densities on the previous line. Because the ash density was assumed to be a constant, the values for these parameters are meaningless for these runs and only non-equal values need be entered.

Line 9)   Fshape is the shape factor for particles. The value of 0.5 was taken from the article by Hill et al. (1998 [DIRS 151040], Table 3).

Line 10)   Airden is the air density. The value of 0.001293 g/cm^3 was taken from the article by Jarzemba et al. (1997 [DIRS 100987], Table 5-1). Airvis is the air viscosity. The value of 0.00018 g/cm-s was also taken from the article by Jarzemba et al. (1997 [DIRS 100987], Table 5-1).

Line 11)   The constant C is the parameter relating eddy diffusivity to particle fall time. The value of 400 was taken from the article by Hill et al. (1998 [DIRS 151040], Table 3).

Line 12)   The upper limit (ρ_{max}) of the outer integral in Equation 6-2 may be limited in ASHPLUME by the log of the value of dmax entered here (Section L3.5). Normally, ρ_{max} is defined as the log of the mean particle diameter specified in line 17 plus five times the value of sigma specified in line 18. For this calculation, using the values specified in line 17 and 18, $\rho_{max} = \log(0.07) + 5 \times 0.8 = 2.8$. Any value of for log(dmax) larger than 2.8 in this case means that the value for ρ_{max} will not be limited. Because no justification exists for limiting ρ_{max} in this calculation, a relatively large number (1,000) was used.

Line 13)   Fdmin, fdmean, and fdmax are the minimum, mean, and maximum waste-fuel-particle diameters. Because this calculation does not consider the fuel transport computation, these values are not utilized.

Line 14)   Hmin is the lower limit of the inner integral of Equation 6-2. A small value greater than 0.0 (e.g., 0.001) is used to avoid numerical problems at the vent exit and to model the full height of the vent from the ground surface.

Line 15)   Acutoff is the lower limit on the ash deposition calculation. It is used to speed program execution by eliminating calculations for receptors outside the plume area.

Line 16)   The constant beta controls the diffusion of particles out of the eruption column. The value of 10.0 was taken from Hill et al. (1998 [DIRS 151040], Table 3).

Line 17)   The mean ash particle diameter of 0.07 cm was taken from Hill et al. (1998 [DIRS 151040], Table 3).

Line 18)   The input parameter sigma is the particle diameter standard deviation (sorting). Hill et al. (1998 [DIRS 151040], pg. 1237) used a range of values for sigma between 0.5 and 1.5. A value of 0.8 was utilized in this calculation.

Line 19)   The incorporation ratio is used to determine the relative mass of fuel particles to waste particles. Because this calculation only considers ash, this parameter is not significant to this analysis.

Line 20)   The mass of fuel is not used in this calculation.

Line 21)   The wind direction was assumed to be directly towards the city of Leon (Figure L-1). A value of 90 degrees was arbitrarily selected to use in the computation and the resulting plume was rotated during the postprocessing step to orient the major plume axis toward Leon for graphical display. This approach allows the receptor grid axis to be aligned with the plume axis, thereby reducing the number of receptor grid locations required to define the plume.

Line 22)   The wind speed of 900 cm/s was taken from Hill et al. (1998 [DIRS 151040], Table 3).

Line 23)   Data for initial eruption velocity for the 1995 Cerro Negro eruption was not provided explicitly by Hill et al. (1998 [DIRS 151040]).   The initial eruption velocity of 10,000 cm/s was stated as a value that velocities drop below only for the upper 200 meters of the column for short eruption columns (<5 km). Thus, this stated value of 10,000 cm/s is utilized here.

Line 24)   Eruption power was determined from Equation L-3 by using a value for H of 2.4 km (Hill et al. 1998 [DIRS 151040], Table 3).

Line 25)   The event duration of 3.46×10^5 s was provided in Hill et al. (1998 [DIRS 151040], Table 3).

Version 1.4LV of the ASHPLUME code was then executed. The program was executed in a MSDOS window using the MSDOS batch file shown in Figure L-4. The following command was used to execute the program:

>**runashp14 cn_1_4**

Because Version 1.4LV of ASHPLUME contains an option for performing either a stochastic analysis or a deterministic analysis, the input logic for Version 1.4LV is different than Version 2.0. For this calculation, the deterministic mode of operation was used. Two input files are required with Version 1.4LV for a deterministic calculation when executing with the above command. The two input files used in this calculation are shown in Figure L-5 and are named *cn_1_4.in* and *cn_1_4.resp*. The file with the .resp filename extension contains the user's

responses to the screen prompts written by the program. The output file produced by the above command is named *cn_1_4.out*. The output file will be discussed in the next section.

The two Version 1.4LV data files were developed using parameter values equal to those used with the Version 2.0 calculation. The conversion of the Version 2.0 data set to the Version 1.4LV data set was done such that the total mass of ash released would be identical in the two versions. The following lists provide a line by line description of how the data in the two files were selected. The first list describes the file *cn_1_4.in*:

Line 1)   The run title.

Line 2)   The receptor grid is identical to Version 2.0.

Line 3)   The receptor grid is identical to Version 2.0.

Line 4)   The receptor grid is identical to Version 2.0.

Line 5)   The receptor grid is identical to Version 2.0

Line 6)   Vlogmin and vlogmax are not used in deterministic mode.

Line 7)   Powlogmin and powlogmax are not used in Version 1.4LV.

Line 8)   Betalogmin and betalogmax are not used in deterministic mode.

Line 9)   The particle mean diameter distribution parameters are not used in deterministic mode.

Line 10)   The particle size standard deviation distribution parameters are not used in deterministic mode.

Line 11)   The ash density is defined to be identical to that used in the Version 2.0 calculation (i.e., constant at 1.2 g/cm^3).

Line 12)   These parameters are used in conjunction with Line 11 to define ash density. The ash density is defined to be identical to that used in the Version 2.0 calculation.

Line 13)   The shape parameter is identical to Version 2.0.

Line 14)   Air density and viscosity are identical to Version 2.0.

Line 15)   The constant C is identical to Version 2.0.

Line 16)   The parameter dmax is identical to Version 2.0.

Line 17)   Fdmin, fdmean, and fdmax are not significant to an ash-only calculation.

Line 18)   Hmin is identical to Version 2.0.

Line 19)   Acutoff is identical to Version 2.0.

Line 20)   The incorporation ratio is not significant to an ash-only calculation.

Line 21)   Uranmin and uranmax are not used in deterministic mode and are not significant to an ash-only calculation.

The next list describes the file *cn_1_4.resp*, the user response file.

Line 1)   A value of 2 specifies a deterministic calculation.

Line 2)   A value of 2 indicates that no additional files containing particle size distribution information are required.

Line 3)   The constant beta is identical to Version 2.0.

Line 4)   The mean ash particle diameter is identical to Version 2.0.

Line 5)   Sigma is identical to Version 2.0.

Line 6)   The incorporation ratio is not significant to an ash-only calculation.

Line 7)   The mass of fuel to incorporate is not significant to an ash-only calculation.

Line 8)   The wind direction is identical to Version 2.0 (i.e., towards Leon).

Line 9)   The wind speed is identical to Version 2.0.

Line 10)   The initial eruption velocity is identical to Version 2.0.

Line 11)   The eruption power was entered identically to Version 2.0; however, this parameter is not used in Version 1.4LV.

Line 12)   The total ash volume in km^3 was determined with Equation L-2 using the value for ash density entered on the next line (1.2 g/cm^3) and the total ash mass calculated for Version 2.0 with Equation L-4. This approach assures that the total ash mass will be the same and allow direct comparison of results with the two version of the code.

Line 13)   The average ash density is assumed to be identical to that used in Version 2.0.

Line 14)   The eruption parameters used with both versions of the code are summarized in Table L-1. ASHPLUME inputs not related to this calculation and inputs developed by the analyst such as receptor grid locations are discussed above and are not shown in the table. All inputs to ASHPLUME for this calculation are within the range of validation as described in the qualification documentation.

L6.   RESULTS

The results of the two ASHPLUME calculations are shown as ash thickness contours in Figure L-6 along with the measured Cerro Negro ash thickness data taken from Wunderman et al. (1995 [DIRS 152504]). Figure L-6 was created using the following procedure.

1) The output file from the Version 2.0 calculation (*cn_2_0.out*) was processed with an Excel spreadsheet (*cn_2_0.xls*) to convert distance in meters to distance in kilometers. This was necessary because the Version 1.4LV output is in kilometers and a common unit must be used for the graphical display. The spreadsheet was also used to convert the ash areal density in g/cm^2 from the ASHPLUME output to ash thickness in cm by dividing the areal density by the ash density of 1.2 g/cm^3. Three columns of data were then exported from the spreadsheet to the text file *cn_2_0.dat*. The three columns contain x and y coordinates in kilometers relative to the volcanic vent and ash thickness in centimeters.

2) The output file from the Version 1.4LV calculation (*cn_1_4.out*) was processed with an Excel spreadsheet (*cn_1_4.xls*) in an identical manner to the Version 2.0 output except that the distance conversion was not necessary because Version 1.4LV output is already in kilometers. The three columns of data containing x,y coordinates and ash thickness were exported to the text file *cn_1_4.dat*.

3) The commercial software Surfer was then used to create contours of the ash thickness results using the files *cn_2_0.dat* and *cn_1_4.dat*.   The files *cn_1_4.grd* and *cn_2_0.grd* contain the binary Surfer grid files and the file *cn_2014.srf* contains the Surfer contour drawing.

4) The file *14neg13f.gif* from Wunderman et al. (1995 [DIRS 152504]) contains ash thickness contours for the 1995 Cerro Negro eruption derived from data collected by M. Kesseler of the University of Geneva. This file was imported into Microsoft PowerPoint and the contours for ash thickness of 0.1, 0.5, 1.0, 2.0, 5.0, and 10.0 cm were manually traced from the *.gif* figure using the drawing capabilities of PowerPoint. Selected base map features were also extracted from the *.gif* figure to provide a reference for overlaying the contours developed with the ASHPLUME calculated data. The traced figure was saved in a separate file (*base_map.ppt*).

5) After adjusting the scale in the Surfer drawing to match exactly to the PowerPoint figure and rotating the Surfer drawing to align the plume to the observed data, the Surfer generated contours were cut and pasted to the PowerPoint drawing. Using the volcanic vent as a reference for location, the two figures were overlaid. Scales were checked to ensure that the correct scales had been maintained in the merging operation. The resulting PowerPoint drawing was saved as file *compare.ppt*. The drawing was imported to this document as Figure L-6. The Surfer contouring algorithm causes the anomaly in the 1.0-cm contour for Version 2.0.

As shown in Figure L-6, the two versions of the code produce similar results. The ASHPLUME calculations compare well with the observed data for distances from the volcanic vent greater

than 10 km. For distances less than 10 km, the ASHPLUME results give ash thickness values greater than the observed data. The lobe on the northern side of the measured ash thickness data indicates that a variation in wind direction and/or speed occurred during the eruption. This probably accounts for some of the discrepancy because ASHPLUME assumes a constant wind speed and direction for a given simulation. To help understand the differences in the results obtained with the two versions of the code, the header portion of the output files are shown in Figures L-7 and L-8 for comparison. Figure L-7 shows the header from the Version 2.0 calculation and Figure L-8 shows the header from the Version 1.4LV calculation. The only significant differences between the two files are the values of event duration (T_d) and column height (H). The constraint of maintaining an equal mass of ejected material for the two versions means that the calculation in Equation L-1 will yield a column height for Version 1.4LV that will differ from that calculated by Version 2.0 using Equation L-3. The unequal column height between the two versions accounts for the differences in the results. As can be seen in Figures L-7 and L-8, the column height from Version 1.4LV (2.0453 km) is slightly less that that calculated by Version 2.0 (2.4000 km), resulting in the slightly reduced downwind transport distance of the ash plume shown in Figure L-6.

Table L-1. ASHPLUME Eruption Parameters used for the Cerro Negro Calculation

Parameter	Value	Source
Fshape	0.5	Hill et al. 1998 [DIRS 151040], Table 3
Airden, g/cm^3	0.001293	Jarzemba et al. 1997 [DIRS 100987], Table 5-1
Airvis, g/cm-s	0.00018	Jarzemba et al. 1997 [DIRS 100987], Table 5-1
C, cm^2/s$^{5/2}$	400	Hill et al. 1998 [DIRS 151040], Table 3
Beta	10	Hill et al. 1998 [DIRS 151040], Table 3
Mean ash diameter, cm	0.07	Hill et al. 1998 [DIRS 151040], Table 3
Sigma[a]	0.5 to 1.5	Hill et al. 1998 [DIRS 151040], p. 1,237
Wind Speed, cm/s	900	Hill et al. 1998 [DIRS 151040], Table 3
Initial Eruption Velocity, cm/s	10,000	Jarzemba et al. 1997 [DIRS 100987], Table 5-1
Power, Watts[b]	7.338×10^9	Hill et al. 1998 [DIRS 151040]
Ash Volume, km^{3}[c]	0.00288	Hill et al. 1998 [DIRS 151040]
Ash Density, g/cm^3	1.2	Hill et al. 1998 [DIRS 151040]
Event Duration, s[d]	3.46×10^5	Hill et al. 1998 [DIRS 151040]

OTES: [a]A value of 0.8 was selected for the calculation after several trials within the range shown.
[b]The power was derived from Equation L-3 using a value of 2.4 km for the column height taken from the cited reference. This parameter is not used in Version 1.4LV.
[c]Volume is not used in Version 2.0. For Version 1.4LV, the volume was calculated with Equation L-2 using the value for mass (3.46×10^{12} g) from Version 2.0 and average ash density (1.2 g/cm^3) from the cited reference.
[d]Event duration is an input parameter in Version 2.0 only.

Figure L-1. Cerro Negro Location Map

Filename = runashp20.bat

```
Echo off
rem.....Run the ASHPLUME V2.0 dll in DOS window
rem..... %1 = input file base name
rem
copy %1.in ashplume.in
D:\Ashplume\V2.0\run_ashp
del ashplume.in
del %1.out
ren ashplume.out %1.out
del %1.log
ren run_ashp.log %1.log
rem
```

Figure L-2. MSDOS Batch File Used to Execute ASHPLUME Version 2.0 [DIRS 152844]

Filename = cn_2_0.in

```
 1) ASHPLUME v2.0 - Cerro Negro, Nicaragua
 2) 1                     ! iscrn, 0 = no screen output, 1 = yes
 3) -10.0   10.0          ! xmin, xmax in km
 4) -2.0   30.0           ! ymin, ymax in km
 5) 21                    ! numptsx
 6) 33                    ! numptsy
 7) 1.2   1.2             ! ashdenmin, ashdenmax in g/cm3
 8) -1.0   0.0            ! ashrholow, ashrhohi
 9) 0.5                   ! fshape
10) 0.001293 0.00018      ! airden in g/cm3, airvis in g/cm-s
11) 400.0                 ! c in cm2/s to the 5/2
12) 1000.0                ! dmax in cm
13) 0.01d0 0.1d0 1.0d0    ! fdmin, fdmean, fdmax all in cm
14) 0.001                 ! hmin in km
15) 1.d-10                ! acutoff in g/cm2
16) 10.0                  ! the constant beta (unitless)
17) 0.07                  ! the mean ash particle diameter (cm)
18) +0.8                  ! sigma for the ash lognormal dist.
19) 0.3d0                 ! the incorporation ratio (unitless)
20) 1.0d7                 ! the mass of fuel to incorporate (g)
21) +90.0                 ! wind direction- relative to due east (deg)
22) 900.0                 ! the wind speed (cm/s)
23) 10000.0               ! the initial eruption velocity (cm/s)
24) 7.3382e9              ! the power (watts)
25) 3.46e+05              ! the event duration (s)
```

Figure L-3. Input File Used with ASHPLUME Version 2.0 [DIRS 152844] Cerro Negro Calculation

Filename = runashp14.bat

```
Echo off
rem.....Run ASHPLUME V1.4 in DOS window
rem..... %1 = input file base
rem
copy %1.in ashplume14.in
D:\Ashplume\V1.4\ashplume14 < %1.resp
del ashplume14.in
del %1.out
ren ashplume.out %1.out
rem
```

Figure L-4. MSDOS Batch File Used to Execute ASHPLUME Version 1.4LV [DIRS 154748]

Filename = cn_1_4.in

```
 1) ASHPLUME v1.4  -  Cerro Negro, Nicaragua
 2) -10.0   10.0             ! xmin, xmax in km
 3)  -2.0   30.0             ! ymin, ymax in km
 4) 21                       ! numptsx
 5) 33                       ! numptsy
 6) -2.54   -2.54            ! vlogmin, vlogmax- logs of volume in km**3
 7)  9.87    9.87            ! powlogmin, powlogmax- logs of P in W
 8)  1.0     1.0             ! betalogmin, betalogmax-logs
 9) -2.0d0 -1.0d0  0.0d0     ! dmeanmin,dmeanmed,dmeanmax-logs of d in cm
10) 0.8      0.8             ! dsigmamin, dsigmamax
11) 1.2      1.2             ! ashdenmin, ashdenmax in g/cm3
12) -1.0     0.0             ! ashrholow, ashrhohi
13) 0.5                      ! fshape
14) 0.001293   0.00018       ! airden in g/cm3, airvis in g/cm-s
15) 400.0                    ! c in cm2/s to the 5/2
16) 1000.0                   ! dmax in cm
17) 0.01   0.1   1.0         ! fdmin, fdmean, fdmax all in cm
18) 0.001                    ! hmin in km
19) 1.d-10                   ! acutoff in g/cm2
20) 0.3                      ! the incorporation ratio (unitless)
21) 1.0e7   1.0e7            ! uranmin, uranmax, the mass of fuel (g)
```

Filename = *cn_1_4.resp* (User Responses)

```
 1) 2              ! Deterministic
 2) 2              ! No files
 3) 10.0           ! the constant beta (unitless)
 4) 0.07           ! the mean ash particle diameter (cm)
 5) 0.8            ! sigma for the ash lognormal dist. (unitless)
 6) 0.3            ! the incorporation ratio (unitless)
 7) 1.0e7          ! the mass of fuel to incorporate (g)
 8)  90.0          ! the wind direction- relation to due east (deg)
 9) 900.0          ! the wind speed (cm/s)
10) 10000.0        ! the initial eruption velocity (cm/s)
11) 7.3382e9       ! the power (watts)
12) 0.00288        ! the volume (km3)
13) 1.2            ! the ash density (g/cm3)
```

Figure L-5. Files used with ASHPLUME Version 1.4LV [DIRS 154748] Cerro Negro Calculation
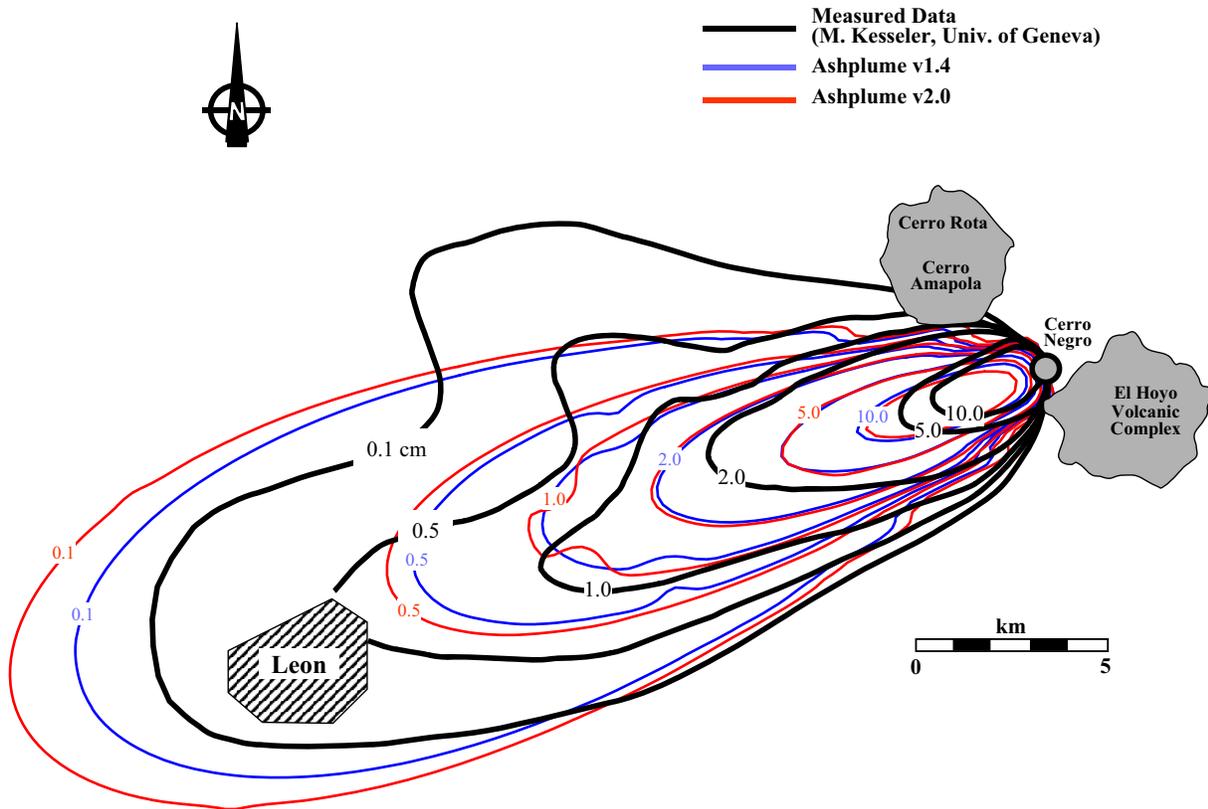
Figure L-6. Comparison of Calculated and Measured Ash Deposit Thickness in cm for 1995 Cerro Negro Eruption

Filename = cn_2_0.out (partial listing)

```
 ASHPLUME version 2.00-dll


***********************************************************************
     Input Parameters (From vin vector):
         Minimum x location (km)............... -10.0000
         Maximum x location (km)...............  10.0000
         Minimum y location (km)...............  -2.0000
         Maximum y location (km)...............  30.0000
         Number of grid points in x............      21
         Number of grid points in y............      33
         Minimum ash density (g/cm^3).........    1.2000
         Maximum ash density (g/cm^3).........    1.2000
         Minimum particle size [log(cm)].......  -1.0000
         Maximum particle size [log(cm)].......   0.0000
         Particle shape parameter.............    0.5000
         Air density (g/cc)................... 1.2930E-03
         Air viscosity (g/cm-s)............... 1.8000E-04
         Eddy diff. constant (cm^2/s^[5/2])....  400.0000
         Size cutoff (cm)..................... 1000.0000
         Minimum waste particle diameter (cm)..   0.0100
         Mode waste particle diameter (cm).....   0.1000
         Maximum waste particle diameter (cm)..   1.0000
         Minimum height of column (km).........   0.0010
         Lower limit for ash deposits (g/cm^2). 1.0000E-10
         Dispersion constant, beta.............  10.0000
         Mean particle diameter (cm)...........   0.0700
         Log particle standard deviation.......   0.8000
         Incorporation ratio...................   0.3000
         Total fuel mass available (g)........ 1.0000E+07
         Wind direction (deg)..................  90.0000
         Wind speed (cm/s).....................  900.0000
         Vent exit velocity (cm/s)............. 10000.0000
         Event power (w)....................... 7.3382E+09
         Event duration (s).................... 3.4600E+05

     Derived Parameters:
         Ash particle minimum log-diameter.....   -5.1549
         Ash particle mean log-diameter........   -1.1549
         Ash particle maximum log-diameter.....    2.8451
         Fuel particle minimum log-diameter....   -2.0000
         Fuel particle mode log-diameter.......   -1.0000
         Fuel particle maximum log-diameter....    0.0000
         Column height (km)....................    2.4000
         Ash mass (g).......................... 3.4600E+12

***********************************************************************
```

Figure L-7. Listing of Header from ASHLUME Version 2.0 [DIRS 152844] Output File for the Cerro Negro Calculation

Filename = cn_1_4.out (partial listing)

```
*********************************************************************
*                                                                 *
*                   realization number                   1        *
*                   wind speed (cm/s)              900.0000        *
*                   wind direction (deg)            90.0000        *
*            mean particle diameter (cm)             0.0700        *
*                        log- std dev                0.8000        *
*                       column ht (km)               2.0453        *
*                   event duration (s)           0.2002E+06        *
*                        ash mass (g)            0.3456E+13        *
*                     event power (W)            0.7338E+10        *
*                               beta                10.0000        *
*              vent exit velocity (cm/s)         10000.0000        *
*              particle shape parameter              0.5000        *
*                    air density (g/cc)          0.1293E-02        *
*                 air viscosity (g/cm-s)         0.1800E-03        *
*         eddy diff. constant (cm2/s5/2)           400.0000        *
*                      size cutoff (cm)           1000.0000        *
*                   incorporation ratio             0.3000        *
*         fuel particle minimum log-diam            -2.0000        *
*          fuel particle median log-diam            -1.0000        *
*         fuel particle maximum log-diam             0.0000        *
*          total fuel mass available (g)         0.1000E+08        *
*                  eruption volume (km3)             0.0029        *
*                   ash density (g/cm3)              1.2000        *
*                                                                 *
*********************************************************************
```

Figure L-8. Listing of Header from ASHPLUME Version 1.4LV [DIRS 154748] Output File for the Cerro Negro Calculation